ADAPTIVE PATH PLANNING FOR AN AUTONOMOUS MARINE VEHICLE PERFORMING COOPERATIVE NAVIGATION FOR AUTONOMOUS UNDERWATER VEHICLES

by

Jonathan Hudson

Submitted in partial fulfilment of the requirements
for the degree of Master of Applied Science

at

Dalhousie University
Halifax, Nova Scotia
April 2012

DALHOUSIE UNIVERSITY

DEPARTMENT OF MECHANICAL ENGINEERING

The undersigned hereby certify that they have read and recommend to the Faculty of Graduate Studies for acceptance a thesis entitled "ADAPTIVE PATH PLANNING FOR AN AUTONOMOUS MARINE VEHICLE PERFORMING COOPERATIVE NAVIGATION FOR AUTONOMOUS UNDERWATER VEHICLES" by Jonathan Hudson in partial fulfilment of the requirements for the degree of Master of Applied Science.

Dated: April 9, 2012

Supervisor: ______________________________

Co-Supervisor: ______________________________

Readers: ______________________________

____

DALHOUSIE UNIVERSITY

DATE: April 9, 2012

AUTHOR: Jonathan Hudson

TITLE: Adaptive Path Planning for an Autonomous Marine Vehicle Performing Cooperative Navigation for Autonomous Underwater Vehicles

DEPARTMENT OR SCHOOL: Department of Mechanical Engineering

DEGREE: MASc CONVOCATION: October YEAR: 2012

____

Signature of Author

Table of Contents

List of Tables

List of Figures

Abstract

Adaptive path planning of an autonomous marine vehicle (surface or subsurface) in the role of a communication and navigation aid (CNA) for multiple autonomous underwater vehicles (AUVs) for survey missions is studied. This path planning algorithm can be run before deployment, based on the planned paths of the survey AUVs, or underway, based on information transmitted by the survey AUVs. The planner considers the relative depth of the CNA and survey AUVs (not previously done) allowing the CNA to better aid survey AUVs that maintain a set distance over the ocean floor while surveying. Results are presented from simulations and in-water trials for both pre-deployment and underway planning modes, the latter being preferred since it can adapt to the survey AUV path during the mission. The necessity of bounding the distance between the CNA and any survey AUV in order to bound survey AUV position error is also described.

List of Abbreviations and Symbols Used

ADCP	Acoustic Doppler Current Profiler
AINS	Aided Inertial Navigation System
ASC	Autonomous Surface Craft
ATR	Automatic Target Recognition
AUV	Autonomous Underwater Vehicle
CAD/CAC	Computer-Aided Detection/Computer Aided Classification
CEP	Circular Error Probability
CML	Concurrent Mapping and Localization (now known as SLAM)
CNA	Communication and Navigation Aid
CNM	Concurrent Navigation and Mapping (now known as SLAM)
CTD	Conductivity, Temperature, and Depth (underwater sensor)
DVL	Doppler Velocity Log (gives AUV speed over seabed)
EKF	Extended Kalman Filter
ESKF	Error State Kalman Filter
FAU	Florida Atlantic University
FOG	Fibre Optic Gyroscope
INE	Inertial Navigation Equations
INU	Inertial Navigation Unit (sometimes INS, "S" for system)
LBL	Long Baseline (navigation)
MCM	Mine Countermeasures
MDP	Markov Decision Process
MLO	Mine-Like Object (in MCM)
MOOS	Mission Oriented Operating Suite
MOOS-IvP	MOOS expansion using Interval Programming
OWTT	One-Way Travel Time (for acoustic navigation)
RI	Reacquire and Identify (in MCM)
ROV	Remotely Operated Vehicle (tethered underwater robot)
SCM	Search-Classify-Map (in MCM)
SLAM	Simultaneous Localization And Mapping
TDMA	Time Division, Multiple Access (communication protocol)
USBL	Ultra-Short Baseline (navigation)
WHOI	Woods Hole Oceanographic Institution, Massachusetts, USA

Acknowledgements

Funding for this effort was provided through Defence Research and Development Canada (Atlantic). Many people provided vital assistance in the completion of this thesis. Some of their names will not appear here due to the forgetfulness of the author. He wishes to apologize. Among the names that should appear here are Warren Connors (C++ and Object Oriented Programming whiz), Mary Beth Lascurain (research engineer, wife of author), Vincent Myers (excellent teacher for all things algorithm), Liam Paull (creator of information gain AUV path planning and the extended Kalman filter used as part of the simulations in this thesis), Aaron Percival (creator of PATHA path planning used as part of the simulations in this thesis), Mae Seto (author's supervisor), and the technicians/technologists of Defence R&D Canada (Atlantic) who made the in-water trials possible, in spite of the odds. Errors remaining in this thesis are the sole responsibility of the author.

Chapter 1 Introduction

Autonomous underwater vehicles (AUVs) are increasingly used for scientific research [1], offshore petroleum [2], and naval applications [3]. One naval application is mine countermeasures (MCM). Formerly, MCM operations required divers and ships to operate within suspected minefields. With advances in marine robotics, it is now possible for most of the dangerous work in MCM to be performed by AUVs. There are however, inherent AUV limitations in fulfilling MCM requirements. Some of these limitations can be addressed by using an additional autonomous marine vehicle as a communication and navigation aid (CNA). This thesis reports on the adaptive path planning of such an autonomous marine vehicle as a CNA for AUVs.

1.1. Thesis Contributions and Organization

This thesis makes several original contributions to autonomous marine vehicle path planning. First, an adaptive three-dimensional path planner for the CNA where the survey AUVs change their relative depths while surveying is the main contribution. This planner considers both an AUV and an autonomous surface craft (ASC) as a CNA vehicle and compares their relative merits in simulation. Second, a distance penalty is used in bounding the distance between the CNA and the submerged survey AUVs, without significant increases in the computational load, in order to bound survey AUV position error growth. Third, this thesis describes the implementation of the path planning algorithm on an autonomous marine vehicle in MOOS-IvP [4] and in-water trials that validate this algorithm in both pre-deployment and underway planning modes. Fourth, simulations of a CNA supporting AUV missions other than lawnmower patterns (Figure 1.1) such as paired-track patterns (Figure 6.3 and [5]) and an adaptive, information-gain based method (Figure 6.5 and [6]) are described. This shows that the path planner is capable of more than the basic lawnmower mission in complexity.

The thesis is organized as follows. Section 1.2 describes the use of AUVs in MCM, and Section 1.3 describes the concept of a CNA vehicle. Chapter 2 reviews the literature relating to CNAs. Chapter 3 describes the new CNA path planning algorithm. Chapter 4 details the implementation of the CNA path planning algorithm using MOOS-IvP.

Chapter 5 reports on simulations in MATLAB®. Chapter 6 describes the algorithm's validation both in simulation and in-water. Chapter 7 recommends areas for future work, and Chapter 8 concludes with a few remarks.

1.2. AUVs in Mine Countermeasures

The MCM mission for AUVs may be thought of as a special case of the underwater object search mission. Non-military examples of this problem include locating shipwrecks or downed aircraft [7]. However, several aspects of the MCM mission make it distinct from other underwater object search missions. First, in some cases there may be a need to conduct MCM covertly [8]. Second, the mission must be completed rapidly, and to within a certain probability of having found all the mines,[1] to reopen ports or shipping lanes to commercial and naval vessels. Third, as much information as possible must be communicated between the AUVs and the operator so that each can adapt as the overall military mission evolves. This relates to the previous point in allowing mines to be inspected and removed or destroyed as their locations are reported to the operator by the minehunting AUVs. A high communication rate is of course desirable in non-MCM applications, but the need is more pressing in MCM since the mission must be completed in a timely fashion. Finally, accuracy is vital; the consequences of falsely concluding that all the mines in an area have been cleared could be dire.

One concept of an MCM mission conducted with autonomous vehicles is to divide the mission into three parts and assign groups of underwater vehicles to each [9, 10]. The first part of the mission, called "search-classify-map" (SCM), typically employs one or more AUVs with side scan sonar travelling in a lawnmower pattern to survey the area of interest (see Figure 1.1). These vehicles are typically envisioned as equipped with some form of automatic target recognition (ATR), also called computer-aided detection and computer-aided classification (CAD/CAC). The goal of ATR is to detect mine-like objects from side scan sonar images [11]. Prior to the use of AUVs, the side scan sonar was towed by a warship, and the sonar image was analyzed by operators in real-time. In

[1] This is often referred to as the "confidence" or "percent clearance."

the second part of the mission, called "reacquire and identify" (RI),[2] other vehicles investigate target locations transmitted (or marked with transponders [12]) by the SCM vehicles by repeatedly "flying" over the targets (typically in some form of a star-shaped pattern) to determine if the target is actually a mine. In the third part of the mission, called "neutralization," targets identified as mines by the RI vehicles are destroyed using divers, remotely-operated vehicles (ROVs), or possibly AUVs. Neutralization vehicles either plant an explosive charge near the mine or else self-destruct with the intent of destroying the mine [9]. The RI and neutralization steps were previously performed by divers, though ROVs are also used. The adaptive path-planning algorithm in this thesis primarily supports the SCM mission, but supporting the RI mission is expected to be possible. In this thesis, minehunting AUVs will be called "survey AUVs" to emphasize the relevance of a CNA vehicle outside the MCM mission.

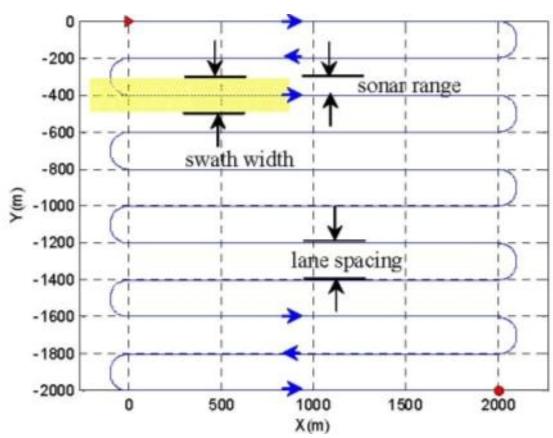

Figure 1.1: Side scan sonar lawnmower pattern (start ►, finish ●) [13]

As stated previously, the primary advantage of using AUVs for MCM is removing ships and sailors from minefields. There are, however, three main limitations when using AUVs. First, AUVs are not able to survey an area as quickly as a surface ship due to the AUVs' lower speed. For example, the Royal Navy's *Sandown* Class minehunting ships have a maximum speed of 13 kts (6.7 m/s) [14], whereas the Hydroid REMUS-100 AUV has a maximum speed of 5 kts (2.6 m/s) [15]. The speed at which either class conducts minehunting will be lower than its maximum speed, but the difference in maximum speeds is representative of the difference in minehunting survey speeds. Second, when a

[2] In some contexts, the SCM and RI missions are actually considered as a three-step process of detecting mine-like objects, identifying actual mines, and then classifying the mines by type (Manta, Rockan, etc.).

surface ship tows a sonar, the images are accessible in near real-time (via the tow cable) to the operator for analysis. Third, when a surface ship tows the sonar there is a bound on the sonar images' position error since the sonar depth and tow cable length are known (the ship's position is also known). In AUV minehunting, the sonar images are not accessible until after the AUV is recovered (though some work on sending snippets of sonar images has been done, [16]), and the position uncertainty is more difficult to bound (discussed below).

The area coverage rate, a measure of survey efficiency, could be recovered to some extent by using multiple AUVs. In addition, multiple AUVs could increase the confidence that all targets are acquired by collaborating to confirm their findings or alter their missions to re-acquire targets as necessary, possibly combining the SCM and RI steps discussed above. Such robotic cooperation/collaboration requires some level of inter-AUV communication.

The best range for underwater communications is obtained via acoustic modems. However, water has inherently low bandwidth, high attenuation, variable sound speed, and multi-path effects for acoustic signals [17-22]. This compromises reliable and long range acoustic propagation; the acoustic communication range in an ocean environment is only on the order of kilometres. This means it is not possible to transmit large quantities of data, such as sonar images, reliably or over long distances in a timely manner. ATR has the potential to reduce the required acoustic bandwidth, as the AUVs would analyze the sonar data on-board during the survey and transmit a summary to another AUV, for an RI search, or to an operator, for final confirmation on a target identity. (Communication challenges and current research are reviewed in Section 2.2.) The value of the sonar images and their subsequent target recognition analysis is related to how well targets in these images can be accurately positioned (geo-referenced). Ambiguity in a target's position means it might not be reacquired to have its identity confirmed. Thus, the requirement for accurate positioning is important in minehunting surveys.

The underwater environment has no absolute references for positioning and navigation such as the global positioning system (GPS). AUVs dead reckon for positioning and navigation using complementary measurements from on-board inertial measurement units (IMUs), Doppler velocity logs (DVLs) [18, 23-25]. (A digital compass is also typically carried.) Consequently, the dead-reckoned AUV position error grows unbounded with time [24]. The AUV can surface periodically for a GPS fix to zero its position error, but this increases the time and energy expended in the mission, especially in deep water. One way to enable more accurate positioning is to use communication and navigation buoys, but these require time to deploy (and recover, if required). Research is currently being done in simultaneous localization and mapping (SLAM) using sonar images [26]. (SLAM is a method of bounding position error by identifying landmarks and revisiting them multiple times to reduce the overall position error of mapped objects and thereby the AUV [27]. SLAM is discussed further in Section 2.3) SLAM could bound navigation error in AUV paths where the same underwater features are revisited, but would not mitigate the underwater communication challenges. Both the communication and navigation limitations of minehunting AUVs can be addressed by a CNA vehicle working cooperatively with survey AUVs.

1.3. Communication and Navigation Aid Vehicle

A CNA is a dedicated vehicle supporting AUV underwater positioning, navigation, and communication. A CNA can be a manned surface ship or an AUV or ASC. A ship as a CNA for MCM has limited effectiveness unless it enters the suspected minefield. If the ship enters the minefield, the advantage of using AUVs has been compromised, as it was stated in Section 1.2 that ships can perform minehunting more effectively (if less safely) than AUVs. Some of the literature also describes two CNAs cooperating to aid submerged AUVs [9, 28, 29].

The CNA aids communication by linking the submerged AUVs to each other (via underwater acoustic communication) and to the operator (via in-air communications), whether on a ship, aircraft or shore station. In the MCM mission, timely communication among the various naval assets involved is vital both for the rapid transition from mine detection to neutralization and for the dissemination of mission information to military commanders.

A CNA aids AUV navigation by providing the CNA's global position (from GPS) to the survey AUVs. The survey AUVs use the CNA's global position, and their position relative to it, to refine their own global position estimates. The survey AUVs determine their position relative to the CNA vehicle by use of range measurements from the CNA.[3] The CNA sends out ranging pings, and the one-way travel time (OWTT) of the ping is measured by all survey AUVs simultaneously, allowing them to calculate their ranges from the CNA (given a measured or assumed speed of sound in water) [30]. The variance of OWTT range measurements has been reported as 3 m in [26]. Over time, the survey AUVs can filter several range measurements (in combination with their onboard sensors such as compass, DVL, and IMU) to establish their own exact position. This process is called cooperative navigation in [31]. Cooperative navigation is simplified if the original position of the survey AUVs is known, e.g. a GPS fix before submerging [29]. In [32], it was stated that range measurements from the CNA will reduce the survey AUV error along the line between the survey AUV and the CNA vehicle, but not in the direction perpendicular to that line, forming the yellow-green ellipse in Figure 1.2 from the larger, unaided, blue ellipse. Therefore, the most desirable location for the next range measurement would be along this perpendicular direction, as stated by [33, 34] and achieved in [31] by using two CNA vehicles in a right-angle formation with a single survey AUV. Similar work was done in [10]. However, with a single CNA vehicle, the optimal next position may not be physically achievable, especially considering the possibility of multiple survey AUVs all needing to be aided. Changing the survey AUVs' paths may be possible in some applications, but in the MCM AUV application, the path of the survey AUV is important to achieving an acceptable level of confidence that all mines in a certain area have been detected with the side scan sonar and ATR process. Thus the problem that this thesis addresses is that of finding the best achievable path for the CNA vehicle to follow in order to minimize the position error for the submerged AUVs.

[3] The use of bearing or bearing and range measurements is also found in the literature [114], but range-only is most common.

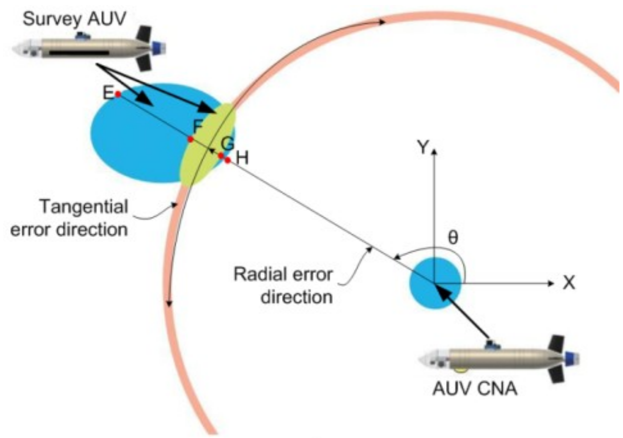

Figure 1.2: Bounded survey AUV position error, adapted, [32]

The use of a CNA vehicle is potentially more time efficient than localization methods where the survey AUV either periodically surfaces for its own GPS position or employs a field of communication and navigation buoys. Consider an AUV surveying at 100 m depth and travelling at 1.5 m/s, unaided by either a field of buoys or a CNA. Assuming that the AUV dives and surfaces at a pitch angle 30° from horizontal, either manoeuvre will take approximately 2 min. The time required to collect an accurate GPS fix may be as much as 5 – 10 min. During this time, the survey AUV will be too far from the ocean floor to collect sonar data. AUV positioning uncertainty is frequently reported as a fraction of distance travelled. In this thesis, the desired maximum error is considered to be a 10-m ellipse in order to minimize the time required to require and identify targets located by survey AUVs. If the positioning error is 0.1% of distance travelled (reported for the very expensive Kearfott T-24 and IXSEA PHINS III inertial navigation units, INUs [35]), a survey AUV would have to surface every 1.9 hrs. Assuming that a surfacing manoeuvre takes 10 m, in an 8-hr mission, the survey AUV would spend a total of 40 min in collecting GPS fixes, 8% of the mission. In many cases this may be acceptable, but what if the survey AUV has more modest internal navigation sensors and, like the Iver2 AUVs used in this thesis, has a positioning error of 0.5% of distance travelled [36]? Now the survey AUV must surface every 22 min for a total of 150 min in an 8-hr mission, or 31% of the mission. In this case, the support of a CNA vehicle would considerably increase the efficiency of the minehunting survey since 0% of the 8-hr mission will be spent surfacing for a GPS fix. A field of communication and navigation buoys could provide similar benefits in terms of improved navigation, but a single CNA vehicle would take less time to deploy and recover than a field of buoys and can manoeuvre to the optimal location for cooperative navigation based on the path of the survey AUVs.

In addition, a single CNA can aid multiple AUVs at one time. When a CNA aids multiple AUVs, the overhead of using a CNA is reduced. For instance, if a CNA supports one AUV, half of the autonomous vehicles deployed are not actually performing the mission (e.g. side scan sonar survey for mines), but if a CNA supports four survey AUVs, the overhead is reduced from 50% to 20%.

Chapter 2 Literature Review

The literature review begins by addressing broad areas of AUV research, namely multiple-vehicle operations, communication, and navigation. Next, literature addressing a CNA vehicle will be reviewed. As mentioned in Section 1.3, the CNA vehicle is a solution to communication and navigation limitations in multiple AUV operations. It is not, however, the only option, and some alternate options are also discussed.

2.1. Multiple-Vehicle Operations with AUVs

Much current research in unmanned vehicles involves the use of multiple vehicles and frequently involves heterogeneous vehicles. Sometimes these heterogeneous vehicles are different autonomous vehicle models of the same type (e.g., REMUS and Bluefin AUVs) [37, 38], but in other cases the vehicles are of different types. Examples of this include ASCs with AUVs [10, 29, 31, 38-44]; ASCs with Unmanned Aerial Vehicles (UAVs) [44-46]; AUVs with UAVs [47]; and UAVs with uninhabited ground vehicles [48]. Some of the work cited above deals with the CNA concept introduced in Section 1.3. Research on this topic will be reviewed in more detail in Section 2.4. Most multiple-vehicle operations require some form of inter-vehicle communication. As mentioned in Section 1.2, the best communication with submerged AUVs is achieved through acoustic modems.

2.2. Acoustic Communications Research

Underwater communication is probably the single biggest obstacle to effective multiple-AUV operations. Because most radio frequency (RF) signals have very limited range underwater as do optical signals, underwater communication is best achieved acoustically.[4] There are many ways in which underwater communications can break down. Eadie and Mace [49] identify low data rates, high error rates, and blackout as possible communication problems in the perpetually turbulent very shallow water (VSW) and in the surf zone (SZ). Desa, Madhan, and Maurya [25] also report that multi-path effects caused by stratified upper water layers and the water surface inhibit acoustic

[4] Though Ludwig [113] does note that in extremely shallow water an AUV could use a surface piercing antenna for RF communications.

communication in the VSW/SZ. The VSW/SZ is at the most shallow end of the littoral water area where AUV minehunting is considered.[5] Various coding schemes to increase data rates have been attempted including a multi-chirp acoustic communications system that mimics the chirping communication used by bats and dolphins [50]. Increasing acoustic data throughput underwater will remain an active area of research for some time.

2.2.1. Acoustic Communications Literature 2000 - 2005

Yuh [18] reviews the state-of-the-art underwater communication and navigation technology in 2000. He reports that an acoustic modem had been developed with 1,200 baud, capable of sending video at very short range. Yuh also mentions modems capable of 500 kbps (at 60 m range), but none of the modems he reviews can communicate further than 5 km (6.5 km in the vertical direction for one modem). The 5-km range modem has a rate of 5 kbps.

Using a REMUS AUV with a Utility Acoustic Modem (UAM) in very shallow water (three to eight metres), Freitag [17] reports that in spite of multipath spanning and high noise levels, his group was able to achieve communication rates of 60-5000 bps. This was done reliably at ranges as great as 5 km. Freitag et al. use a 32-byte AUV status message; this continues to be the most common length for acoustic communication messages with AUVs.

Von Alt et al. [51] describe their work on the REMUS 100 AUV that applied to MCM, focussing on the communications aspect of AUV operations. They discuss the concept of an underwater docking platform connected to a shore-based operator by a fibre optic link or a buoy with a satellite or radio link. If having a buoy constantly on the surface is undesirable, the buoy could be placed on a winch and only raised to the surface at specific transmission times. The platform would be used for recharging vehicles, downloading data, and uploading new missions. Other equipment includes a towed transducer called RANGER, available to send command signals such as “return home” and to provide emergency tracking; and PARADIGM, which employs two-channel acoustic communication from small buoys. One channel is used to help the REMUS

[5] Littoral waters are divided into four zones (surf zone, very shallow water, shallow water, and deep water) in [3].

navigate while the other allows the operator to track the AUV. Von Alt et al., report that WHOI is working on a way to integrate PARADIGM with an acoustic modem to allow the AUV to send sensor data to the operator and the operator to send mission commands to the AUV. This would appear to be the basis of at least some of the work reviewed in Section 2.2.3.

According to Marr and Healey [19], stationary acoustic communications in shallow water can achieve rates of 20 kbps but, referring to [52], shallow water communication at ranges of hundreds of meters between moving vehicles is limited to 1.2 kbps. However, Marr and Healey conducted multiple experiments in the waters of Monterey Bay, and concluded that reliable communications ("nearly 100% reliability") could be achieved at almost 300 metres with maximum rates of just 0.8 kbps [19]. On the other hand, [22] reports that the average data rate "operationally" is actually 10-50 bps. Also, four years before [19], rates of 60-5000 bps were possible at ranges of 5 km [17]. Beyond the hardware used, there are a myriad of possible environmental factors that may cause this discrepancy. It should be remembered that no matter the data rate, there will be times and situations where no communication is possible (blackout) and any fielded minehunting AUV solution must be able to handle this situation.

2.2.2. Rajala et al., 2005 - 2009

Rajala, Edwards, and O'Rourke consider the situation of a formation of AUVs hunting for mines with one AUV acting as leader [53]. The focus of their paper is how to determine when an AUV in the formation needs to be replaced due to a failure and what to do if the decision to replace the AUV was mistaken (i.e. a communication blackout was falsely interpreted as AUV failure). Rajala, Edwards, and O'Rourke simulate a spherical transducer so that all vehicles could hear the messages but only one vehicle can transmit at a time. This communications simulation uses a 32-byte message. They establish a communications procedure whereby each vehicle is able to transmit on a five-second interval (that is to say, the communication cycle is 5 sec × the number of AUVs). AUV formations may not be optimal in cases where there is a reasonable probability of an AUV setting off a mine because of the risk of destroying multiple AUVs with a single mine detonation. However, correctly identifying the need to replace an AUV is also important in decentralized AUV minehunting. Rajala, Edwards, and O'Rourke discuss the need to prioritize lists of messages waiting to be sent by an AUV (as has been done in [38]). They also use a fuzzy logic controller to make the determination using obstacle locations and local communication environment.

The work by Coleman et al. [20] is unique because it uses a Design Failure Mode and Effects Analysis (DFMEA) approach to communication failure underwater. DFMEA is an objective evaluation of possible ways a design can fail and the effects of these failures [54]. Two challenges to communication identified by Coleman, et al., are propagation effects (including multipath and ray bending) and restricted data rates. Data rates are restricted in acoustic communication because more energy is absorbed by the water at higher frequencies than lower frequencies [20, 55]. Coleman et al., identify three possible communication failure modes. An AUV can fail to send a message when it should, send a message when it should not, or send a message with errors (wrong information, incomplete information, or garbled information) at the right time. Of these failure modes, Coleman et al. rate the sending of wrong information at the right time as the most detrimental to the mission. They state that the strict communication protocol that they have developed should keep miss-timed communications quite rare.

Further work by Rajala, Edwards, and O'Rourke [56] expands on the underwater communications and lost vehicle decision topics. Their work includes an AUV communication language called *AUVish.* They report that they are working on a 13-bit micro packet available on the WHOI modem rather than the current 32-byte packet. At the time of writing, Rajala, O'Rourke, and Edwards were designing logic to deal with corrupted messages (though they report that the WHOI modem does not allow access to corrupted messages).

Another paper by Rajala and Edwards [57] deals with the need for each minehunting AUV to have a complete map of the underwater area. Because of the limited communications bandwidth, map information is difficult to transmit between vehicles, but every vehicle needs a complete map due to the possibility of any number of AUVs failing. Their solution to this problem is to divide the map into cells and give each cell a value from 0 to 5 to indicate the cell contents (no information, clear, unidentified obstacle, non-lethal objects, lethal objects, dangers to AUVs). They suggest that the accuracy lost by dividing the map into cells is not significant in light of the navigation error experienced by AUVs. However, the size of the cells is not specified.

Johnson et al. [58] advocate maintaining both a low and a high-resolution map on each AUV. The low-resolution map is updated more frequently than the high-resolution map. The maintenance of maps on each AUV limits the amount of data to be lost should an AUV be lost. Maintaining two maps on each vehicle reduces the probability of losing much data with the loss any one AUV. Johnson et al. have a 30-second communication cycle capable of handling a formation of five AUVs (one of which is designated as the leader). The communication cycle uses both the 13-bit and 32-byte messages and provides for queries to long baseline navigation beacons (discussed in Section 2.3). The 13-bit messages contain information about the AUV's location, the location of mine-like objects, and which other AUVs the AUV has heard from (using a "connection vector"). It is used to update the low-resolution map. If an AUV has not been heard from by any member of the formation for two communication cycles (1 min), the AUV is declared to be inactive or lost by the remaining AUVs [58]. This is in contrast to the fuzzy logic controller proposed previously by Rajala, Edwards, and O'Rourke [53] and seems like a very low threshold given the acoustic communications experience from this thesis. When a vehicle is declared to be lost, the area from just behind to just ahead of the AUV's last known position is declared to be a dangerous area [58]. The 32-byte message is used to maintain the high-resolution map containing the locations of mine-like objects (MLOs). MLOs are referenced to 5 x 5-m grid squares on the high-resolution map rather than absolute coordinates. While this does reduce the accuracy of the map, Johnson et al. do not believe that this map accuracy is significantly reduced when compared to the achievable AUV navigation accuracy. Johnson et al. also consider the possibility of the same MLO being located multiple times in slightly different locations and therefore being incorrectly identified as multiple MLOs. They state that this is an acceptable error since it is better to overestimate the number of MLOs in the water than to underestimate it. In addition, Johnson et al. express a belief that post-mission processing of the MLO location data would be able to identify which MLOs are in fact incorrectly identified as multiple

MLO's. This ignores the possibility of a burdensome number of MLO contacts identified by the AUVs. In [59], these "false alarms" are actually discussed at length. A large number of false alarms would make it difficult to complete the RI and neutralization steps in a timely manner. In the 32-byte message described by Johnson et al., only the MLO locations are transmitted. Johnson et al. state that additional information could be transmitted (such as the type of MLO), but just as by transmitting a grid reference rather than an absolute reference, transmitting the minimum of information allows for more MLO locations to be transmitted in a single message. This paper's chief contributions are the use of different message sizes, the proposed communication cycle, and the use of the "connection vector" in deciding when to declare an AUV inactive or lost.

2.2.3. Stokey et al., 2005

The Compact Control Language developed by Stokey et al. [16] works with a large variety of AUVs and display systems in addition to WHOI-developed AUVs and systems. The WHOI Micro-Modem allows for time-division multiple access (TDMA) communication on a master-slave polled system or a random peer-to-peer system. If the message traffic is light, the two systems can apparently be used during the same mission, although "light traffic" is not defined. Stokey et al. report that 16 addresses are available using the WHOI Micro-Modem. This is expected to be more than sufficient for most multi-AUV applications. Using the WHOI Micro-Modem, each AUV can receive and process every message sent (whether or not it is an addressee). This allows an AUV to maintain situational awareness, particularly awareness of message traffic density. Stokey et al. describe what they consider to be a typical communication cycle, which is based on a central communications node (such as a communications buoy) sending commands from the human/computer controller to multiple AUVs but also provides for communication among the AUVs as peers (the buoy acts as a relay). Two communications cycle innovations by Stokey et al. include the use of an acknowledgment message and an event-driven message. The acknowledgement can inform the controlling agent that a command message has been received. The event-driven message takes advantage of the random access option on the WHOI Micro-Modem to send high priority messages that cannot wait for the AUV's scheduled turn to transmit. Users can create custom messages or use messages that have been constructed previously. Messages are usually sent in the minimum possible packet size for a WHOI Micro-Modem (32 bytes), but larger packets are possible. In 1999 tests, REMUS vehicles using the Utility Acoustic Modem were able to communicate with an over-the-side acoustic receiver on a surface ship; at a frequency of 15 kHz, a range of 4 km was possible. Also in 1999, the Utility Acoustic Modem was used to send compressed pieces of side scan sonar images in real time to a base station. This capability allows an extra-vehicular agent (or operator) to examine the image and determine if an MLO is in fact a mine (very useful given the sometimes large computational load of ATR programmes [60]). Finally, Stokey et al. report that the compact control language has been used during US-Navy-sponsored MCM exercises to aid in searcher/investigator collaboration missions [16]. These missions are similar to the concept of operations presented in Section 1.2. The Compact Control Language is an important contribution to multiple-AUV operations. The work of Stokey et al. was the basis of work by Schneider, discussed in Section 2.2.7.

2.2.4. Perrier, Brignone, and Drogou, 2007

Perrier, Brignone, and Drogou [43] consider the case of multiple unmanned marine vehicles operating on and below the surface. In characterizing the challenges of underwater communication, they state that bandwidth is typically confined to "a few tens of bits/sec up to a few kbits/sec." They list four objectives for communication aiding multi-vehicle operation in order of increasing complexity (navigation, task coordination, mission control, and human supervision). Perrier, Brignone, and Drogou also present four communication configurations above water only (radio or satellite), below water only (acoustic), above and below water simultaneously, and above or below water singly (the vehicle is capable of both, but can only perform one at a time) [43]. While it would seem obvious that an ASC or a surfaced AUV could simultaneously send or receive both above water communications (since they are on the surface) and acoustic communication (since at least part of the vehicle remains in the water), an AUV with its acoustic modem mounted on top of the hull (possibly useful for communication when close to the ocean floor) may not be able to communicate acoustically from the surface. Even a surfaced AUV with its acoustic modem mounted below the hull may have trouble communicating acoustically if it is moving quickly or being bounced by waves. Perrier, Brignone, and Drogou discuss communication for positioning in a way that leads one to consider a CNA vehicle. They suggest that a ship or ASC could provide AUVs with an absolute position via long baseline (LBL) or ultra-short baseline (USBL) navigation (refer to Section 2.3 for discussion of acoustic navigation techniques). This could lead to a moving LBL navigation technique proposed in [28], which is considered the basis of much of the later CNA work [29]. They also suggest that AUVs might aid each other to improve their navigation accuracy using range and possibly bearing measurements between vehicles based on acoustic message travel time. This was later done in [61]. Perrier, Brignone, and Drogou present many ideas which other researchers have also used in their work.

2.2.5. Kunz et al., 2008

Working in the Arctic Ocean, Kunz et al., appear to have been able to communicate between their command ship and their AUVs at ranges of seven to ten kilometres [21]. To accomplish this, they used frequency-shift keying (FSK) between 8 and 12 kHz on the AUV's WHOI Micro-Modem. The maximum bandwidth was found to be 80 bps using either 32-byte packets or 13-bit "mini-packets." Because the modem was being used for both navigation (by LBL, see Section 2.3) and communication, Kunz et al. typically used a 90-second communication cycle (a TDMA cycle) to coordinate use of communication packets. Each TDMA cycle allows for a 32-byte packet to be sent from both the ship and the AUV and for three interrogations of the LBL navigation network. Thus the effective bandwidth for AUV-to-ship communication is only 3 bps (presumably the same for ship-to-AUV communication). While communication from the AUV happens during each TDMA cycle (sending a location estimate, information on the mission goal, and the most recent sound travel times for the LBL navigation), the ship only communicates with the AUV to send it waypoints to a hole in the ice so that it can be recovered through it [21]. It should be noted that the communication range achieved in the Arctic may be impossible in other areas of operation due to the higher levels of ambient noise and possibly poorer propagation conditions outside the Arctic.

2.2.6. Driscoll et al., 2005 - 2006

Florida Atlantic University (FAU) has developed an air-droppable navigation and communication buoy for use with AUVs [62, 63]. This buoy is equipped with both a WHOI micro-modem and an FAU Dual Purpose Acoustic Modem (DPAM), and these two modems can operate "simultaneously." Using a combination parachute and anchor along with an intelligent mooring spool, the buoy can remain moored on most bottom types in up to sea state 3 (waves between 0.5 m and 1.25 m) and 3-kt currents in water depths of 5 m to 200 m. Above water, the float is designed for mounting GPS, radio, and satellite antennas. The WHOI and FAU acoustic modems can provide communication between AUVs and the surface (by connecting to the above water antennae) as well as provide LBL and USBL navigation for the AUVs [62]. As such, it represents a complete communication and navigation solution for multiple-AUV operations. It has some drawbacks as discussed in Section 2.4.10. The acoustic modems were able to communicate at ranges up to 3 km at rates up to 860 bps, although 72 bps was found to be most reliable [62].

2.2.7. Schneider and Schmidt, 2010 – 2011

Building on [16], Schneider and Schmidt developed the communications system used in this thesis for use with MOOS-IvP and the WHOI Micro-Modem. The WHOI modem, in their usage, is able to run at 20 bps (low rate) up to 2,000 bps (high rate) [38]. As discussed above, environmental conditions affect communication reliability. Schneider and Schmidt state that the higher rates are more sensitive than lower rates [38]. They also state that reliability can change through the day, it is affected by vehicle orientation and modem mounting position, and it is most difficult in very shallow water (approximately 20 m depth). They state that in shallow water they lost communications for "tens of minutes … especially at ranges of more than several hundred meters." In deeper water (100 m) they were able to send data at 2,000 bps at ranges up to 1.6 km. Their recommendation is to alternate between low- and high-rate transmissions to maximize data transfer while ensuring that some messages will get through [38]. The work of Schneider and Schmidt is reviewed in more detail below because their communications process was employed on AUVs used for trials in this thesis. The version of *pAcommsHandler* (MOOS-IvP process developed by Schneider) described in [64] has three TDMA medium access control (MAC) modes, centralized (polled by master modem), decentralized (assigned slots), and decentralized with automatic discovery of new modems. It appears that the version of *pAcommsHandler* installed on the AUVs used in this thesis is slightly older and only supports decentralized control with automatic discovery. The result is a slightly slower than needed communications cycle due to a silent period to allow new "nodes" to join the cycle. (Nodes will typically be AUVs or ASCs, but may also include a modem suspended from a support ship.) A new version of *pAcommsHandler* has recently been released. Among other improvements, it uses Google Protocol Buffers instead of XML files for defining acoustic messages [65]. Perhaps future releases will use some WHOI Micro-Modem features described by other authors but not used to date in *pAcommsHandler*. These features include the 13-bit message [53] and the transmission of sonar image snippets [16].

The major contribution of Schneider and Schmidt is the Dynamic Compact Control Language (DCCL) and their method of queuing multiple messages based on importance and time sensitivity [66]. DCCL uses the Extensible Markup Language (XML) to encode data to save message space (e.g. a float numeral with no decimal places takes the same space as an integer of the same value). Also, unlike the Compact Control Language, DCCL's XML messages do not require rebuilding of the source code in order to implement a new message. Messages can be sent in packages of 32, 64, or 256 bytes and can be encrypted using the open source Crypto++ [66]. Messages of smaller sizes can be combined into larger packages and sent at the same time [64]. This is in addition to queuing messages as mentioned above. Finally, Schneider and Schmidt developed a user interface called *iCommander* where the operator can manually specify values for an XML message to be sent by the WHOI Micro-Modem [66]. This interface is typically used for issuing commands to the autonomous marine vehicles (such as "begin mission" or "stop mission and return"), but can also be used to send autonomous marine vehicles simulated data (such as target locations) in trials. DCCL and its associated components, *pAcommsHandler* and *iCommander,* have proven to be reliable and fairly easy to learn.

2.2.8. Plueddemann et al., 2012

Plueddemann et al. [67] report on the use of a lightweight AUV under the Arctic ice. For recovery, they modified a REMUS 100 AUV to use USBL homing towards a net suspended below a hole cut in the ice. A hook attached to the AUV grabs the net so the AUV can be recovered. During preliminary tests, it was discovered that 25 kHz acoustic ranging system had a maximum range of 2.5 – 3.5 km. Given that there was very little variation in the underwater speed of sound in the trials area, it was decided to use a lower frequency (10 kHz) ranging system. The benefits of the lower frequency were lower sound absorption (approximately 2 dB/km) and reduced scattering (both off the bottom and the underside of the ice). In actual trials with the maximum range was only 1.25 km as ice conditions “precluded determination of the maximum range of the 10-kHz acoustics,” [67]. While it was noted in [67] that lowering the acoustic frequency would increase the achievable range, it should be remembered that lower frequency transducers are larger and require more power than higher frequency transducers, limiting the acoustic frequencies that can be used on small AUVs.

2.2.9. Conclusion

This section has reviewed acoustic communication environments, rates, ranges, languages, and implementations. Given the literature (summarized in Table 2.1), it would appear that 2 kbps at 1.6 km should generally be possible. Using the WHOI Micro-Modem on the Iver2 AUVs, a TDMA communication cycle time of approximately 15 sec per vehicle was observed. Messages of 32 bytes were sent using Schneider’s *pAcommsHandler*. Messages were exchanged at a maximum range of just over 1 km.[6] Fixed underwater docking stations could be used as communications aids in addition to providing charging capabilities, but they would be hard to move at short notice due to their size and weight. The use of a communications buoy has many advantages, and the air-droppable version described in [62, 63] has more flexibility than most. There remains, however, a distinct advantage to using an autonomous marine vehicle (surface or subsurface) as a communication (and navigation) aid since it can adapt its path to the path of multiple AUVs.

[6] To date a maximum achievable range has not been established with the DRDC(Atlantic) Iver2 AUVs. The distance reported is merely the maximum range observed during trials of the path planning algorithm. According to [97], the maximum range of the WHOI Micro-Modem (used on the Iver2 AUVs) is 2-3 km in the open ocean.

Table 2.1: Summary of acoustic communication rates and ranges from the literature

Frequency	Range	Data Rate	Year, Source
-	60 m	500 kbps	2000, [18]
-	6500 m (vert.)	16 kbps	2000, [18]
-	5000 m	5 kbps	2000, [17, 18]
-	300 m	0.8 kbps	2004, [19]
15 kHz	4000 m	-	1999, [16]
8-12 kHz	7000 -10,000 m	0.08 kbps	2008, [21]
-	3000 m	0.072 – 0.86 kbps	2006, [63]
25 kHz	1600 m	0.02 – 2 kbps	2011, [38]
25 kHz	3500 m	-	2012, [67]
10 kHz	>1250 m	-	2012, [67]

2.3. AUV Navigation Research

In order to be useful, minehunting AUVs must be able to detect mines (usually with sonar) and indicate to the operator (through some form of communication) the location of the mines so that the mines can be avoided, removed, or destroyed at the commander's discretion. Locating mines requires the minehunting AUV to have an accurate idea of its own position at all times. If the AUV is not able to effectively navigate because it's positioning accuracy is too low, it is essentially useless for minehunting operations. Navigation systems discussed in this section include acoustic homing, inertial navigation, geophysical navigation, and GPS.

2.3.1. Theseus and Explorer AUVs, 1997 - 2011

During the early and mid 1990's, Canadian defence scientists worked with ISE Research Ltd. on the navigation system for a nearly 9,000 kg [68] AUV called *Theseus*. *Theseus* was designed to lay cable under sea ice in the high Arctic. *Theseus'* first mission was 175 km each way; a second mission of 160 km each way was also run [69]. Most of the navigation was done by dead-reckoning with velocity-aided inertial navigation (laser-ring gyro), but terminal navigation and position fixes along the route were provided by acoustic homing beacons. Depth and altitude in the water was obtained from a pressure transducer and sonar. In total, four navigation systems were employed (inertial navigation system, Doppler sonar, pressure transducer, and acoustic homing) [69]. Acoustic transponders were deployed on ropes through the ice at important locations to allow for acoustic homing. Results from the testing of these acoustic homing beacons are presented in [70]. During the first mission, a navigation accuracy of 0.5% of distance travelled was achieved. Results for the second mission were not stated [69]. Recently, Canadian scientists have been operating the smaller *Explorer* AUVs in the high Arctic, collecting data for Canada's submission to UNCLOS in 2013 [71, 72]. Work on the *Theseus* and *Explorer* AUVs represents state-of-the-art on-board navigation aided by stationary acoustic beacons. This is not a complete solution for MCM because the on-board navigation systems are expensive, and (as will be discussed in Section 2.4) stationary beacons have limitations (particularly, mobility).

2.3.2. Stokey et al., 1999 - 2005

In 1999, Stokey and Austin published a paper on LBL navigation for the REMUS 100 AUV [73]. The primary contributions of this paper are a discussion of sources of error in acoustic navigation and the author's method of accounting for AUV motion during acoustic transmissions for LBL navigation. The sources of error fall into two categories, errors caused by variations in the speed of sound (due to changes in salinity or temperature) and errors caused by geometry. Geometry errors include moving parallel to the baseline between the two transponders (which can be eliminated by using a third transponder) and, under certain conditions, having the vehicle located on the baseline, as some errant range measurements will result in the inability to calculate a position. The author's method of accounting for AUV motion during an LBL update is to use dead reckoning (preferably with DVL, but with propeller revolutions when this is not possible). Because the time interval is short, the dead reckoning error (even using propeller revolutions) should be small.

Stokey et al. [74] present results of navigation system trials with the REMUS 600 AUV[7]. Their REMUS 600 has a Kerfott KN-4902 INU integrated with the standard REMUS LBL navigation system. The REMUS 600 measures altitude and speed over ground with its acoustic-Doppler current profiler (ADCP). (Typically, speed over ground, altitude, and local ocean currents are all measured with the same acoustic device. In determining speed over ground and altitude, this device is typically called a DVL. In determining local ocean currents, this device is typically called an ADCP. Stokey et al. [74] here differ somewhat from what appears to be the convention). GPS fixes are available through the

[7] The numbers used to designate REMUS AUV models indicates the AUV depth rating in metres.

AUV's mast when on the surface. Using the INU, the AUV ran for twenty minutes between position fixes and the errors were approximately 3 or 4 m, the same order of magnitude as the GPS being used to track the error [74]. The vehicle speed was not stated. Stokey et al. recommends LBL navigation for near shore operations rather than using sophisticated (expensive) INUs and surfacing periodically. Their reasons are the time involved in surfacing for GPS fixes and the danger to the AUV posed by surface craft [74].

2.3.3. Other Underwater Navigation, 1998 – 2005

Leonard et al. [24] review the 1998 state-of-the-art in AUV navigation techniques. They cite three methods of AUV navigation: dead-reckoning and inertial navigation, acoustic navigation, and geophysical navigation (including concurrent mapping and localization). Their review of these methods is discussed below.

Leonard et al. regard dead reckoning and inertial navigation as the most established and obvious method of AUV navigation but with two major drawbacks. First, high performance inertial navigation systems cannot be placed in small AUVs because of the cost, power, and space requirements. Second, ocean currents near shore (where minehunting AUVs would work) "can exceed 2 kts" [24]. With AUV speeds rarely greater than 6 kts, position estimates are frequently poor [24], although inertial navigation can still be an attractive option for some AUVs. The use of an acoustic device called a DVL can give an AUV velocity over ground when it is operating within range of the bottom. When combined with the inertial navigation system (INS) in a Kalman filter, DVLs can produce significantly improved navigation results [24]. For instance, DARPA's[8] UUV[9] had a navigation error of "0.01% of distance traveled using an integrated INS/DVL system,"[10] though the position error increases with distance travelled without bound [24]. The rate of increase is determined by ocean currents, AUV speed, and the quality of the navigation sensors. The error can be reduced by having the AUV surface periodically to get a position fix with radio or satellite navigation systems (presumably GPS in most cases) with the maximum time between surface position fixes

[8] Defense Advanced Research Projects Agency
[9] Unmanned Underwater Vehicle
[10] [24]. However, the source that they cite [8] indicates an error of nearly 0.02%.

determined by the accuracy of the dead reckoning or inertial navigation system. Three problems with frequent surfacings for position fixes are the danger of collisions with shipping, the inability to surface if operating under the ice, and the time and power required to surface when working in deep water [24].

Leonard et al. discuss two primary acoustic navigation systems, LBL and USBL. Long baseline navigation uses an array of beacons whose deployed locations are surveyed. The AUV "pings" the beacons, and the beacons each respond with a ping. The vehicle determines its position using the known location of the beacons and the time of travel of each beacon's ping using an assumed or measured local speed of sound. Two techniques employed to localize the AUV are calculating the intersection of the spheres whose radii are the distances from the beacons to the AUV and integrating the sound time-of-flight from the beacons with a Kalman filter. In environments where there are multipath acoustic effects, identifying the false returns from the beacons is important. With the sphere calculation method [24], incorrect distances can be ruled out, and if using the Kalman filter, a gate can be placed on the time-of-flight values to eliminate the errant data. Hyperbolic navigation is a variant of LBL navigation where the AUV does not ping (interrogate) the beacons, but instead listens for the beacons to transmit in their specific sequence and at their designated frequencies. Thus, the AUV knows which beacon it is hearing and is able to combine the time-of-flight with the location of the beacon to determine its own position. The main advantage of hyperbolic navigation is that the AUV can localize itself without the power expenditure of pinging the beacons as in standard LBL navigation. Leonard et al. report that hyperbolic navigation works well for multiple AUV operations [24]. Typically, LBL systems operate at 10 kHz where the maximum range is a few kilometres and the accuracy is in the order of a few metres. However, some systems operate at 300 kHz and are accurate to as little as 1 cm, though the operating region is reduced to a triangular area 100 meters on each side [24].

USBL navigation is a variation of a system used for tracking underwater vehicles from a surface ship and is used for local AUV navigation, especially homing and docking. USBL navigation uses an array of receivers on the AUV and a single beacon in the water. The difference in arrival times to the receiver array elements from a single beacon ping is used to determine the bearing from the AUV to the beacon. The distance to the beacon can be determined if the beacon will respond with a ping to an interrogation from the AUV (allowing the round-trip travel time of the sound to be measured). Thus the AUV can calculate both distance and bearing to the beacon [24].

With both LBL and USBL navigation, the primary sources of error are the location of the beacons and the assumed local speed of sound, for which Leonard et al. presents mitigation techniques [24]. Navigation errors caused by uncertainty in the sound speed profile overlap somewhat with problems in acoustic communication described in Section 2.2. An inaccurate estimation of the sound speed profile will result in a bias in the calculated distance. In addition, multipath and reflection errors will yield errant time-of-flight values, giving erroneous positions. Leonard et al. report that LBL navigation works well in deep water when the beacon array covers only a few kilometres. However, in shallow water and at larger distances, complex propagation effects can increase the rate of errant position fixes. In areas where the bottom has dramatic topographic features, the AUV may find that it is unable to communicate with one or more beacons at times during the mission. Finally, the sound speed profile is subject to change during the mission [24]. Leonard et al. cite Deffenbaugh on long-range LBL navigation in dynamic acoustic environments, especially in the Arctic.[11] Leonard et al. discuss estimating the sound speed profile with acoustic tomography and how acoustic tomography, navigation, and communication are inter-related [24]. Acoustic tomography is the use of "travel time information between one or more vehicles and vertical hydrophone arrays to estimate the sound speed profile … at various places in the intervening water column" [24]. Using an AUV for acoustic tomography requires the AUV to have a precise navigation estimate. The propagation paths to each hydrophone also need to be traced, and these paths are needed for effective acoustic communication [24]. However, acoustic tomography does not appear frequently in more recent literature.

Leonard et al. also discuss three techniques of geophysical navigation: geomagnetic, gravitational anomaly, and bathymetric. The basic concept of geophysical navigation is to use the AUV's sensors to match its current position with a location on a database map.

[11] [24] referencing [116] and [117]

The advantage of geophysical navigation is its independence from a deployed array of beacons such as those used in LBL navigation. The two main disadvantages are the time and expense of developing the database maps and the computational cost of matching the AUV's present location and orientation to the database map. Geomagnetic and gravitational anomaly navigation are two novel geophysical navigation techniques presented by Leonard et al. The earth's magnetic flux density varies with latitude and ocean depth in addition to natural and man-made anomalies. Small and predictable variations between day and night also occur in the magnetic flux; however, large changes caused by magnetic storms can make magnetic maps useless for the duration of the storm. Leonard et al. cite several authors who have implemented bathymetric navigation on AUVs.

In the absence of a recent, high quality bathymetric map, concurrent mapping and localization (CML) becomes an attractive option [24]. CML, now more commonly known as SLAM, is an active area of AUV research [26]. The other forms of geophysical navigation discussed in [24] do not appear frequently in the research, though they are discussed in [75]. Dead reckoning, inertial navigation, and LBL and USBL navigation are regularly used in AUV operations today.

Fulton and Cassidy [76] discuss the fusion of navigation data to obtain a position fix using an extended Kalman filter (EKF) on an AUV. Their AUV uses a compass, DVL, and LBL navigation. LBL navigation suffers errant range readings due to acoustic multipath effects, errors in signal processing, and the noise of the vehicle itself. To compensate for this, Fulton and Cassidy's EKF uses two forms of outlier rejection to prevent the introduction of errors in position estimation from poor range measurements. Time domain gating determines if a sensor measurement is accurate to within some threshold and rejects the inaccurate measurements. Spatial domain gating determines if a computed position fix is accurate and rejects the inaccurate positions fixes. Fulton and Cassidy include the results of several simulations (using data collected on two different REMUS 100 AUV trials) as well as their Kalman filter parameters. At the time of writing, Fulton and Cassidy were working to implement their filtering algorithm on a real AUV [76]. In [29], it is argued that Kalman filtering is not optimal for acoustic range measurements due to the (incorrect) assumption of Gaussian noise and the subsequent long-term bias caused by outlier range measurements. The outlier rejection in [76] seems to be satisfactory (position error held to a 10-m radius when proper gating used), and it is unfortunate that this outlier rejection on an EKF was not compared to the cooperative navigation algorithm discussed in [29].

2.3.4. Le Bouffant et al., 2005

Le Bouffant et al. [77] present an automatic mission control system for a minehunting AUV including Concurrent Navigation and Mapping (CNM, like CML now known as SLAM). Le Bouffant et al. begin by defining "short-term navigation" as "absolute geographical positioning" based on inertial navigation, sonar, and other positioning systems combined with state estimation techniques like Kalman filters. They state that short-term navigation can be as accurate as 2% to 5% of the distance travelled. According to Le Bouffant et al., the advantage of SLAM over short-term navigation is that the AUV does not need to surface for GPS fixes; this they mention is important when the AUV cannot or must not surface such as during under-ice or covert operations [77].

A second advantage of SLAM is that it uses terrain landmarks to find the relative position between landmarks and between the AUV and these landmarks (whether they be rocks, inert man-made objects, or mines) while keeping their absolute positions available. Le Bouffant et al. claim that this makes the relative positioning of objects independent of the AUV's position and therefore independent of time [77]. Le Bouffant et al. apply, in simulation, SLAM to two scenarios, surveillance and exploration. Surveillance works from a database map containing known underwater objects while the object of exploration is to build a database map [77]. The purpose of surveillance is to update the database map with new objects and remove old objects that are no longer present. SLAM has the potential to solve some underwater navigation problems, especially on vehicles equipped with side scan sonar for minehunting missions. However, there are some drawbacks to SLAM, discussed in more detail in Section 2.3.8.

2.3.5. Reed et al., 2005

In their paper on fusing sonar image mosaics, Reed et al. discuss the use of SLAM (calling it CML) on side scan sonar data collected by SACLANT[12] Undersea Research Centre in 2002 [78]. The purpose of SLAM is to form a landmark-based map of the underwater environment. The landmarks can then be used to establish the location of the AUV within the map. Reed et al. also use the SLAM map to geo-reference their sonar images. The specific method employed for SLAM by Reed et al. is a stochastic map with a Rauch-Tung-Striebel (RTS) smoother [78]. A stochastic map uses a Kalman filter in building the map; according to Reed et al., this Kalman filter maintains all the correlations and covariances for the states (vehicle and landmark positions). Having fully correlated states allows the correction of the whole map from the observation of a single landmark. After the mission, the RTS smoother filters all the measurements for the states iteration-by-iteration (using all the data before and after each iteration). This improves the accuracy of the map and aids the creation and positioning of the sonar mosaics [78]. As mentioned in Section 2.3.4, SLAM does not eliminate the need for a CNA vehicle. More discussion on the topic is found in Section 2.3.8.

2.3.6. Desa, Madhan, and Maurya, 2006

Desa, Madhan, and Maurya [25] discuss acoustic transponders, GPS, DVL, and pressure sensors in their review of AUV systems. They propose deploying an array of transponders on the seafloor for AUV position triangulation. They indicate that this is expensive and requires a support ship, but claim that 2-m accuracies are possible [25]. A variation of the bottom transponders is the free-floating transponder. This they say can be equipped with differential GPS (DGPS) and be linked by radio to the support ship. When the AUV pings the buoys, the support ship can calculate the AUV's position [25]. A second method of AUV navigation proposed by Desa, Madhan, and Maurya is a combination of dead reckoning and GPS fixes. A DVL and a pressure sensor are used to calculate three-dimensional motion while underwater; when the cumulative error from the dead reckoning is greater than some acceptable threshold, the AUV surfaces to get a GPS fix. This is a common navigation method; however, the main drawback of this method is the time and energy expended in surfacing. The drawback of using stationary

[12] Supreme Allied Command Atlantic (NATO); the centre is now called the NATO Undersea Research Centre (NURC)

beacons is the time taken in laying and recovering them (especially if they need to be moved during a mission) as well as (in MCM) the danger to the ship or boat that must position them.

2.3.7. Sáez et al, 2006

Sáez et al. [79] discuss a vision-based approach to 3-D SLAM underwater using an entropy minimization technique. A trinocular L-shaped array of cameras for depth perception and a six-degree-of-freedom inertial measurement unit (IMU) for motion sensing were used. The mapping results provided by Sáez et al. are based on post-mission processing of images collected by tele-operation of their underwater vehicle [79]. While vision-based navigation is not viable in the cold water where the experiments for this thesis were conducted, SLAM is based on extracting features from sensor returns (whether sonar or video) and relating them to features that have been found previously and using this relation to correct the vehicle's position estimate. Therefore, after the features have been identified in either the video or the sonar image, the SLAM process is essentially the same. The main issue preventing Sáez et al. from using their SLAM technique for navigation underway is the time required for their entropy estimation [79]. Even once this issue is overcome, there are still problems with SLAM as discussed in Section 2.3.8.

2.3.8. Hölscher-Höbing and Larsen, 2006

Hölscher-Höbing and Larsen discuss an aided inertia navigation system (AINS) for AUVs [80, 81]. The AINS has five main parts. The IMU is the core sensor of the AINS. It "consists of orthogonal triads of gyros and accelerometers" and is rigidly attached to the AUV. Three possible kinds of IMUs are listed, micro electro-mechanical systems (MEMS), ring laser gyros (RLG), and fibre optic gyros (FOG). The IMU sends changes in velocity (ΔV) or attitude ($\Delta\theta$) to the second AINS part, the inertial navigation equations (INE). The INE computes the AUV's position, orientation and velocity from its initial conditions and from the ΔVs and $\Delta\theta$s measured by the IMU. Because this method of inertial navigation will quickly lose accuracy, the INE are also given corrections from the third part of the AINS, an error state Kalman filter (ESKF). This filtering creates what is called "tightly coupled" or "closed loop" AINS operation. The ESKF takes the information from the INE and any other sensors on the AUV (such as GPS or DVL) and estimates the measurement errors in the inertial navigation and the other sensors. The inertial navigation errors are sent to the INE as corrections, bounding the inertial navigation errors and limiting the effect of linearization errors implicit in Kalman filtering. The fourth part of the AINS, the sensor models, is used by the ESKF update its error estimates by comparing the actual sensor measurements with the expected (modeled) sensor measurements. The final part of the AINS is a post-processing technique called optimal smoothing [80]. It uses all the sensor measurements (past and future, over a specified interval) to find the most likely actual position for every point in time of the AUV mission. This has been done without degrading the inertial navigation dynamics or consuming significant time [81].

Two navigation techniques cited as using the AINS are Synthetic LBL and SLAM. Larsen claims that when used together, synthetic LBL and SLAM can give an AUV "long-term covert autonomous navigation with bounded error and superior relocation accuracy" [81]. The basic principle of Synthetic LBL is quite simple; a single beacon is used underwater instead of several. The AUV collects range measurements to the beacon, and since the beacon is not moving, the Kalman filter is able to use the range measurements to bound the position error.[13] To accomplish this, the state vector includes the beacon position, and the initial uncertainty in the beacon's position is mitigated by the values assigned in the covariance matrix [81]. Larsen reports that the AINS SLAM works much like the Synthetic LBL but with multiple seabed features used instead of the beacon. Prior knowledge of the seabed feature positions can be used by initializing them in the state vector and covariance matrix. Synthetic LBL and SLAM were evaluated from data collected in two trials. One evaluation is done simulating real-time measurement and another evaluation is done with the post-processing optimal smoothing discussed above [81].

The data from their main trial was processed offline to compare Doppler/inertial dead-reckoning, SLAM, and Synthetic LBL. Larsen compares the three navigation techniques with and without the offline optimal smoothing. Considering first the "real-time"

[13] This is essentially the same as a stationary CNA vehicle. A stationary CNA vehicle was used in [84].

navigation errors, Larsen shows that the Doppler/inertial and SLAM position errors grow together until the vehicle revisits the seabed landmark features. Revisiting the features eliminates the SLAM position error. The maximum position error for both SLAM and Doppler/inertial navigation is about 2.5 m during this 140-minute mission. The Synthetic LBL error barely exceeds 1 m at the very end of the seabed survey. Larsen demonstrates a dramatic rise in position error for all three methods during diving and surfacing because the DVL does not have a bottom fix. Optimal smoothing removes these diving and surfacing errors. In optimal smoothing, the Doppler/inertial radial position error[14] barely exceeds 2 m; the SLAM error reaches a peak of approximately 1.6 m; and the Synthetic LBL navigation error peaks at approximately 0.8 m and was less than 0.5 m for more than 90% of the mission. However, when the smoothed circular error probability[15] for SLAM and Synthetic LBL are compared and the larger than expected DVL scale factor error is considered, SLAM and Synthetic LBL generally provides similar accuracy after post-processing, though the results show Synthetic LBL is superior to SLAM in handling poor dead-reckoning performance [81]. According to [82], the SeaOtter Mk. II AUV is being sold with the AINS. Unfortunately further information on the effectiveness of its AINS could not be found. Other authors are working on AINS, including [83].

While actual test results of the AINS with SLAM and Synthetic LBL do not seem to be available, [80, 81] appear promising especially since SLAM would not require beacons in the water—a procedure which would cost time and could be dangerous in MCM. There are, however, drawbacks with the work in [80, 81]. First, sophisticated inertial navigation systems can be prohibitively expensive, especially for smaller AUVs. Second, the AINS described uses a variant of the Kalman filter. According to [29], even occasional outlier range measurements from a single beacon can introduce significant bias. Third, while a buoy for synthetic LBL navigation would likely be cheaper than most kinds of CNA vehicle, the relative bearing change required to effect the range-only navigation must be done by the AUV. In a side scan sonar survey mission such as minehunting, the path of the AUV is determined by the need to survey the area of interest to a required confidence level. Deviations in AUV course to aid synthetic LBL (similar to that done in [84]) would

[14] The difference between the AINS position estimate and the LBL reference position [81].
[15] Circular error probability (CEP) describes "a circle about a mean value which includes 50% of the population" [35].

be to the detriment of the mission objectives. In addition, synthetic LBL would not work well for an underwater transit as the AUV's bearing from the beacon would change slowly and the beacon would eventually be out of range. Fourth, the SLAM used in [80, 81] was processed after the mission. To be truly effective, SLAM would have to work on-board while the vehicle is underway. This requires some form of ATR. As ATR can suffer from a high number of false alarms [59], real-time SLAM requires more research before it will be viable. In addition, SLAM requires targets to be seen at least twice, making it unsuitable for underwater transits. Finally, the best results presented in [81] were based on post-mission optimal smoothing. If the MCM mission is to include mine-like target positions being passed from the detecting AUV to an inspection and/or neutralization vehicle (probably an ROV), post-mission navigation analysis (while useful for research) will not help speed-up the mine-clearing process. On the other hand, a mobile CNA vehicle as described in this thesis would use GPS fixes to correct navigation error (rather than post-mission processing) and is flexible enough (due to its mobility) to handle both large area searches and long distance transits.

2.3.9. Kinsey, Eustice and, Whitcomb, 2006

Kinsey, Eustice, and Whitcomb [85] reviewed state-of-the-art underwater navigation systems in 2006. The main challenge in underwater navigation is (x,y) location as depth, heading, pitch, and roll can be measured with bounded uncertainty. High-frequency (300 kHz or more) LBL navigation can provide sub-centimetre accuracy, but (due to the high frequency) has a very short maximum range. LBL navigation at 12 kHz can work at ranges of up to 10 km, but the precision is reduced to 0.1-10 m (depending on range). Filtering of range measurements (such as with EKF) can improve both accuracy and precision to a limited extent. Fixing the LBL transponders to the sea-floor, sea-ice, or the hull of a ship is the more traditional method of deployment; using buoys with LBL transponders and GPS receivers is a more recent development. Kinsey, Eustice, and Whitcomb briefly discuss the use of a ship as a CNA, providing ranging pings to bound AUV position error in a manner like that discussed in Section 1.3. (More detail on their approach is found in [30]). This thesis argues instead for the use of an autonomous marine vehicle as a CNA since it can follow an adaptive path more easily than a manned boat or ship and, in MCM operations, using an autonomous marine vehicle allows free movement of the CNA in the minefield without endangering human lives. However, the intention of the path planning algorithm in this thesis is to support OWTT range measurements as described in [85].

Kinsey, Eustice, and Whitcomb also discuss IMUs, navigation filters, and SLAM. IMUs can dramatically reduce error in AUV position estimates, but high accuracy IMUs can draw significant power and cost $100,000 or more [85]. Many small AUVs cannot provide this much power. It is reported in [85] that navigation filters such as Kalman Filters and EKFs typically use kinematic plant models. One work, [86], is cited as modeling vehicle dynamics, but this is in post-mission processing, and is thus less useful in the MCM scenario described in Section 1.2. Other filters such as Unscented Kalman Filters and Particle Filters are highly regarded because they do not have the linearization errors of the Kalman Filter and EKF [85]. However, these non-linearized filters have not been widely adopted in AUVs. According to Kinsey, Eustice, and Whitcomb the major problem with SLAM is identifying sea-floor features and matching them to previous views of the same feature. They report that success has been achieved with both optical sensors and sonar, but do not state whether this success was during the mission or in post-processing.

Kinsey, Eustice, and Whitcomb present a thorough review of AUV navigation in 2006, and their work may be regarded as an update on [24]. The main advances in [85] are SLAM and ranging from a single beacon (on a ship in [85]) using OWTT. For the purposes of this thesis, the major contribution of [85] is the OWTT ranging as the CNA vehicle path planning algorithm assumes that this ranging is used to correct survey AUV position estimates.

2.3.10. Kunz et al., 2008

Kunz et al. [21] discuss work with under-ice AUV operations and focus on LBL. As mentioned in Section 2.2.5, Kunz et al. use the same onboard WHOI Micro-Modem for LBL navigation and communication between ship and AUV. Since the AUVs have their own depth sensors, only two moored LBL beacons are needed to fix the location of the AUV. However, to increase the area they could survey at one time, Kunz et al. used four

Benthos LBL beacons with a 7-km range. The AUVs interrogate the beacons, and each beacon responds to the query at its own frequency. The two-way travel time was used to determine the AUV's range from each beacon. During AUV recovery, another set of LBL beacons were lowered over the side of the support ship. Two methods were implemented to localize the AUV from the support ship. First, direct ranging measurements were made using the ranging mode on the WHOI modem as well as a back-up beacon on the AUV. Second, the LBL interrogations and responses were monitored to calculate the AUV's position from the ship [21]. To account for LBL blackouts caused by underwater topography (discussed in Section 0), the AUVs actually navigated by Doppler bottom tracking when possible, using the LBL when the bottom tracking was not available [21]. In future Arctic missions, Kunz et al. intend to incorporate the OWTT range-only navigation discussed in [30, 85]. This method of navigation has been noted as part of the theoretical background of the present thesis.

2.3.11. Panish and Taylor, 2011

Panish and Taylor [35] report on the use of Kearfott T-24 and IXSEA PHINS III INUs (two of the best quality INUs currently available) with the Bluefin 12" AUV (12-in being the approximate vehicle diameter). Using trial runs of more than 5 km underwater with varying amounts of turning (a major factor in increasing position estimate error), Panish and Taylor demonstrate that the specified error of 0.1% of distance travelled (CEP) for both INUs is actually exceeded in trials. The CEP drift for the Kearfott INU is 0.05% of distance travelled and 0.07% for the IXSEA INU. The Kearfott INU actually achieves 0.1% error in 81% of the dives examined, while the IXSEA INU achieves 0.1% error in 83% of the dives. The Kearfott-equipped Bluefin 12" in this paper was equipped with a synthetic aperture sonar (SAS) capable of 400-m survey swaths (Figure 1.1). Panish and Taylor report that contacts in SAS images could be located with an accuracy of 10 m.

It should be remembered that inertial navigation solutions do not eliminate or bound positioning errors but rather reduce the drift. No matter how accurate the INU, at some point an external aid (e.g. GPS, LBL, CNA) will be required. Also, the very best INUs are also very expensive; in some cases it may be less costly to use a CNA vehicle rather than INSs for each survey AUV. Finally, the effect of turning on position uncertainty was not documented in [35], and the accuracy will likely degrade when a significant number of turns have been made (e.g. at the end of lanes shown in Figure 1.1), increasing the need for an external aid.

2.3.12. Medagoda et al., 2011

Medagoda et al. [87] report on trials using ADCP measurements to limit AUV position error growth between diving (losing GPS fix) and coming into DVL range of the ocean floor (called "bottom lock"). ADCP is an acoustic device that measures water current by measuring acoustic reflections off "scatterers" in the water column (such as plankton). Currents are measured in the *x,y* direction in a predetermined number of "bins" in the *z*-direction. In [87], the ADCP/DVL is mounted under the AUV. On some AUVs, ADCP/DVLs are mounted above and below the AUV. Medagoda et al. state that DVL range is a much as 200 m for low-frequency DVLs (150 kHz) and as little as 45 m for high-frequency DVLs (1500 kHz) [87]. The advantage of the high-frequency DVL is lower power consumption, higher accuracy, and a lower minimum altitude. This lower minimum altitude is especially useful to Medagoda et al. as they are using stereo vision for SLAM at 2-m altitude. They use a sparse extended information filter (SEIF) to combine sensor measurements (including SLAM and ADCP) to form the AUV's position estimate. They state that the incorporation of ADCP measurements in the filter obviates the need for acoustic navigation (LBL or USBL) when the AUV dives and surfaces. The filter can maintain the entire AUV state history, and thus "be re-linearized to correct for linearization errors," or it can remove positions and states that are no longer observed to reduce the filters computational requirements. In both cases, the position uncertainty grows during the AUV's dive, but when the entire state history is used, the error does not grow as rapidly during the dive and actually decreases (rather than grows) during the ascent [87]. This is presumably because the GPS fix when surfaced is filtered backwards through the ascent.

While an important paper, there are several reasons to conclude that [87] does not present an AUV solution in direct competition to the CNA solution advocated in this thesis. First, given that the AUV uncertainty with ADCP still grows while diving, some form of acoustic navigation (perhaps a CNA) would still be needed for arbitrarily deep ocean surveys. Second, using the entire state history is less useful in MCM operations outlined in Section 1.2 than in scientific missions because the locations of detected MLOs are reported immediately by the detecting AUV. This means that the transmitted position of the MLO does not benefit from later refinements in the estimated position of that MLO. The full benefit of maintaining the entire state history is only found in processing the data *after* the AUV is recovered though there would be a partial benefit during the mission. Third, of the two missions shown in [87], the minimum position uncertainty in the shorter mission is approximately 3 m and the minimum uncertainty in the longer mission is approximately 10 m. The estimated position error for an AUV benefitting from OWTT range measurements in [26] is 3 – 5 m, making the use of a CNA at least as effective as the SLAM method employed in [87]. Finally, as with other work with SLAM, [87] does not solve the communications limitations that must be overcome for effective AUV MCM operations.

2.3.13. Conclusion

Underwater navigation is a difficult but well-studied problem in AUV research. Much research has focused on acoustic navigation (particularly LBL and USBL). Acoustic navigation beacons can typically handle both communication and navigation, but static beacons are time consuming to deploy, and a ship-based solution is inadvisable for MCM operations. Sophisticated inertial sensors and filters are useful, but reduce rather than bound position estimate error drift. SLAM can bound navigation error, but cannot handle submerged transits and does not address the communication issues.

2.4. CNA Research, Including Alternatives

The use of a single vehicle (surface or subsurface) as a communication aid [19, 41, 44, 88] or navigation aid [85, 89, 90-92] to an AUV has been considered. One or two vehicles have been used to aid both communication and navigation [9, 13, 28-30, 32, 43, 61, 94-96]. The primary alternatives to a CNA vehicle are buoys (or bottom beacons) that are surveyed in place or buoys that are dropped into position and determine their position with GPS. One example of the latter option is discussed in Section 2.4.10.

2.4.1. Baccou and Jouvencel, 2003

Baccou and Jouvencel [34] address range-only navigation for AUVs. They present simulations using either a stationary beacon and a single AUV or two AUVs where one leads and the other follows. The range measurements are calculated from round-trip travel time and include measurements that are affected by Gaussian noise or random outliers. An EKF is used to determine the AUV's position. Like other range-only navigation research (Section 1.3), Baccou and Jouvencel state the most effective range measurements occur when there is a 90^{o} change in relative heading between the beacon and the AUV. Unlike much other AUV research, they do not assume that the AUV has an accurate (i.e. GPS) position fix at the beginning of the mission. Instead, they have the AUV take range measurements from the beacon (or leader AUV) while turning in a circle in order to initialize its position with respect to the beacon. Once the circle is complete, the mission proper begins. The multi-AUV range-only navigation presented primarily differs from this thesis in two ways. First, their work has the follower AUV adjust yaw to improve its position estimate whereas this thesis discusses path planning for the "leader" vehicle (assumed to have the better position estimate). Second, their follower AUV mimics the movements of the leader AUV whereas in this thesis the survey AUVs define their own paths (typically under operator direction prior to the mission) and the vehicle providing the range measurements adapts its path based on its knowledge of the survey AUV paths. However, the goal of bounding the error on the "follower" or "survey" AUV is the same in both cases.

2.4.2. Bahr et al., 2009

Bahr et al. [29] propose a method whereby two CNA vehicles maintain a prescribed distance from the survey AUV and, in a second scenario, two CNA vehicles maintain a right-angle formation with the survey AUV (survey AUV held at apex of right angle, as shown in Figure 2.1). This right angle formation, while not an optimized path, provides a bounded positioning solution for the AUVs consistent with the principles of range-only navigation discussed earlier. Employing two CNAs is a disadvantage if satisfactory navigation with a single CNA is possible because of the higher overhead of two vehicles instead of one. Later work by the author [31] considers the use of a single CNA vehicle (Section 2.4.7).

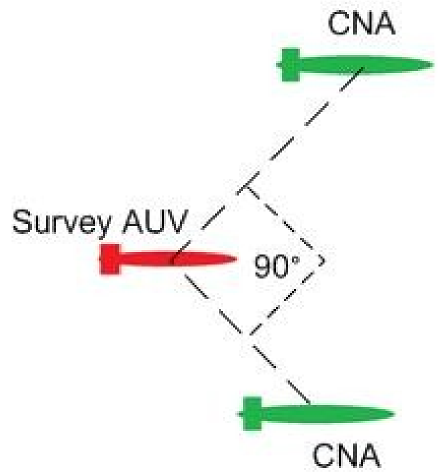

Figure 2.1: Single survey AUV supported by two CNAs.

2.4.3. Fallon et al., 2011

Building on their own previous work [61, 94, 97] as well as [28, 31], Fallon et al. discuss a combination of SLAM and cooperative CNA navigation [26]. Their work focuses on improving the navigational accuracy of an AUV attempting to reacquire a target using side-scan sonar. SLAM bounds the AUV position error while the AUV performs the reacquisition search over the target but the cooperative navigation does not due to the lack of relative motion between AUV and CNA. However, the CNA vehicle bounds the navigation error when the AUV transits between targets. The CNA path (in some trials, surface ship) was not discussed. An adaptive CNA path (as proposed in this thesis) would be more effective during the reacquisition search as the CNA would be able to ensure effective relative motion between the AUV and the CNA.

2.4.4. Fallon et al., 2010

In 2010, Fallon et al. [61] propose a CNA solution that differs from the CNA concept presented in Section 1.3 in two ways. First, it does not use a dedicated CNA vehicle for multi-AUV surveys. All but one AUV uses a very accurate INU. The AUV with the modest INU surfaces as required for GPS fixes which it then shares with the others to update their positions.[16] The AUV with the modest INU contributes to the survey/surveillance mission between its GPS fixes. Second, all the AUVs exchange their position and range estimates to improve their EKF navigation estimates. Each AUV's filter combines measurements from multiple sensors (weighted by respective accuracies)

[16] In [115], the possibility of using a single AUV with a very accurate INU to surface for GPS updates was suggested as an alternative.

to yield the best position estimate. A possible combination of [61] and the CNA path planning presented in this thesis is discussed in Section 0.

2.4.5. Benjamin et al., 2006

Benjamin et al. demonstrate the ability of MOOS-IvP to arbitrate competing AUV behaviours [84]. In their example, one behaviour's objective is to drive in a rectangular path and the other is to manoeuvre the AUV to improve its position relative to a stationary CNA vehicle. More often in the literature (as shown below) the CNA does the manoeuvring, not the AUV. Benjamin et al. here highlight the MOOS-IvP behaviour-based control. Their method determines the relative path between AUV and CNA based on the previous *N* positions. The new position is selected to increase the spatial extent and relative angle of the *N* previous positions. The goal of this manoeuvring behaviour is to minimize the AUV position error using a model similar to that described in Section 1.3. This manoeuvring behaviour does not consider motion by the CNA, and thus, unlike [13, 33, 93], does not benefit from the other vehicle's motion in its path optimization. While their work only considers two-dimensional motion, it should extend to three dimensions. This manoeuvring method was effective because the distance between the AUV and CNA vehicle is bounded (CNA is stationary and the AUV drives in a rectangle). To use this manoeuvring method on a non-stationary CNA vehicle, other behaviours would be required to maintain minimum and maximum distances from the AUV to prevent collisions and stay within acoustic modem range. Such behaviours exist in MOOS-IvP [98]. This thesis presents a path planning algorithm complete with bounded distances for a CNA that has been tested in harbour trials.

2.4.6. CNA Path, 2009 – 2010

Among researchers who use a single non-stationary CNA vehicle, few optimize its path. A non-optimized zigzag path was previously used while the submerged AUV followed a lawnmower path (Figure 1.1) [94]. A zigzag and an encirclement path were employed by a single ASC CNA where both CNA paths adapted to the AUV path [97].

2.4.7. Bahr, 2009

Another approach [31] determines a discrete set of *M* CNA positions that can be reached prior to the next update. The CNA selects the position that minimizes the survey AUV's position error and, in the process, optimizes its own path. The AUV position error, summarized by its position and covariance matrix, is sent to the CNA. The CNA determines its new position using this information and a short-term prediction of the AUVs' future paths. Permutations of one or more AUVs working with one or more CNAs are studied. In the case of multiple CNAs, each CNA selects a position to minimize the AUVs' position errors. Each CNA takes into account position selections communicated by the other CNAs, in addition to information from the AUVs, as it seeks to optimize its own path. Unlike other cases in the literature, this approach does not assume a constant CNA speed. However, in the single CNA case highlighted, the maximum speed was chosen by the path planner out of a range of speeds. Variable depth on the part of either the CNAs or the AUVs was not considered [31] as it has been in this thesis.

2.4.8. Chitre et al., 2010

Chitre [32, 93] optimizes the CNA path through minimizing the survey AUV(s) position error estimates. By assuming constant depths for both CNA vehicle and survey AUV(s), it was possible to path plan in two dimensions. Simulations were shown for one and two survey AUVs aided by one CNA vehicle. The CNA vehicle path could be determined in *underway* or *pre-deployment* modes. In pre-deployment mode, the CNA vehicle knows the survey AUVs' planned paths and the survey AUVs know the CNA's planned path *a priori.* In underway mode, the CNA vehicle still knows *a priori* the survey AUVs' planned paths but is also able to accept updates to the survey AUVs' planned paths which may change. This information allows for adaptive path planning by the CNA vehicle. This adaptation is important in the dynamic underwater environment but requires increased communication and computation for the CNA vehicle. Underway path planning results from field trials have been reported [99].

In [93], the CNA vehicle plans its path with knowledge of the survey AUVs' paths and uses an optimization that minimizes the survey AUVs' position errors. As mentioned above, the result of the planned CNA path is a reduction in the radial direction error but not the tangential one. In Figure 1.2, the blue ellipse near the survey AUV represents its unaided (by the CNA) position error and the green ellipse represents its error when aided by CNA range measurements. The blue circle near the CNA AUV represents its own position error. Notice the survey AUV's position error reduces significantly in the radial direction from E-H to F-G but the tangential error is unchanged. The green ellipse is used to determine the CNA's next waypoint. Ideally, the CNA vehicle selects its next waypoint on the major axis of the green ellipse since this minimizes the survey AUV's overall position error [33]. However, since this may not be achievable given a CNA vehicle's dynamics, a planner is used to find the best possible next position given a finite set of heading options. The approach in [93] served as the starting point for this thesis and is referred to again throughout.

2.4.9. Teck and Chitre, 2011

Teck and Chitre [33] used the same error model as [93], but with a different solution to the problem of minimizing the survey AUVs' position errors. This problem is formulated as a Markov Decision Process (MDP) with the path planning solution (CNA heading for the next time step) solved with a Cross-Entropy method [33]. The Cross-Entropy method learns the path planning control policy to map its states to actions. The authors applied a smoothing filter to the Cross-Entropy method, preventing the algorithm from converging on a local minimum instead of the optimal solution. Candidate CNA manoeuvres which will bring it closer than 100 m or farther than 1000 m from any survey AUV are heavily penalized to prevent selection. Their simulations discretize the ±40° possible CNA vehicle heading angle change into 8 discrete options, and used a 20-second time step (τ) between heading decisions.

Teck and Chitre published simulations with two survey AUVs comparing three methods for selecting the next CNA heading change. The first method simply manoeuvres to aid the survey AUV with the higher position error and ignores the other AUV. This method causes the CNA to move closer to the survey AUV with the higher position error, reducing the CNA's ability to effectively aid the other survey AUV. The second method kept the CNA equidistant from the two survey AUVs. This method is the unintended result of the algorithms employed earlier [13, 93]. The third method (similar to that in [13, 93]) was to select a desired CNA heading based on the sum-squared of the AUVs' position errors. This is the preferred method because it produced better results than the first method and was simpler than the second method [33].

The AUV position errors reported for simulations with two survey AUVs are comparable to those reported in [93], although differences in the parameters (e.g. the time-step τ) prevent direct comparisons. They state that while the computational load in [93] grew with the number of heading options and look-ahead levels (described in Section 3.1), the MDP/Cross-Entropy approach in [33] is independent of the number of possible actions (analogous to the number of heading options in [93]). Their simulations assume that the CNA and both the survey AUVs travel at a constant speed of 1.5 m/s. Their stated intention is to allow different CNA and AUV speeds in future work. [33]. No distinction between path planning prior to deployment versus underway was made as was done in [93]. As in [93], they do not consider depth changes by either the CNA vehicle or the survey AUVs.

2.4.10. Driscoll et al., 2005 - 2006

The drawbacks of the FAU GATEWAY buoy [62, 63] in comparison to the CNA vehicle advocated in this thesis are these. First, the FAU GATEWAY buoy is restricted to operating in 5 m to 200 m of water. Another device would be required for AUV operations in deeper water. Second, due to its large surface presence (see Figure 2.2), the GATEWAY buoy may be unsuitable for operations where stealth is required. An AUV CNA that only surfaces periodically would have a much lower surface presence. Third, in some situations, it could be too time consuming to recover a field of (two or more) GATEWAY buoys. This is a problem in protected marine environments and fishing areas as the buoy is not designed to scuttle itself after a mission. A CNA vehicle could transit to the recovery point along with the AUVs. Finally, the GATEWAY buoy is stationary. If GATEWAY buoys were to support a long distance transit or a large area search by AUVs, multiple GATEWAY buoys would have to be laid, rather than deploying a single CNA vehicle. For these reasons, the CNA vehicle is preferred above a stationary GATEWAY buoy. On the other hand the air-droppable GATEWAY buoy will reach its full potential when used with air-droppable AUVs (i.e. dropped from an aircraft like a torpedo). Only very small air-droppable AUVs are currently on the market; larger AUVs would likely be quite expensive due to the need for hardening for air-drops. In this situation, there may be cases where a field of GATEWAY buoys would not only be cheaper but sufficiently useful to employ rather than an additional air-dropped AUV as a CNA.

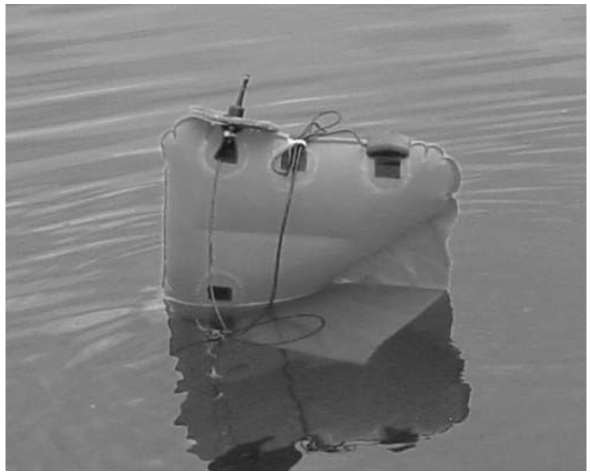

Figure 2.2: Float for the Florida Atlantic University air-droppable GATEWAY buoy, from [62]

2.4.11. Conclusion

There are advantages to using a single autonomous marine vehicle (surface or subsurface) as a CNA. There has been very little work on adaptive path planning for CNA vehicles. The work that does exist has not addressed the effect of changing depth in the survey AUV(s) path(s), nor does it typically address more than two survey AUVs. These points are addressed in this thesis.

Chapter 3 CNA Path Planning for Variable Survey AUV Depth

As shown in Section 2.4, previous work assumes constant depth for both the survey AUVs and the CNA vehicle. The assumption is valid for some applications, but minehunting missions with side scan sonar require the survey AUV to maintain constant altitude above a varying seabed. (One guideline is an AUV altitude set point of 10% of the side scan sonar range.) Dramatic changes in underwater topography are not unusual in littoral waters of depths to 100 m where minehunting with AUVs is considered. This thesis reports on work that includes variable survey AUV and CNA vehicle depths in optimizing the CNA's path.

As in [93], the CNA vehicle transmits an update to the *N* survey AUVs every τ seconds and determines its own heading change, δ_t^{CNA}, based on the CNA's model of survey AUV position error shown in Figure 1.2. The angle between the CNA vehicle and any survey AUV, *k,* (out of a group of *N* survey AUVs) is described by $\theta_{t+1}^{k} = \angle\left(x_{t+1}^{k} - x_{t+1}^{CNA}\right)$ (Figure 1.2).

As shown in Figure 1.2, the CNA vehicle models survey AUV position errors in two orthogonal directions – radial and tangential. The AUV position error in the radial, θ_{t+1}^{k} direction is modeled as zero-mean Gaussian radial error, $\varepsilon_t^k = \sigma$. Other authors have also modeled this error as independent of range [29, 94], but as described in the literature review (particularly [29]) the assumption of Gaussian noise with range measurements does not account for periodic measurements affected by multi-path and thus not described by Gaussian noise. However, these extremely poor range measurements can be rejected as described in [76], so the assumption is convenient and not entirely unrealistic. The AUV position error in the tangential direction, $\varepsilon_t^{\perp k}$, based on the survey AUVs dead-reckoned velocity estimates is described by (1). Parameter α represents the survey AUVs' velocity estimate error [93].

$$\varepsilon_{t+1}^{\perp k} = \sqrt{\frac{\left(\varepsilon_t^k \varepsilon_t^{\perp k}\right)^2}{\left(\varepsilon_t^k \cos\gamma_t^k\right)^2 + \left(\varepsilon_t^{\perp k} \sin\gamma_t^k\right)^2} + \alpha\tau} : \quad \gamma_{\mathrm{t}}^k = \theta_{t+1}^k - \theta_t^k \tag{1}$$

Building on [93], this thesis deliberately considers changes in survey AUV depth (and the possibility that if the CNA vehicle is itself an AUV it too can change depth) to adequately model AUVs in MCM missions. In the case of an AUV CNA, ϕ represents CNA vehicle pitch angle (for an ASC CNA vehicle, $\phi = 0$, since no change in depth occurs). At each time step, the CNA determines its new heading (ψ, first line of (2), from a set of A discrete options) and pitch angle (second line of (2), for AUV only). The pitch change, β_t^{CNA} (positive for AUV nose up), for which there are B possible options, is constrained to not exceed the maximum AUV CNA pitch rate, $\dot{\phi}_{\max}$, i.e. $\beta_t^{CNA} \le \left|\dot{\phi}_{\max}^{CNA} \times \tau\right|$ or the maximum AUV CNA pitch angle, $\phi_{\max}$. The CNA vehicle position at time t is shown in (2) where s^{CNA} is the CNA speed.

$$\begin{bmatrix} \psi_{t+1}^{CNA} \\ \phi_{t+1}^{CNA} \\ x_{t+1}^{CNA} \\ y_{t+1}^{CNA} \\ z_{t+1}^{CNA} \end{bmatrix} = \begin{bmatrix} \psi_t^{CNA} + \delta_t^{CNA} \\ \phi_t^{CNA} + \beta_t^{CNA} \\ x_t^{CNA} + \tau \cdot s^{CNA} \cos\left(\psi_{t+1}^{CNA}\right)\cos\left(\phi_{t+1}^{CNA}\right) \\ y_t^{CNA} + \tau \cdot s^{CNA} \sin\left(\psi_{t+1}^{CNA}\right)\cos\left(\phi_{t+1}^{CNA}\right) \\ z_t^{CNA} - \tau \cdot s^{CNA} \sin\left(\phi_{t+1}^{CNA}\right) \end{bmatrix} \tag{2}$$

Each heading-pitch combination produces estimates of errors ε_{t+1}^{k} and $\varepsilon_{t+1}^{\perp k}$ for each survey AUV. The CNA chooses the heading (and pitch) that minimizes the cost function, (3), which considers the position error for each survey AUV. Low cost correlates directly to low survey AUV position error [93].

$$C(S_t, a_t) = \sum_j \left[\left(\varepsilon_{t+1}^{j}\right)^2 + \left(\varepsilon_{t+1}^{-j}\right)^2\right] \tag{3}$$

Considering depth changes in both survey AUVs and the CNA vehicle allows the CNA vehicle to better maintain required minimum and maximum distances. With an AUV CNA, changes in CNA depth place it in *x-y* locations that may be unachievable at constant speed since a speed component will be used for changing depth. An increased number of waypoint values, $A \cdot B$ over A, theoretically allows the AUV CNA to reduce the survey AUVs' position error further than with an ASC CNA.

3.1. Cost Function for Impact of Current Decisions on Future

To improve the CNA path-planning algorithm performance, a look-ahead function considers the cost of current heading decisions L time steps (τ) into the future [13, 93]. As in the cost function without look-ahead (3), the CNA vehicle chooses the heading option that minimizes the survey AUVs' position errors. Simulations with different CNA vehicle heading options, pitch options, vehicle speeds, look-ahead levels, and one to five survey AUVs show the survey AUV positioning error reduces with increase in the number of heading values (A), CNA speed, and look-ahead time steps [13, 93]. Simulations with an AUV CNA do not show this trend with increasing the number of pitch options (B). This will be discussed further in Section 5.3. Not unexpectedly, increasing the number of heading options, pitch options, and look-ahead time steps increases the on-board computation effort. This is a concern both when the CNA plans its path underway and less so when planning prior to the mission, as discussed in Chapter 5 .

Figure 3.1 shows a cost determination with A = 3 heading options and look-ahead level L = 2. With no look-ahead levels the minimum cost out of options $[A_1, A_2, A_3]$ is selected. Say the dotted line for cost $C_{0,A3}$ is the minimum of the 3.

For L = 1, each branch at A_1, A_2, A_3 is explored and the minimum cost of each of these branches is added to the L = 0 cost. For example, the minimum of [$C_{1,A1}$ $C_{1,A2}$ $C_{1,A3}$] is added to $C_{0,A3}$. The CNA will choose the heading option out of $[A_1, A_2, A_3]$ that has the minimum combined $C_{0,Ax} + C_{1,Ax}$. Similarly, for L = 2, each branch will be explored to the $C_{2,Ax}$ level and the minimum $C_{1,Ax} + C_{2,Ax}$ will be added to each $C_{0,Ax}$ (a total of 9 numbers per $C_{0,Ax}$). The CNA will choose the heading option $[A_1, A_2, A_3]$ that has the minimum combined $C_{0,Ax} + C_{1,Ax} + C_{2,Ax}$.

One can appreciate that the number of calculations grows as A^{L+1} for an ASC CNA. In the case of an AUV CNA, the number of calculations would grow as $(A \cdot B)^{L+1}$. In the case of multiple survey AUVs, the number of calculations grow as $N \cdot (A \cdot B)^{L+1}$.

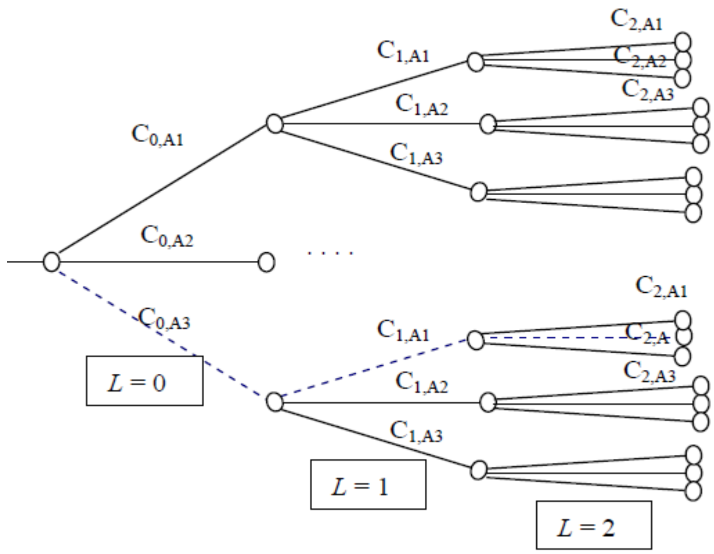

Figure 3.1: Cost determination for path optimization with A = 3 heading options and L = 2 look-ahead levels to select optimal heading options for one survey AUV

3.2. Distance Penalty

As discussed in [13], distance limitations are imposed to penalize candidate CNA position values, $\boldsymbol{x}_t^{CNA}$, that the CNA might otherwise choose when those position values violate maximum and minimum distances between it and any survey AUV. In the case of an AUV CNA, maximum and minimum depths as well as maximum absolute pitch angle are also imposed.

The maximum distance between the CNA and a given survey AUV is maintained to ensure reasonable quality acoustic communication between the two. The minimum distance between the CNA and a given survey AUV is maintained to avoid collisions. Beyond [13], the effect of distance limitations on optimizing the CNA path-planning has not been explored in detail, though the need for it was mentioned in [33, 93].

Every τ seconds (CNA update interval) the path-planning algorithm evaluates (3) for each heading/pitch value based on that heading/pitch's ability to reduce the position error in all survey AUVs. At the same time, the distance between the CNA and any given AUV is calculated. If this distance is less than the minimum distance or less than the maximum distance, a revised cost is calculated, (4) or (5) respectively, which penalizes that heading value so that it is less likely to be chosen. If a heading/pitch option does not violate either the minimum or the maximum distance, no penalty is applied. The consequences of any vehicles coming too close are more serious than having vehicles too far apart (collision versus loss of communication). Therefore, the distance penalty penalizes "too close" heading options more severely than "too far" ones as shown in (4) and (5), respectively.

if distance < min_dist ("too close" penalty)

$$C'(S_t, a_t) = 2 \times \left(C(S_t, a_t) + 2 \times \left(\text{min\_dist} - min\left(\boldsymbol{x}_t^j - \boldsymbol{x}_t^{CNA}\right)\right)\right) \quad (4)$$

for given δ_t^{CNA}

if distance > max_dist ("too far" penalty)

$$C'(S_t, a_t) = 2 \times \left(C(S_t, a_t) + max\left(\boldsymbol{x}_t^j - \boldsymbol{x}_t^{CNA}\right) - \text{max\_dist}\right) \quad (5)$$

for given δ_t^{CN}

The magnitude of the distance violation is incorporated into (4) and (5) so that if all heading options are either too far or too close, the least undesirable heading option will be selected. In the case of multiple survey AUVs, it is possible that a heading option may put the CNA too close to one survey AUV and too far from another. When this happens, the distance penalty function applies the "too close" penalty rather than the "too far" penalty to prevent collisions. In the look-ahead function (because the calculated costs do not immediately affect the CNA's motion), a simple penalty is used where the costs of options that are too close to or too far from any survey AUV are doubled. Differentiating between the "too close" and "too far" cases did not initially seem necessary as heading/pitch options in the look-ahead function are not about to be used as they are in the main function. Results of the investigation of this penalty formulation and some alternatives are shown in Section 5.1.

Chapter 4 Implementation in MOOS-IvP

The algorithm described in Chapter 3 (1 to 5) was first implemented in MATLAB®, and results from these simulations are reported in Section **Error! Reference source not ound.**. The MATLAB® simulations demonstrate pre-deployment path planning for both ASC and AUV CNAs. For testing the underway path planning mode in simulation, as well as in-water testing (underway and pre-deployment modes), the path-planning algorithm was implemented in MOOS-IvP. To date, only the ASC CNA path planning is implemented in MOOS-IvP.

The Mission Oriented Operating Suite (MOOS), and its extension, MOOS-IvP (Interval Programming) were developed by the Massachusetts Institute of Technology (MIT) for marine robotics applications [4]. It is used by Defence R&D Canada (DRDC) for marine autonomy research and is implemented on DRDC's three Iver2 AUVs (Figure 4.1). MOOS is a publish-subscribe architecture [4] where processes publish and subscribe to variables in the MOOS database (MOOSDB). Processes include path-planning, navigation, communication, control, and sensor interfaces. The *pHelmIvP* process manages the use of behaviours such as waypoint following, operating area definition, and collision avoidance to determine vehicle waypoints [4]. The process and behaviour configuration files are customized to a mission's specific requirements [98]. The DRDC implementation of MOOS-IvP is based on the use of two processors on the AUVs. A backseat processor uses MOOS-IvP to make heading, speed, and depth decisions (in *pHelmIvP* through the arbitration of the active behaviours). A frontseat processor is used to control the AUV in compliance with the MOOS-IvP objectives [100].[17] MOOS-IvP processes developed as part of this thesis are highlighted in Figure 4.2. All other behaviours and processes were originally written by others. The implementation of the algorithm described in Chapter 3 is in the *pCnaPathPlanning* process, which provides waypoints to *pHelmIvP's* waypoint behaviour. A second process, *pParseSegList*, manipulates waypoint lists for acoustic transmission to all vehicles, enabling underway CNA path planning.

---

[17] Because a waypoint following behaviour, including optional path following, was available in MOOS-IvP and actual vehicle control was already implemented on the Iver2 AUV, non-linear waypoint and path following control such as described in [111] did not need to be implemented in this thesis.

Figure 4.1: Iver2 AUVs operated by Defence R&D Canada

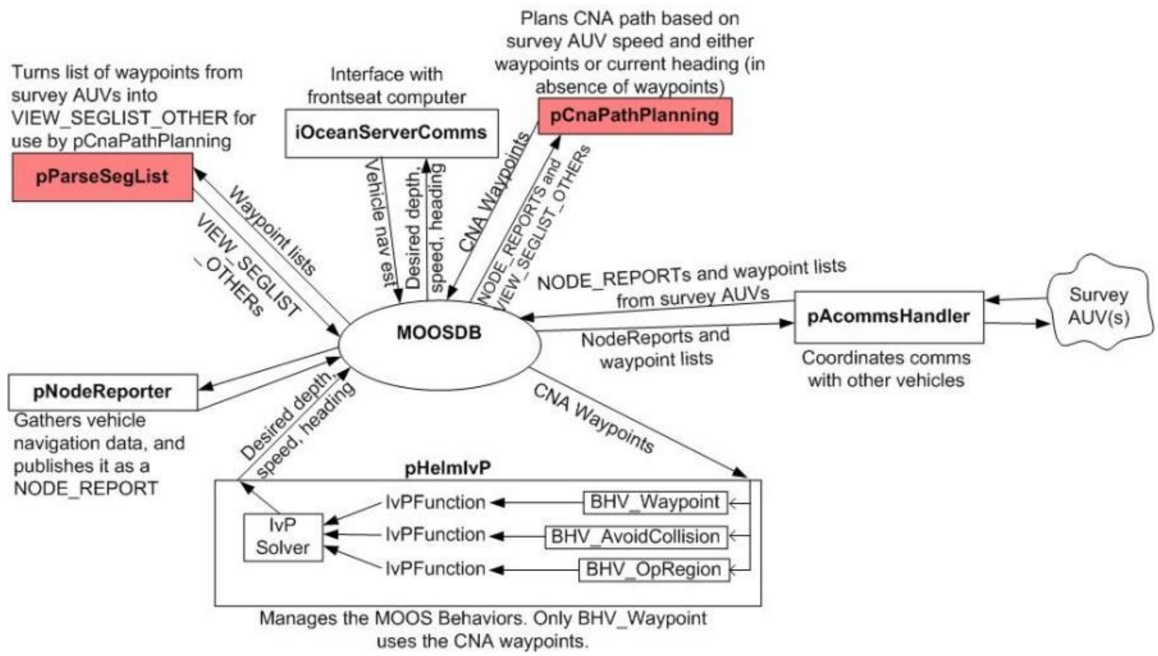

Figure 4.2: Partial diagram of CNA MOOS-IvP processes for underway path planning trials. Shaded processes created by the author. Diagram' general arrangement based on [4]

4.1. Pre-Deployment Path Planning Mode

CNA path planning in pre-deployment mode works like the CNA path planning implemented in MATLAB® for simulations but is able to pilot a vehicle in the water. The ASC CNA accesses a static file with the *a priori* survey AUVs' *x,y,z* positions listed as a function of time over the entire mission. The path planner performs linear interpolation on this position data to determine the survey AUVs' positions at the times that the CNA makes heading decisions (*i.e.* every τ seconds). Each heading decision (at assumed constant speed) results in an *x,y* waypoint. (Depth is 0 m for ASC CNA implementation). Once the waypoints for the entire mission are planned, they are sent to MOOSDB as a single string. This string is subscribed to by the waypoint behaviour. For in-water AUV operations, an additional waypoint behaviour instance causes the CNA to travel from where it enters the water to where its mission begins.

In-water trials of pre-deployment path planning were conducted in Halifax Harbour with an Iver2 AUV as an ASC CNA. The main goal of pre-deployment mode trials was to prove that the non-holonomic Iver2 AUV can turn at the rate specified by the planner and hence can keep up with the planner. Weather during pre-deployment trials included waves of up to two feet (sea state two) with surface currents of 0.5 -1 m/s. The Iver2's best speed on the surface is 1.5 m/s.

Figure 4.3 shows a mission conducted in pre-deployment mode. The interpolated (30-second time steps) path of the survey AUV is shown by the green dashed line. The red dashed line indicates the operating region in which the ASC CNA vehicle is confined. The planned CNA vehicle (Iver2 as an ASC) waypoints are marked with asterisks connected with a dark blue line. The actual (logged) path of the CNA vehicle is shown in magenta. The AUV CNA entered the water on the far right of the plot and headed for the first planned waypoint at (0, 0). Several of the waypoint positions are covered more than once as the Iver2 follows its planned path. Spikes in the magenta path near the bottom of the figure are due to jumps in the vehicle GPS position. The ASC CNA glided to a stop after reaching its final waypoint. Notice that the vehicle entered the water outside the operating region. The MOOS-IvP operating region behaviour (*BHV_OpRegion*) is not active until the ASC CNA has been inside the operating region for a specified time [98].

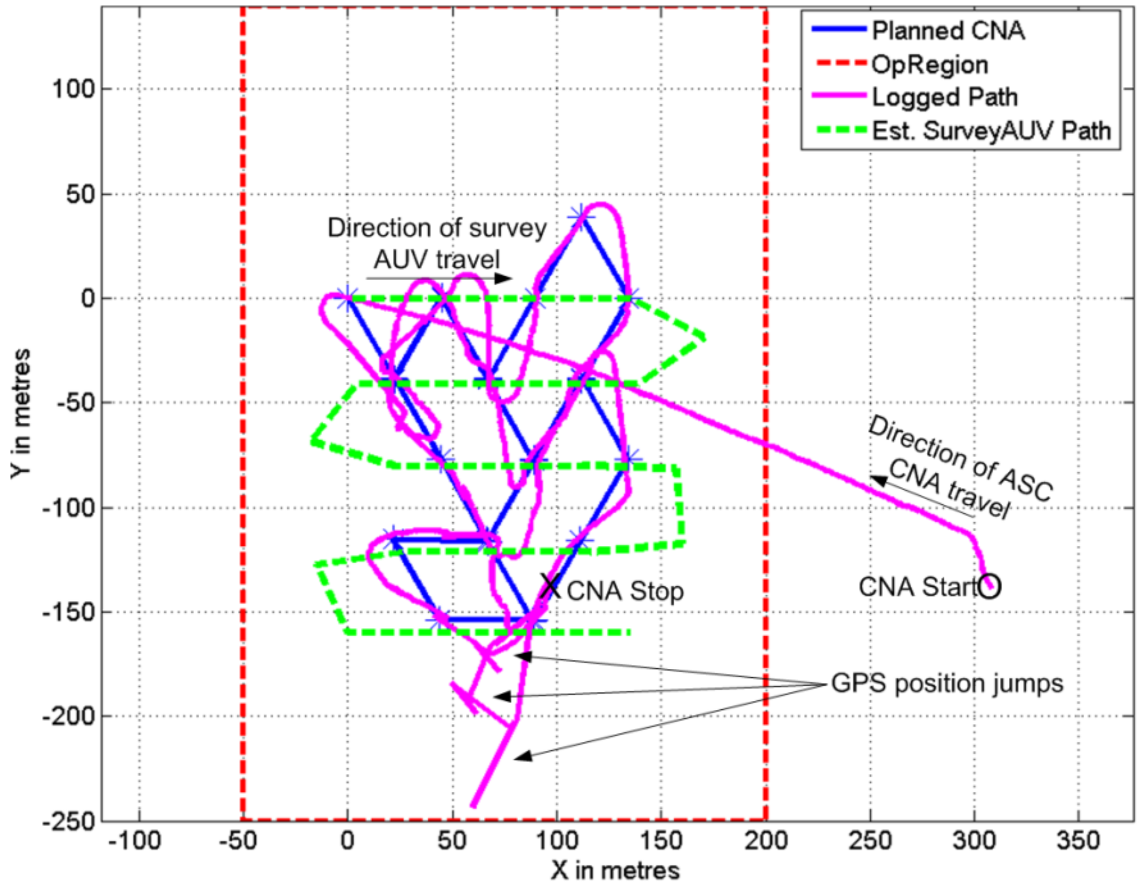

Figure 4.3: Planned and actual (logged) paths from at-sea trials with an Iver2 AUV as the ASC CNA with a speed set point of 1.5 m/s

In Figure 4.3, the Iver2 AUV is able to achieve the planned turn rate of 4°/sec at a decision time step (τ) of 30 sec. A 30-sec decision time step (higher than that in [33] or [93]) was selected to align with an anticipated underwater communication rate of one message every 30 sec [61]. However, in the implementation of the MOOS-IvP acoustic communication process (*pAcommsHandler*) used in this paper, the communication rate is 15 sec per vehicle. Thus in an in-water trial with one survey AUV and a CNA, each vehicle transmits once every 30 sec (as anticipated), but in a trial with two survey AUVs and a CNA, each vehicle transmits once every 45 sec. Future implementation of a cooperative navigation methodology may require modifying the current communication cycle such that the transmission rate of the CNA vehicle is every 30 sec, independent of the number of survey AUVs. It is not meaningful to lower the decision time step below the communication rate as there is no benefit for cooperative navigation in making heading decisions at a higher frequency than the range transmissions to the survey AUVs.

On the other hand, maximizing the time between heading decisions increases the time available for calculating the next heading, allowing for higher look-ahead levels and therefore more effective cooperative navigation. (The computation time in pre-deployment mode is typically on the order of a few seconds, but grows exponentially as look-ahead level increases, maximum look-ahead levels in underway mode are examined in Section 6.5.2) It was decided that the turn rate in the planner did not need to be increased even though the AUV is certainly able to achieve a higher turn rate. This is to maintain consistency with previous work [13, 93] and to avoid the case where turns of more than 180° are possible since the resultant heading from a hard left turn would overlap the resultant heading from a hard right turn (and vice versa).

4.2. Underway Path Planning Mode

Since a real AUV MCM survey mission is influenced by such environmental considerations as currents and underwater topography, the planned survey mission and the actual survey mission may differ. The goal of the underway path planning mode is to adapt the CNA vehicle's path to the survey AUVs' actual paths during the mission. Unlike [93], the CNA vehicle does not have any information about the survey AUV paths before the mission begins. This simplifies implementation, but requires that the CNA receive acoustic messages from each survey AUVs prior to initiating its path planning.

The underway path planning implementation in this paper uses the same algorithm as the pre-deployment implementation, but plans only one waypoint at a time, sending each waypoint to the MOOS waypoint behaviour as the behaviour indicates that it is ready for another waypoint. There are also functions in *pCnaPathPlanning* that infer the current and future positions of the survey AUVs. A flowchart describing the underway path planning mode is shown in Figure 4.4

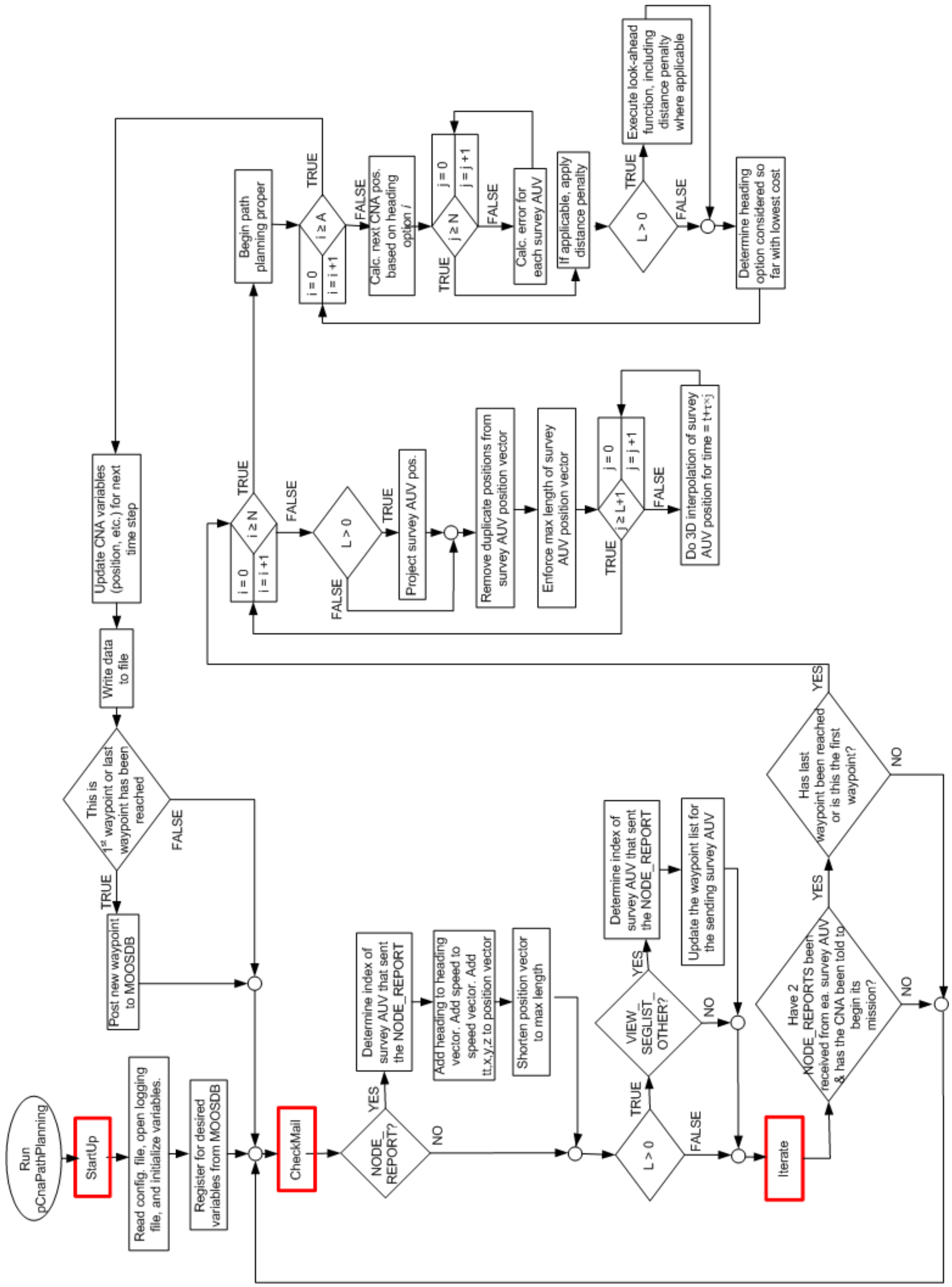

Figure 4.4: Flowchart of underway path planning algorithm.
Blocks outlined in red belong to the CMOOSApp base class.[18]

Path planning begins once two acoustic messages have been received from each survey AUV in the mission. This increases the likelihood that the survey AUVs have actually

[18] Layout of MOOS-IvP process based on [98]. Flowchart style based on [118].

commenced their missions and are not waiting for the command to start from the operator. The acoustic messages contain a NODE_REPORT which is a MOOS variable string that contains a vehicle's position summary (e.g. *x,y,z* position, heading, and speed) [98]. A function inside *pCnaPathPlanning* feeds the NODE_REPORTs into a vector containing all recently reported and projected positions. A function in *pCnaPathPlanning* maintains an upper limit on the number of positions stored in the aforementioned vector.

If the survey AUVs are using waypoints in their path planning, their next three waypoints are transmitted in the acoustic message and assembled into a MOOS string, VIEW_SEGLIST_OTHER, by the *pParseSegList* process on the CNA vehicle. This string has the same format as the VIEW_SEGLIST string [98]. The CNA path planning process uses VIEW_SEGLIST_OTHER to create its own list of survey AUV waypoints. Before the *pCnaPathPlanning* generates a new CNA waypoint, it consults the list of survey AUV waypoints (if updated since the last CNA waypoint was generated) and determines the times for the future waypoints based on the assumption that the last reported survey AUV speeds remain constant until the next update. This assumption is reasonable given that a constant speed is generally required for survey AUVs with side scan sonar. Presently, the number of future waypoints considered is based on the look-ahead level in the path planning algorithm. Later versions of *pCnaPathPlanning* will use all waypoints transmitted by the survey AUVs, regardless of the look-ahead level.

Survey AUV depths are likewise assumed constant between updates. This assumption may not be optimal when the survey AUVs are changing depth, but it was used for the following reasons. In an altitude-keeping survey AUV mission, the survey AUVs do not know their future depths (knowing instead their altitude set points) and so are not able to transmit that information. The high probability of missed messages with underwater acoustic communication precludes the use of a simple extrapolation function by the CNA since the extrapolated depth using the last two transmitted depths will quickly grow to an unreasonable value (much too deep or shallow) between infrequently received acoustic updates. On the other hand, if the CNA had access to a reasonably good chart of the mission area (not always available) and knew the altitude set point on the survey AUVs (easily added to the acoustic message), the CNA could in principle estimate the probable depth of the survey AUVs with reasonable accuracy. Since this capability is not currently available, the constant depth assumption has been used so that a reasonable depth value is used by the CNA. The error in assumed depth will be corrected next time an acoustic message is received from the survey AUV.

The acoustic communications uses a micro-modem, developed by the Woods Hole Oceanographic Institution (WHOI), run by the MOOS process *pAcommsHandler* [66]. The version of *pAcommsHandler* used generated messages of 32 bytes using an XML file customized by the author. Larger message sizes are available (64 and 256 bytes), but the 32-byte message size remains the most common [9, 38, 66]. The only message used in this work sends a NODE_REPORT, three future vehicle waypoints, and basic vehicle health data (*e.g.* battery life), using 27 bytes of the 32-byte maximum. (See Appendix C.) The decision to send only three waypoints is based on two factors. First, the need to conserve space in the 32-byte message for future capabilities (such as ATR reports), and second, the fact that three waypoints are sufficient to transmit the length of the longest survey leg any time the message is sent. In Figure 4.5, a message is sent immediately before the survey AUV reaches a waypoint. In this case, the survey AUV is practically at its next waypoint, but that waypoint is still transmitted as the next waypoint. The distance between the survey AUV's current position and that waypoint is too short to provide the CNA with significant information about the survey AUV's intended path, especially in the event that the CNA does not hear from the survey AUV again for several minutes. However, since three waypoints are sent, the corner at the end of the next leg is sent, providing the CNA with enough information to plan a useful path for some time. If another acoustic update is not received by the CNA before the survey AUV reaches the third waypoint, the CNA assumes the survey AUV continues in a straight line and the effectiveness of the CNA path decreases. There will be a limiting case, especially in very poor acoustic communication conditions, where the lawnmower legs are too short for three waypoints to provide sufficient information to the CNA for path planning. In this case, it would be necessary to increase the number of waypoints transmitted.

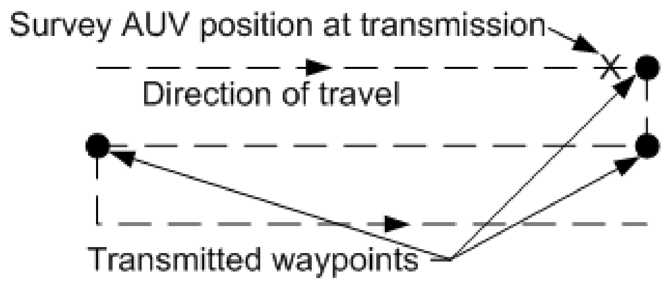

Figure 4.5: Acoustic transmission of waypoints

In order to run an underway path planning mission with multiple vehicles in-water, other processes and behaviours were used. Some of these are shown in Figure 4.2. The MOOS interface *iOceanServerComms* is designed specifically for frontseat-backseat computer communication on the Iver2 AUV. [100] Heading, depth, and speed decisions from *pHelmIvP* are sent to the frontseat computer for execution. In the in-water trials shown in this thesis, the navigation was done by the frontseat computer, and the resulting position, speed, and attitude variables were passed to the backseat computer. However, an EKF has been implemented in MOOS for the DRDC Iver2 AUVs by University of New Brunswick PhD student Liam Paull. The EKF takes the raw data from the navigation sensors (GPS, DVL, and compass) and determines the AUV's most likely position and the associated uncertainty in that position estimate. This EKF was used by the Iver2 AUVs in the altitude keeping trials shown in Section 6.5.3. The *pNodeReporter* process produces the navigation summary NODE_REPORT, discussed above, at the rate stipulated in its configuration file [4]. The *pHelmIvp* process and the waypoint behaviour were discussed above. Two other behaviours used in this work are *BHV_OpRegion* and *BHV_AvoidCollision. BHV_OpRegion* allows the user to define a convex polygon where the vehicle can operate (red dashed line in Figure 4.3) [98]. After the vehicle enters the operating region, *BHV_OpRegion* stops the vehicle if it leaves the operating region for more than a user specified length of time [98]. (A new version of the operating region behaviour, *BHV_OpRegionBounce,* has been developed that avoids shutting down MOOS in most cases by "bouncing" the vehicle back into the operating region [101]. This new behavior has been used in some of the trials with the original *BHV_OpRegion* retained for redundancy). While a distance penalty was applied to prevent collisions between the CNA vehicle and the survey AUVs, *BHV_AvoidCollision* adds an important layer of vehicle safety, especially since the distance penalty does not consider the distance between the CNA and the survey AUVs between CNA waypoints. In multiple vehicle trials, each vehicle is provided with an instance of *BHV_AvoidCollision* [4]. The CNA vehicle initiates collision avoidance manoeuvres at a greater range than the survey AUVs because it is much more important for the survey AUVs (simulating minehunting side scan sonar surveys) to follow the specified path between waypoints than for the CNA vehicle on its navigation and communication support task.[19] Additional processes and behaviours were also employed during in-water trials (e.g. data logging with *pLogger*, [4]), but those discussed above are the most important in the present work.

[19] Note that the manoeuvres resulting from *BHV_AvoidCollision* are not in accordance with the maritime collision regulations (known as COLREGS or Rules of the Road) used by surface ships. Collision avoidance in accordance with the Rules of the Road is a separate set of MOOS behaviours [112] and has not been examined as part of this thesis.

Chapter 5 Results from MATLAB® Simulations

Given the large number of possible combinations of CNA path planning parameters, finding the optimal parameters for a specific set of survey AUV missions or a general case is a legitimate but time consuming task. Previous work [13, 93, 96] has shown increasing CNA vehicle speed, heading options, and look-ahead level generally improves path-planning performance. Of course, the look-ahead level, number of heading options, and (in the case of a AUV CNA) number of pitch options have an upper limit imposed by the capacity of the processor to handle the number of variables to be calculated and its ability to make those calculations in a timely manner. For some combinations of path planning parameters, the time required for calculating the CNA path in pre-deployment mode on the backseat processor may be greater than the time the mission will take to actually run. An off-board super-computer could even be employed to make the calculations. However, in underway mode the backseat computer must be able to calculate a waypoint every τ seconds in order to keep the CNA vehicle moving at a constant speed, as assumed by the path planning algorithm. The parameters in Table 5.1 are used in all the simulations and in-water trials presented in this thesis. Other parameters are listed for specific simulations and trials.

Table 5.1: Fixed simulation & in-water trial parameters

Parameter		Value
survey AUV *k* error in radial direction at $t = 0$	ε_0^k	1 m
survey AUV *k* error in tangential direction at $t = 0$	$\varepsilon_0^{\perp k}$	1 m
uncertainty of survey AUVs' velocity estimate	α	0.1 m^2/sec
CNA maximum turning rate	$\psi_{\max}^{CNA}$	4°/sec
CNA maximum pitch rate	$\varphi_{\max}^{CNA}$	1.5°/sec
Maximum distance	-	1000 m
Minimum distance[20]	-	100 m

The CNA path planning algorithm was first implemented in MATLAB® before translation into C++ for use in MOOS-IvP. The MATLAB® implementation only supports path planning in the pre-deployment mode (where the CNA has *a priori* access to *x,y,z* positions for all the survey AUVs for the entire mission), and work has been done

[20] This number needs to be large enough to allow for somewhat clumsy collision avoidance manoeuvres by both the CNA and the survey AUV to still prevent a collision.

to evaluate the performance of the path planning algorithm in pre-deployment mode. Pre-deployment mode simulations are entirely deterministic, allowing simulations to be run only once for a set of parameters.

5.1. Distance Penalty, Initial Investigation

In [13], the effect of the distance penalty using the (4) and (5) cost functions was shown through MATLAB® simulations for an ASC CNA. The distance penalty does not prevent all violations of maximum and minimum distances between the CNA vehicle and survey AUVs. In some instances, the path planning algorithm is unable to maintain the specified distances from all the survey AUVs and must select the heading option that is the least undesirable of the available options.

As discussed, and in [13, 93] look-ahead reduces the overall survey AUV position error by adding the cost (an estimate of survey AUV position errors) of future decisions to the cost of current decisions each time a heading (and pitch, if an AUV CNA) decision is made. It seems that in most of the cases considered, look-ahead alone should be sufficient to bound survey AUV position error, provided that enough look-ahead can be computed by the processor. (This assumes that the CNA can physically maintain the specified maximum distance from all survey AUVs. If the distance between any two survey AUVs is greater than 2 × max_dist, the CNA will not be able to maintain the required max_dist from both survey AUVs). However, sufficient look-ahead levels (L) cannot always be realized due to the exponential increase in computational load with increased look-ahead. For instance, sufficient look-ahead to reduce survey AUV position error to the same level without a distance penalty as with could not be found for five survey AUVs, but position error without a distance penalty could match position error with a distance penalty for two survey AUVs with a look-ahead level of 4 (or higher) (Figure 5.1). If a high enough look-ahead level were possible, five or more survey AUVs could be satisfactorily supported without a distance penalty. However, in the case of 2 survey AUVs and no distance penalty, the distance and position error versus time trends (not shown), suggest the distances and errors are not bounded when using a look-ahead level of 4 and are bounded with a look-ahead of 5.

For the case of two survey AUVs, with a look-ahead level of 4, the distance penalty bounds the error and the distance between the CNA and survey AUVs. Without the distance penalty, the error and distance are not bounded even though the costs are similar with and without distance penalty, though there is a practical limit to the value of large look-ahead in a dynamic environment if the survey AUVs deviate significantly from the planned paths.

In the case of one survey AUV with $L = 0$, the initial distance between the CNA vehicle and AUV determines whether the distance penalty reduces or bounds the AUV position error. In the example of a CNA and survey AUV initially separated by approximately 140 m, the distance penalty makes no difference in reducing or bounding AUV position error. In a second example, the CNA and survey AUV are initially just over 1 km apart (including depth). Here, the distance penalty is needed to bound the survey AUV's position error because while the CNA vehicle chooses the best manoeuvre for each time step, the overall effect takes the CNA further and further away from the survey AUV. The addition of the distance penalty effectively discourages the CNA from selecting a heading option that will cause it to move too far away from the survey AUV, effectively adding a global optimality vote for the path planning that look-ahead would generally provide at higher computational cost. Therefore, the distance penalty is of particular value when the CNA and the survey AUV must be deployed far apart.

In most cases simulated by the author, the addition of a distance penalty is sufficient to bound the survey AUVs' position error, and, as mentioned, the addition of the distance penalty does not add significant computational load to the CNA path-planning algorithm. In other cases, such as when the CNA vehicle travels slower than the survey AUVs, the path-planning algorithm is often unable to plan manoeuvres that will bound the survey AUV position error. Whether or not the survey AUV position error is bounded by the CNA's planned path, the proposed use of a cooperative navigation algorithm will bring the survey AUV position error lower than would be possible were the survey AUVs to navigate independently.

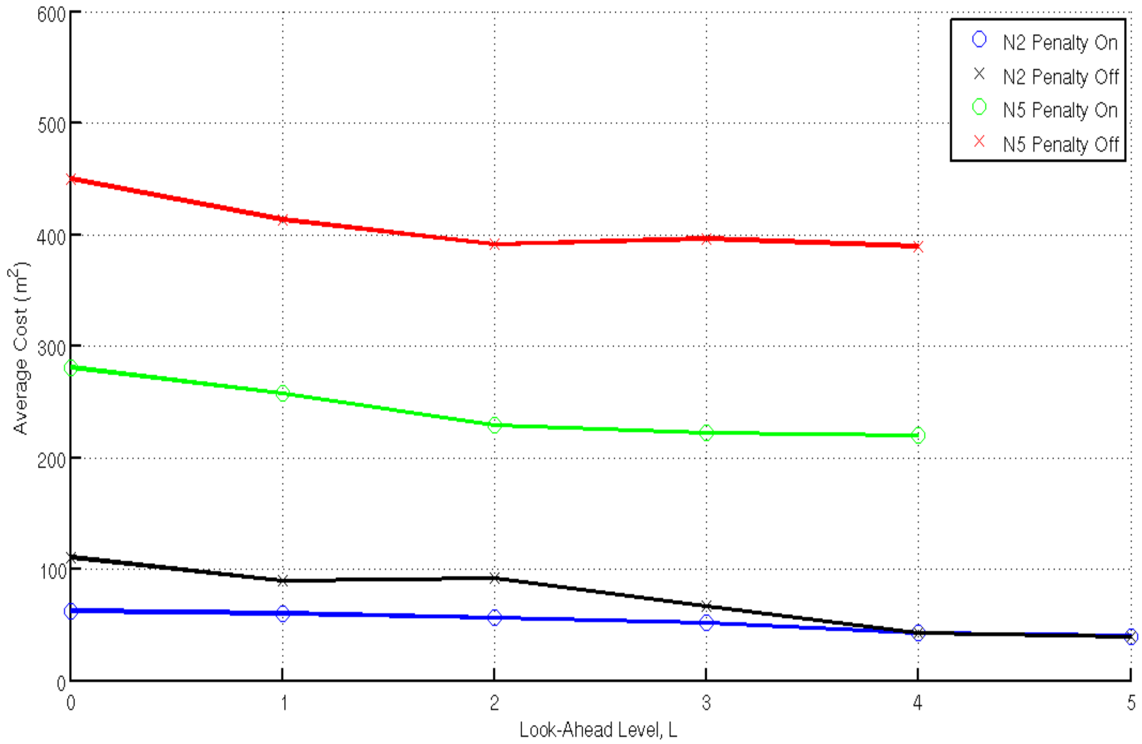

Figure 5.1: Average Cost ((3), ≈ survey AUV position error) vs. look-ahead for simulations with 2 and 5 survey AUVs with and without distance penalty

5.2. Distance Penalty, Follow-On Investigation

It was suggested by Gregson, [102], that formulations of the distance penalty other than (4) and (5) (such as a quadratic equation) might improve compliance with the distance limitations. Therefore the equation sets below, (6 - 12), were tested in MATLAB® simulations. $C'(S_t, a_t)_{\text{LA\_TC}}$ is the distance penalty as applied in the look-ahead function if a pitch-heading combination is too close to any survey AUV; $C'(S_t, a_t)_{\text{LA\_TF}}$ is the distance penalty as applied in the look-ahead function if a pitch-heading combination is too far from any survey AUV. All in-water trials and most simulations described in this thesis used (11), (12) is only used in a few simulations. In the figures below, the legends use Table 5.2 to indicate the primary and look-ahead penalties applied in each set of simulations.

$$\begin{bmatrix} C'(S_t, a_t)_{\text{TooClose}} \\ C'(S_t, a_t)_{\text{TooFar}} \end{bmatrix} = \begin{bmatrix} 2\left(C(S_t, a_t) + 2\left(\text{min\_dist} - min\left(\boldsymbol{x}_t^j - \boldsymbol{x}_t^{CNA}\right)\right)^2\right) \\ 2\left(C(S_t, a_t) + \left(max\left(\boldsymbol{x}_t^j - \boldsymbol{x}_t^{CNA}\right) - \text{max\_dist}\right)^2\right) \end{bmatrix} \tag{6}$$

$$\begin{bmatrix} C'(S_t, a_t)_{\text{TooClose}} \\ C'(S_t, a_t)_{\text{TooFar}} \end{bmatrix} = \begin{bmatrix} 2\left(C(S_t, a_t) + 2\left(\text{min\_dist} - min\left(\boldsymbol{x}_t^j - \boldsymbol{x}_t^{CNA}\right)\right)^3\right) \\ 2\left(C(S_t, a_t) + \left(max\left(\boldsymbol{x}_t^j - \boldsymbol{x}_t^{CNA}\right) - \text{max\_dist}\right)^3\right) \end{bmatrix} \tag{7}$$

$$\begin{bmatrix} C'(S_t, a_t)_{\text{TooClose}} \\ C'(S_t, a_t)_{\text{TooFar}} \end{bmatrix} = \begin{bmatrix} 5\left(C(S_t, a_t) + 5\left(\text{min\_dist} - min\left(\boldsymbol{x}_t^j - \boldsymbol{x}_t^{CNA}\right)\right)\right) \\ 2\left(C(S_t, a_t) + max\left(\boldsymbol{x}_t^j - \boldsymbol{x}_t^{CNA}\right) - \text{max\_dist}\right) \end{bmatrix} \tag{8}$$

$$\begin{bmatrix} C'(S_t, a_t)_{\text{TooClose}} \\ C'(S_t, a_t)_{\text{TooFar}} \end{bmatrix} = \begin{bmatrix} 5\left(C(S_t, a_t) + 5\left(\text{min\_dist} - min\left(\boldsymbol{x}_t^j - \boldsymbol{x}_t^{CNA}\right)\right)^2\right) \\ 2\left(C(S_t, a_t) + \left(max\left(\boldsymbol{x}_t^j - \boldsymbol{x}_t^{CNA}\right) - \text{max\_dist}\right)^2\right) \end{bmatrix} \tag{9}$$

$$\begin{bmatrix} C'(S_t, a_t)_{\text{TooClose}} \\ C'(S_t, a_t)_{\text{TooFar}} \end{bmatrix} = \begin{bmatrix} 5\left(C(S_t, a_t) + 5\left(\text{min\_dist} - min\left(\boldsymbol{x}_t^j - \boldsymbol{x}_t^{CNA}\right)\right)^3\right) \\ 2\left(C(S_t, a_t) + \left(max\left(\boldsymbol{x}_t^j - \boldsymbol{x}_t^{CNA}\right) - \text{max\_dist}\right)^3\right) \end{bmatrix} \tag{10}$$

$$\begin{bmatrix} C'(S_t, a_t)_{\text{LA\_TC}} \\ C'(S_t, a_t)_{\text{LA\_TF}} \end{bmatrix} = \begin{bmatrix} 2\left(C(S_t, a_t)\right) \\ 2\left(C(S_t, a_t)\right) \end{bmatrix} \tag{11}$$

$$\begin{bmatrix} C'(S_t, a_t)_{\text{LA\_TC}} \\ C'(S_t, a_t)_{\text{LA\_TF}} \end{bmatrix} = \begin{bmatrix} C(S_t, a_t) + \left(\text{min\_dist} - min\left(\boldsymbol{x}_t^j - \boldsymbol{x}_t^{CNA}\right)\right)^3 \\ C(S_t, a_t) + \left(max\left(\boldsymbol{x}_t^j - \boldsymbol{x}_t^{CNA}\right) - \text{max\_dist}\right)^2 \end{bmatrix} \tag{12}$$

In considering the various non-look-ahead distance penalties, it is useful to consider the failure point for each pair of equations. Failure would be the point where the penalized cost for a heading and pitch option that is too far from one of the survey AUVs is lower than the penalized cost for another heading and pitch option that is too close to one of the survey AUVs (causing the CNA to come too close to a survey AUV and risk a collision). In comparing the original distance penalties, (4) and (5), with the assumption that the original cost in both the "too close" and "too far" cases are the same (not true, but the costs will be relatively close), the "too close" option will be chosen over the "too far" option when the magnitude of the violation for the "too far" option is greater than twice the magnitude of the violation for the "too close" option, as shown in (13) (TF = too far, TC = too close). Using the maximum and minimum allowable distance used in this thesis (1000 m and 100 m respectively), the failure point would occur when $max(\mathbf{x}^{\mathbf{j}}_{\mathbf{t}} - \mathbf{x}_{\mathbf{t}}^{\mathbf{CNA}}) + 2 \times min(\mathbf{x}^{\mathbf{j}}_{\mathbf{t}} - \mathbf{x}_{\mathbf{t}}^{\mathbf{CNA}}) > 1200$ m. This could occur in any number of combinations, but one example would be where $min(\mathbf{x}^{j}_{t} - \mathbf{x}_{t}^{CNA}) = 99$ m and $max(\mathbf{x}^{j}_{t} - \mathbf{x}_{t}^{CNA}) = 1003$ m.

$$\left(max\left(\boldsymbol{x}_t^j - \boldsymbol{x}_t^{CNA}\right) - \text{max\_dist}\right)_{\text{TF}} > 2\left(\text{min\_dist} - min\left(\boldsymbol{x}_t^j - \boldsymbol{x}_t^{CNA}\right)\right)_{\text{TC}} \quad (13)$$

The failure point for (6) is actually more easily found than for (4) and (5) as shown in (14), but there is an advantage to using (6) when all heading/pitch options are either too far or too close (primarily in the single AUV case) as the worst of the unsatisfactory (too far or too close) options will be substantially less likely to be chosen than the least unsatisfactory option. Similarly, the failure point for (7) is even lower than for (6) as shown in (15), but there remains the potential benefit of cubing the magnitude of the distance violation.

$$\left(max\left(\boldsymbol{x}_t^j - \boldsymbol{x}_t^{CNA}\right) - \text{max\_dist}\right)_{\text{TF}} > \sqrt{2}\left(\text{min\_dist} - min\left(\boldsymbol{x}_t^j - \boldsymbol{x}_t^{CNA}\right)\right)_{\text{TC}} \quad (14)$$

$$\left(max\left(\boldsymbol{x}_t^j - \boldsymbol{x}_t^{CNA}\right) - \text{max\_dist}\right)_{\text{TF}} > \sqrt[3]{2}\left(\text{min\_dist} - min\left(\boldsymbol{x}_t^j - \boldsymbol{x}_t^{CNA}\right)\right)_{\text{TC}} \quad (15)$$

The failure points for (8), (9), and (10) are shown in (16), (17), and (18) respectively. As above, the calculation of the failure point assumes that the cost of the too close option is equal to the cost of the too far option. If Cost = 0 (a conservative simplifying assumption), (8) would fail when the magnitude of the “too far” violation was more than 12.5 times the magnitude of the “too close” violation, (9) would fail when the magnitude of the “too far” violation was more than just 3.5 times the magnitude of the “too close” violation, and (10) would fail when the magnitude of the “too far” violation was more than just 2.3 times the magnitude of the “too close” violation. If different powers were employed, such as in (12), the failure point is shown in (19).

$$\left(max\left(\boldsymbol{x}_t^j - \boldsymbol{x}_t^{CNA}\right) - \text{max\_dist}\right)_{\text{TF}} > \tfrac{3}{2}\text{Cost} + \tfrac{25}{2}\left(\text{min\_dist} - min\left(\boldsymbol{x}_t^j - \boldsymbol{x}_t^{CNA}\right)\right)_{\text{TC}} \quad (16)$$

$$\left(max\left(\boldsymbol{x}_t^j - \boldsymbol{x}_t^{CNA}\right) - \text{max\_dist}\right)_{\text{TF}} > \sqrt{\tfrac{3}{2}\text{Cost} + \tfrac{25}{2}\left(\text{min\_dist} - min\left(\boldsymbol{x}_t^j - \boldsymbol{x}_t^{CNA}\right)\right)_{\text{TC}}^2} \quad (17)$$

$$\left(max\left(\boldsymbol{x}_t^j - \boldsymbol{x}_t^{CNA}\right) - \text{max\_dist}\right)_{\text{TF}} > \sqrt[3]{\frac{3}{2}\text{Cost} + \frac{25}{2}\left(\text{min\_dist} - min\left(\boldsymbol{x}_t^j - \boldsymbol{x}_t^{CNA}\right)\right)_{\text{TC}}^3} \tag{18}$$

$$\left(max\left(\boldsymbol{x}_t^j - \boldsymbol{x}_t^{CNA}\right) - \text{max\_dist}\right)_{\text{TF}} > \left(\text{min\_dist} - min\left(\boldsymbol{x}_t^j - \boldsymbol{x}_t^{CNA}\right)\right)_{\text{TC}}^{\frac{3}{2}} \tag{19}$$

Given the discussion above, it would appear that the best distance penalty would be (8). A series of simulations was run for two and five survey AUVs testing various distance penalties with both an ASC CNA and an AUV CNA. The survey AUVs run at a constant depth of 90 m. Both the CNA and the survey AUVs run at a constant speed of 1.5 m/s. Each survey AUV covers an area of 500 × 1500 m. The survey AUV areas are side-by-side starting from (0, 0) and going east, similar to Figure 5.26. Since the survey AUVs move in parallel, the maximum distance between survey AUVs in the two-survey AUV case is 500 m and the maximum distance between survey AUVs in the five survey AUV case is 2000 m. Given a maximum allowable distance between the CNA and any survey AUV is 1000 m (based on a conservative estimate of acoustic communication range), the five-survey AUV case would seem to be on the outer limits of the CNA's capability to support multiple survey AUVs. For multiple survey AUV operations in a wider area (e.g. five or more survey AUVs each covering an area greater than 500 m wide) it may be most beneficial to divide the survey AUVs into two or more independent groups each supported by a CNA. Alternatively, [31] presents a method of coordinating multiple CNAs for a single group of survey AUVs. This requires more coordination through acoustic communication, but could be more effective if the acoustic messages are able to be exchanged frequently enough.

Table 5.2: Distance penalty cases used in simulations (LA = look ahead)

Case No. and Legend Entry	Primary Penalty	LA Penalty	Description
1:Orig.(Orig. in LA)	(4) & (5)	(11)	Orig. Penalty (Orig. Penalty in LA)[21]
2a:Orig. (None in LA)	(4) & (5)	None	Orig. Penalty (No Penalty in LA)
2:No Penalty	None	None	No Penalty at All
3:None (Orig. in LA	None	(11)	Orig. Penalty only in LA
4:Orig.^{2} (Orig. in LA)	(6)	(11)	Orig. Penalty Squared (Orig. Penalty In LA)
5:Orig.^{2} (None in LA)	(6)	None	Orig. Penalty Squared (No Penalty in LA)
6:Orig.^{3} (Orig. in LA)	(7)	(11)	Orig. Penalty Cubed (Orig. Penalty in LA)
7:Orig.^{3} (None in LA)	(7)	None	Orig. Penalty Cubed (No Penalty in LA)
8:5×Cost (Orig. in LA)	(8)	(11)	5×Cost (Orig. Penalty in LA)
9:5×Cost (None in LA)	(8)	None	5×Cost (No Penalty in LA)
10:5×Cost^2 (Orig. in LA)	(9)	(11)	5×Cost Squared (Orig. Penalty in LA)
11:5×Cost^2 (None in LA)	(9)	None	5×Cost Squared (No Penalty in LA)
12:5×Cost^3 (Orig. in LA)	(10)	(11)	5×Cost Cubed (Orig. Penalty in LA)
13:5×Cost^3 (None in LA)	(10)	None	5×Cost Cubed (No Penalty in LA)
2b:Orig. (New in LA)	(4) & (5)	(12)	Orig. Penalty (New Penalty in LA)
3a:None (New in LA)	None	(12)	New Penalty only in LA
4a:Orig.^{2} (New in LA)	(6)	(12)	Orig. Penalty Squared (New Penalty in LA)
6a:Orig.^{3} (New in LA)	(7)	(12)	Orig. Penalty Cubed (New Penalty in LA)
8a:5×Cost (New in LA)	(8)	(12)	5×Cost (New Penalty in LA)
10a:5×Cost^2 (New in LA)	(9)	(12)	5×Cost Squared (New Penalty in LA)
12a:5×Cost^3 (New in LA)	(10)	(12)	5×Cost Cubed (New Penalty in LA)

Considering the case of two survey AUVs supported by an ASC CNA, Figure 5.2 shows the average cost (a measure of the position error of all survey AUVs) as the look-ahead level (L) increases for all the distance penalties tested; Figure 5.3 shows the best 12 cases from Figure 5.2; Figure 5.4 shows the maximum distance between the ASC CNA and either survey AUV as look-ahead level (L) increases; Figure 5.5 shows the best 12 cases from Figure 5.4; and Figure 5.6 shows the minimum distance between the ASC CNA and either survey AUV as look-ahead level (L) increases.

[21] Case numbers are not sequential as they evolved during experimentation and are copied from the author's log book for simplicity of reference.

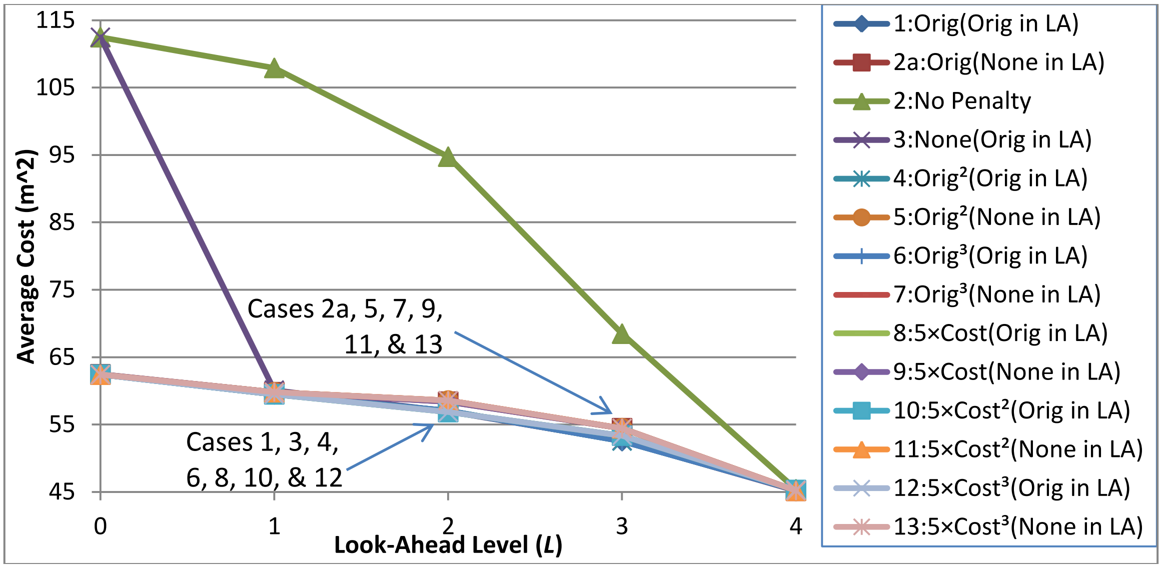

Figure 5.2: Average cost (3) vs. look-ahead for $N = 2$ case with an ASC CNA, illustrating the effect of different distance penalties

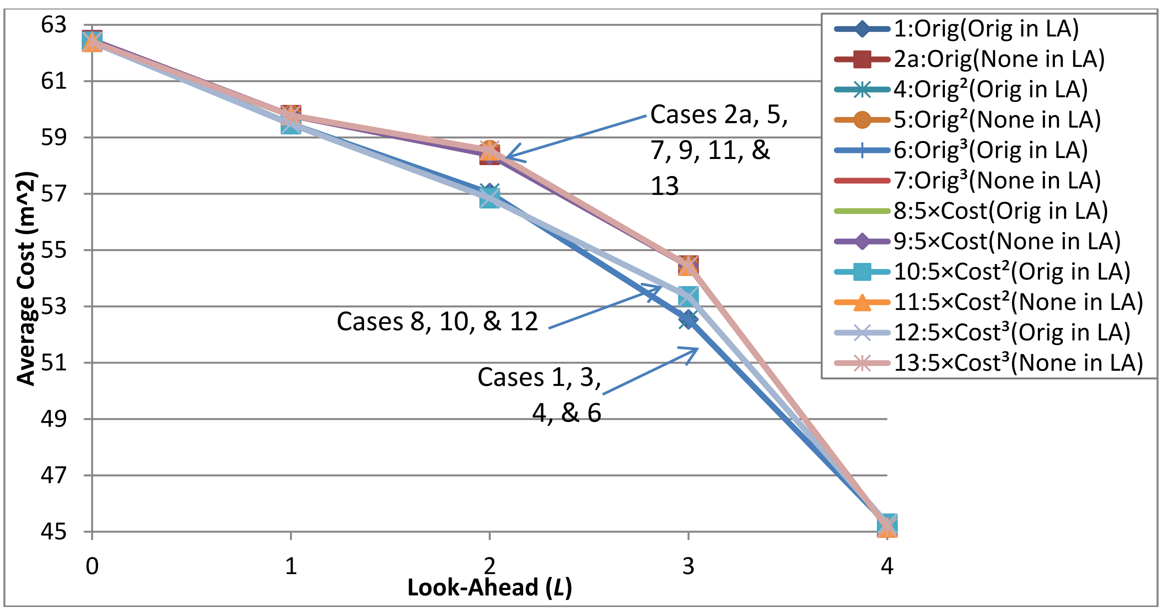

Figure 5.3: Average cost (3) vs. look-ahead for $N = 2$ case with an ASC CNA, illustrating the effect of different distance penalties; best results

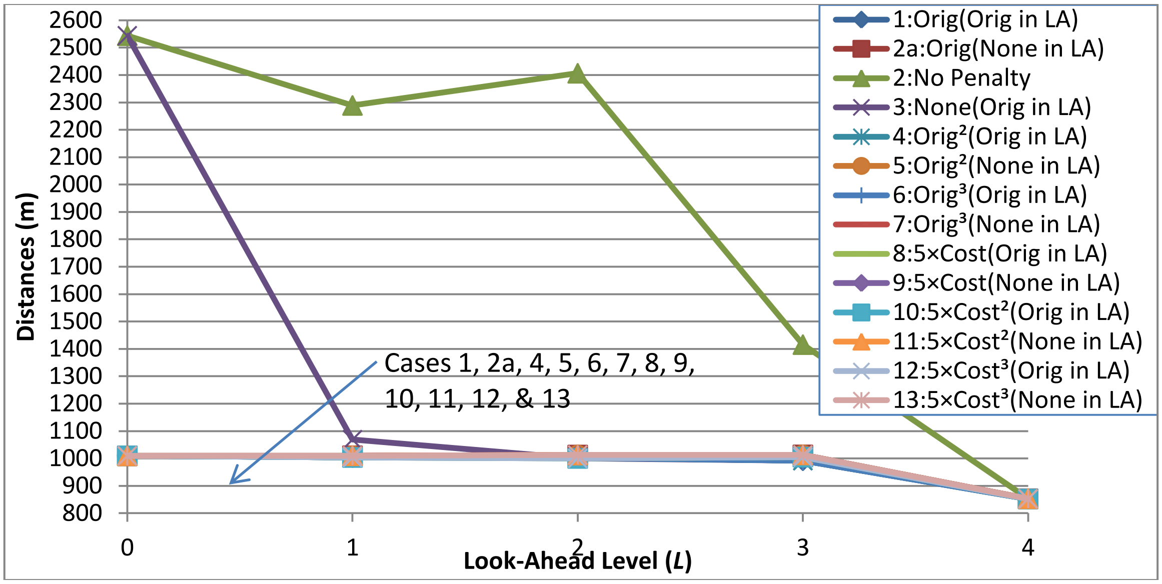

Figure 5.4: Maximum distance vs. look-ahead for $N = 2$ case with an ASC CNA, illustrating the effect of different distance penalties

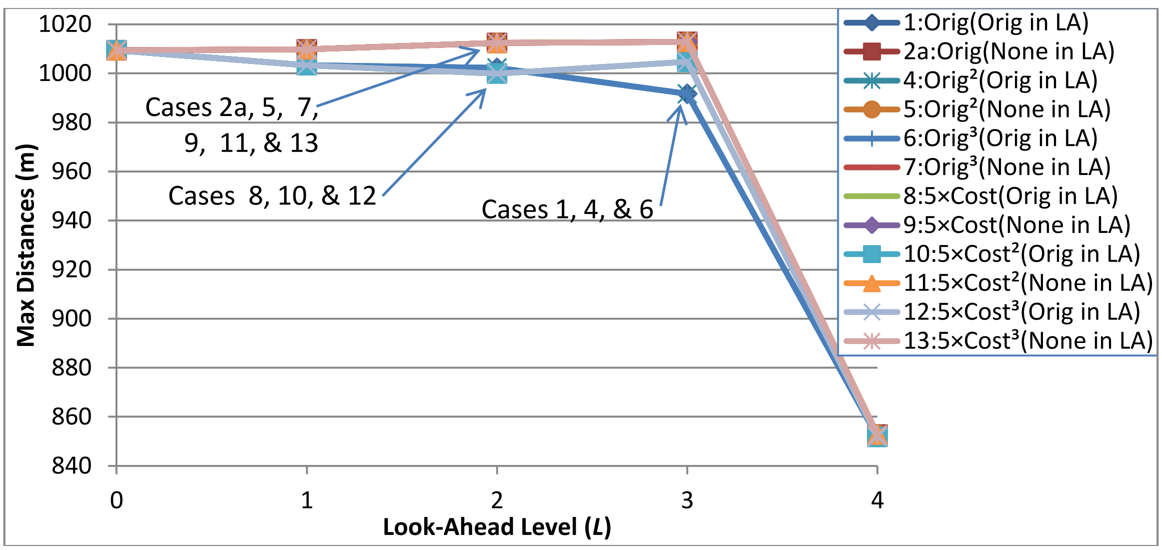

Figure 5.5: Maximum distance vs. look-ahead for $N = 2$ case with an ASC CNA, illustrating the effect of different distance penalties; best results

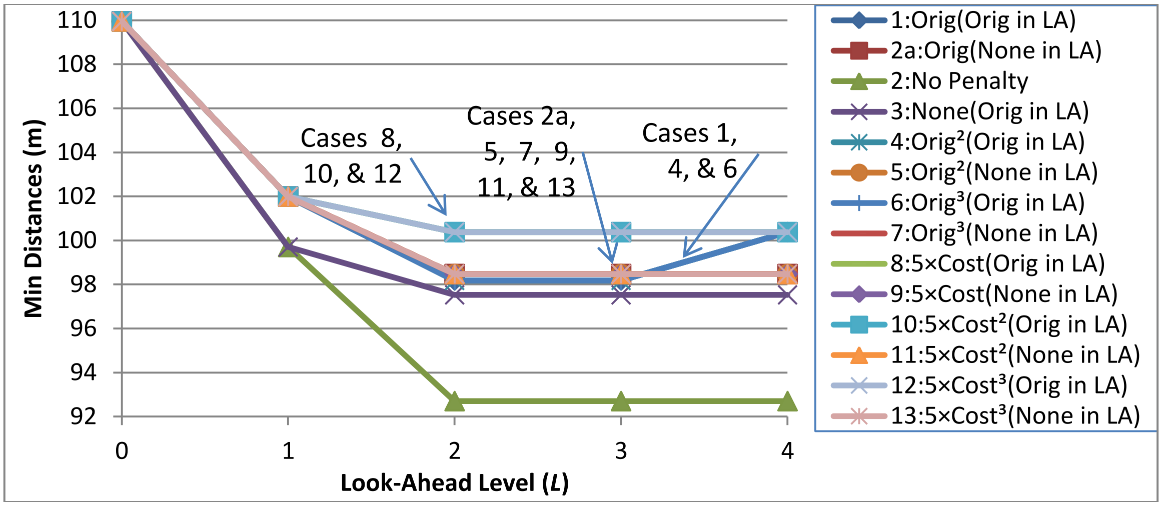

Figure 5.6: Minimum distance vs. look-ahead for $N = 2$ case with an ASC CNA, illustrating the effect of different distance penalties

Some conclusions may be drawn from these plots. First, any penalty is better than no penalty at all, although look-ahead $L = 4$ is able to bring the no penalty case into line with the best penalty cases for average cost and maximum distance (maintaining minimum distance is not possible without a penalty as the path planning algorithm does not consider it). Notice that the case where the distance penalty is only applied in the look-ahead function (case 3) is the same as the no penalty case (case 2) when $L = 0$. Second, cubing or squaring the magnitude of the distance violation does not measurably affect the results of the simulations (though it does slightly increase the computational load). Third, (considering Figure 5.3) it appears that cases 1, 4, and 6 have the lowest average cost overall, though not much lower than cases 8, 10, and 12. Fourth, (considering Figure 5.3 and Figure 5.5) including the penalty in the look-ahead function (simple though it is) does serve to improve both average cost (a measure of survey AUV position error) and maintenance of desired distances. Based on this information, case 8 (5×cost with the original penalty in the look-ahead) appears to be the best distance penalty combination considered for the ASC CNA with two survey AUVs.

The simulations for the two survey-AUV case above were repeated with five survey AUVs. Figure 5.7 shows the average cost (a measure of the survey AUVs' position error), Figure 5.8 shows the maximum distance of the ASC CNA from any survey AUV, and Figure 5.9 shows the minimum distance of the ASC CNA from any survey AUV.

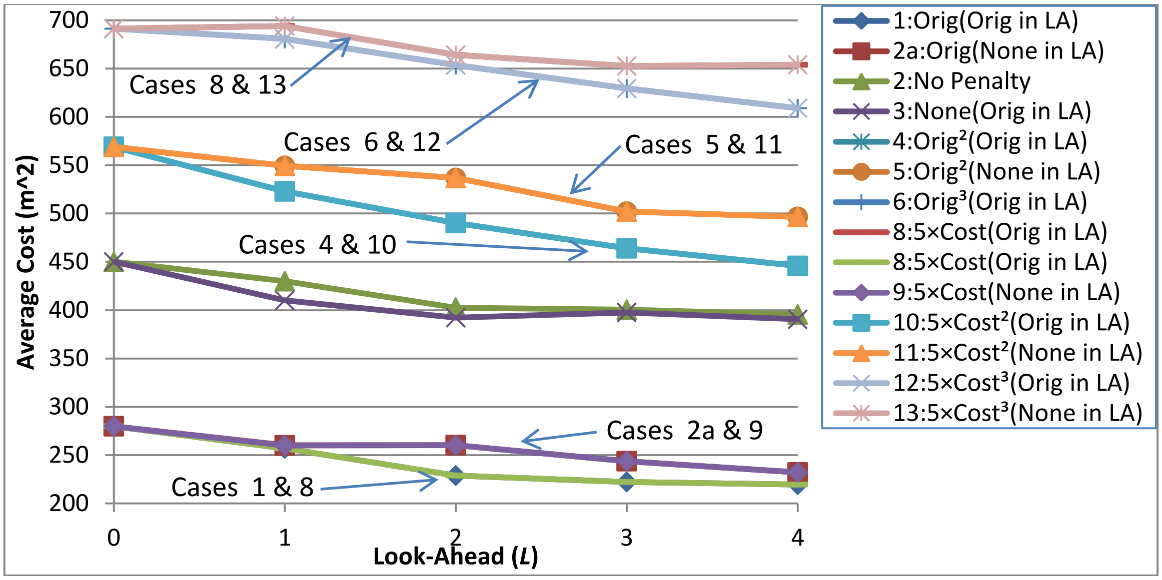

Figure 5.7: Average cost (3) vs. look-ahead for $N = 5$ case with an ASC CNA, illustrating the effect of different distance penalties

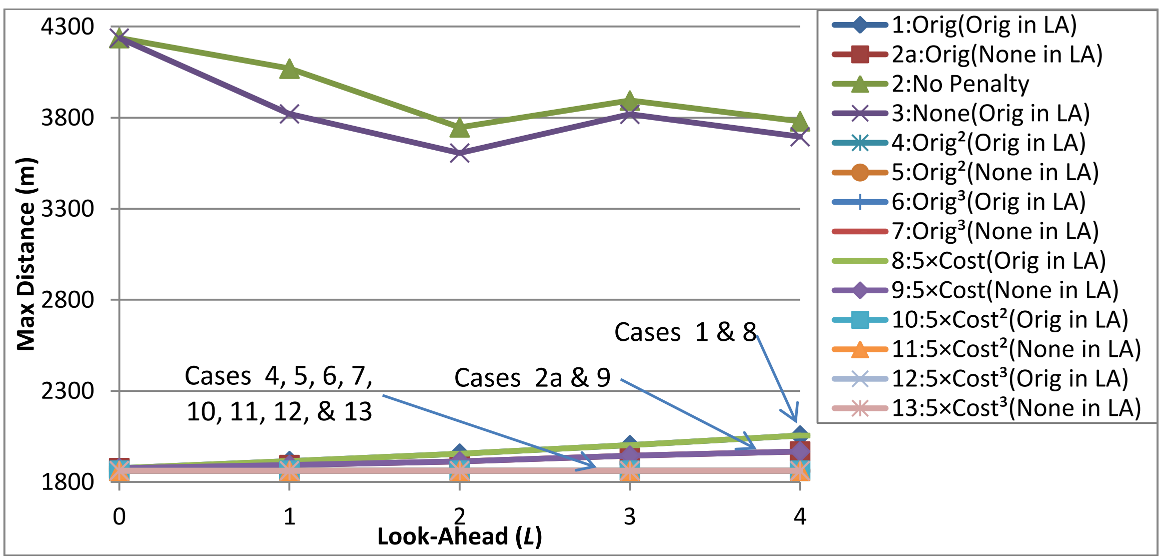

Figure 5.8: Maximum distance vs. look-ahead for $N = 5$ case with an ASC CNA, illustrating the effect of different distance penalties

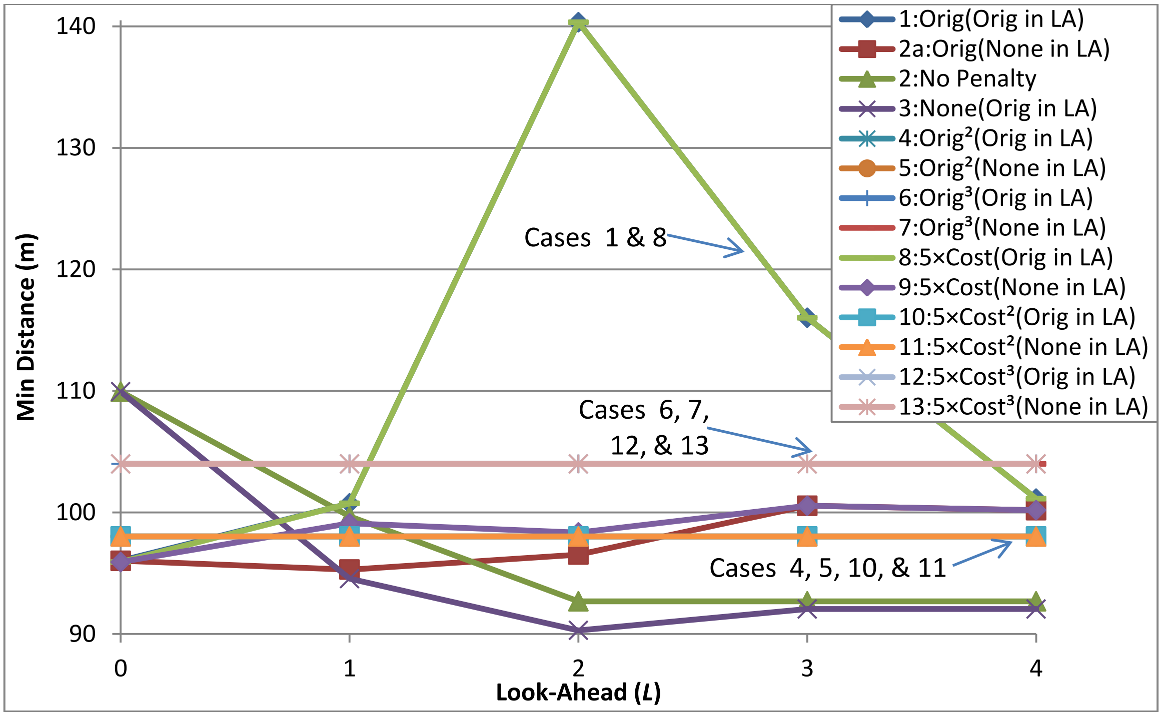

Figure 5.9: Minimum distance vs. look-ahead for $N = 5$ case with an ASC CNA, illustrating the effect of different distance penalties

The results of this set of simulations are significant. First, unlike the two survey AUV case, using no distance penalty at all is does *not* produce the worst results. In Figure 5.7, the penalties including cubed or squared terms (cases 4 – 7 and 10 - 13) produce poorer results than cases 2 and 3. As was discussed in the context of Figure 5.1, a look-ahead level greater than $L = 4$ was not possible with five survey AUVs due to the size of the matrices required for the computations. One would assume that if arbitrarily higher levels of look-ahead were possible, the average cost of all distance penalty configurations would converge on a single, low average cost as is seen in Figure 5.2. Second, unlike the two survey AUV case, squaring or cubing the distance penalty does significantly affect the results of the simulations. As noted above, the squared and cubed distance penalties result in a much higher cost than the other penalties. However, the squared and cubed penalties do not allow the maximum distance between the CNA and any survey AUV to exceed the initial distance between the CNA and the furthest survey AUV (1862 m), Figure 5.8. From Figure 5.9, it can be seen that the cubed penalties (cases 6, 7, 12, and 13) are able to maintain the required minimum distances while the squared penalties (cases 4, 5, 10, and 11) cannot. Third, (considering Figure 5.7) the lowest average cost is achieved by cases 1 and 8. The second best average cost is achieved by these penalties with no penalty in the look-ahead function (cases 2a and 9). In fact, turning off the penalty in the look-ahead function increases the average cost for all distance penalty cases. Considering Figure 5.7, Figure 5.8, and Figure 5.9, cases 1 and 8 seem to be the most effective penalties. This is clear from Figure 5.7, but the increasing trend in Figure 5.8 was not expected nor was the parabolic curve described in Figure 5.9. The best explanation seems to be that the $N = 5$ case is near the limit of the planner's ability to effectively aid the survey AUVs, especially considering the maximum distance requirement of 1000 m. The squared and cubed distance penalties may perform poorly in terms of average cost because the magnitude of the distance penalty is so much greater than the original cost calculation (based on (1)) that the best subsequent CNA heading in terms of survey AUV position error is not significant. The challenge of maintaining both minimum and maximum distances cannot be done throughout by the squared distance penalties (cases 4, 5, 10, and 11), though the cubed distance penalties (cases 6, 7, 12, and 13) were able to do this (Figure 5.8 and Figure 5.9). This is surprising in light of the failure point discussion above where it was decided that cubed penalties ((7) and (10)) were much more susceptible to favouring a too close option over a too far option than squared terms ((6) and (9)). An explanation of this result is not presently forthcoming. The violations of the minimum distance limit can be attributed to insufficient penalties. Specifically, other than with the squared and cubed distance penalties, in this set of simulations, a penalty is required in the look-ahead function (cases 2a and 9) but is not sufficient on its own (case 3). In addition, it was shown in [93] that increasing the look-ahead level typically decreases the minimum distance in the mission (cases 2 and 3). Why (8) does not outperform (4) in maintaining the minimum distance for $L = 0$ (Figure 5.9) is also unknown; based on the failure point discussion, it certainly should have.

The distance penalty simulations above dealt with the ASC CNA case. The AUV CNA case is similar, but has the additional need to maintain maximum and minimum depths. In the look-ahead function, proper depth is maintained with a simple 2×Cost penalty. In the main path planning function, proper depth is maintained by removing the offending heading/pitch options as done for distance in [93].

The results for the $N = 2$ AUV CNA case closely resemble those of the $N = 2$ ASC CNA case. There are however some differences. First, case 3 performs much better in the AUV CNA simulations than the ASC CNA simulations (Figure 5.10 through Figure 5.13); in fact it is among the very best. However, it poorly manages the minimum distance requirement (Figure 5.14). From Figure 5.11 it appears that apart from cases 1 and 2a, the presence of the penalty in the look-ahead function does not affect the simulation. In case 1, the penalty in the look-ahead function is helpful. Also in Figure 5.11, the average cost for cases 1, 2a, 4, 5, 6, and 7 alternates in value with cases 8 – 13 from $L = 1$ to $L = 4$. Presumably, they will converge at $L = 5$ or shortly thereafter. Like the ASC CNA case, cubing or squaring the penalty is not helpful. Maximum distances are all quite close together except case 2a. In Figure 5.14, as in Figure 5.10, results for cases 1, 2a, 4, 5, 6, and 7 are quite close together as are the results for cases 8 – 13. Cases 8 – 13 generally do the best job of maintaining the required minimum distances. Thus for simulations with two survey AUVs and an AUV ASC the best distance penalties are still Cases 8 and 9.

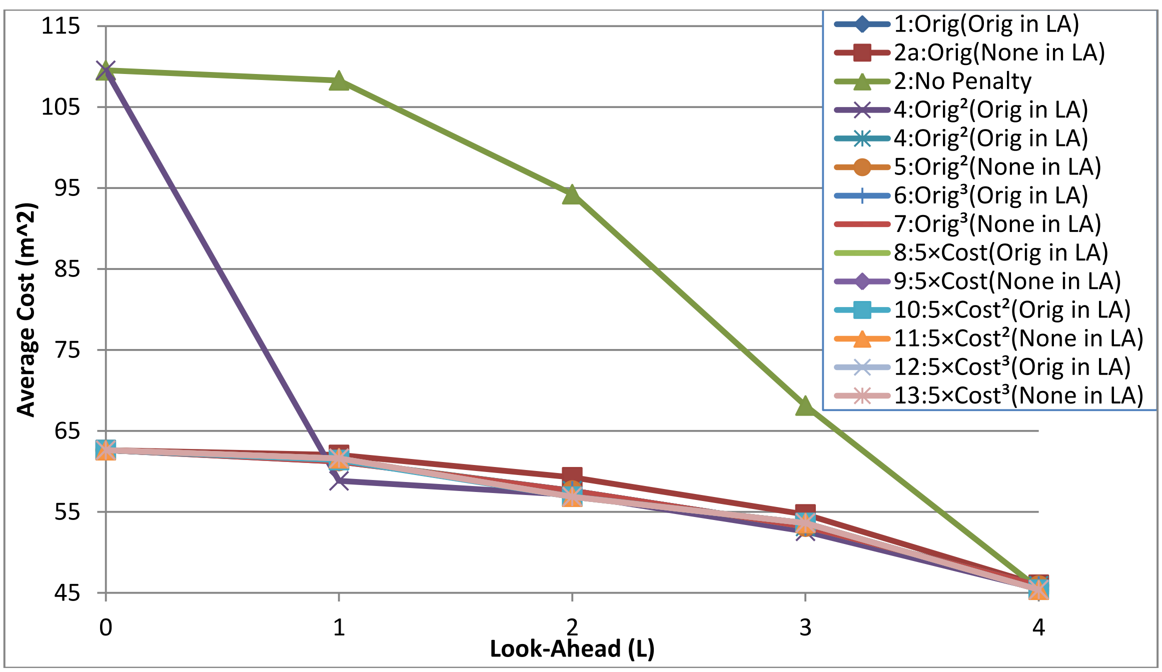

Figure 5.10: Average cost (3) vs. look-ahead for $N = 2$ case with an AUV CNA, illustrating the effect of different distance penalties (detail view in Figure 5.11)

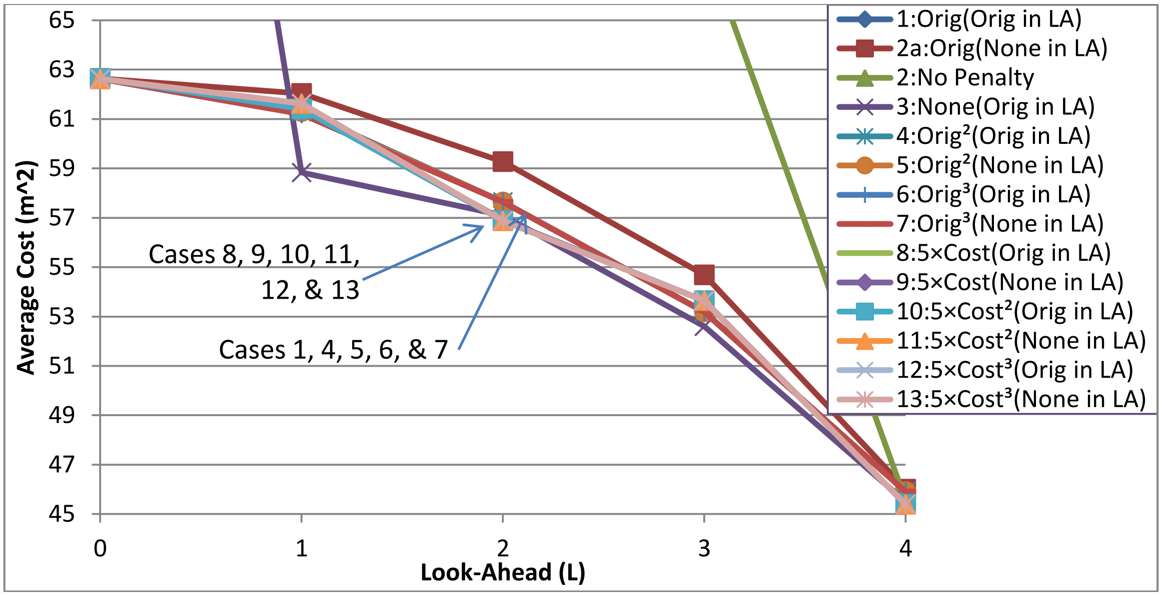

Figure 5.11: Average cost (3) vs. look-ahead for $N = 2$ case with an AUV CNA, illustrating the effect of different distance penalties, detail view

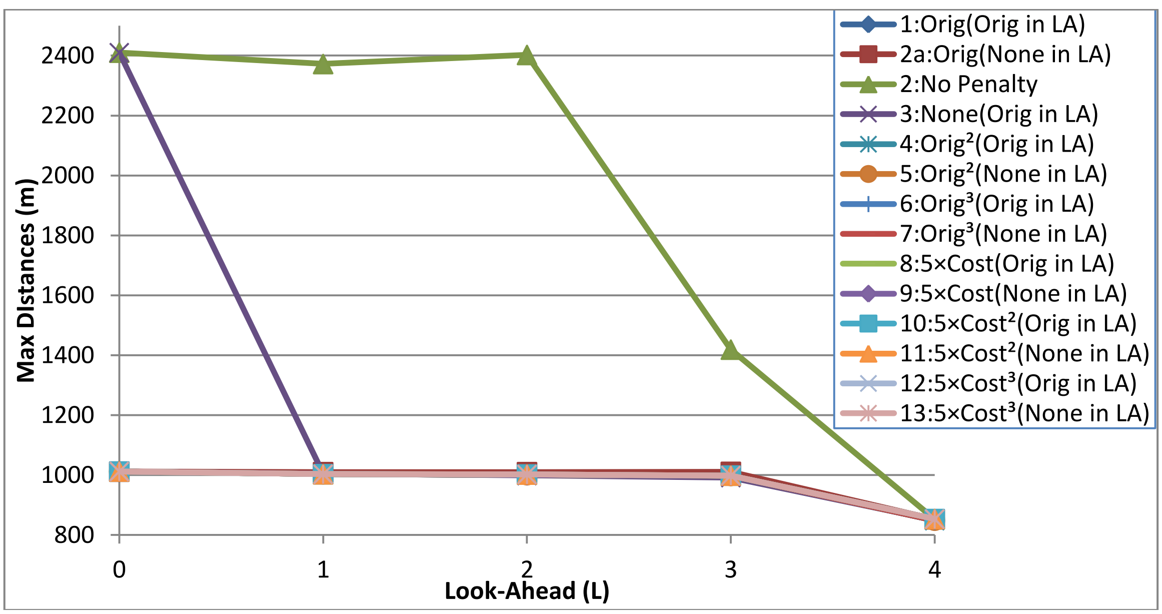

Figure 5.12: Maximum distance vs. look-ahead for $N = 2$ case with an AUV CNA, illustrating the effect of different distance penalties (detail view in Figure 5.13)

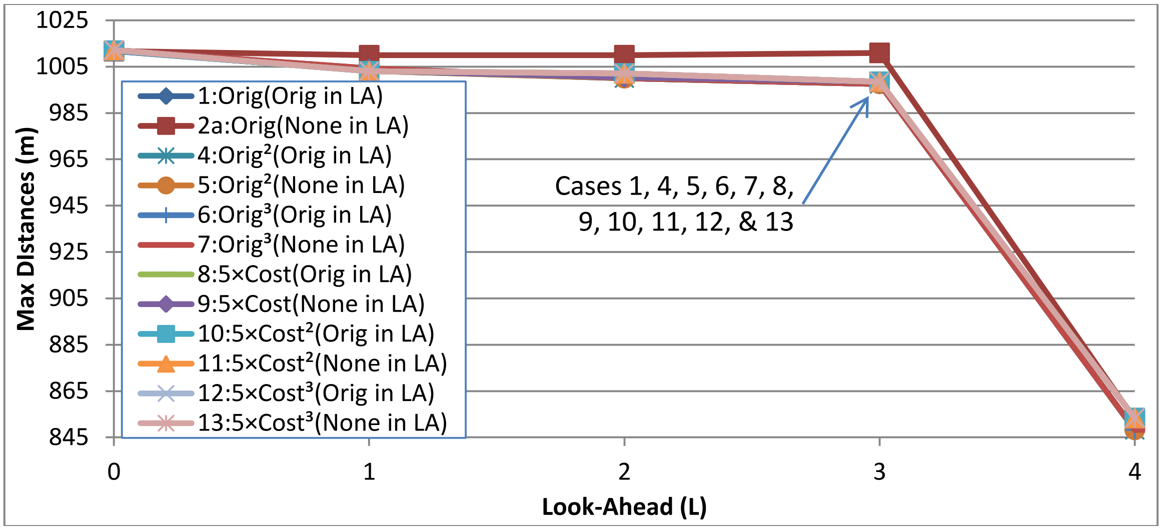

Figure 5.13: Maximum distance vs. look-ahead for $N = 2$ case with an AUV CNA, illustrating the effect of different distance penalties, best results

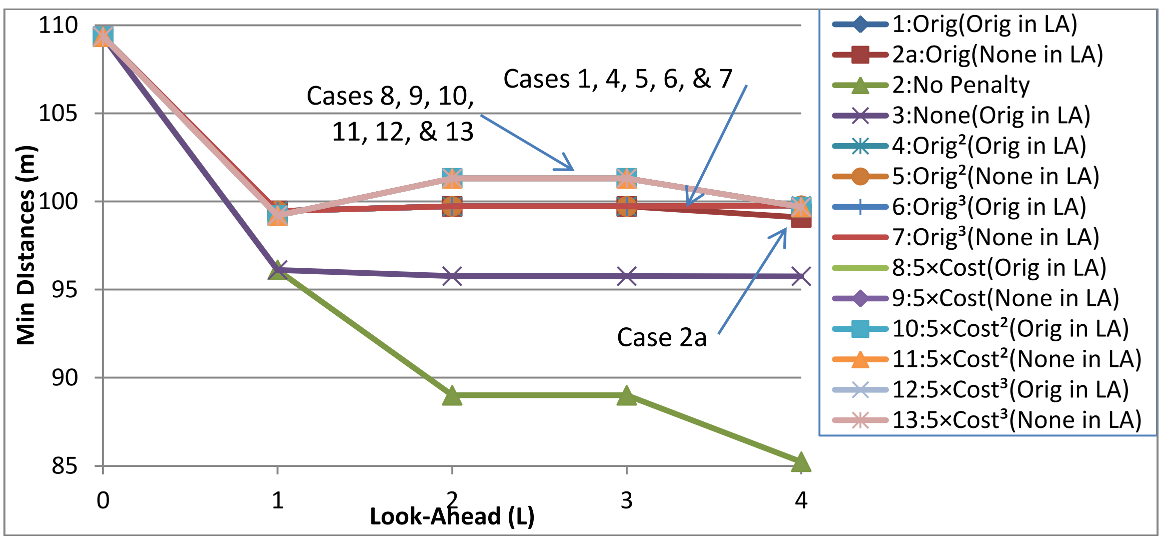

Figure 5.14: Minimum distance vs. look-ahead for $N = 2$ case with an AUV CNA, illustrating the effect of different distance penalties

The five survey-AUV simulations with an AUV CNA resemble the five survey-AUV simulations with an ASC CNA. There are however some significant differences. First, in Figure 5.15, the worst cases are 6, 7, 12, and 13. The next worst cases are 4 and 5 followed by 10 and 11. The best performers were cases 1, 8, and 9. In Figure 5.17 and Figure 5.18, as in Figure 5.8, the maximum distance is best maintained by the squared and cubed penalties (at the initial maximum distance of 1862 m) while cases 1, 2a, 8, and 9 have an increasing maximum distance with increasing look-ahead (there was no reason to expect this other than that it was seen in the ASC CNA simulations). Figure 5.19 is similar to Figure 5.9 in that the cubed and squared penalties with and without look-ahead penalties hold consistent minimum distances across look-ahead levels. Also, the cubed penalties are within the minimum limit and the squared penalties are outside the minimum limit. The major difference between Figure 5.19 and Figure 5.9 is the extremely poor performance of case 1 compared to cases 8 and 9 when $L = 1$. This is not unexpected as cases 8 and 9 are designed to improve on case 1's handling of the "too close" situation. It is interesting that from $L = 2$ to $L = 3$ the look-ahead seems to make up for the shortcomings of case 1 provided there is a penalty in the look-ahead function. At $L = 4$, a penalty in the look-ahead function is not needed to maintain the minimum distance in Case 1 or 2a. For cases 8 and 9, the penalty in the look-ahead function has no effect. This non-effect of the look-ahead distance penalty for cases 8 and 9 is the most significant result of the $N = 5$ AUV CNA simulations. As case 9 was better than case 8 in the ASC CNA case, the author's recommendation is to use case 9 since the increased computational cost is negligible.

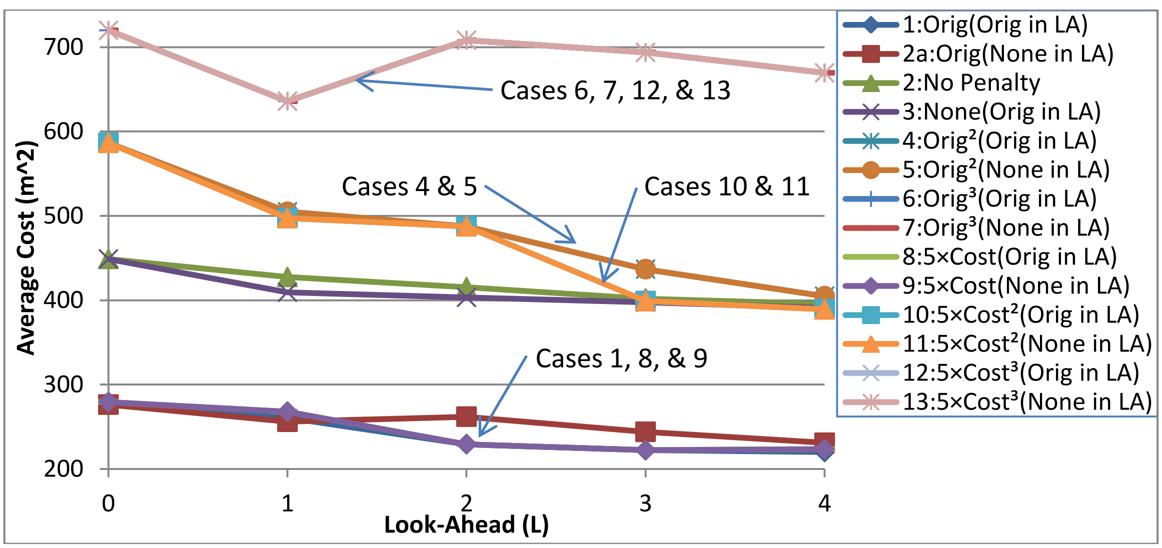

Figure 5.15: Average cost (3) vs. look-ahead for $N = 5$ case with an AUV CNA, illustrating the effect of different distance penalties

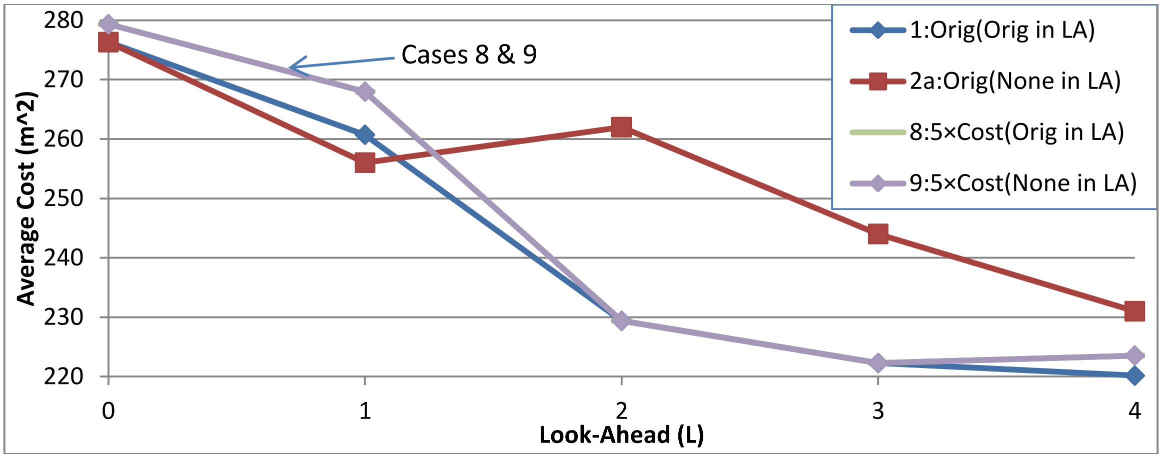

Figure 5.16: Average cost (3) vs. look-ahead for $N = 5$ case with an AUV CNA, illustrating the effect of different distance penalties, best results

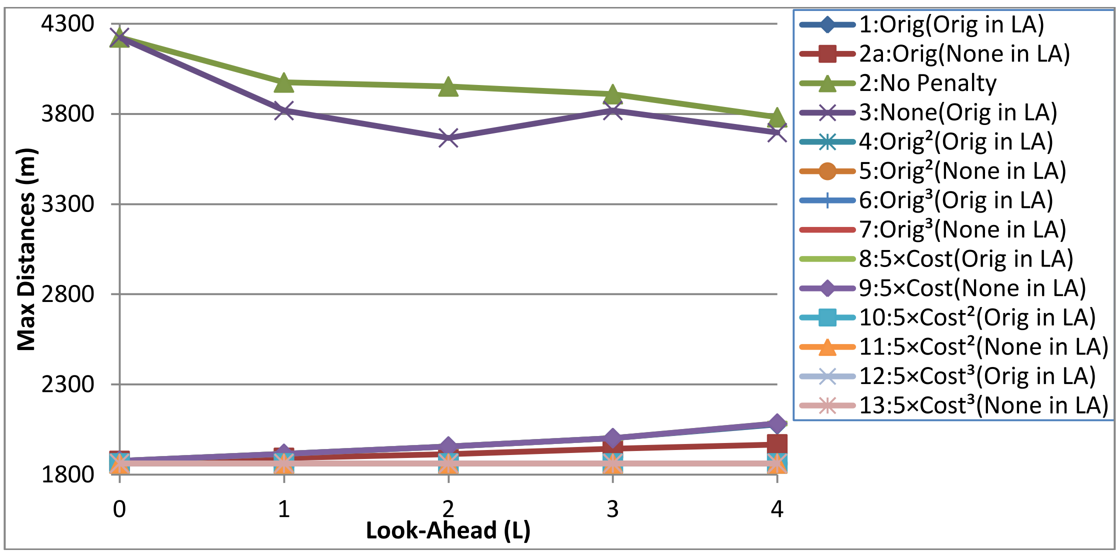

Figure 5.17: Maximum distance vs. look-ahead for $N = 5$ case with an AUV CNA, illustrating the effect of different distance penalties (detail view in Figure 5.18)

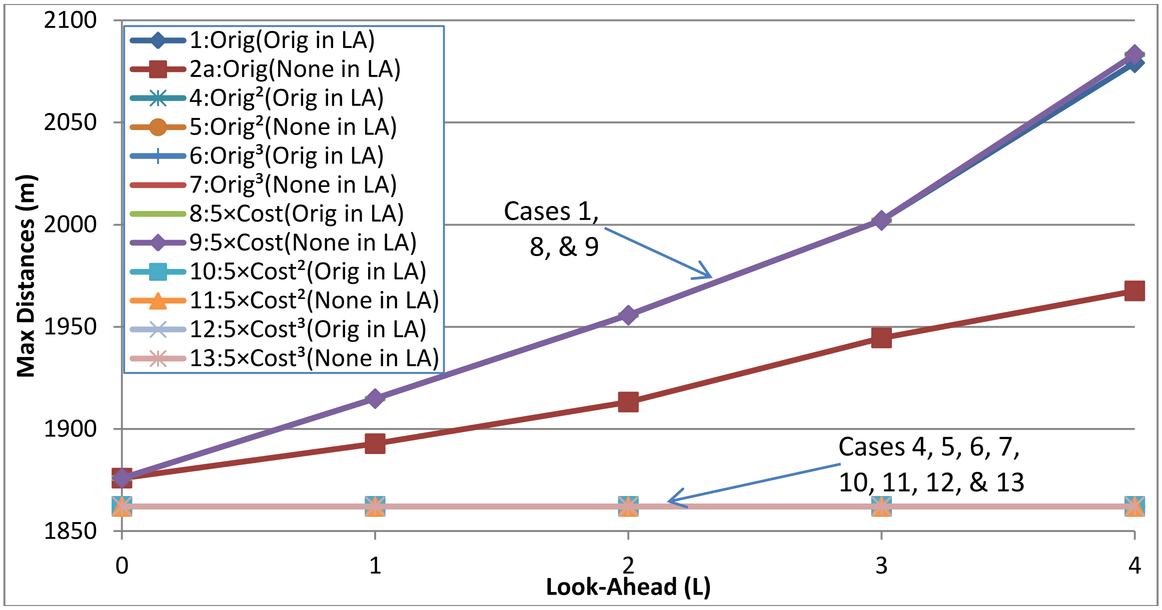

Figure 5.18: Maximum distance vs. look-ahead for $N = 5$ case with an AUV CNA, illustrating the effect of different distance penalties, best results

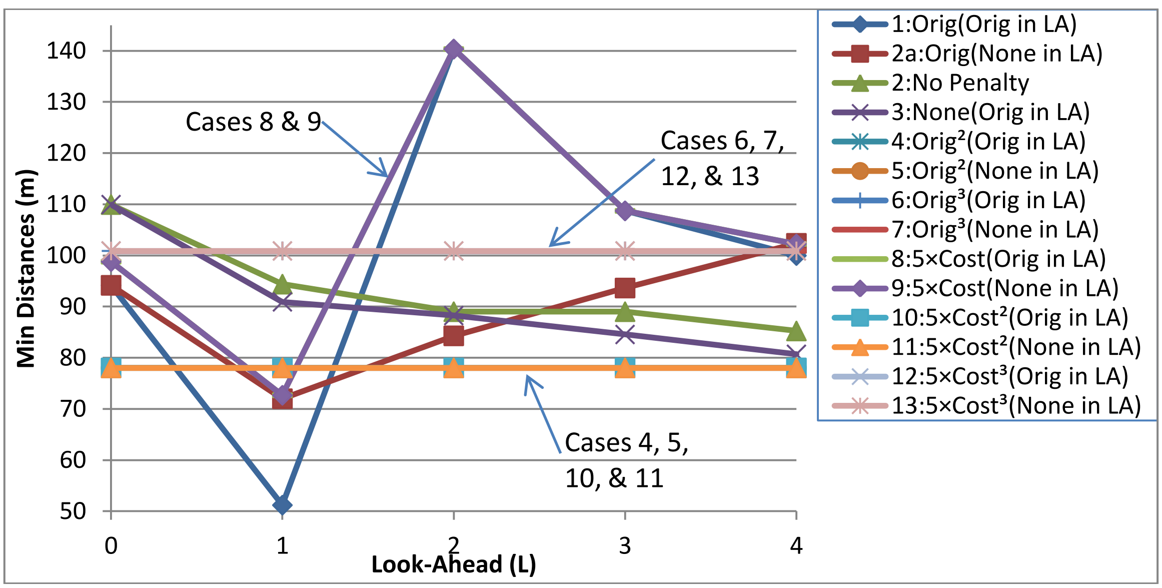

Figure 5.19: Minimum distance vs. look-ahead for $N = 5$ case with an AUV CNA, illustrating the effect of different distance penalties

The look-ahead function distance penalty described in (12) was a logical extension of the other distance penalties used. It was tested in AUV CNA simulations[22] for $N = 2$ and $N = 5$. As (12) adds some computation cost to the simulation (a squared or cubed term to the look-ahead function, which is run $(A \cdot B)^L$-times per time step), there would need to be an improvement in performance to justify its usage. Reviewing the figures for the $N = 2$

[22] The $L = 0$ case for $N = 2$ has not been done. This was an oversight, but since the look-ahead penalty does not apply in $L = 0$ case, no data was lost.

case (Figure 5.20 through Figure 5.22), none of the simulations with (12) have better performance than simulations with (11) or no look-ahead penalty. Reviewing the figures for the $N = 5$ case (Figure 5.23 through Figure 5.25), none of the simulations with (12) has lower average cost or more consistent maximum distance than the previous simulations, though cases 6a and 12a do have the best minimum distance compliance. It is therefore concluded that using (12) in the look-ahead function is not advantageous. If further simulations were to be run, using (8) in the look-ahead function could be a profitable investigation as it has previously proved to be quite effective.

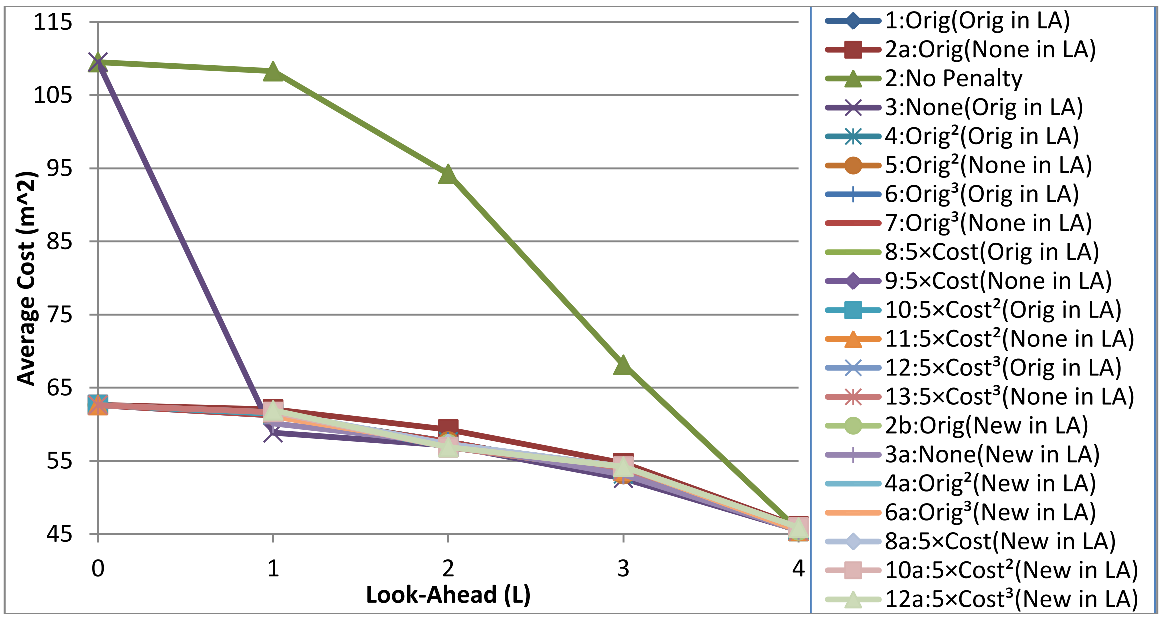

Figure 5.20: Average cost (3) vs. look-ahead for $N = 2$ case with an AUV CNA, illustrating the effect of the modified look-ahead distance penalties (compare with Figure 5.10)

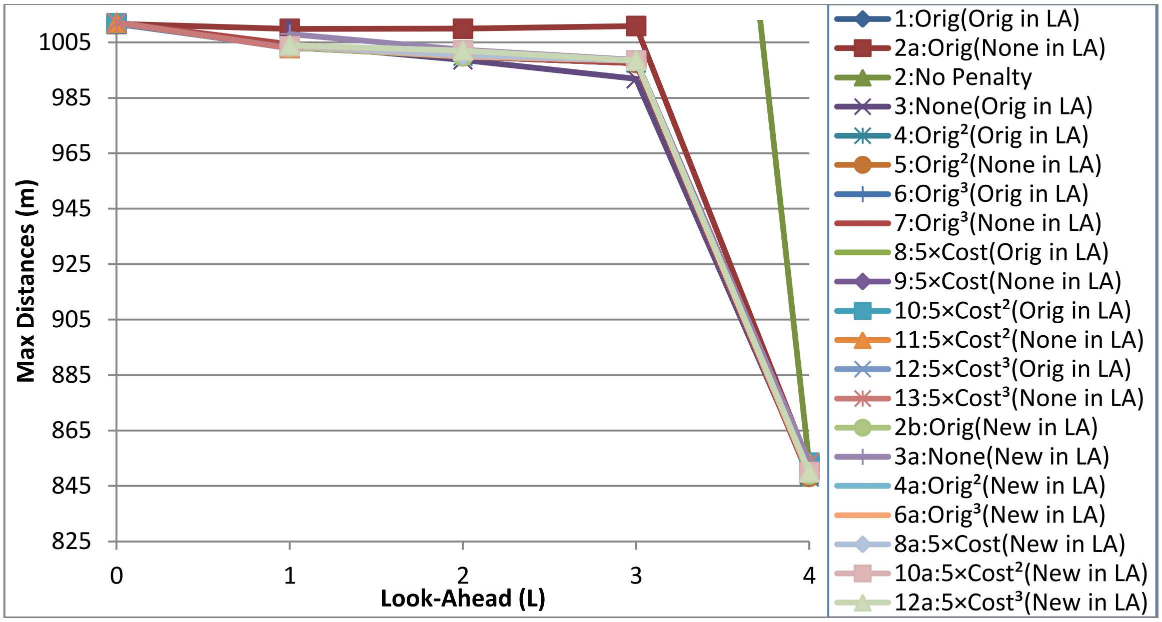

Figure 5.21: Maximum distance vs. look-ahead for $N = 2$ case with an AUV CNA, illustrating the effect of the modified look-ahead distance penalties (compare with Figure 5.12)

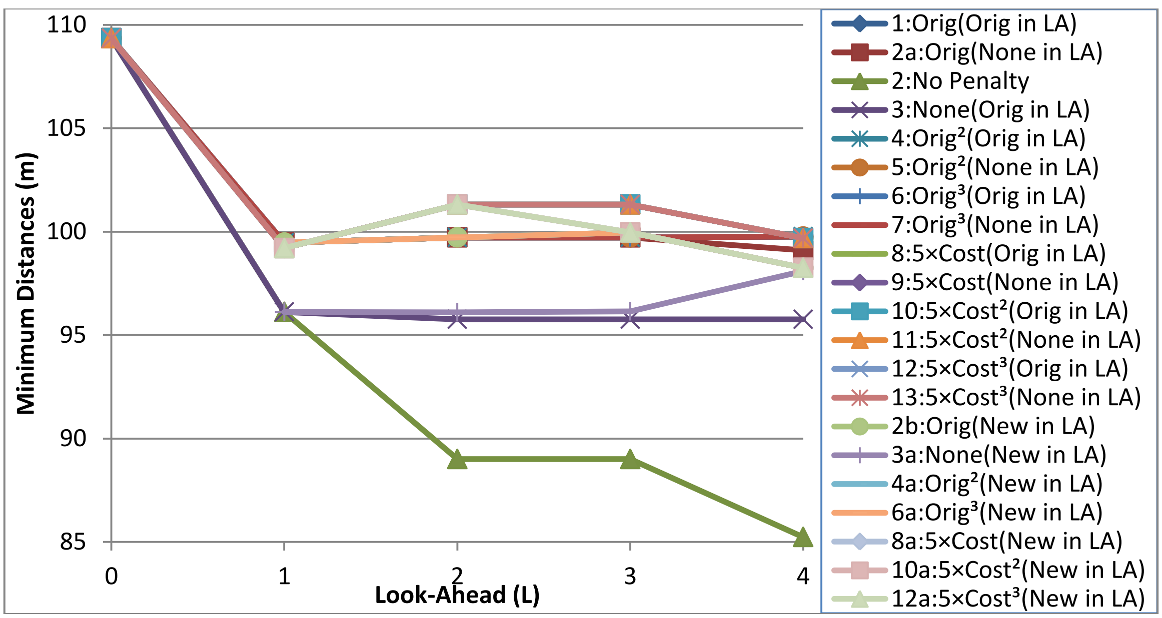

Figure 5.22: Minimum distance vs. look-ahead for $N = 2$ case with an AUV CNA, illustrating the effect of the modified look-ahead distance penalties (compare with Figure 5.14)

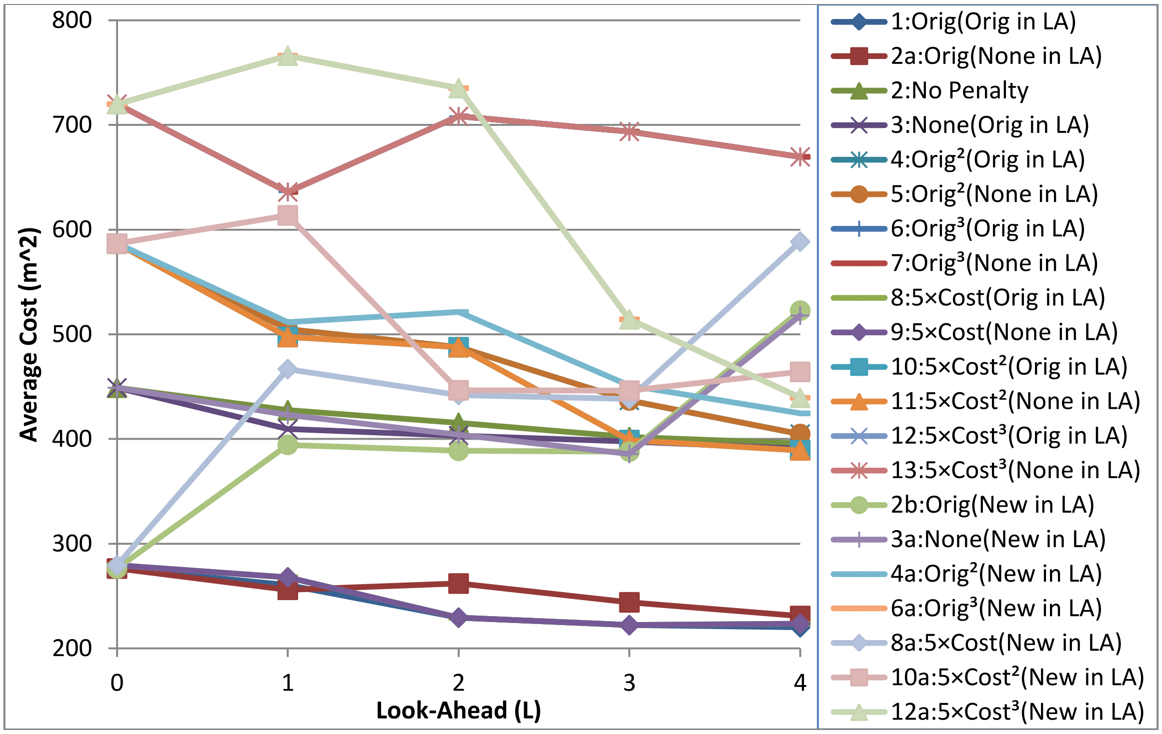

Figure 5.23: Average cost (3) vs. look-ahead for $N = 5$ case with an AUV CNA, illustrating the effect of the modified look-ahead distance penalties (compare with Figure 5.15)

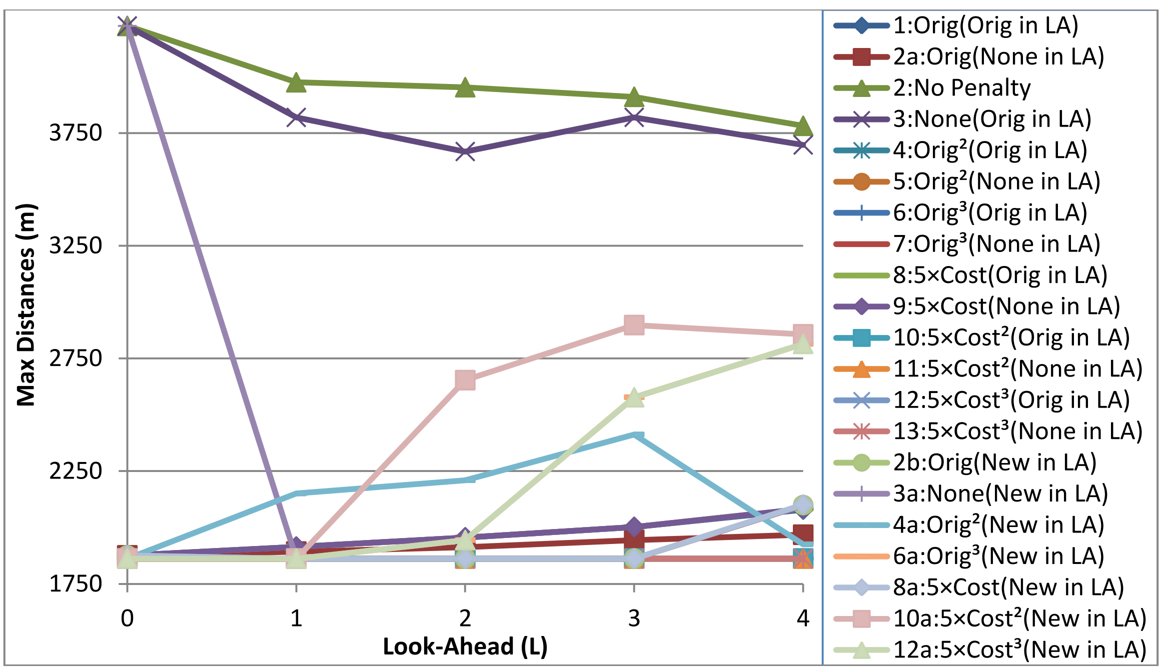

Figure 5.24: Maximum distance vs. look-ahead for $N = 5$ case with an AUV CNA, illustrating the effect of the modified look-ahead distance penalties (compare with Figure 5.17)

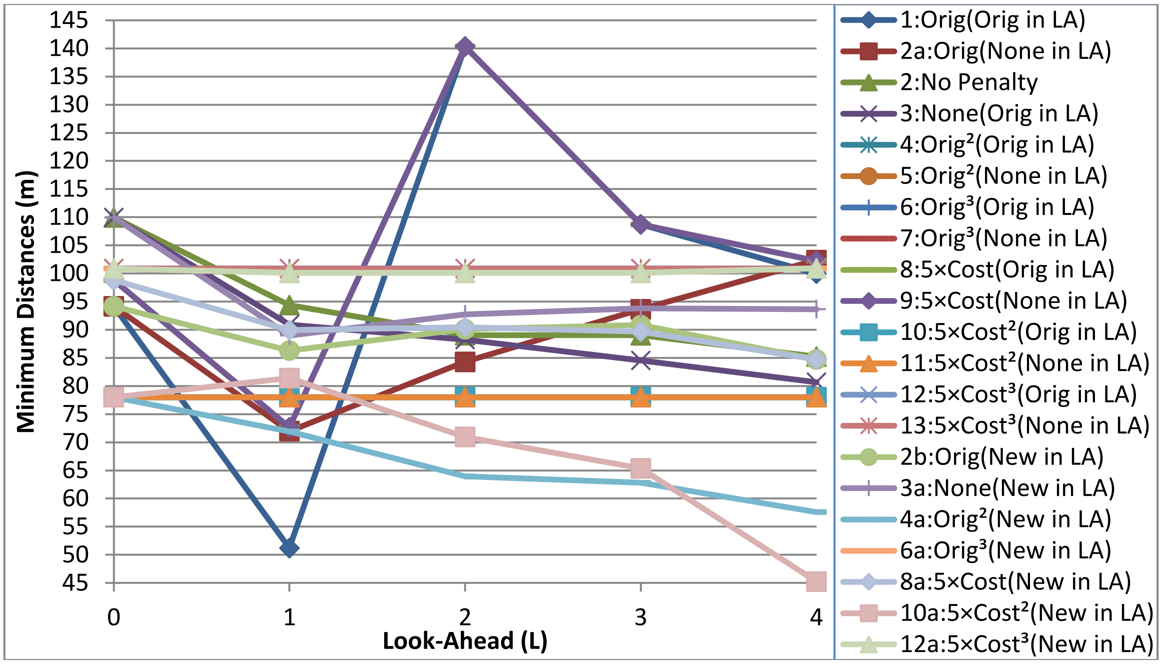

Figure 5.25: Minimum distance vs. look-ahead for $N = 5$ case with an AUV CNA, illustrating the effect of the modified look-ahead distance penalties (compare with Figure 5.19)

5.3. Effect of Variable Depth

In order to demonstrate the algorithm's effectiveness with multiple survey AUVs, simulations were performed with 1, 2, 3, 4, and 5 survey AUVs. Both an ASC and an AUV are used as the CNA vehicle. The time step was $\tau = 10$ sec. Heading options (A) were varied from 3 to 9, look-ahead levels (L) from 0 to 3, pitch options (B, AUV CNA only) from 2 to 6, and CNA speeds (s^{CNA}) from 0.5 m/s to 4 m/s. In the simulations shown here, each survey AUV covered an adjacent 500 × 1000 m area (Figure 5.26). Each vehicle operates at its own assigned mean depth, oscillating up and down in depth in a sinusoidal manner with a unique frequency and period, (20). The five survey-AUV case was discussed in [96].

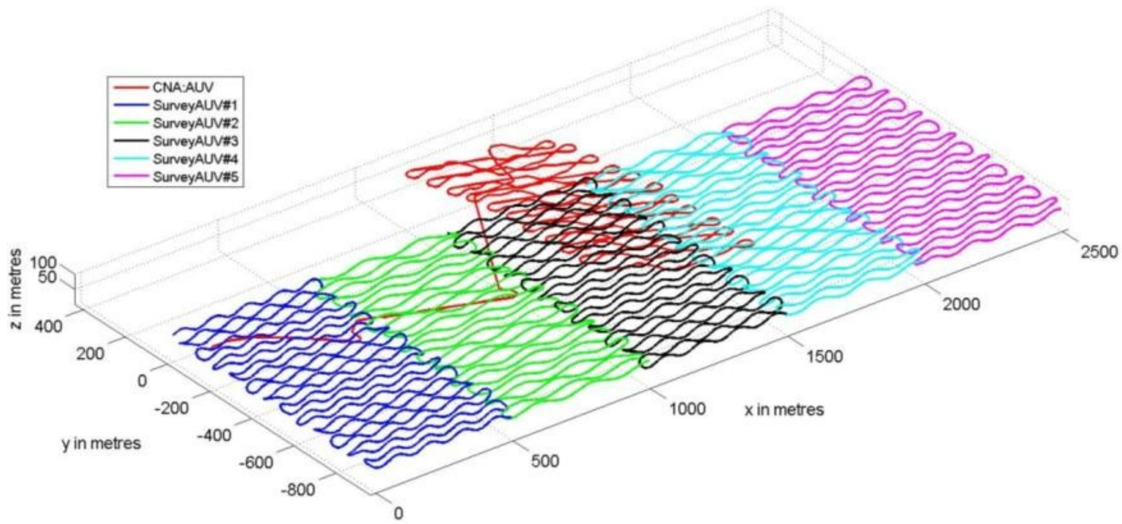

Figure 5.26: Simulation of five survey AUVs aided by an AUV CNA

$$depth_{SurveyAUVs} = \begin{bmatrix} z_1 \\ z_2 \\ z_3 \\ z_4 \\ z_5 \end{bmatrix} = \begin{bmatrix} 10\sin\left(1.0\,{}^{\pi}\!/_{40}t + 0\right) + 90 \\ 10\sin\left(0.6\,{}^{\pi}\!/_{40}t + {}^{\pi}\!/_{2}\right) + 85 \\ 10\sin\left(0.9\,{}^{\pi}\!/_{40}t + \pi\right) + 80 \\ 10\sin\left(0.7\,{}^{\pi}\!/_{40}t + {}^{3\pi}\!/_{2}\right) + 75 \\ 10\sin\left(0.8\,{}^{\pi}\!/_{40}t + 2\pi\right) + 70 \end{bmatrix} \tag{20}$$

Table 5.3: Best results, *N*=5, MATLAB® simulation, sorted by avg. cost

CNA	s^{CNA} (m/s)	A	B	L	Avg. Cost (m^2)	Max Error (m)	RMS Error (m)
AUV	4	3	6	3	142.0	8.27	6.75
ASC	4	6	-	3	150.0	8.67	7.02
AUV	4	5	4	3	150.0	8.62	6.92
AUV	4	5	3	3	150.7	8.39	6.99
AUV	4	7	4	2	153.3	9.36	7.02
AUV	3.5	3	3	3	154.3	9.24	7.14

Table 5.4: Best results, *N*=5, MATLAB® simulation, sorted by max error

CNA	s^{CNA} (m/s)	A	B	L	Avg. Cost (m^2)	Max Error (m)	RMS Error (m)
AUV	4	3	6	3	142.0	8.27	6.75
AUV	4	6	3	3	156.1	8.37	7.10
AUV	4	5	3	3	150.7	8.39	6.99
AUV	4	4	5	3	158.5	8.39	7.14
ASC	4	5	-	3	165.9	8.40	7.31
AUV	3	3	5	3	163.5	8.51	7.05

Table 5.5: Best results, N=5, MATLAB® simulation, sorted by RMS error

CNA	s^{CNA} (m/s)	A	B	L	Avg. Cost (m^2)	Max Error (m)	RMS Error (m)
AUV	4	3	6	3	142.0	8.27	6.75
AUV	3	3	4	3	157.1	8.62	6.86
AUV	4	5	4	3	150.0	8.62	6.92
AUV	3	3	3	3	156.8	8.66	6.94
AUV	4	5	3	3	150.7	8.39	6.99
AUV	4	7	4	2	53.3	9.36	7.02

Tables in this thesis representing multiple survey AUV simulations, “Maximum Error” and “RMS Error” represent the highest value for any survey AUV in the simulation. Since organizing the data by descending average cost also represents maximum error and RMS (root-mean-square) error in fairly good order in Table 5.3, the rest of the MATLAB® simulations will also be organized by average cost. Currently, 4 m/s is not an achievable speed for many AUVs, including the Iver2 AUVs used in this thesis. In Table 5.9, the best eight results are shown (all being an ASC CNA) followed by the best AUV CNA result. As stated previously, these simulations are deterministic, and so it would seem that for this particular survey AUV case, the AUV CNA parameters are better able to manage the average cost. Note, however, that the maximum error for the AUV CNA listed in Table 5.9 is lower than any listed for an ASC CNA. Due to its greater number of possible motions (pitch as well as heading), an AUV CNA needs more look-ahead than an ASC to avoid local minima as it attempts to minimize survey AUV position error. This may explain why the best results are achieved by an ASC CNA rather than an AUV CNA.

One of the goals of these simulations was to determine whether there is a trend correlating decreased survey AUV error as the number of pitch options (B) increased for an AUV CNA. No such trend was found. This is counter-intuitive, especially in cases where the number of pitch options is an odd number, since the AUV CNA does not need to change pitch, enabling it to match the ASC CNA case (since it is essentially an AUV CNA that cannot change depth). The best explanation is again the number of look-ahead steps. Were it computationally possible for the CNA to consider all the time steps for the entire simulation, the AUV option (at least with an odd number of pitch options so that constant pitch and depth were possible) should be the best option every time since it has more possible motions to consider. However, since only a limited number of time steps are considered at a time (through look-ahead), the AUV CNA option is settling into local minima in some cases. Due to its higher number of motion options, the AUV CNA would be more susceptible to this than an ASC CNA. Nevertheless, it can be seen from the tables in Section 5.3 that the AUV CNA option is better in some cases even though the effect of increased pitch options is not always beneficial in reducing survey AUV position error.

Table 5.6: Best results, *N*=4, MATLAB® simulation, sorted by avg. cost

CNA	s^{CNA} (m/s)	A	B	L	Avg. Cost (m^2)	Max Error (m)	RMS Error (m)
ASC	4	9	-	3	68.5	5.44	4.78
ASC	4	7	-	3	68.7	5.45	4.79
ASC	4	8	-	3	68.8	5.45	4.79
ASC	4	5	-	3	68.9	5.48	4.80
ASC	4	6	-	3	69.2	5.47	4.81
ASC	4	4	-	3	69.6	5.51	4.81
ASC	4	3	-	3	69.7	5.49	4.82
AUV	4	7	3	3	69.7	5.47	4.82

Table 5.7: Best results, *N*=3, MATLAB® simulation, sorted by avg. cost

CNA	s^{CNA} (m/s)	A	B	L	Avg. Cost (m^2)	Max Error (m)	RMS Error (m)
ASC	4	5	-	3	44.3	5.25	4.05
ASC	4	3	-	3	44.5	5.20	4.03
ASC	4	6	-	3	44.5	5.21	4.06
ASC	4	9	-	3	44.7	5.53	4.05
ASC	4	7	-	3	44.5	5.54	4.05
ASC	4	4	-	3	44.6	5.37	4.06
ASC	4	8	-	3	44.6	5.47	4.06
AUV	4	4	6	3	44.6	5.28	4.10

Table 5.8: Best results, *N*=2, MATLAB® simulation, sorted by avg. cost

CNA	s^{CNA} (m/s)	A	B	L	Avg. Cost (m^2)	Max Error (m)	RMS Error (m)
AUV	4	9	3	3	22.2	4.82	3.36
AUV	4	4	5	3	22.2	4.71	3.35
AUV	4	8	3	3	22.3	4.91	3.37
ASC	4	6	-	3	22.4	4.76	3.36
AUV	4	7	4	3	22.4	4.83	3.36
AUV	4	7	6	3	22.4	4.84	3.38
AUV	4	8	6	3	22.5	4.82	3.36
AUV	4	6	4	3	22.5	4.90	3.37

Table 5.9: Best results, *N*=1, MATLAB® simulation, sorted by avg. cost

CNA	s^{CNA} (m/s)	A	B	L	Avg. Cost (m^2)	Max Error (m)	RMS Error (m)
ASC	4	4	-	3	4.56	2.77	2.14
ASC	4	9	-	3	4.57	2.74	2.14
ASC	4	6	-	3	4.58	2.74	2.14
ASC	4	5	-	2	4.60	2.89	2.14
ASC	4	5	-	3	4.60	2.76	2.14
ASC	4	7	-	2	4.60	2.95	2.15
ASC	4	3	-	2	4.61	2.84	2.15
ASC	4	8	-	2	4.62	2.90	2.15
AUV	4	9	2	3	4.90	2.57	2.21

Chapter 6 Results from MOOS-IvP Simulations and Trials

Development in MATLAB® was followed by implementation in MOOS-IvP as described in Chapter 4 . The MOOS-IvP implementation supports an ASC CNA in pre-deployment and underway path planning modes. The MOOS-IvP implementation was used as part of the tank and harbour trials as well as simulations.

6.1. Operating Autonomous Marine Vehicles in the Underwater Environment

Many of the issues in underwater operations have been mentioned earlier, but are discussed here for clarity. AUV motion can be inhibited by currents which are influenced by winds and tides. Near the surface, AUVs must also deal with waves which are again influenced by winds and tides. Any class of underwater vehicle will at some point be unable to overcome the effects of waves and currents as these effects can be almost an order of magnitude more powerful than the AUV. AUV navigation typically uses GPS on the surface and dead-reckoning (perhaps with acoustic navigation aids such as LBL, USBL, or CNA vehicle) underwater. As has been stated, dead-reckoning position estimate error grows over time and must be periodically corrected either by surfacing for a GPS fix or by the aforementioned acoustic navigation aids. Acoustic communication (including communication from navigation aids) is the most reliable method of underwater communication, but is prone to difficulty. The re-direction of underwater sound is caused by changes in the speed of sound (this effect is known as multi-path). The speed of sound is itself influenced primarily by the temperature and salinity of the water. Two major causes of temperature and salinity changes in the ocean are major currents (e.g. the Gulf Stream comes from the warm Gulf of Mexico up the Eastern Seaboard and then crosses the cold North Atlantic) and fresh water from rivers that empty into the ocean. However, there are other variations in temperature and salinity which are difficult to predict and change quickly over time and space, e.g. the daily heating of the water by the sun can make noticeable changes in the speed of sound. Topography can also inhibit underwater communications. An extreme case would be two AUVs surveying in parallel underwater canyons, they would not be able to communicate because there would likely be no path for the sound to follow between vehicles. In addition, water absorbs underwater sound, especially at higher frequencies, and acoustic signal can be lost in the presence of noise such as ships and marine life. Lower frequencies travel further, but require larger transducers and more power to produce, limiting the frequencies that can be used by lightweight AUVs. Finally, the nature of underwater communication limits the amount of information (bandwidth) that can be transmitted even in the absence of other complicating conditions.

6.2. ASC/AUV CNA Tradeoffs

One goal early in this research was to examine trade-offs between the effectiveness of an AUV and an ASC in the role of a CNA. The results shown in this thesis do not indicate that either vehicle is better. Future work may resolve some of this ambiguity, but there will remain several issues that are beyond an extension of the simulations and experiments described in this thesis.

First, there is the issue of covertness. This is not always a requirement, but if it is required, it will be a very important consideration. Most ASCs are too easily observed by the human eye to be considered covert. However, semi-submersibles such as ISE's DORADO vehicle [103, 104] may be covert enough and would path-plan in the same manner as an ASC CNA. AUVs are obviously more covert. This issue of covertness is considered purely from the standpoint of visibility to the human eye or surface radar. Issues of acoustic signatures (from the acoustic communications and radiated noise from vehicle systems such as the propeller and prime mover) and electromagnetic signatures (from in-air communications and from radiation from vehicle systems such as servo motors) could also be important in some applications, and techniques of mitigating these signatures (especially communications) without impeding the mission would need to be developed. Steps for AUV magnetic signature mitigation were taken as part of [105], but the resulting magnetic signature was not reported.

Second, there is the issue of computation power. In general, an ASC will have more power than an AUV. The ASC may even have an internal combustion engine rather than batteries. In this case, the ASC could be equipped with a much more powerful path-planning processor than an AUV. This would allow the ASC to path plan more effectively than an AUV using the algorithm discussed in this thesis. Refer to Sections 3.1 and 6.5.2 for more discussion of the algorithm's computational load.

Third, additional tasks could be assigned to the CNA vehicle. An ASC CNA, (especially one with an internal combustion engine rather than battery power) could serve as an AUV docking, recharging, and data download station [106]. (A catamaran or SWATH hull configuration is typically envisioned in this case. A towed acoustic modem might need to be winched aboard prior to docking with an AUV, making the time required for docking an issue if other AUVs are still operating underwater as the ASC will not be providing CNA support.) An ASC CNA that could autonomously dock with AUVs could simplify AUV recovery by a large ship as the ASC could retrieve the AUVs one at a time, and the ship's crew would have the (hopefully) simpler task of recovering the relatively large ASC multiple times rather than recovering multiple small AUVs. On the other hand, if the survey AUVs had sufficiently accurate onboard navigation systems, an AUV CNA might periodically cease its CNA role to reacquire and identify mine-like contacts reported by the survey AUVs. Depending on how much time the AUV CNA could spend on the secondary reacquisition mission, the mission might begin to resemble the mission proposed in [61] rather than the adaptive path-planned mission described in this thesis.

Fourth, there is the issue of the accuracy of the CNA's navigation fix. Being above the water, the ASC may be assumed to always have a position fix within the accuracy of the onboard GPS. The AUV CNA, on the other hand, will have growing position uncertainty when it is underwater, forcing periodic surfacings which have not been accounted for in the simulations in this thesis. The rate at which the AUV CNA will need to surface will vary based on the quality of the onboard sensors and (to a lesser extent) the sea conditions in the operating area (e.g. high currents will degrade the position accuracy faster, and high sea state will make it more difficult for the AUV to keep its mast above water when it attempts to acquire a GPS fix).

Fifth, as with the navigation fix, an ASC CNA will have much better in-air communications (satellite, radio, Wi-Fi, etc.) than an AUV CNA because the ASC mast will be further above the water surface. This is not to say that an AUV CNA will not work, but that an ASC will be better able to maintain an in-air communications link. Indeed, an ASC CNA will be much faster because an AUV CNA will have to re-establish its connection when it surfaces rather than as soon as it has information to relay as the ASC CNA would.

Sixth, partially related to the previous two considerations is the consideration of sea-keeping. Sea-keeping is the ability of a marine vehicle to overcome waves and currents. In the case of a CNA vehicle, sea-keeping is the ability to travel to the planned points in spite of waves and currents. Any marine vehicle or ship will have a maximum sea state in which it can operate. The maximum desired operating sea state should be considered carefully when selecting autonomous marine vehicles for any application. While an AUV could typically dive below the effects of sea states and winds, it must periodically surface for GPS fixes and in-air communications. In general, it may be considered that the sea-keeping ability of an ASC will be better than that of a surfaced AUV

Seventh, this thesis (as well as [13, 93]) has shown that higher CNA speed tends to improve the effectiveness of the CNA path planning algorithm. In most cases, an ASC will be capable of higher speeds than an AUV.

Finally, there is the matter of acoustic communications reliability. Here, the AUV CNA has advantages over the ASC CNA. As discussed in Section 6.5.3 and in [31], the effectiveness of the acoustic modem when mounted on the hull of a vehicle on the surface is not very high. However, as discussed in Section 6.5.3 the acoustic communication of a submerged AUV with a hull-mounted acoustic modem is satisfactory (likely due to the lower sea state and ambient noise), and according to [31], the acoustic communication of a surface craft towing a modem is more satisfactory than a hull-mounted modem. The advantage of the AUV CNA is that the ASC CNA may not be able to tow its modem at its highest speed as the modem will not be able to transmit and receive effectively, possibly removing the speed advantage of the ASC.[23] An ASC powered with an internal

[23] Having an ASC CNA move at high speed from point to point (following a path-planning algorithm) and pausing at these points to transmit may prove ineffective because the modem would not be able to "hear" the survey AUVs. Messages from the survey AUVs to the CNA are very important because they may contain 1) locations of mine-like targets from their sonar images, 2) future waypoints needed for CNA path planning (see Section 4.2), including major changes in plan, or 3) notice of survey AUV malfunctions such as plane jams or leaks. These are not messages the CNA should deliberately risk missing. Instead, a constant speed that allows for good acoustic communication will probably be most effective.

combustion engine (suggested to help with some of the previously mentioned factors) would also need some special attention in the area of vibration isolation on engine mounts and noise insulation on the hull (such as anechoic tiles used on submarines [107]) to prevent the engine noise from drowning out the acoustic modem. This would not be a trivial problem to overcome. In addition, variations in the salinity and temperature of the water in the operating area could create regions where the survey AUVs and CNA could not communicate with each other.[24] If the survey AUVs could provide salinity and temperature information to the CNA (through an on-board conductivity, temperature, and depth sensor, CTD), the CNA (knowing its own local water salinity and temperature) could plot probable regions of good and poor communication areas and incorporate that information into its path planning decisions. However, the acoustic environment is constantly changing, and in some cases it may be changing too fast for collected CTD data to be useful for path planning. An AUV CNA would have more manoeuvring options in this situation than an ASC CNA. Similarly in the case of higher sea states, an AUV CNA has an advantage over an ASC CNA because it could generally dive deep enough to escape the motion caused by the sea state. On the other hand, some sea state effects on an ASC-towed acoustic modem could be mitigated by putting some elasticity in the towing cable. A similar solution was implemented on air-dropped sonobuoy microphones [108], but the towing application is much more complicated and has not, to the author's knowledge, been implemented successfully.

These seven measures of performance have been discussed as additional considerations to the ability of an AUV or ASC to effectively minimize survey AUV position error using the algorithm described in this thesis. As neither type of vehicle is significantly better at minimizing survey AUV position error, these additional considerations may be the factors upon which a selection of CNA vehicle is made. Based on the simulations presented in Section 5.3, either an ASC or AUV can effectively bound survey AUV position error satisfactorily, leaving the operator to decide on a CNA vehicle type based on his own special requirements as outline above.

[24] The speed of sound in water is affected by salinity and temperature. Sound waves traveling through changes in sound speed will bend at the interface much the way light bends at the air water interface, causing a pencil in a glass of water to appear bent. These changes in sound-wave path can cause communication blackouts between vehicles.

6.3. Hardware

The hardware used for in-water trials in this thesis consists primarily of three OceanServer Technology, Inc. Iver2 AUVs and a laptop computer connected to a 25 kHz WHOI acoustic Micro-Modem (for simulating additional AUVs and monitoring the real AUVs, see Figure 6.1). The three AUVs (Figure 4.1) have a diameter of approximately 15 cm and are 1.5 – 1.8 m long (depending on the vehicle's specific equipment fit). All three vehicles have Wi-Fi for moving mission files, code, log files, and sonar data on and off the AUVs. In addition, the AUVs each have a pressure transducer for depth measurement, a six-beam DVL/acoustic Doppler current profiler for altitude and speed-over-ground measurements, and magnetic compass (corrected for local declination angle), differential GPS for navigation on the surface, and 16 GHz Intel Atom processors as frontseat and backseat computers. They are also equipped with 25 kHz WHOI Micro-Modems for communication between the AUVs and the modem deck unit used as part of the path planning algorithm in this thesis. The Iver2 AUVs are capable of 0.5 – 2 m/s submerged and can run for at least 8 hrs at optimum speed (1.25 m/s) depending on the duty cycle for the sonar usage. It was discovered that the AUV's maximum speed on the surface was approximately 1.5 m/s.[25] This is presumed to be caused by the increased drag experienced by the vehicle when on the surface. One of the Iver2 AUVs is equipped with a YellowFin™ side scan sonar (capable of 260, 330, 770 kHz operation), another is equipped with a MarineSonics™ side scan sonar (900 or 1800 kHz operation), and the third AUV is equipped with a DeltaT™ multibeam bathymetric sonar and a CTD sensor. As with many other autonomous marine vehicles, the Iver2 AUVs periodically experience a variety of faults; these include but are not limited to leaks, major jumps in GPS position while on the surface (also experienced with other AUVs [35]), and unexpected tripping of safety settings. These problems, coupled with the wind and waves make running sea trials very challenging.

[25] Because AUVs are designed to run underwater, their maximum speed on the surface is less than their maximum speed. During the trials shown in this thesis, an AUV was sometimes used in the role of an ASC CNA, as such it has a lower maximum speed than the survey AUVs. However, the author considers that a real ASC will generally be faster than a submerged AUV (though actual maximum speeds will depend on the particular models of ASCs and AUVs considered).

Figure 6.1: Towfish and 25 kHz transducer, WHOI photo [109].
The transducer is the black cylinder in the lower left of the photograph

6.4. Pre-Deployment Mode MOOS-IvP Validation

As mentioned in Section 4.1, the main goal of the in-water trials in pre-deployment planning mode was to prove the AUVs were able to turn at the rate specified by the planner. This was demonstrated in Figure 4.3. Pre-deployment mode simulations were conducted using the same simulated survey AUV path as the in-water trials and yield the same results in terms of survey AUV error as if the parameters were tested in the water. All MOOS-IvP simulations and experiments use a time step of $\tau = 30$ sec. The simulations summarized in Table 6.1 are consistent with the results described in [93] and [13], namely that higher speeds, numbers of heading options (*A*), and look-ahead levels (*L*) improve (lower) survey AUV position error. The complete set of offline results are shown in Appendix A. *A* was varied from 2 to 9. *L* was varied from 1 to 9. s^{CNA} was varied from 0.5 m/s to 4 m/s. Due to the exponentially increasing size of the arrays used in computations, the maximum number of look-ahead levels possible on the processor decreased as the number of heading options increased.

Table 6.1: Best results for pre-deployment simulations of an ASC CNA supporting a single survey AUV on a lawnmower path at 90 m

A	L	s^{CNA} (m/s)	Max Error (m)	RMS Error (m)
7	5	3.50	2.29	2.22
7	5	3.75	2.33	2.22
9	2	4.00	2.30	2.22
8	4	3.75	2.31	2.22
8	3	3.75	2.29	2.22
9	4	4.00	2.29	2.22

Note: Data is sorted by RMS Error and rounded to two decimal places.

6.5. Underway Mode MOOS-IvP Testing and Validation

Validation of the CNA path planning algorithm in the underway mode was conducted in the following three phases: (1) path planning simulations on a single computer using *pMOOSBridge* [98] to communicate among the simulated vehicles; (2) path planning trials among multiple vehicles over their acoustic modems while the vehicles were stationary (and in very close range) in a freshwater test tank, and (3) path planning among multiple vehicles while underway in Halifax Harbour. Each phase validates a different aspect of the whole underway path planning mode. Underway path planning simulations on a single computer test the concept and perform parametric sensitivity analyses. Trials in the test tank allowed for testing with the acoustic modems, the development of *pParseSegList,* the testing of mission plans in the safety of simulation, and some limited parametric analysis. In-water testing proved that an Iver2 AUV could perform the manoeuvres planned for it, that the AUV was able to run the path planning process at the anticipated rate, and that the path planning algorithm was robust to real-world communications limitations.

In these trials, a maximum of two survey AUVs were used due to the number of vehicles available (typically, at least one of the three OceanServer Technology Inc. Iver2 AUVs was broken). The actual maximum number of vehicles the algorithm can support will be based on the processing capacity of the computer running the algorithm; faster processors will support more survey AUVs. However, if the distance between survey AUVs (Figure 5.26) becomes too great, the CNA path planning algorithm will break down as the maximum distance limitations will not be attainable for all the survey AUVs.

6.5.1. Computer Simulations

During the testing of the underway path planning mode on a single processor, it was discovered that various aspects of the MOOS-IvP architecture make each underway path-planning simulation a little bit different. Therefore, approximately three simulations were run with each combination of parameters for two survey AUVs on orthogonal lawnmower tracks over a 480 m × 480 m area (Figure 6.7 illustrates an orthogonal lawnmower simulation with different dimensions). The survey AUVs surveyed at 1.5 m/s, one AUV at 100 m depth and the other at 90 m. Both survey AUVs surface and return to the start point at the end of their survey. The ASC CNA continues planning even after the survey AUVs park at the start/end point as shown in Figure 6.2. Once the survey AUVs have stopped, the ASC CNA begins circling them following the path planning algorithm. Summary data is presented in Table 6.2. Heading options (*A*) of 3, 5, and 7, look-ahead levels (*L*) of 0 to 5, and CNA speeds of 1.5 m/s to 2 m/s (in increments of 0.25 m/s) were tested.

Table 6.2: Best results for underway simulations of an ASC CNA supporting two survey AUVs on orthogonal lawnmower tracks

A	L	s^{CNA} (m/s)	Max Error (m)	RMS Error (m), 95% Confidence Interval:	Std Dev:
7	4	2	4.15	2.88± 0.0347	0.0306
7	5	2	4.74	2.90±0.0230	0.0204
7	3	2	4.00	2.92±0.001398	0.01091
5	3	2	4.01	2.96±0.01840	0.0230
7	3	1.75	4.32	2.97±0.01215	0.01073

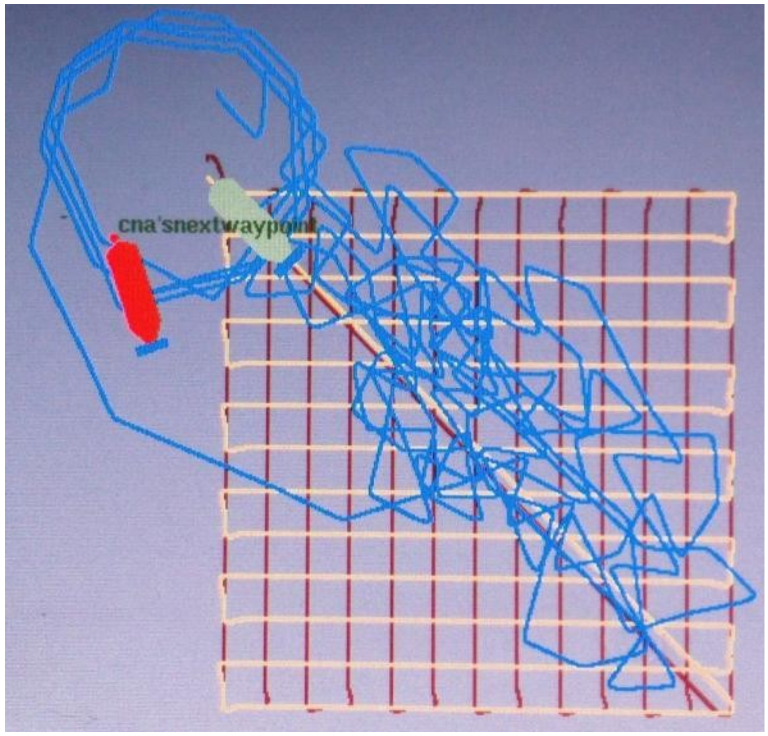

Figure 6.2: End of underway path planning computer simulation, $N = 2$, $A = 7$, $L = 4$, and $s^{CNA} = 2$ m/s

Other simulations conducted on a single processor included the testing of the CNA's performance against two non-lawnmower survey AUV patterns. The first pattern used was an optimally spaced set of tracks for a specified confidence level (confidence that all mine-like objects will be detected given a specified level of sonar performance) for a 1 km × 1 km area for an AUV travelling at 1.5 m/s. This mission takes approximately 8 hrs to complete (running in real time, just as it would if run in the harbour) with the survey AUV at a constant depth of 90 m. The ASC CNA uses a time step (τ) of 30 seconds (based on an assumed communication cycle time for the in-water trials that followed) and has five heading options (A). Results for six sets of CNA parameters are shown in Table 6.3. Each set of parameters was run only once, as the single survey AUV with its set parameters should have little variance. The optimal survey AUV tracks (36 in all, some overlap, producing a confidence level of 94%) were laid out using software tools described in [5], Figure 6.3.

Table 6.3: Results from underway path planning simulation for *N*=1 using survey AUV path from [5]

L	s^{CNA} (m/s)	Max Error (m)	Error RMS (m)
3	2.0	4.39	2.62
2	2.0	4.69	2.86
1	2.0	5.55	3.73
2	1.5	5.97	3.79
3	1.5	5.65	3.56
1	1.5	6.35	4.10

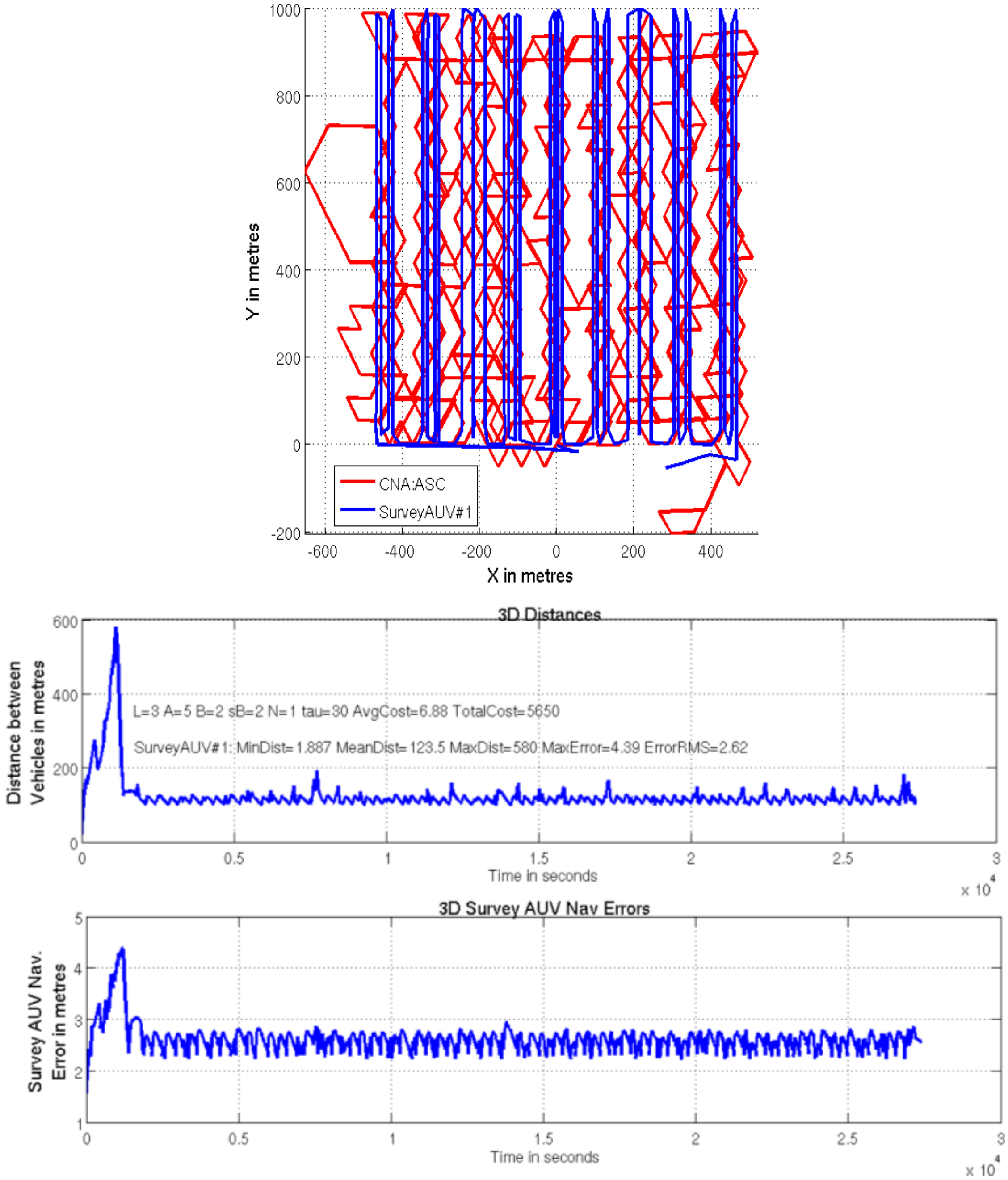

Figure 6.3: ASC CNA simulation supporting a survey AUV path of 1 km x 1 km area with 36 tracks

This pattern was repeated on a smaller area (200 m ×400 m) with the same CNA path planning parameters and same survey AUV speed (1.5 m/s). Using the software tools from [5], eight survey AUV tracks (four overlapping tracks) were laid out for a confidence level of 94%, Figure 6.4. This mission takes approximately 50 min, and each mission was only run once. Unlike the simulations in Figure 6.3, the survey AUV did not maintain a constant depth; instead it spent 5 min at 10 m followed by 1 min at 0 m as was done in many of the harbour trials.[26] This periodic depth is illustrated in Figure 6.30. As can be seen by comparing Table 6.3 with Table 6.4, the survey AUV maximum error is higher in the longer set of simulations, but the error RMS is not consistently higher or lower in either set of simulations. However, since both the depths and the simulation lengths are different, it is not possible to indicate which factor is the most significant. Notice also that while the maximum error is arranged in ascending order, the lowest error RMS for both s^{CNA} = 2.0 m/s and 1.5 m/s occurs with L = 2 rather than L = 3. This is an exception to the general rule of improving performance with increasing look-ahead.

Table 6.4: Underway simulation for N=1 using Survey AUV Path from [5] with variable depth

L	s^{CNA} (m/s)	Max Error (m)	Error RMS (m)
3	2.0	3.20	2.72
2	2.0	3.27	2.69
1	2.0	3.46	2.77
3	1.5	3.61	2.90
2	1.5	3.65	2.86
1	1.5	3.67	2.95

[26] A MOOS-IvP behaviour called *BHV_GoToDepth,* is used to achieve this periodic depth [98].

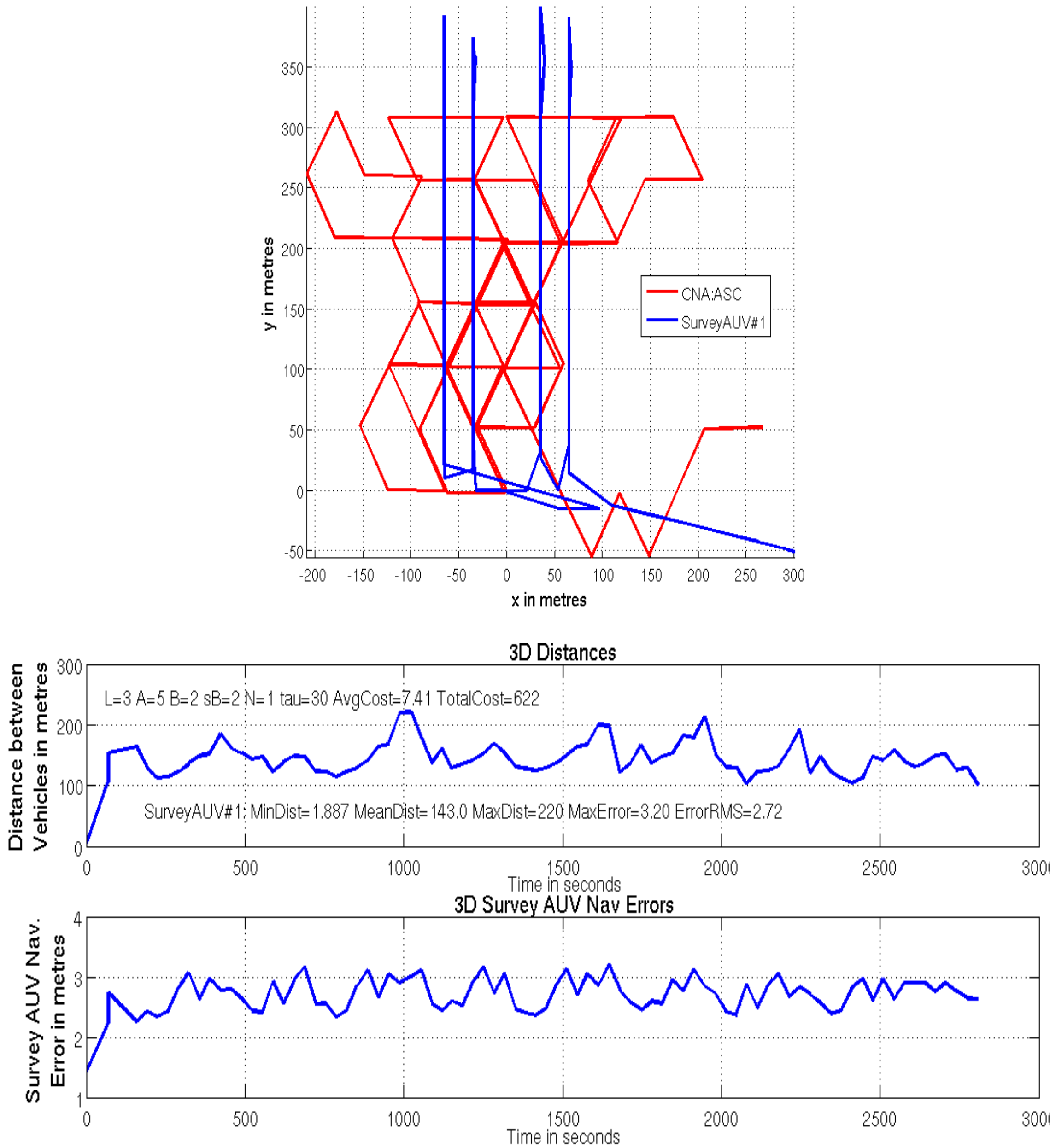

Figure 6.4: Underway path planning simulation for a single survey AUV over a 200 m x 400 m area

Given the differences between the simulations summarized in Table 6.3 and Table 6.4, it seemed prudent to run another set of simulations using the survey AUV waypoints shown in Figure 6.4 at a constant depth of 90 m. The results for this set of simulations are shown in Table 6.5. Comparing these results with the results of the variable depth simulations in Table 6.4, it would appear that the error RMS is lower with the constant depth, but there is no particular trend in the maximum errors. Comparing all three sets of simulations with survey AUV paths based on [5], it seems possible that the higher maximum errors in

Table 6.3 are the result of the longer mission and that the CNA path planner is better able to handle constant depths due to its assumption of constant depth between updates from the survey AUV (explaining why the error RMS is lower in Table 6.5 than Table 6.4).

Table 6.5: Underway simulation for N=1 using Survey AUV Path from [5] with constant depth

L	s^{CNA} (m/s)	Max Error (m)	Error RMS (m)
3	2.0	2.87	2.51
2	2.0	3.29	2.59
1	2.0	3.15	2.61
3	1.5	3.37	2.74
2	1.5	3.83	2.79
1	1.5	3.61	2.84

The second pattern is an adaptive pattern for covering an arbitrarily shaped region to a specified confidence level. This pattern used algorithms from [6] implemented as MOOS-IvP behaviours by Paull. It is significantly different from both the standard lawnmower pattern and the previous pattern in that it does not generate waypoints which can be transmitted to the CNA vehicle. Instead, the algorithms of [6] are implemented as a set of behaviours. These behaviours are able to cover an area described by a non-convex polygon, as shown in Figure 6.5. Because the area coverage planner uses behaviours instead of generating waypoints, the CNA must use the survey AUV's last reported position, speed, and heading to extrapolate its probable next position, rather than interpolating between the survey AUV's current position and its next waypoint(s) as is done in the other survey AUV patterns described in this paper. As seen in Table 6.6, the results suggest that look-ahead has limited value in this case.

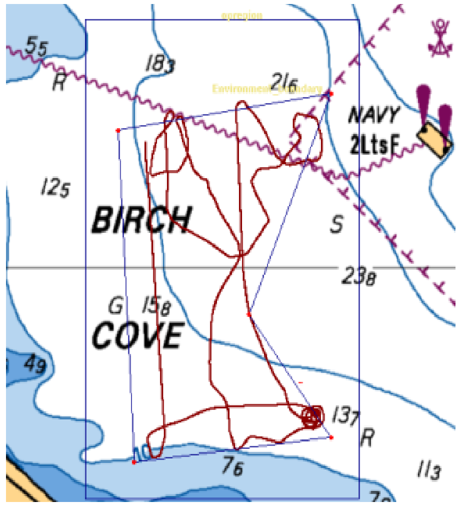

Figure 6.5: Reactive side scan sonar survey of non-convex polygon approximately 200 × 300 m using [6]

The area covered by the survey AUV in these missions is a non-convex polygon inside a rectangle of approximately 200 × 300 m at a speed of 2 m/s. The total simulation time is just under 30 min (corresponding to a harbour trial time of approximately 30 min). The AUV surveys at a constant depth of 10 m, so errors in the CNA path planner's assumption of constant depth do not come into play. As in the other MOOS-IvP simulations (and trials), the ASC CNA uses a time step (τ) of 30 seconds between heading decisions.

The data presented is based on approximately six simulations for each set of CNA parameters. The parameters tested were A = 3, 5, 7; L = 0, 1, 2, 3, 4; and s^{CNA} = 2.00, 2.25, 2.50. Six runs were used to compensate for the variability in the simulations because not only is each underway simulation slightly different, but also each run using Paull's MOOS-IvP behaviours is a bit different (compare the tracks in Figure 6.5 and Figure 6.6). While this number of runs isn't conclusive, it does give an indication for the effectiveness of the CNA path planning algorithm with this survey AUV path. As seen with other paths, increasing CNA speed and number of heading options (A) increases the performance of the algorithm (reduces survey AUV position error). However, unlike other cases, increasing the look-ahead level (L) does not improve performance. The greedy case of L = 0 was run in this set of simulations and was found less than optimal. However, the best results were obtained from L = 1 instead of the higher look-ahead levels tested. This would appear to be a result of the lack of waypoints in this survey

AUV path. In the absence of waypoints from the survey AUV, the CNA infers that the survey AUV maintain a straight course. While this is generally correct, especially in the short term, it is not a valid assumption over many time steps. Hence the best value in these simulations is $L = 1$ in Table 6.6 rather than $L > 1$ (particularly $L = 4$) which assume a straight line path for longer periods of time.

Table 6.6: Best results from underway path planning simulation for N=1 using survey AUV path from [6]

A	L	s^{CNA} (m/s)	Max Error (m)	RMS Error (m), 95% Confidence Interval	Std Dev
7	1	2.50	2.85	2.45±0.0226	0.0283
7	2	2.50	3.00	2.47±0.0295	0.0368
7	3	2.50	3.03	2.48±0.0305	0.0382
7	2	2.25	2.90	2.49±0.01663	0.0208
7	1	2.25	2.98	2.49±0.01175	0.01468
5	1	2.50	2.92	2.49±0.01233	0.01541
5	2	2.50	2.97	2.52±0.01560	0.01591
7	2	2.00	2.93	2.54±0.01464	0.01670
5	3	2.50	3.01	2.54±0.0289	0.0330

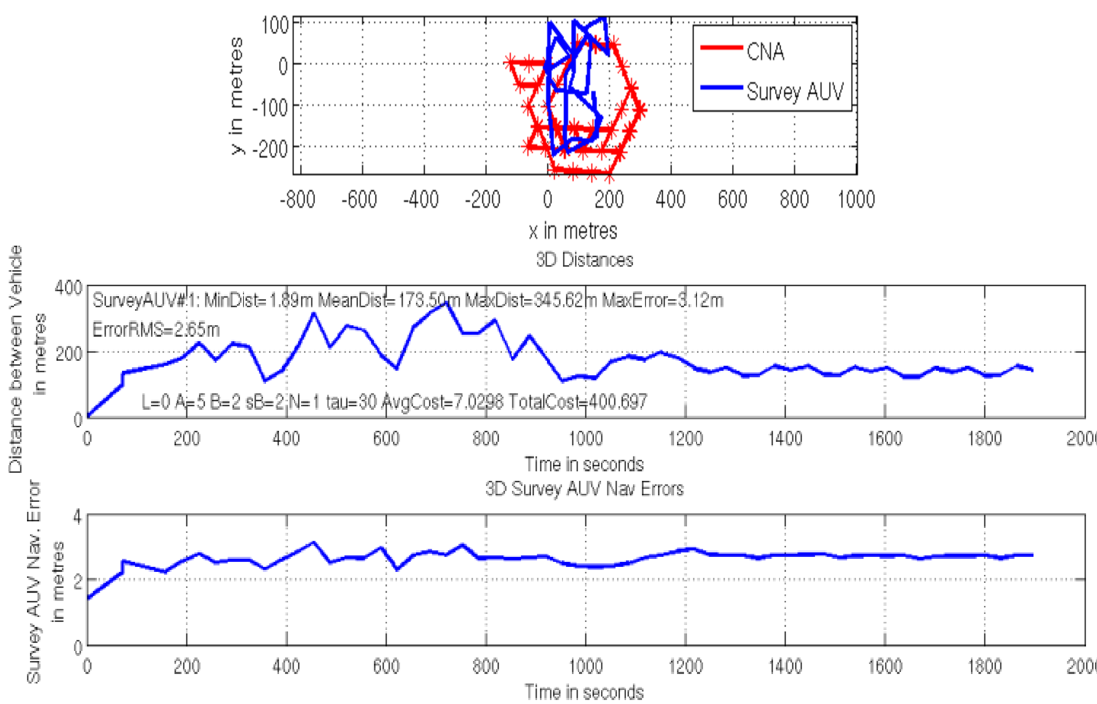

Figure 6.6: Underway path planning simulation of ASC CNA supporting an AUV operating as described in [6]

6.5.2. Tank Trials

Testing with multiple vehicles in the tank served to prove aspects of the path-planning process which could best be observed when using an acoustic modem Simulation tools for the acoustic modem are available in MOOS-IvP [110], but physical equipment was used in simulation since it was available and testing of the actual hardware would be required prior to harbour trials whether or not simulation tools were used. Testing of system capacities was also done.

One system capacity test performed in the tank was to determine the maximum number of look-ahead levels that could be handled by the backseat computer. As discussed in Section 3.1, the computational load of the CNA path planning algorithm increases exponentially with increased look-ahead level (L), $\sim\mathcal{O}(N \cdot (A \cdot B)^{L+1})$. It was meaningful to test the maximum look-ahead value in simulation because it was likely that an unachievable look-ahead level could cause *pCnaPathPlanning* or the entire MOOS-IvP community to stop. The simulation conducted to determine this value used two Iver2 AUVs and a laptop connected to the deck-mounted version of the WHOI Micro-modem. One of the Iver2s acted as the CNA, while the other AUV and the laptop acted as survey AUVs. In these simulations, two levels of failure occurred in the case of an unachievable look-ahead level. In the first level, outright failure, *pCnaPathPlanning* shut down as soon as it should have started planning. In the second level, unsatisfactory performance, *pCnaPathPlanning* is not able to provide a new waypoint to the waypoint behaviour in the 30-second time interval (τ). In this latter failure level, the CNA vehicle circles the previous waypoint until calculations for the next waypoint are complete. The circling is due to the user-configured settings in the MOOS-IvP waypoint behaviour. Obviously, neither failure level can be tolerated, outright failure because the path planner stops working and unsatisfactory performance because the path planning algorithm is based on the assumption that the vehicle travels at a constant speed and reaches a new waypoint every τ seconds. In these simulations (where $N = 2$), it was determined that the highest satisfactory (no failure) look-ahead level for the case of five heading options ($A = 5$) was $L = 5$ and the highest satisfactory look-ahead level for $A = 7$ was $L = 4$. It should be noted that these simulation results are slightly more conservative than would be needed for in-water trials because the backseat processor must simulate vehicle control in the tank, but in the water it simply hands heading, speed, and depth decisions to the frontseat processor for action. The heading, speed, and depth decisions are made by the backseat processor in both simulations and in-water trials. In-water trials using the CNA path planning algorithm have typically run at $A = 5$ and $L = 5$. Optimizing these parameters has not been done in water due to time constraints. Instead in-water trials have been used to validate computer and tank simulation results.

Figure 6.7 shows a tank trial with two survey AUVs (blue and green) supported by an ASC CNA (red). All vehicles begin their missions outside (south west of) the survey area. This is consistent with an AUV MCM mission where the autonomous marine vehicles are launched without the ship entering the minefield. The asterisks indicate vehicle positions and waypoints broadcasted by acoustic modem. This trial demonstrated that the CNA could maintain a bounded error during a relatively long-duration mission, as shown in Figure 6.8 (approximately three hours). The main differences between testing in the tank and testing in Halifax Harbour are the impact of water conditions (such as current and waves) on the vehicles' actual paths and the impact of vehicle motion and water conditions on acoustic communication. Any fielded algorithm must be robust to these realities.

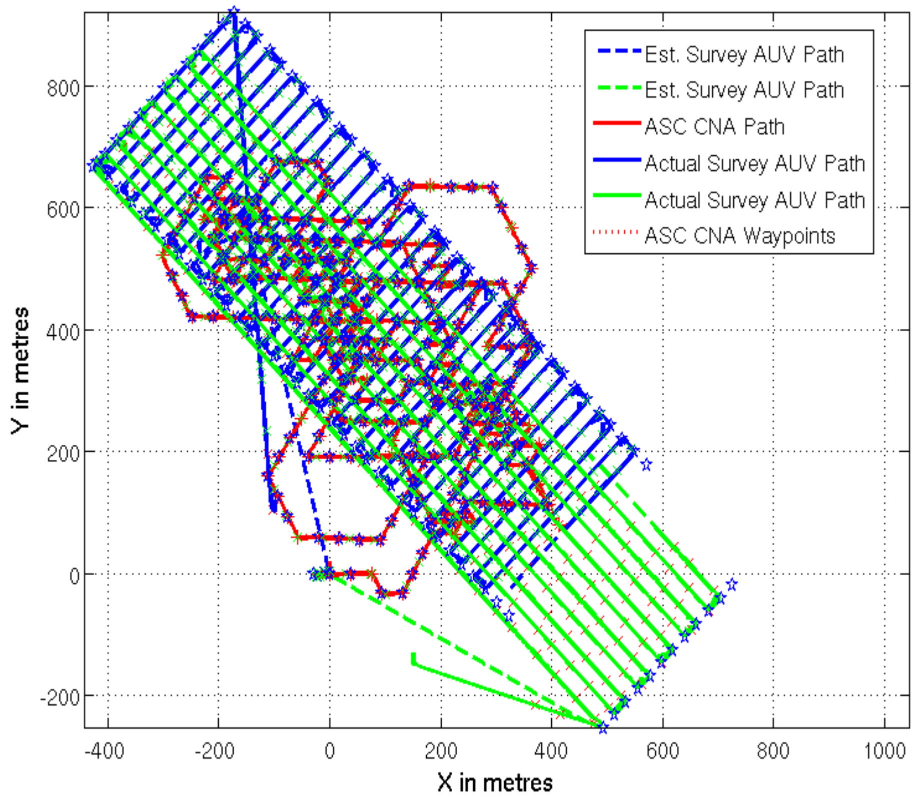

Figure 6.7: Trial of ASC CNA supporting survey AUVs on orthogonal headings over a 350 m x 1300 m area (10 m mode depth)

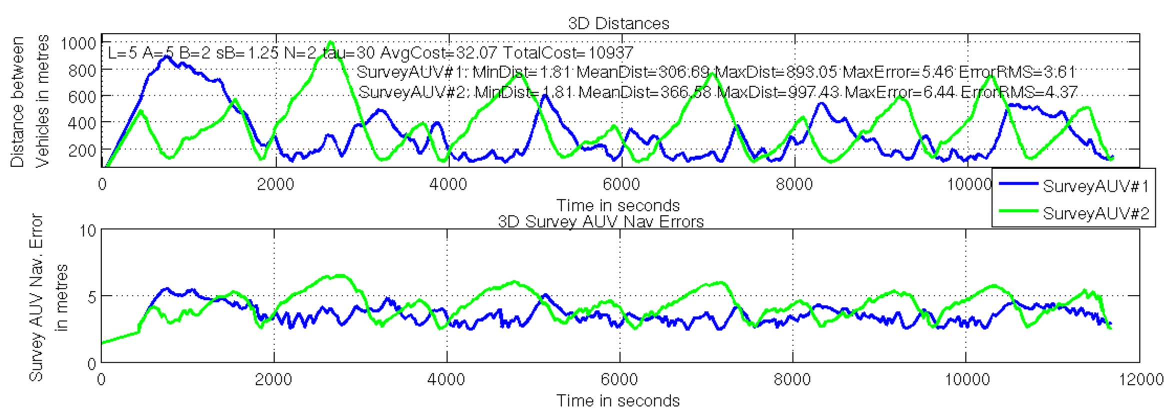

Figure 6.8: Distance and survey AUV position error vs. time for trial shown in Figure 6.7

A similar trial is shown in Figure 6.9 through Figure 6.11 where the two survey AUVs return to their park points part way through the mission and the CNA must react to this dramatic change in survey AUV path. The CNA's estimate of the survey AUVs' paths is noted with the light dashed line in Figure 6.9. The command to return is executed at approximately 9300 sec for the blue survey AUV and at approximately 9500 sec for the green survey AUV. As seen in Figure 6.10, the CNA has not been able to bound the position error of the survey AUVs at their park points before it too is told to return. In computer simulations, it was observed that the CNA, following its path planning algorithm, would circle a stopped survey AUV. The case of two or more stopped survey AUVs was not tested, but the author would expect the CNA to circle all the stopped survey AUVs, circle between the survey AUVs, or some variation of this behaviour such as circling the survey AUVs in a figure-eight path.

Figure 6.11 is a screen shot from *pMarineViewer* (a MOOS-IvP viewing interface) at the end of the trial. The thin green lines connect dots indicating survey AUV positions transmitted to the CNA. (The actual survey AUV path does not follow the line exactly, but connecting the dots allows for a fairly good estimate of survey AUV path). The thick green line indicates the CNA's path over the previous 2 min (approximately). The red "doughnut" indicates the CNA's return point, and the orange line between the CNA and the green AUV ("Alpha," marked in blue in Figure 6.9 and Figure 6.10) is produced by *BHV_AvoidCollision* described in Section 4.2. The blue line near the middle of the plot is an artifact of a collision avoidance maneuver by the CNA in response to the movements of the red AUV ("Bravo," marked in green in Figure 6.9 and Figure 6.10).[27]

[27] The colour of the line between vehicles in a collision avoidance maneuver changes (blue to green to orange to red) as the distance decreases. The ranges at which these colours change is specified by the user [98].

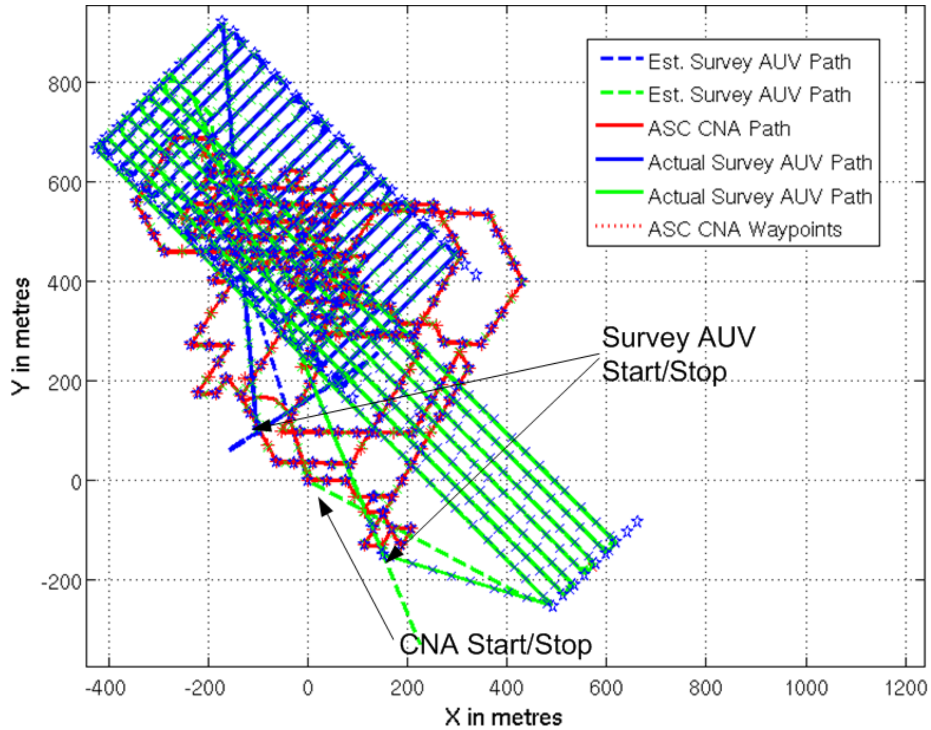

Figure 6.9: Tank trial of ASC CNA supporting survey AUVs which return to their park points part way through the trial; mode depth of 10 m

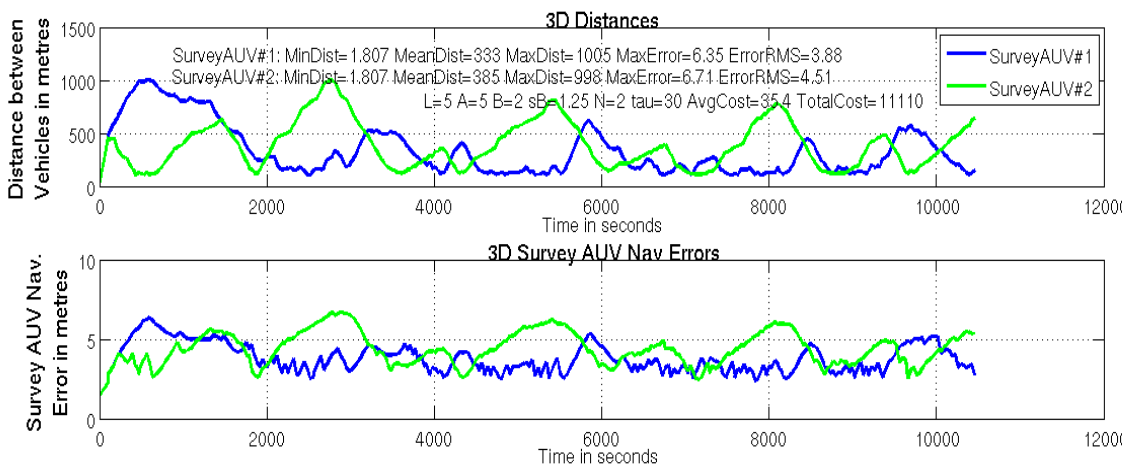

Figure 6.10: Distance and survey AUV position error vs. time for tank trial in Figure 6.9

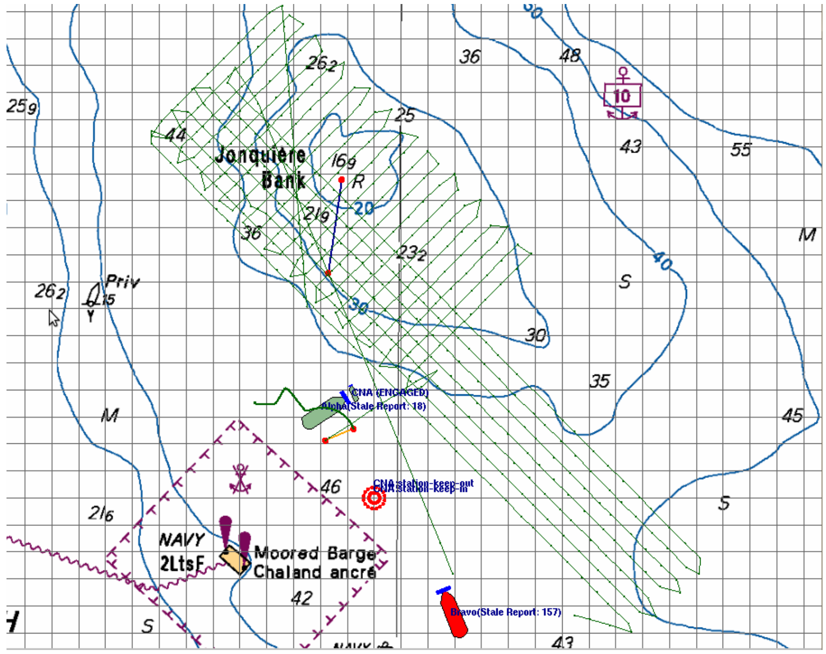

Figure 6.11: Screen shot from *pMarineViewer* at the end of the tank trial shown in Figure 6.9

Another trial performed in the tank used all three Iver2 AUVs (as survey AUVs) and the WHOI Micro-modem connected to a laptop simulating an ASC CNA. Below are the results of the initial tank trial with three survey AUVs. Survey AUV #2 was started four minutes after Survey AUV #1, but Survey AUV #3 was not started until 35 min after Survey AUV #2. This lag likely represents the time required to fetch and set-up Survey AUV #3 for the trial as the other two AUVs had been used all day in the tank, but Survey AUV #3 was only used for this single trial on the day in question. By the time the first two updates were received from Survey AUV #3, the CNA path planner had been running for 53 min. This caused the long jump between the beginning of the distance and error plots in Figure 6.12 and the beginning of the actual path planning. This also serves to illustrate the need to allow survey AUVs to be added and dropped from the survey group because of time wasted waiting for the third AUV. In this case the first two AUVs would be done approximately half an hour ahead of the Survey AUV #3. In a “real” operation, the first two survey AUVs would be recovered shortly after they finished their missions. With these survey AUVs safely on the deck of the support ship, the CNA would have no need to support their navigation and communication and should be able to drop them from its list of survey AUVs and focus on the remaining survey AUV. The full trial was run twice more and is described later.

There are several ways to implement the capability to drop or add survey AUVs, and some combination may produce the best results. For the case of a failed/sunken AUV, the method of determining loss could be done with the fuzzy logic method described in [53]. In the case of survey AUVs parking on the surface at the end of their missions, they could be dropped by the CNA when it receives a "surfacing and returning to recovery location" message.[28] In the case of a covert mission where the survey AUVs loiter underwater while waiting for the recovery time, the CNA would obviously continue to provide support to all survey AUVs until they are actually recovered by the support ship or submarine.

The long excursions in the estimated survey AUV paths are caused by prolonged losses in communication with the survey AUVs. There seem to be two primary causes of communication loss during tank trials. The first cause is modem orientation. The WHOI modem (attached to a laptop simulating an ASC CNA) was suspended at a depth of approximately 3 m in a 4.5 m tank. This tank has tiling on its sides and part of its bottom to prevent reverberation. The Iver2 AUVs were on the surface of the tank. The horizontal separation between the modem and the AUVs was two to three metres. This resulted in a relatively acute angle (33^o to 45^o) between the modem and AUVs. Given that the WHOI modem (complete with towfish assembly, see Figure 6.1) and the AUVs had almost no translation and very slow rotation (being loosely tied in place), if there developed a poor orientation for acoustic communication (e.g. the towfish body blocks reception of acoustic transmissions from the AUVs), the loss of communication would likely last for some time.[29] The second cause was air bubbles in the tank and on the modem surfaces. Air bubbles were caused by the operation of a circulation pump, particularly if the pump was cavitating. The effects of a cavitating pump would dissipate within an hour or two of stopping the pump. When either of these effects was observed, mitigation steps were taken such as manually rotating the towfish or AUVs to improve orientation or shaking the AUVs to loosen air bubbles on the surface of the modems. While acoustic communications during tank trials were often very reliable (hardly any missed

[28] Alternately, the survey AUVs might transit to the park point underwater and then surface. In this case, the CNA might stop aiding them when they begin their return path (leaving the AUVs to surface for a GPS fix as required) or when they surface at the park point.
[29] According to [97], orientation can also cause acoustic communication drop-outs due to propeller wake. However, in the trials run in this thesis the relative orientation changed frequently, so this should not have caused prolonged drop-outs during harbour trials.

transmissions), the prolonged drop-outs were never as long in the harbour trials as in the tank trials making the acoustic communication in the harbour trials slightly more reliable.

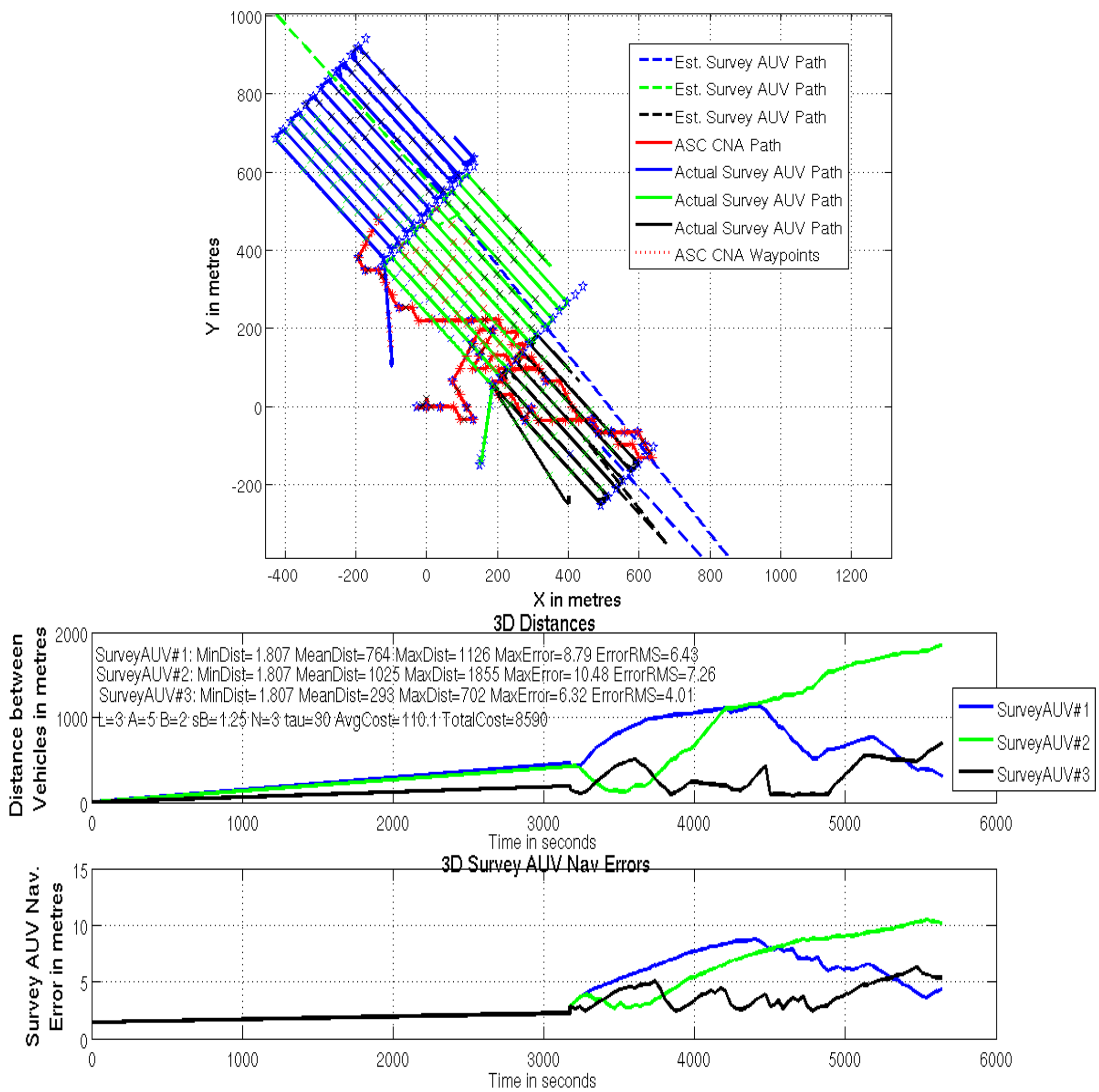

Figure 6.12: Partial tank trial with three survey AUVs (10 m mode depth)

The full three-survey AUV tank trial was run twice. In the first trial (Figure 6.13), the survey AUVs simulated diving to a depth of 10 m for 5 min, surfacing for 1 min, and then diving again. In the second trial (Figure 6.14), the survey AUVs simulated diving to a depth of 5 m. The *x-y* path of the survey AUVs is the same in both trials and the survey AUVs travel at 1.25 m/s. The ASC CNA travels at 1.25 m/s with five heading options (*A*) and three look-ahead time steps (*L*). The survey AUVs each have their own initial locations south of their assigned areas. This same point is their recovery point after completing their assigned surveys. The blue (Alpha) and green (Bravo) survey AUVs begin their surveys at the south corner of their assigned areas, but the black (Charlie) survey AUV begins its survey at the west corner of his assigned area. This is simply the result of the lawnmower path planning function in the MOOS-IvP waypoint behaviour; however, it is significant because multiple vehicle simulations presented in this thesis have all survey AUVs running in the same direction (except for orthogonal lawnmower patterns such as Figure 6.7). As can be seen in Figure 6.13 and Figure 6.14, the error is bounded even with survey AUVs travelling in different directions.

In these figures, the blue asterisks indicate waypoints transmitted by the vehicle on whose path the asterisk lies and received by at least one of the other vehicles. The dashed lines indicate the survey AUV path as estimated by the CNA based on acoustic messages received from the survey AUVs. In both trials, there are significant drop-outs in communications from one of the survey AUVs, causing the estimated paths of the survey AUVs to continue in a straight line rather than changing heading at the waypoints. The cause of these drop-outs was explored above. Unfortunately, the drop-outs prevent the two trials from being accurately compared for the effect of survey AUV depth.

There were other drop-outs in communications, but the length of the survey AUV lawnmower legs and the transmission of the next three waypoints prevent these drop-outs from impacting the accuracy of the CNA's estimate of the survey AUV paths. This was the plan in the use of three waypoints. The triangle formed by the estimated and actual survey AUV paths at the end of the lawnmower pattern is due to the fact that the survey AUV's return waypoint is not presently sent to the CNA until the final lawnmower waypoint is reached and the active survey AUV behaviour becomes the return waypoint behaviour. There is doubtless a way to remedy this issue, but in the meantime, there will always be a slight divergence between estimated and actual survey AUV paths as the CNA will assume a straight-line path for the survey AUVs until it hears that they are heading for their return points.

The path to the return point is on the surface. In an actual implementation with cooperative navigation, the CNA would not need to support the survey AUVs during a surface transit. However, it may be beneficial for the survey AUVs to transit to, and from, their survey areas under water due to their better mobility underwater (avoiding higher drag experienced on the surface and much of the sea-state effects). Should covertness be a mission requirement, the survey AUVs would have to spend the entire mission submerged with an AUV CNA surfacing only for its own GPS fixes (Section 6.2).

The ASC CNA paths in Figure 6.13 and Figure 6.14 are somewhat distinct from the CNA path in simulations such as Figure 5.26. This can partly be attributed to the increase in τ from 10 sec to 30 sec and to the poorer estimate of survey AUV position in underway path planning with acoustic communications. The paths of the survey AUVs (not all in the same direction and not arriving at waypoint synchronously) may also have an effect. However, the primary cause seems to be the start point of the CNA. Unlike the pre-deployment simulations, the CNA starts outside the survey area. Given that the CNA path is determined by the combination of the path planning algorithm and the distance penalties (when applicable), there is no inherent reason for the CNA to enter the survey area. In Figure 6.13, except during the prolonged communication black-out with the green survey AUV (#2) and towards the very end of the trial, the CNA stays near the south-west side of survey AUV #2. The path of this survey AUV generally represents the average position of all three survey AUVs at any time. By staying near the average position and staying to one side, the CNA is able to maintain maximum and minimum distances from the survey AUVs and use survey AUV motion to its advantage in maximizing the change in relative bearing with the survey AUVs in order to minimize the size of their position error ellipses (Figure 1.2) as part of the path planning algorithm.

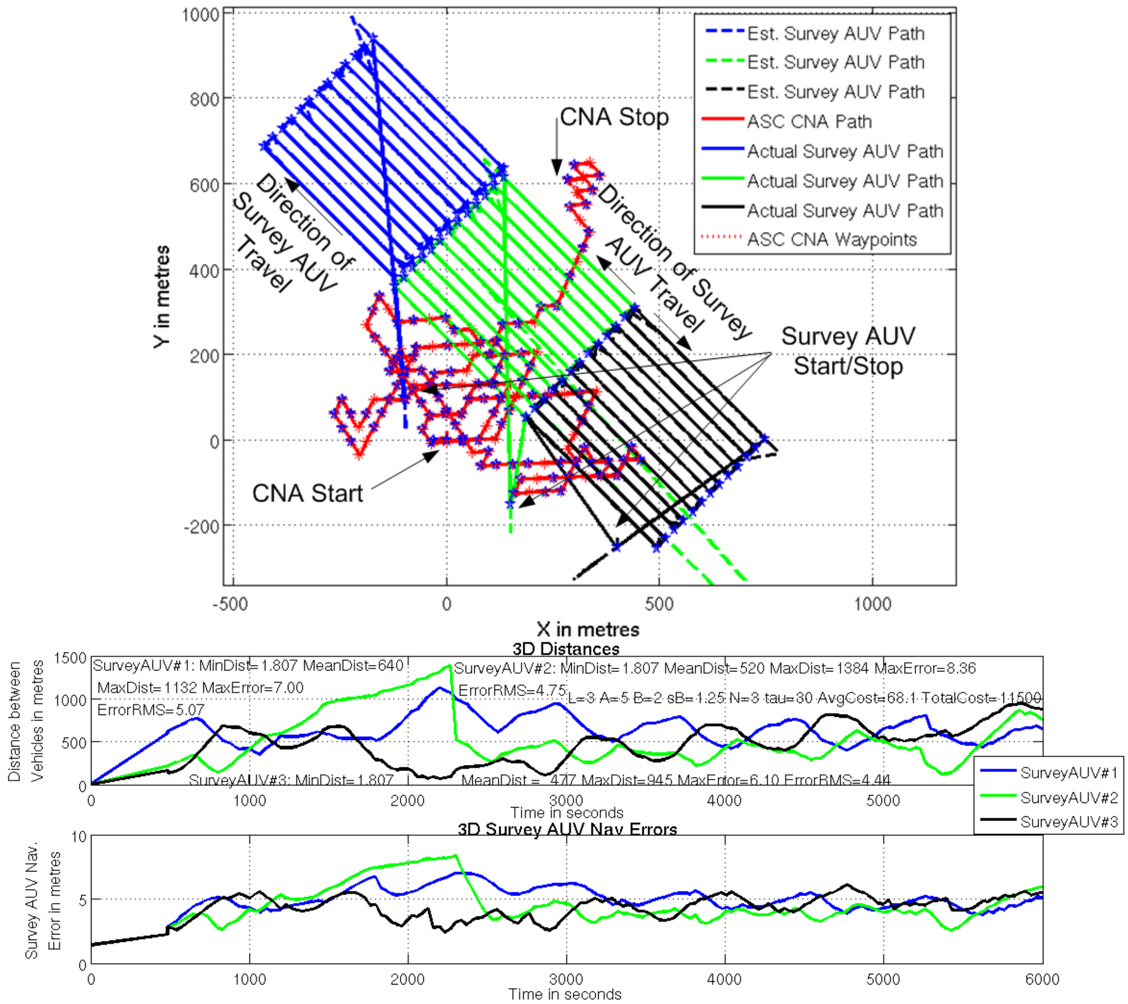

Figure 6.13: Tank trial with three survey AUVs, mode depth of 10 m

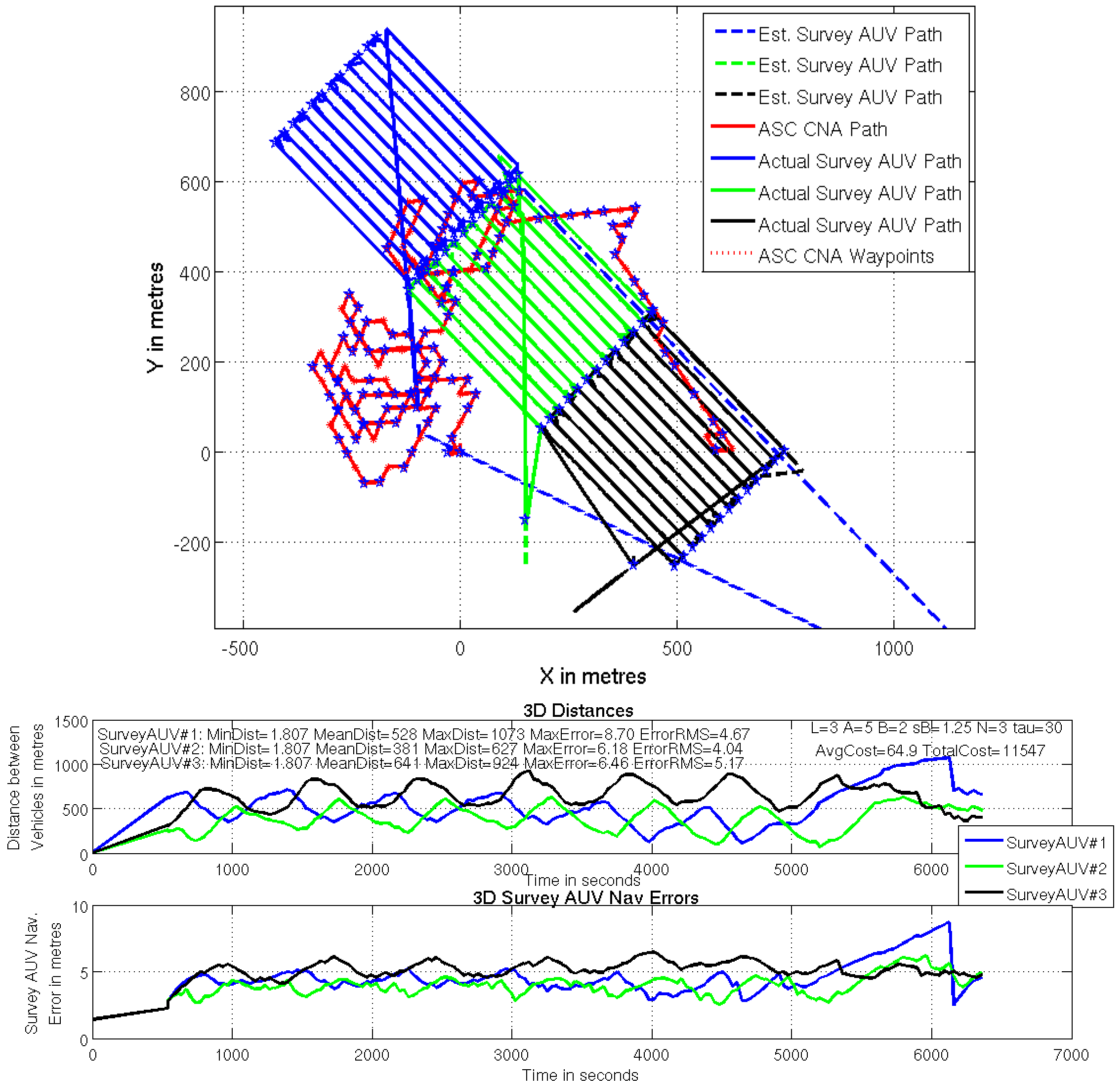

Figure 6.14: Tank trial with three survey AUVs, mode depth of 5 m

Other tank trials include repeating harbour trials as shown in Section 6.5.3 and the additional tank trials in Appendix B. A complete list of completed and planned tank and harbour trials is shown in Table B.1, and the main trials from that table are shown in Table 6.7.

Table 6.7: Primary tank and harbour trials

N	Pattern	Depth	CNA Params	1st Harbour Trial	2nd Harbour Trial	Tank Trial
1	Lawnmower	10 m	A=5,L=5	Figure 6.18		Figure 6.20
1	Lawnmower	10 m	A=3,L=0	Figure 6.23		Figure 6.26
1	Lawnmower	5 m	A=5,L=5	Figure 6.28	Figure 6.36	Figure 6.32
1	Lawnmower	5 m	A=3,L=0	Figure 6.38	Figure 6.39	Figure 6.40
1	Lawnmower	Alt.	A=5,L=5	Figure 6.42	Figure 6.44	
1	Lawnmower	Alt.	A=3,L=0	Figure 6.46		
2	Ortho.Short	10 m	A=5,L=5	Figure 6.47		Figure 6.49
2	Ortho.Short	10 m	A=3,L=0	Figure 6.53		Figure 6.54
2	Ortho.Short	5 m	A=5,L=5	Figure 6.56		Figure 6.57
2	Ortho.Short	5 m	A=3,L=0	Figure 6.58		Figure 6.61
2	Ortho.Short	Alt.	A=5,L=5	Figure 6.63		Figure 6.64
2	Ortho.Short	Alt.	A=3,L=0	Figure 6.66		Figure 6.67

6.5.3. Harbour Trials

Harbour trials were conducted with one or two survey AUVs and a single ASC CNA. In some cases the ASC CNA role is filled by an Iver2 AUV and in other cases it is simulated on a laptop connected to the WHOI Micro-modem deck unit. The survey AUVs were likewise either an Iver2 or a laptop connected to a WHOI Micro-modem deck unit. It was discovered during these trials that best communication results were achieved when the ASC CNA was simulated by a laptop and a WHOI modem rather than when the ASC CNA was simulated by a surfaced AUV. This is due to the flow noise generated by the water moving around the AUV’s acoustic modem when it is near the surface. The survey AUVs spend the majority of their time underwater, and the WHOI modem, connected to the laptop, is held stationary at 4-5 m depth (the key being the lack of motion more than the depth). This is consistent with the results of [31], which recommends suspending the modem below an ASC rather than attaching it to the hull.

Figure 6.15: An Iver2 AUV during harbour trials

In MCM missions, AUVs maintain a specified altitude over the seafloor. In some cases this altitude may be as little as 3 m or as much as 10 m, depending largely on sonar swath width (Figure 1.1) and frequency. Testing the effect of altitude keeping on the communication rate between the CNA and the survey AUVs was desired as part of this thesis. To this end, five altitude keeping missions were conducted, including two missions with two survey AUVs, in addition to two preliminary tests. These missions were run at an altitude of 10 m. Lower altitude missions were not run due to concerns about MOOS-IvP's ability to control depth fast enough to prevent grounding.[30] The communications concern was that at low altitudes, the acoustic communication from the survey AUVs would be lost as the bottom absorbed or reflected (depending on the bottom type) most of the signal. This may very well be the case at altitudes lower than 10 m or over other bottom types. Figure 6.16 shows adequate communication at 10 m altitude during one of the test runs. Figure 6.17 shows the results of the second test run. (The other altitude keeping trials are shown at the end of the single and multiple survey AUV trial discussions. The seafloor in this part of the harbour is quite muddy.) If acoustic communication degrades in these conditions, consideration should be given to mounting the acoustic modem transducer on the top of the AUV rather than its current location

[30] Altitude keeping in MOOS-IvP is performed by giving the frontseat a desired depth based on MOOS-IvP's desired altitude and its estimate of current total water depth. It may be possible to create an altitude domain in MOOS's HelmIvP (similar to the current depth, speed, and heading domains) so that a desired altitude can be passed directly to the frontseat to work around the latency in MOOS-IvP's architecture. However this may require modification of the current backseat-to-frontseat interface (iOceanServerComms [100]) and frontseat-to-backseat interface (Remote Helm [119]).

below the mast on the Iver2. The loss of acoustic communication when surfaced could be overcome by using the installed 900 MHz radio.

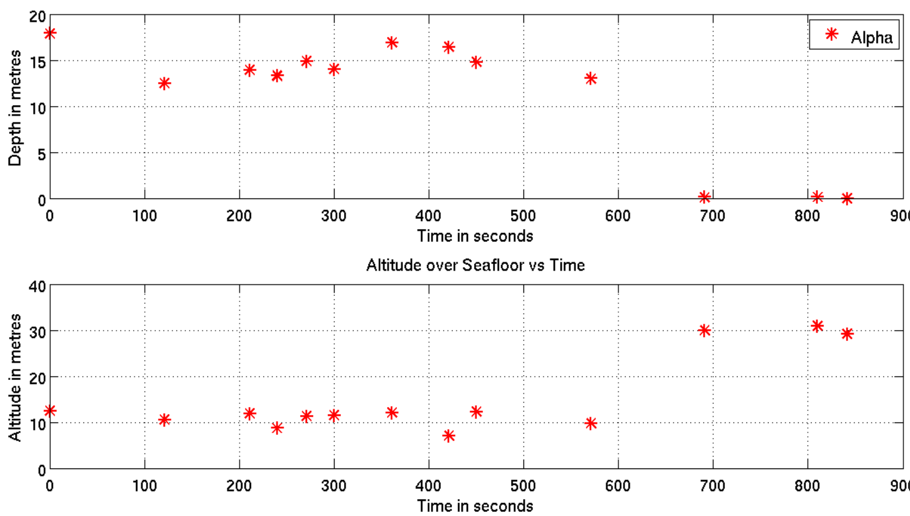

Figure 6.16: Plots of depth and altitude of survey AUV at times its acoustic transmissions were received by simulated ASC CNA

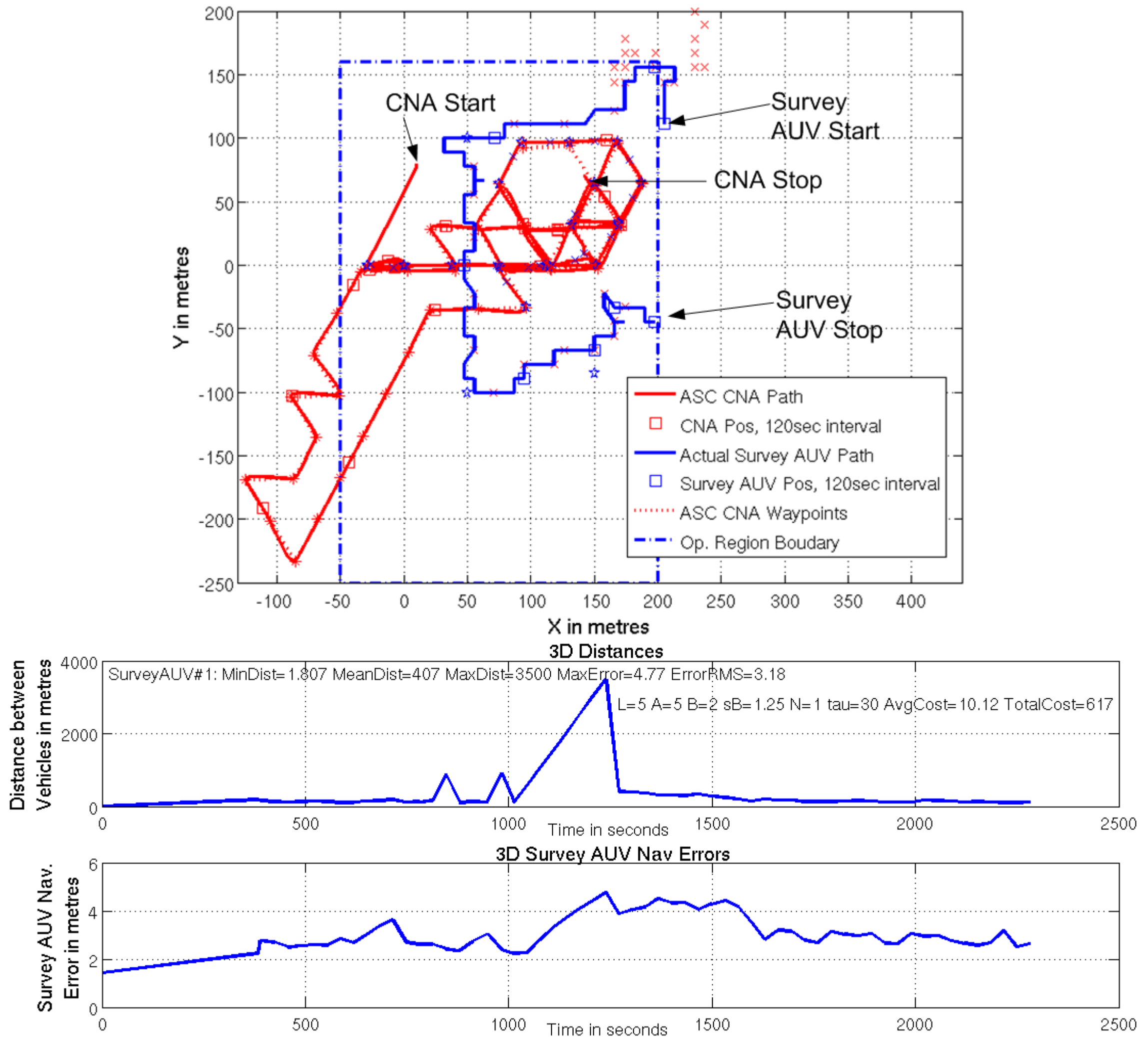

Figure 6.17: Results of a second altitude keeping test run

A complete list of all planned and conducted in-water trials is found in Table B.1 with the primary trials listed in Table 6.7. The harbour trials shown in this section progress in the following manner: One-survey AUV trials at 10-m depth (good and poor path planning parameters); one-survey AUV trials at 5-m depth (good and poor path planning parameters); one-survey AUV trials at 10-m altitude (good and poor path planning parameters); two-survey AUV trials on orthogonal tracks at 10-m depth (good and poor path planning parameters); two-survey AUV trials on orthogonal tracks at 5-m depth (good and poor path planning parameters); two-survey AUV trials on orthogonal tracks at 10-m altitude (good and poor path planning parameters); and two-survey AUV trials on parallel tracks at 10-m depth (good and poor path planning parameters). The last two harbour trials had limited success but are shown since they are the longest harbour trials run as part of this thesis. Where possible, tank trials matching the harbour trials are shown. The poor CNA path planning parameters (A = 3, L = 0) and the good parameters (A = 5, L = 5) are shown to demonstrate that better parameters do result in improved performance of the path planning algorithm. Some short duration harbour trials were run multiple times when time remained on a particular trial day for only a short run. Further tank trials for which corresponding harbour trials were not run are found in Appendix B.

Figure 6.18 shows an Iver2 AUV acting as an ASC CNA (red) and a survey AUV simulated by a laptop connected to the WHOI Micro-Modem deck unit. The WHOI acoustic modem is suspended over the side of a barge moored beside the trials area. The CNA operates at 1.25 m/s while the survey AUV(s) operate at 1 m/s. These speeds are consistent across all in-water trials. The survey AUV varies its depth on a predetermined cycle of 10 m for 5 min followed by 0 m for 1 min before diving to 10 m again. (This diving and surfacing cycle is illustrated in Figure 6.30.) The survey AUV begins by transiting to the upper left of the plot, follows the lawnmower pattern to the bottom of Figure 6.18, and then transits to a recovery point. The CNA enters the water on the right of the plot and transits to a pair of waypoints before commencing its adaptive path planning mission. While the CNA is transiting to these first two waypoints, it receives two acoustic messages from the survey AUV. The purpose of the two initial waypoints is to bring the CNA to the planner's assumed start point with roughly the assumed heading (due east). Later versions of *pCnaPathPlanning* may have the planner use the CNA's initial location and heading as its starting point rather than requiring the CNA to transit to the planner's start point when in underway path planning mode. Figure 6.19 shows the results of this trial in terms of distance between vehicles and navigation error estimate.[31]

[31] The minimum distance listed for all the tank and harbour trials is 1.807 m. This is due to the assumed initial positions of the survey AUVs and is not accurate. Later versions of pCnaPathPlanning will remove this assumption.

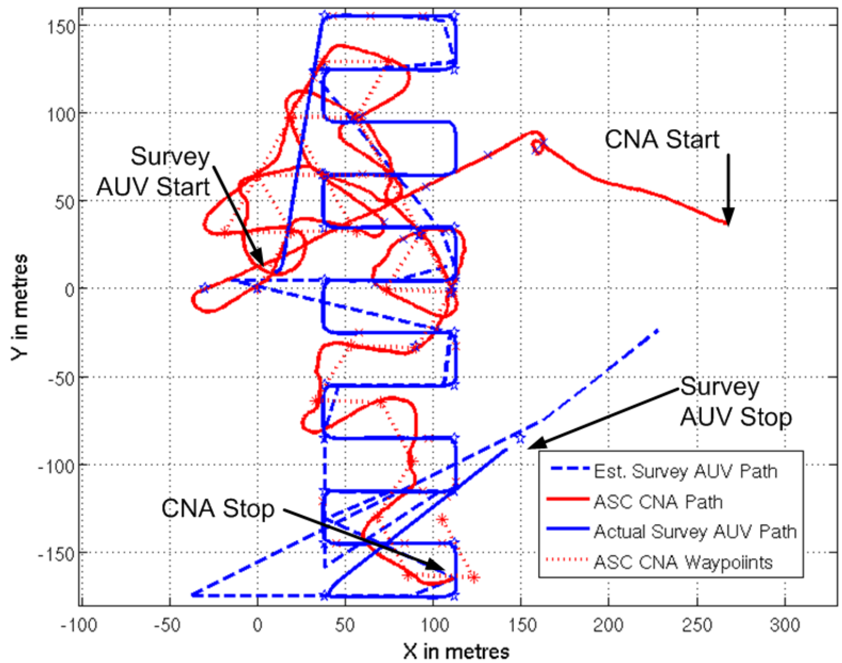

Figure 6.18: An Iver2 AUV acting as an ASC CNA plans its path while underway in a harbour trial to support a simulated AUV with variable depth (mode of 10 m)

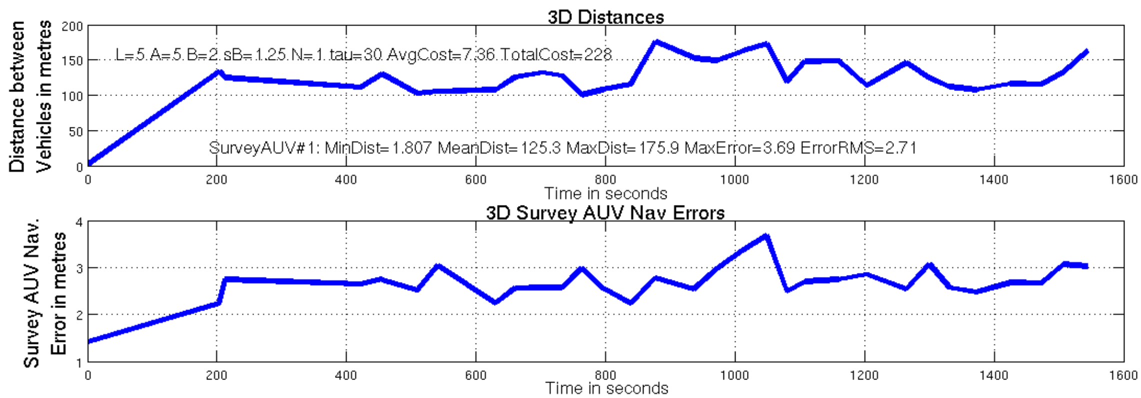

Figure 6.19: Distance and survey AUV position error vs. time for in-water trial shown in Figure 6.18

Figure 6.20 shows a tank trial repeating the harbour trial in Figure 6.18. The results are shown in Figure 6.21, and the two trials are overlaid in Figure 6.22. While the CNA paths are obviously quite different, comparing the numbers in Figure 6.19 and Figure 6.21 shows that the results are consistent. The differences in paths are cause by differing estimates of survey AUV position, which are in turn caused by differing times for acoustic updates.

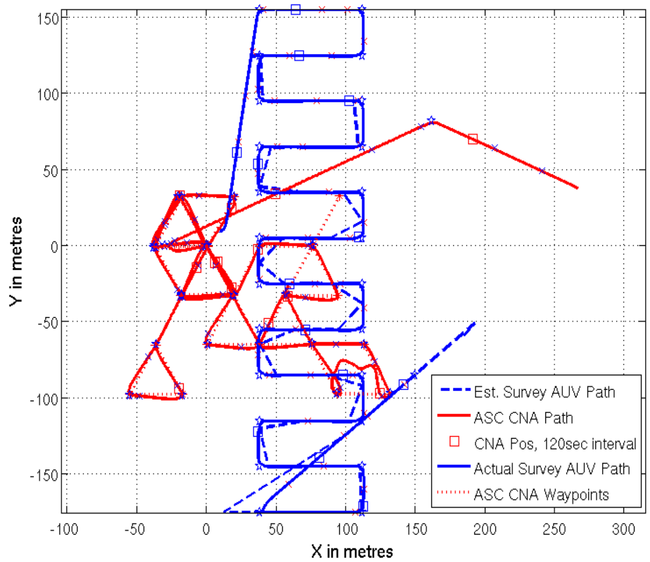

Figure 6.20: Tank trial of in-water trial shown in Figure 6.18 (10 m mode depth)

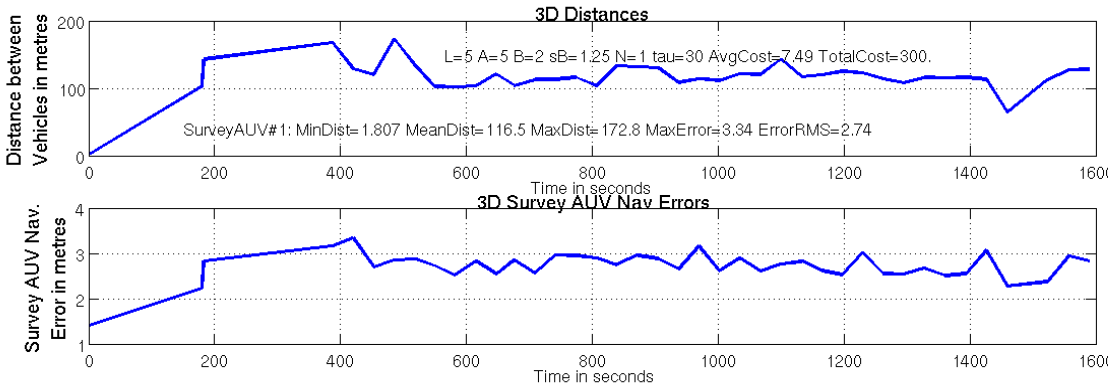

Figure 6.21: Distance and survey AUV position error vs. time for tank trial shown in Figure 6.20

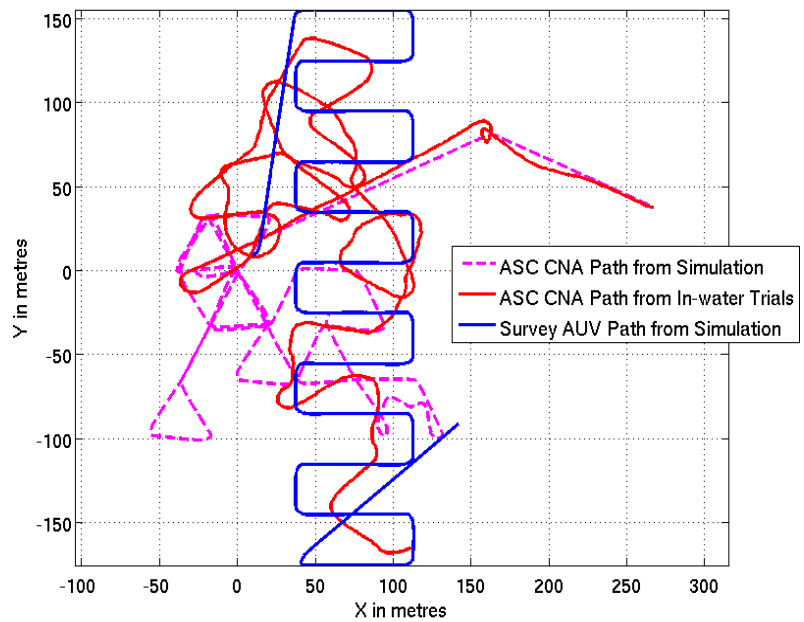

Figure 6.22: Position plots from Figure 6.18 and Figure 6.20 overlaid

Figure 6.23 shows the results of another in-water trial. The survey AUV has a mode depth of 10 m as in Figure 6.18, but in this case, the number of heading options (A) has been reduced to three, and there is no look-ahead (L). For safety, the CNA is simulated since the reduced path planning parameters ($A = 3$, $L = 0$) are less likely to stay within the operating region. The distance and error plots are shown in Figure 6.24. While the errors are similar to those shown in Figure 6.19 and Figure 6.21, the mean and maximum distances are higher. In addition, Figure 6.25 shows that the CNA path does not follow the survey AUV as closely with the reduced planning parameters. The CNA path ends near (-25,-75), showing it heading generally away from the survey AUV (now attempting to park) and explaining the upward trend at the end of the plots in Figure 6.24. This happens sooner in many A=3, L=0 trials, and the trend seems only to be checked by the distance penalty (see Figure 6.38) showing the effectiveness of the distance penalty.

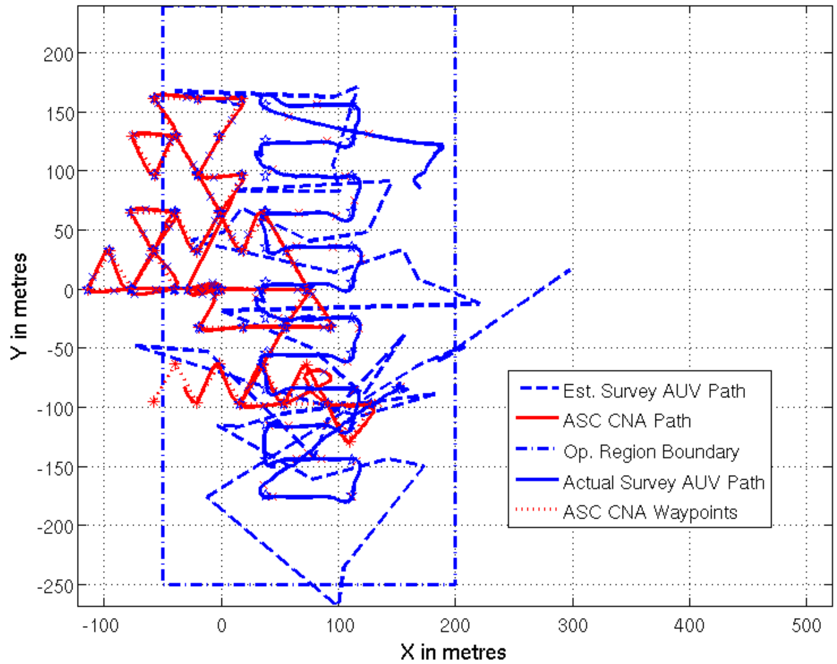

Figure 6.23: A simulated ASC CNA plans its path underway to support an Iver2 AUV following a variable depth lawnmower pattern in Halifax Harbour (mode depth of 10 m)

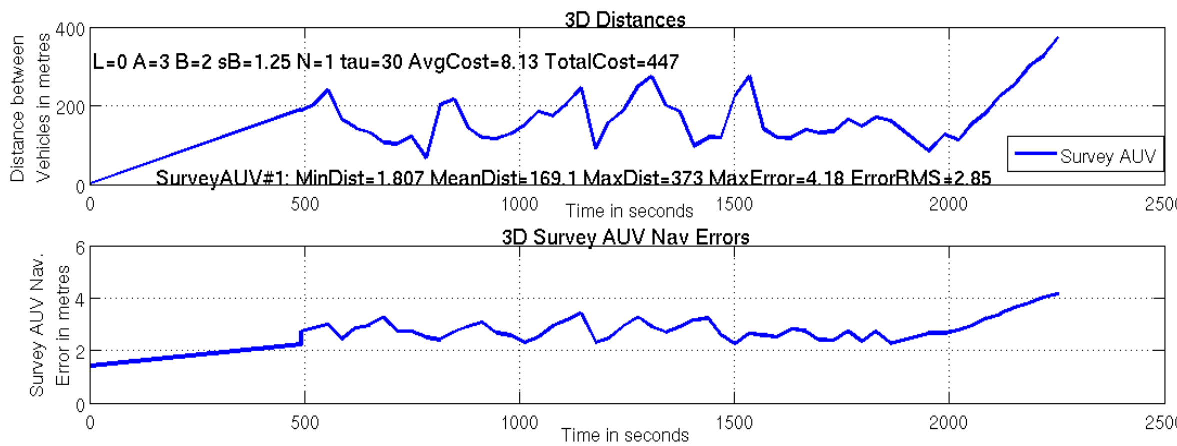

Figure 6.24: Distance and survey AUV position error vs. time for in-water trial shown in Figure 6.23

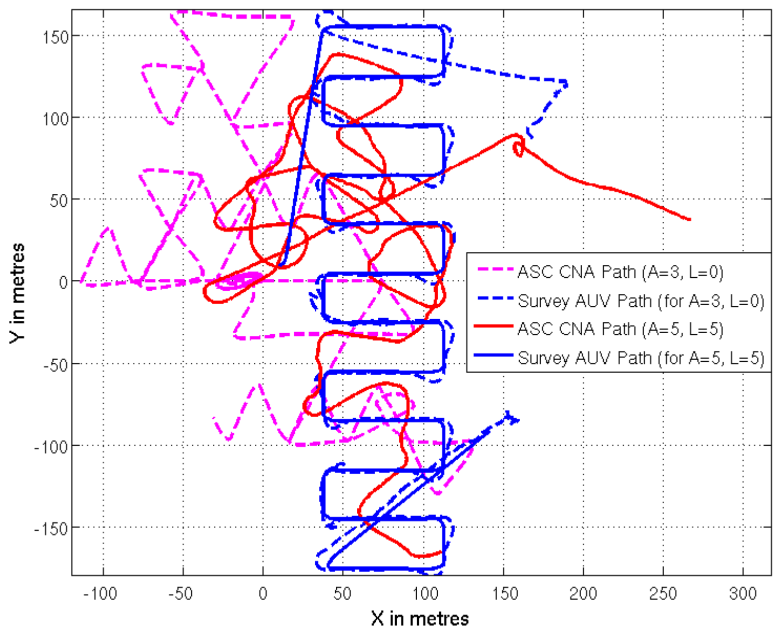

Figure 6.25: Overlay of Figure 6.18 and Figure 6.23 demonstrating the tighter looping of the more effective CNA parameters Figure 6.18

Figure 6.26 is a tank trial repeating the harbour trial in Figure 6.23. The distance and error plots are in Figure 6.27. The paths are once again quite different. This is attributed to a better acoustic communication environment experienced in the tank during this trial. Evidence of the better communication is seen in the reduced number of CNA orbits between (0, 30) and (0, 0) in Figure 6.26 and by the higher number of red ×'s on the survey AUV path, indicating the survey AUV's position when an acoustic transmission was received by the CNA. The error in Figure 6.27 is very close to that in Figure 6.24, but the increasing error and distance in Figure 6.24 (and the diverging path in Figure 6.23) are not observed in this tank trial. This may again be attributed to the better communication environment, though the diverging path may have developed if the tank trial had run longer. (See Figure 6.38 for an extreme case.)

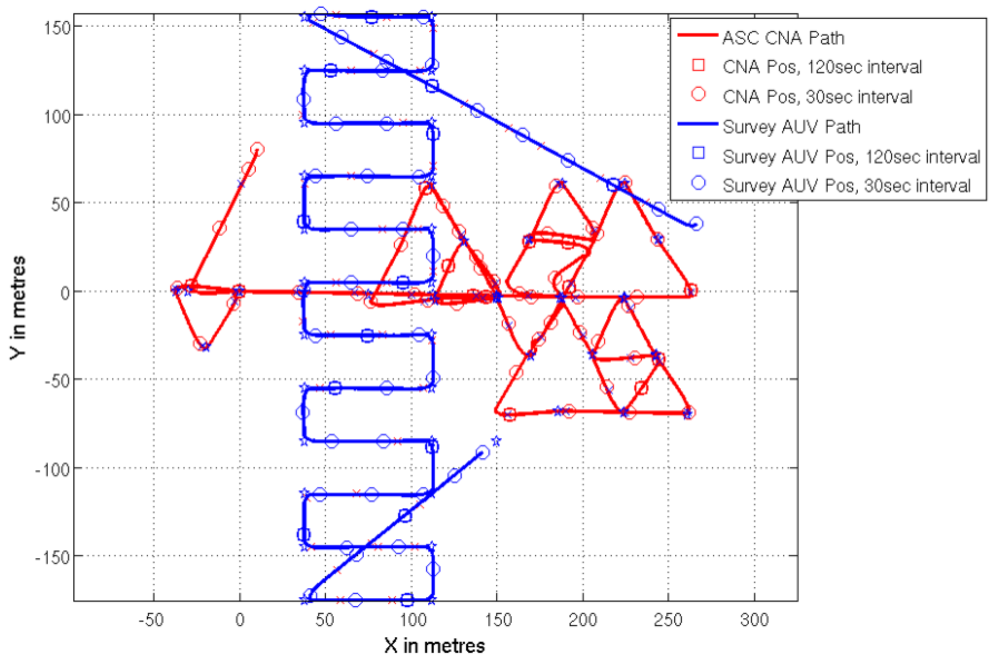

Figure 6.26: Tank trial of harbour trial shown in Figure 6.23

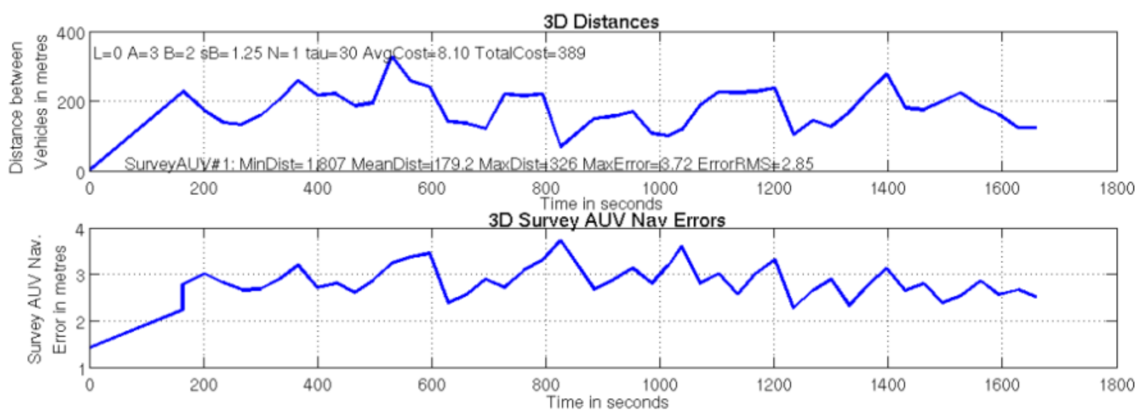

Figure 6.27: Distance and survey AUV position error vs. time for tank trials shown in Figure 6.26

Figure 6.28 illustrates a harbour trial where an Iver2 AUV acts as an ASC CNA to support a simulated survey AUV. The distance and error plots are shown in Figure 6.29. In Figure 6.29, there is a jump in the data between 1128 sec and 1623 sec. This is caused by the CNA leaving the operating region near (-50, -150), stopping due to *BHV_OpRegion* (marked in red because it is defined for the CNA vehicle, which is plotted with red lines), drifting back into the operating region, and resuming the mission.[32] Near (225, 75), the CNA once again leaves the operating region and stops. This time the CNA was recovered, and the broad arc in the path back to the (275, 50)

[32] The author's expectation, based on [100], was that the MOOS-IvP mission would actually shut down after the operating region had been violated for more than a few seconds and the basic frontseat mission would take control of the vehicle.

start point is the CNA travelling in the recovery boat. Note that a final waypoint was inadvertently reached while the CNA was in the boat. This results in another jump in Figure 6.29, this time from 2160 sec to 2375 sec (final data point). Figure 6.30 illustrates the depth-keeping cycle used in the trials for this thesis.

The reader will notice that the CNA's estimate of the survey AUV's path is quite poor at the beginning and end of the mission. The poor estimate near the beginning of the mission is related to the two early acoustic updates received (illustrated by the two red ×'s on the survey AUV's approach to its first waypoint) followed by a prolonged transit to the CNA's first planned waypoint. This means that when the CNA was finally able to plan its next waypoint, the survey AUV had moved quite far away. Future versions of *pCnaPathPlanning* that begin underway path planning from the place where the CNA enters the water will not have this problem. There is a significant deviation in the position estimate at the beginning of the third waypoint from the final leg. This would probably be caused by missed acoustic messages, and the waypoint at the beginning of the second from final leg does not appear to have been received by the CNA (absence of the blue star). The most notable error, however, is at the end of the mission because the planner did not expect the survey AUV to stop at its park point due to a limitation in the code. This error will correct itself once the survey AUV reports its speed (approximately 0 m/s) from the park point, but in the meantime, there will be some error in the position estimate.

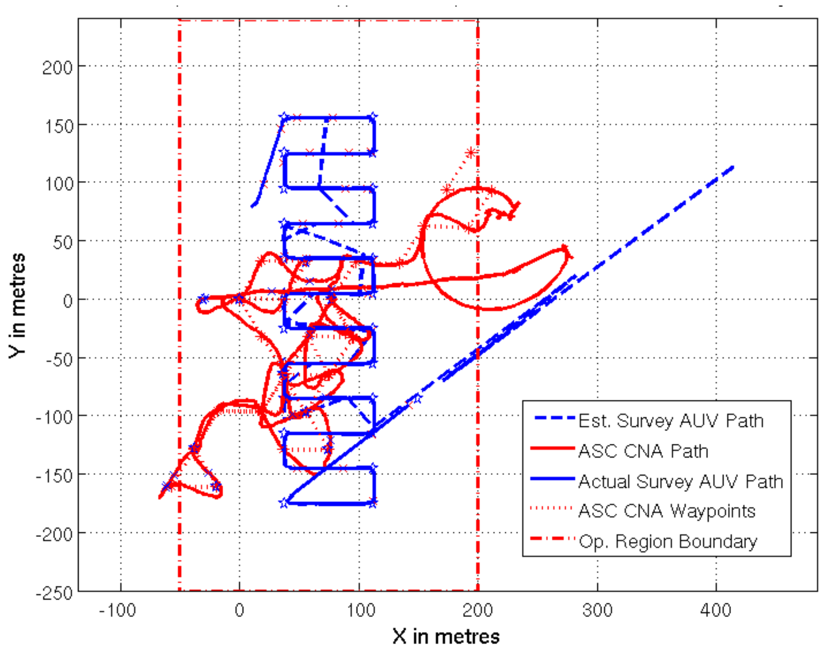

Figure 6.28: An Iver2 AUV acting as an ASC CNA plans its path underway in Halifax Harbour to support a simulated survey AUV with varible depth (mode of 5 m vs. mode of 10 m shown in Figure 6.18)

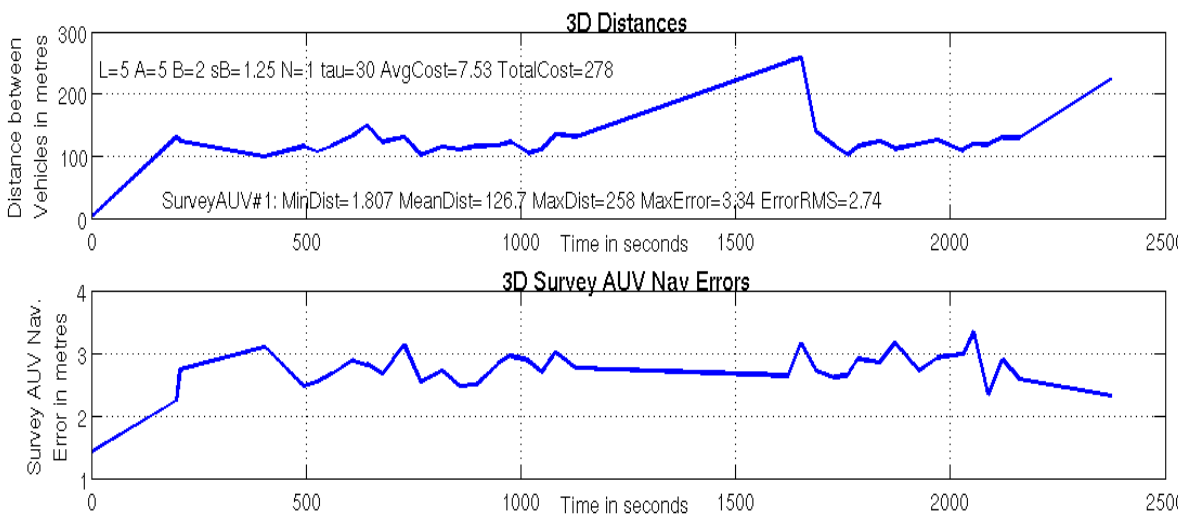

Figure 6.29: Distance and survey AUV position error vs. time for in-water trial shown in Figure 6.28

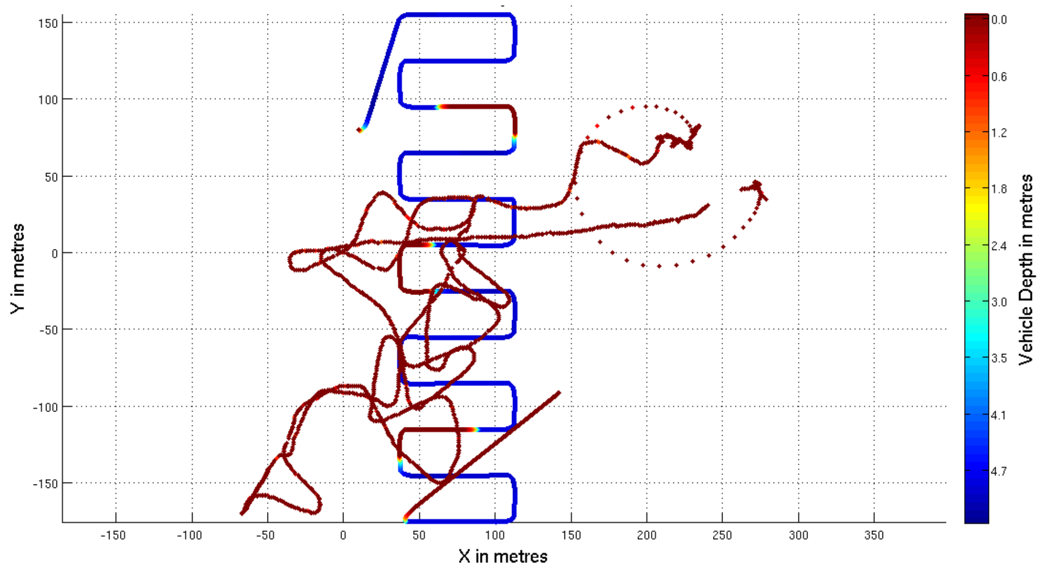

Figure 6.30: Figure 6.28 modified to show vehicle depths

Figure 6.31 shows an overlay of two harbour trials where the survey AUV varied its depth at either 5 m or 10 m. Notice that despite the issues with the 5-m run outlined above, both paths are quite close to the survey AUV path.

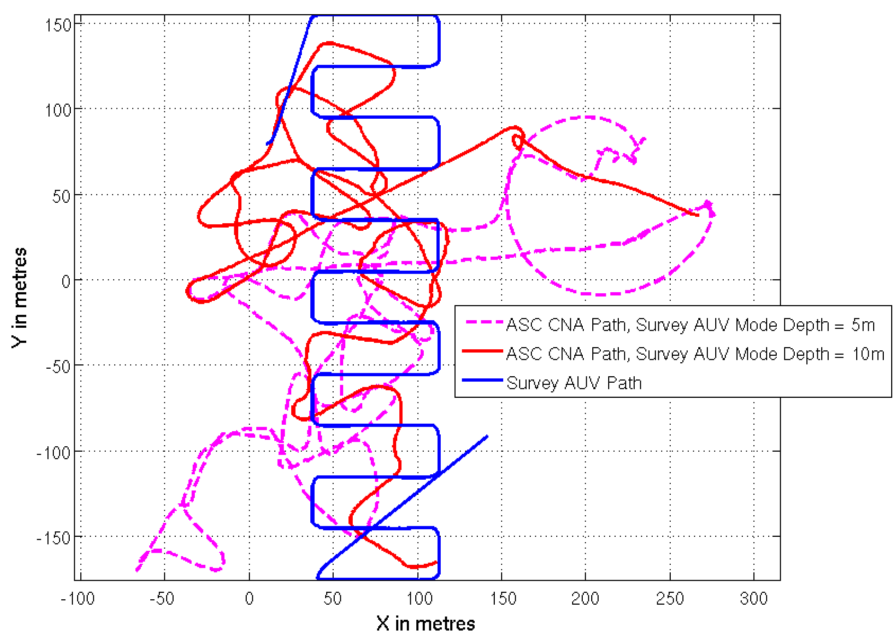

Figure 6.31: Overlay of Figure 6.18 and Figure 6.28 illustrating the potential effect of different survey AUV mode depths (5 m and 10 m)

Figure 6.32 depicts a tank trial repeating the harbour trial in Figure 6.28. The distance and error plots are in Figure 6.33. Due to the absence of the issues with the harbour trial described above, the distances and errors in the tank trial are much better. However, the total cost (the sum of all the cost calculations made for each CNA waypoint and therefore a measure of the survey AUV position error) is slightly higher in Figure 6.33. The author believes this to be due to the larger number of CNA waypoints covered during the tank trial than during the harbour trial. Once again, this relates to the issues experienced during the harbour trial. The CNA paths for the two trials are overlaid in Figure 6.34.

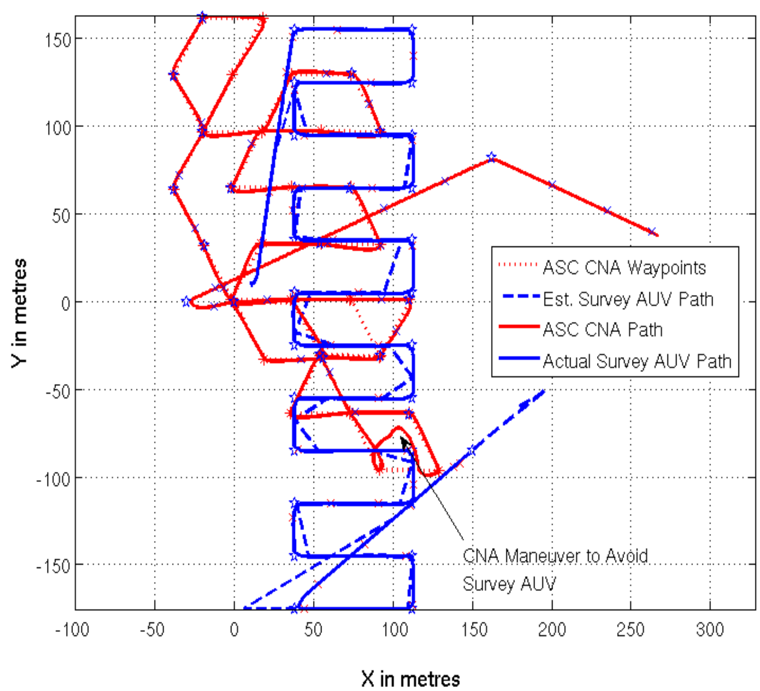

Figure 6.32: Tank trial of harbour trial shown in Figure 6.28 (5-m mode depth)

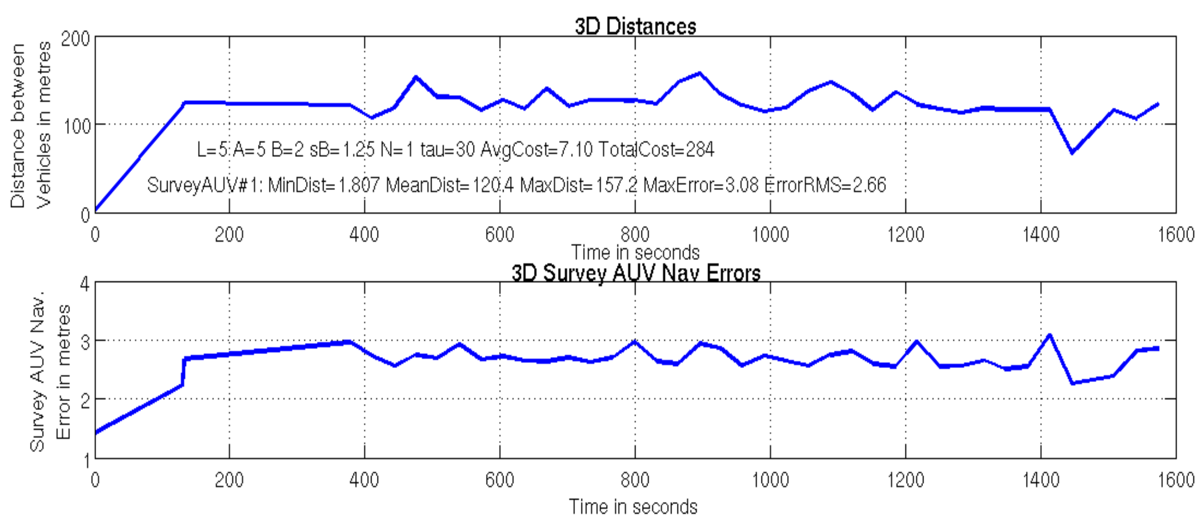

Figure 6.33: Distance and survey AUV position error vs. time for tank trial shown in Figure 6.32

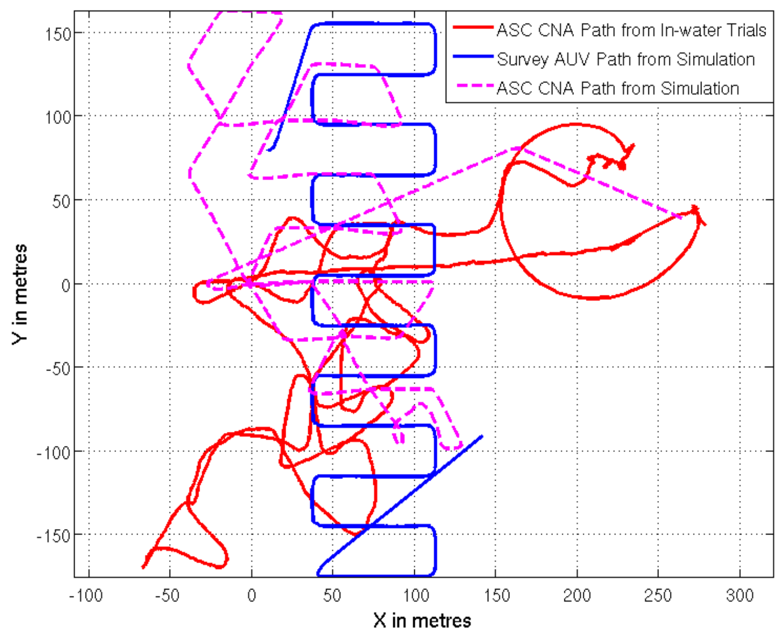

Figure 6.34: Overlay of Figure 6.28 and Figure 6.32 comparing in-water trial with tank trial (5-m mode depth)

Figure 6.36 shows a repeat of the harbour trial in Figure 6.28 but with an Iver2 AUV as the survey AUV and a simulated ASC CNA. Unhindered by an operating region, the simulated CNA performs much better in this trial, though the numbers (save for the total cost) are practically identical. The much higher total cost in Figure 6.36 is attributed to the higher number of CNA waypoints covered, as in Figure 6.33, since the total cost is the sum of the cost from each waypoint generated by the CNA.

The path of the survey AUV shows a problem that developed in the MOOS-IvP logged data following an update to the Iver2 AUV's frontseat processor. The problem manifests itself in rectangular crabbing of the (x,y) path (depth and altitude readings do not seem to be affected). On closer examination, it appears that the frontseat is not passing updated (x,y) positions to the backseat fast enough. While this makes for a very odd-looking plot, given the relatively slow rate of acoustic communication, the problem did not seem likely to affect the outcome of trials with an Iver2 AUV in the survey AUV role.

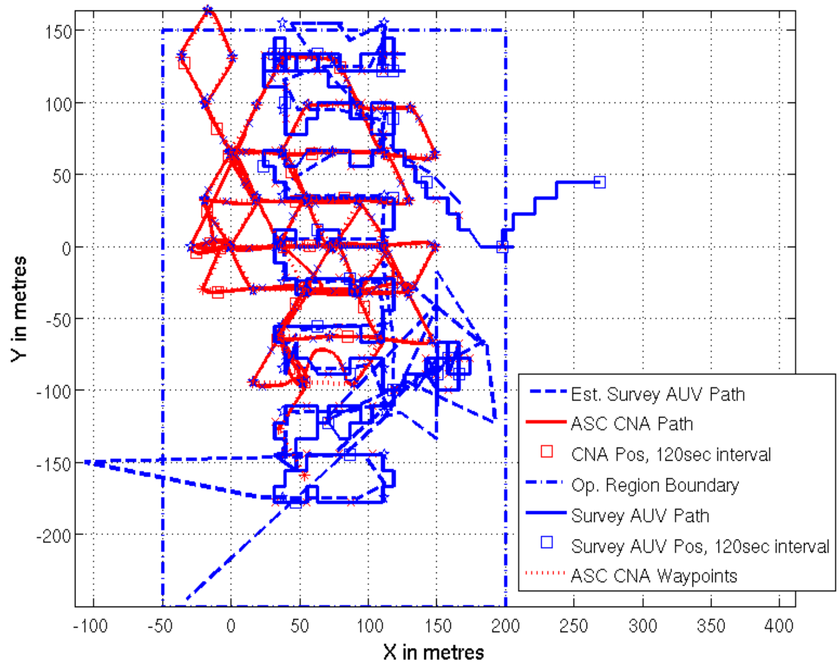

Figure 6.35: Repeat of the harbour trial in Figure 6.28 but with the Iver2 as the survey AUV rather than the CNA (mode depth of 5 m)

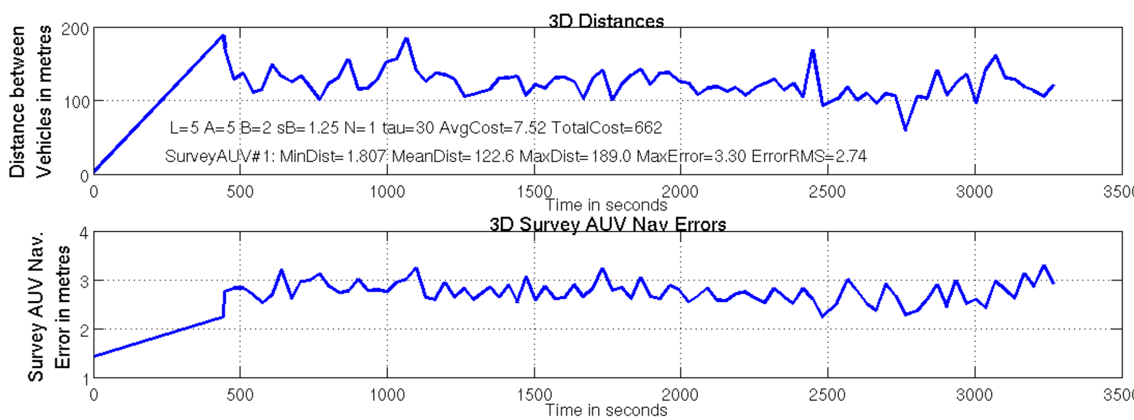

Figure 6.36 Distance and survey AUV position error vs. time for Figure 6.35

Figure 6.38 shows the results of a harbour trial where a simulated ASC CNA (using a laptop and the WHOI micro-modem deck box) supports an Iver2 AUV on a lawnmower survey mission. The survey AUV mission is identical to that used in Figure 6.28 (5-m mode depth), but the CNA parameters have been reduced to $A = 3$ and $L = 0$ (influencing the decision to use a simulated ASC rather than a surfaced Iver2 as the CNA). The trial was repeated, and the results are shown in Figure 6.39.

The trial in Figure 6.39 is obviously much better than the trial in Figure 6.38. The cause is best attributed to the rate and timing of received acoustic updates. In the case of Figure

6.38, the survey AUV had difficulty starting on its mission, forcing a restart, but not before it had sent several acoustic messages to the CNA. These are evidenced by the many red × marks on the upper right part of the operating region. The long delay between the first messages received by the CNA and the survey AUV actually reaching its first waypoint may have set the CNA off in the wrong direction. The distance and error plots in Figure 6.38 indicate that it is actually the distance penalty that bounds the error rather than the planner. The trial in Figure 6.39 does not set off in the wrong direction until much later in the mission. The cause of this wrong direction may be caused by the survey AUV heading to its park point. Using the look-ahead function should have prevented the issues in Figure 6.38, but would have taken time to help with the trial in Figure 6.39 as the planner would be basing future survey AUV position estimates on the transit speed (1.25 m/s) until the survey AUV transmitted from the park point (speed of 0 m/s).

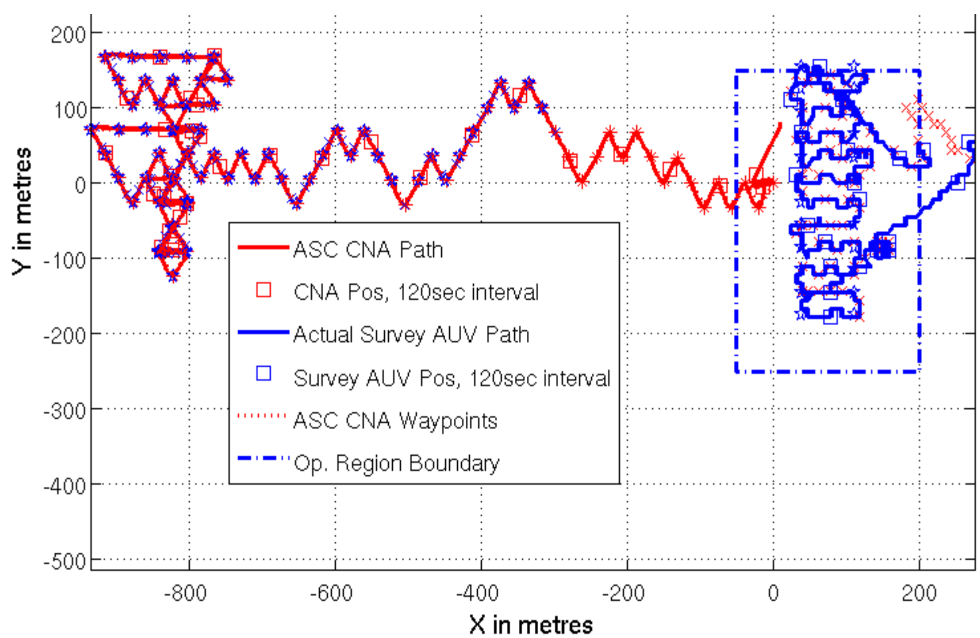

Figure 6.37: Simulated ASC CNA plans its path underway to support an Iver2 AUV following a variable depth lawnmower pattern in Halifax Harbour (mode depth of 5 m)

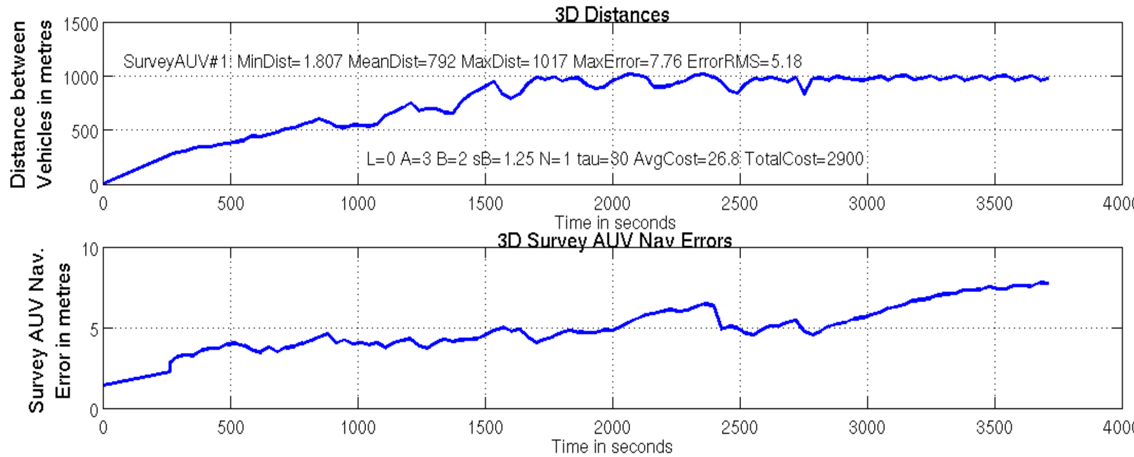

Figure 6.38: Distance and survey AUV position error vs. time from Figure 6.37

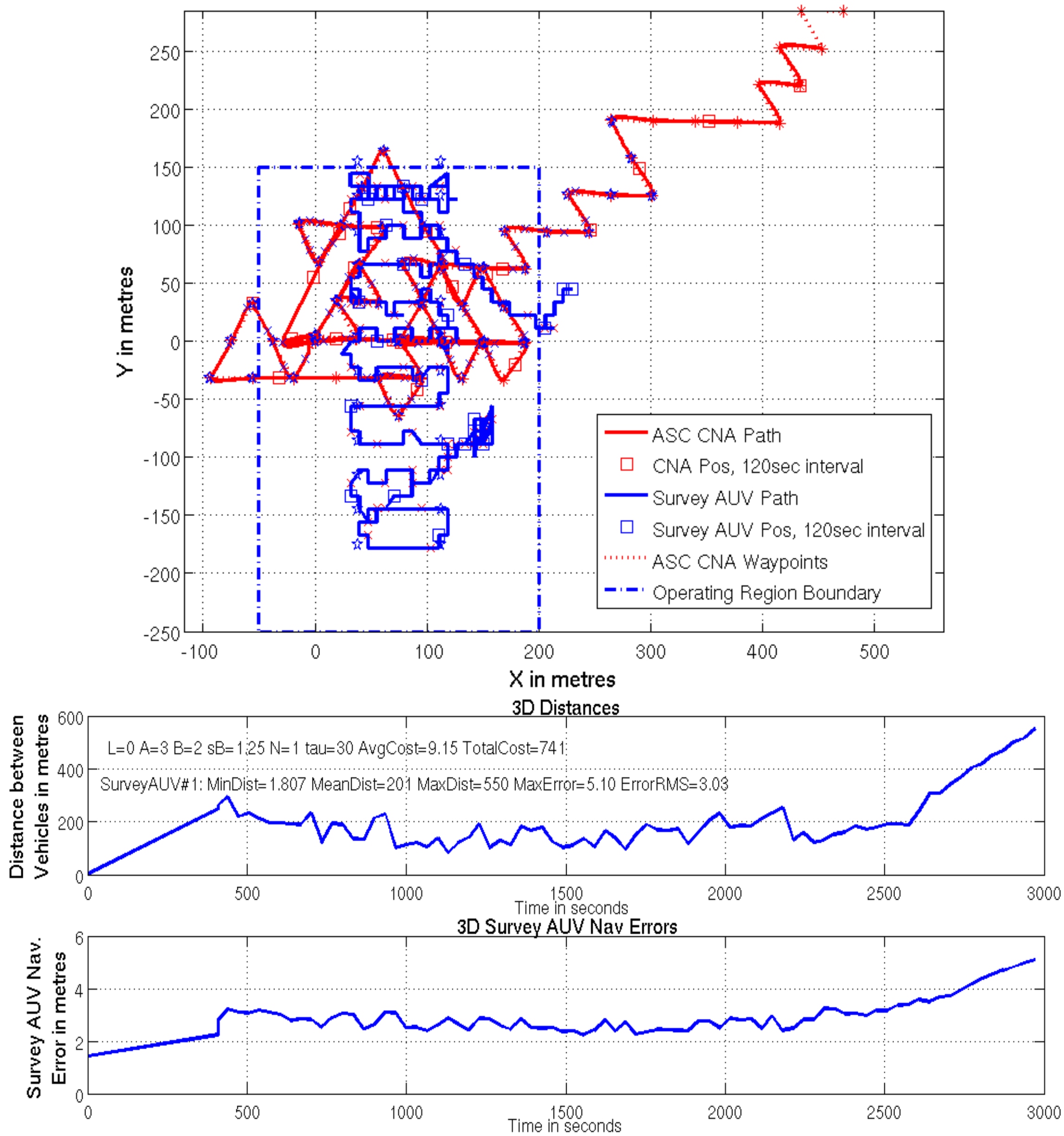

Figure 6.39: Harbour trial repeating harbour trial in Figure 6.38 (5 m mode depth)

Figure 6.40 shows the results for a tank trial duplicating the harbour trials shown in Figure 6.38 and Figure 6.39. In this trial, *BHV_OpRegionBounce* (Section 4.2) was employed for the ASC CNA and shortly after the path planner began to work, the planner determined two waypoints that were outside the operating region. *BHV_OpRegionBounce* prevented the ASC CNA from reaching these waypoints, effectively ending the trial as the CNA circled inside the operating region nearest its next waypoint for most of the duration of the trial. For this reason, the operating region is typically only defined on moving vehicles.

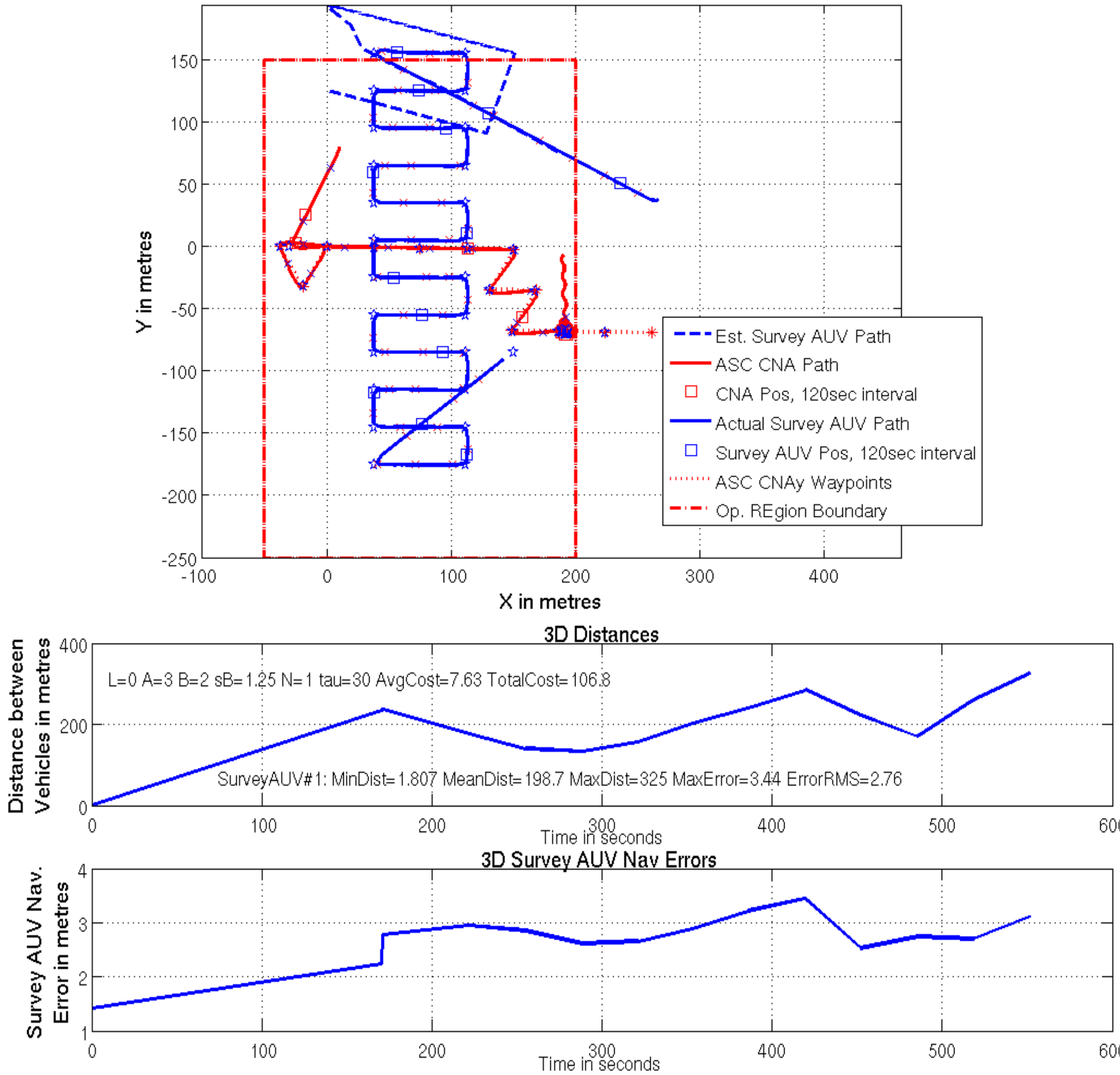

Figure 6.40: Tank trial repeating harbour trials shown in Figure 6.38 and Figure 6.39 (5 m mode depth)

Figure 6.42 shows the first full altitude-keeping mission run for this thesis. In the altitude-keeping missions, the survey AUV (an Iver2) attempts to maintain an altitude of 10 m from the seafloor. This resulted in an average depth of approximately 13 m. Meanwhile, an EKF implemented in MOOS by Paull monitors the AUVs actual position error (rather than the estimated position error used by the CNA). When the position error exceeds the limit, the EKF posts a variable to MOOSDB causing the AUV to switch from altitude keeping to a depth = 0 m behaviour until the position error (aided by GPS) is reduced to a lower limit and the EKF reposts a variable to MOOSDB causing the AUV to switch back to altitude keeping. In this mission, the minimum error was set at 2 m and the maximum error was set at 5 m. This caused the AUV to surface more often than desired, and following the fifth leg, the AUV was not able to bring its position error low enough to allow the AUV to return to altitude keeping and the AUV spent the remainder of the mission on the surface. The reason for this inability to dive may be that the AUV was trimmed too low (placing the mast very close to the water) for the GPS to get a sufficiently accurate fix. Later missions used a minimum error of 3 m and a maximum error of 15 m. This proved more satisfactory with the AUV surfacing only once near the end of the mission. In spite of the issues experienced by the survey AUV, the CNA was able to support the survey AUV well and the CNA's estimate of the survey AUV path is quite accurate until the survey AUV executes the return and park portions of its mission.

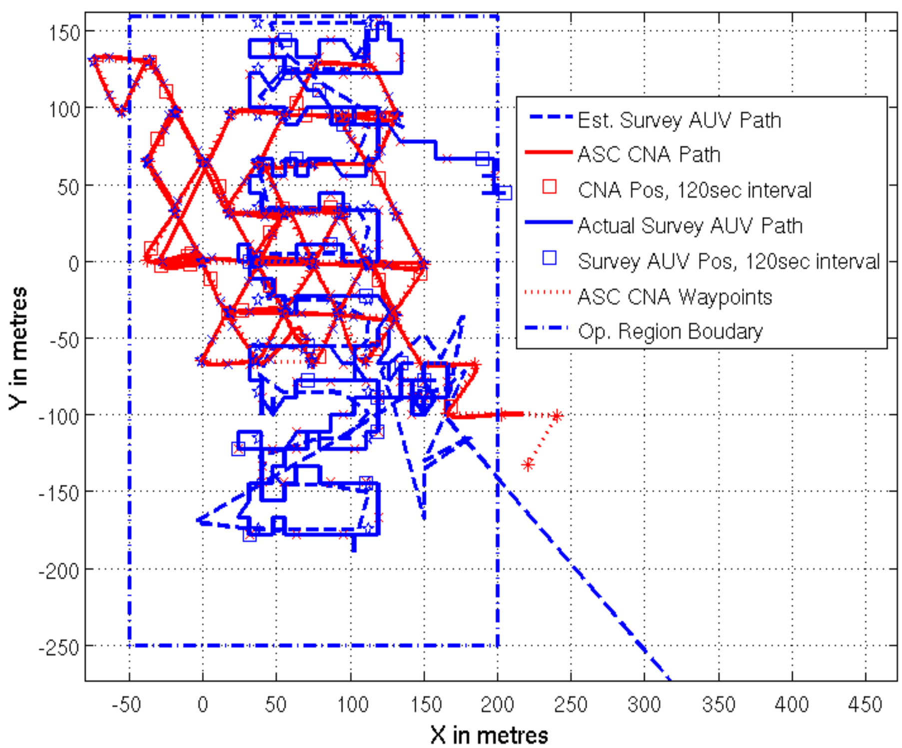

Figure 6.41: Simulated ASC CNA plans its path underway to support an Iver2 AUV following a lawnmower pattern in Halifax Harbour at 10 m altitude

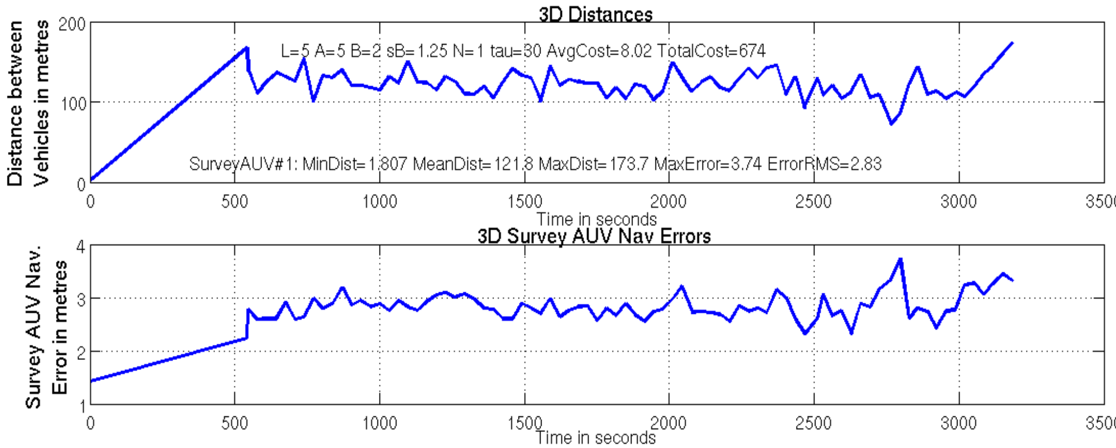

Figure 6.42: Distance and survey AUV position error vs. time from Figure 6.41

Figure 6.44 repeats Figure 6.42 with the improved EFK surfacing parameters described above. The results in the distance and error plots are largely the same. The CNA's estimate of the survey AUV's position is quite good in both trials until the survey AUV reaches the park point. This is at least partly due to the fairly fast surface current at the time, forcing the survey AUVs to move around to maintain the park location. While the survey AUVs are moving, their reported speeds will be used by the CNA's planner to predict the future position of the survey AUV. As mentioned earlier, the planner does not realize that the survey AUV will stop at the park point. This could be remedied in a future version of *pCnaPathPlanning*.

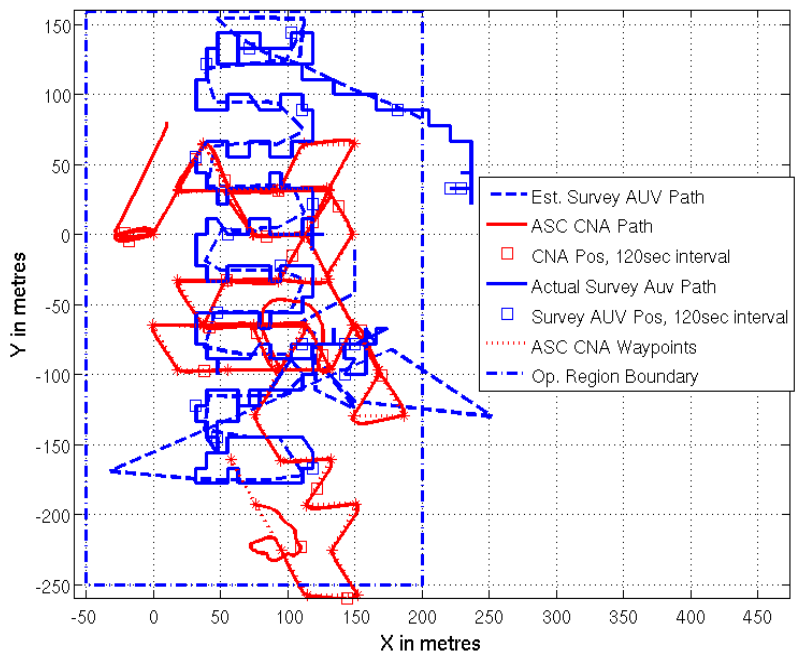

Figure 6.43: Repeat of the harbour trial in Figure 6.42 (10 m altitude) with modified surfacing requirements

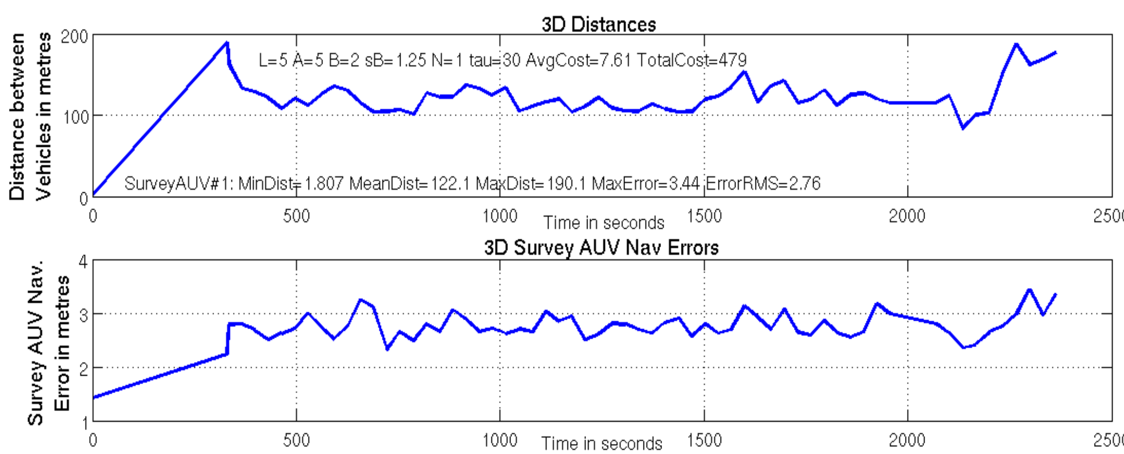

Figure 6.44: Distance and survey AUV position error vs. time

Figure 6.46 shows a repeat of the trial from Figure 6.44 but with reduced CNA path planning parameters. As in Figure 6.38, the CNA vehicle heads in the wrong direction, and it is the distance penalty that brings the survey AUV position error under control. As shown in the inset, the estimated survey AUV position is quite poor. This is partly due to the rate of received communications, but is also due to the fact that the planner does not consider more than one future waypoint when there is no look-ahead. This aspect of the planner's code was implemented during computer testing (Section 6.5.1) in order to reduce unnecessary computations. However, it was discovered during in-water testing that since acoustic transmissions are frequently missed, the planner would have benefitted from keeping information transmitted on all future waypoints instead of relating the number of waypoints kept to the number of look-ahead steps (particularly when the lawnmower legs are short). To keep the trials consistent, this correction was not made during the harbour trials.

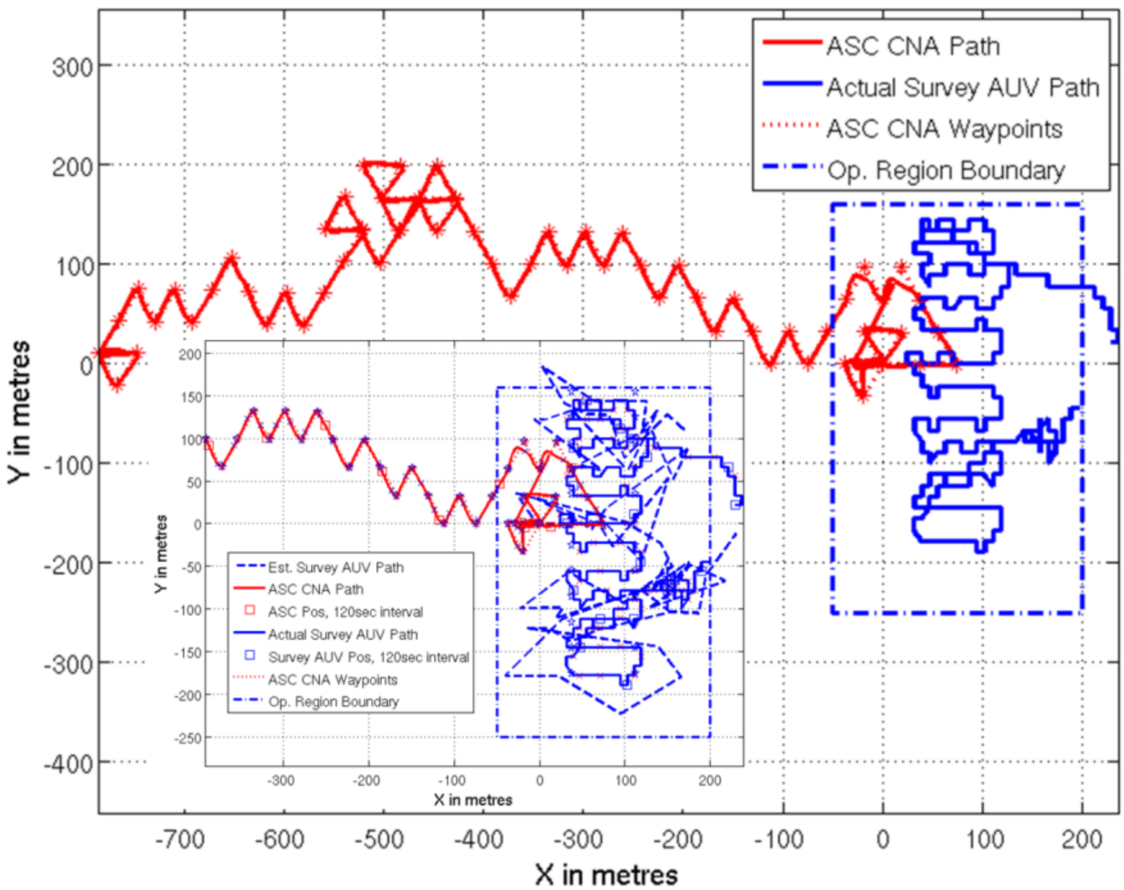

Figure 6.45: repeat of the harbour trial in Figure 6.44 (10 m altitude) with reduced CNA path planning parameters

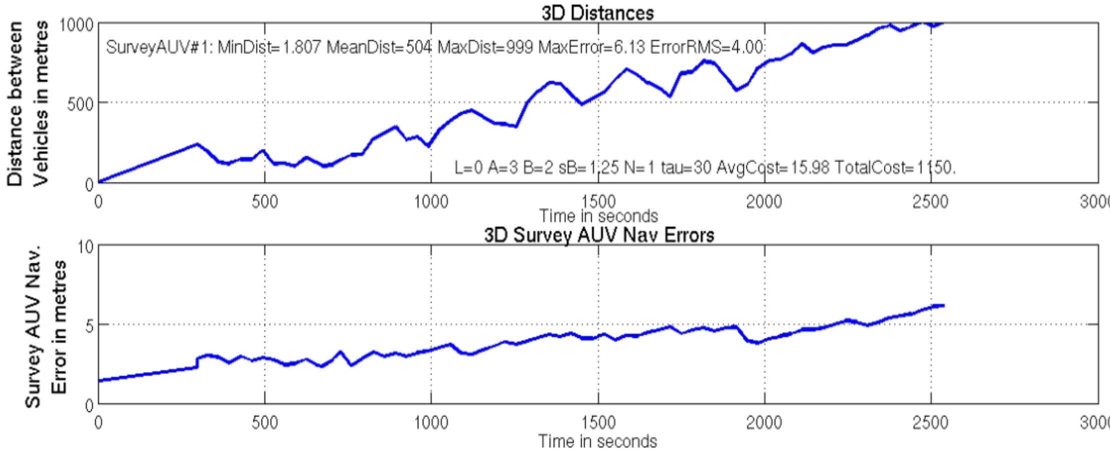

Figure 6.46: Distance and survey AUV position error vs. time from Figure 6.45

Figure 6.47 shows two Iver2 AUVs on orthogonal lawnmower paths during a harbour trial. As in Figure 6.18, the survey AUVs cycle between depths of 10 m and 0 m. The blue survey AUV works across the plot from top to bottom while the green survey AUV works from left to right. Both proceed to the same recovery point after completing the lawnmower pattern. However, they were not shut-off until inside the small boat being used to monitor the trial. This is the cause of the upward curving path of the green survey AUV. The survey AUVs are supported by a simulated ASC CNA.

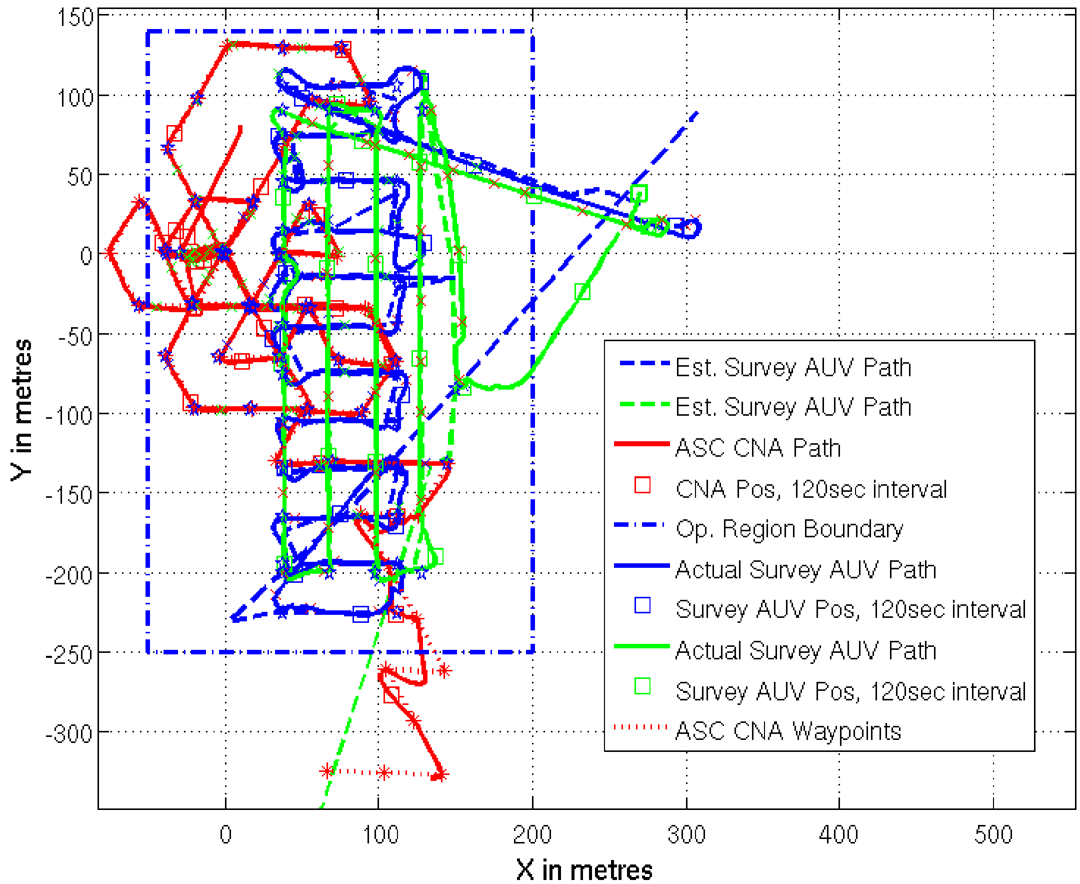

Figure 6.47: Harbour trial with Iver2 AUVs on orthogonal lawnmower paths (10 m mode depth), supported by a simulated ASC CNA

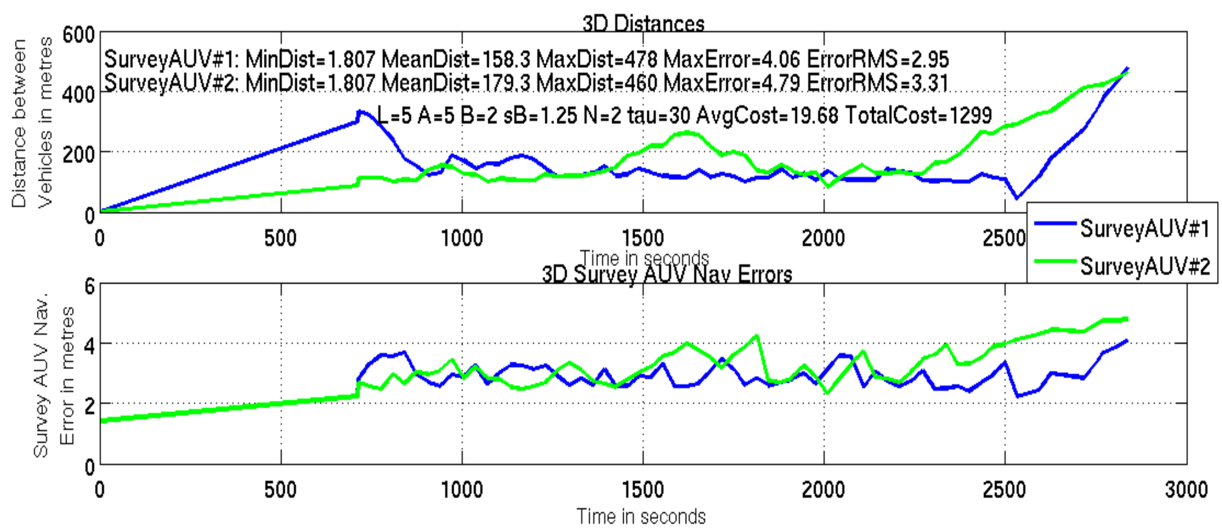

Figure 6.48: Distance and survey AUV position error vs. time for harbour trial shown in Figure 6.47

Figure 6.49 is a tank trial of the harbour trial shown in Figure 6.47 with distance and error plots in Figure 6.50. The two trials are overlaid in Figure 6.51. The two trials are very similar, though the average and total costs are higher in the harbour trial even though the CNA's estimate of survey AUV path is better. It is possible that these differences in cost are not significant, but multiple tank and harbour trials would have to be run to test that hypothesis.

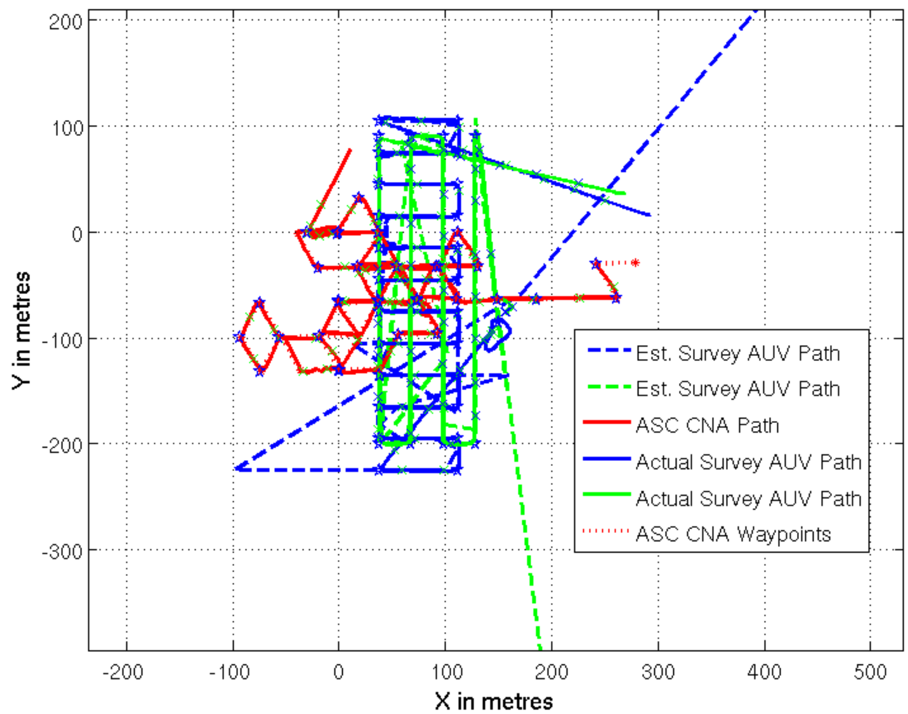

Figure 6.49: Tank trial of harbour trial shown in Figure 6.47 (10-m mode depth)

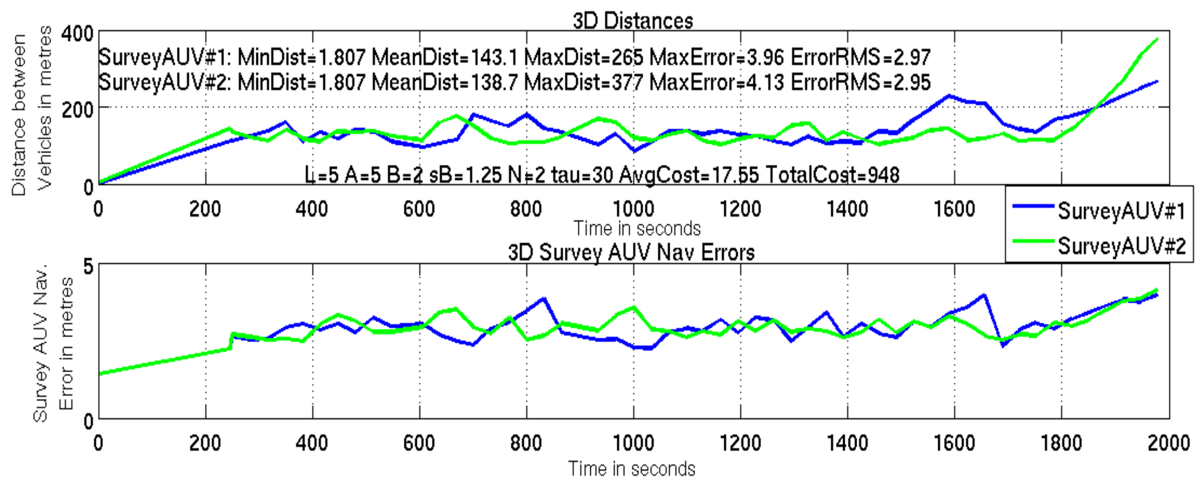

Figure 6.50: Distance and survey AUV position error vs. time for in-water trial shown in Figure 6.49

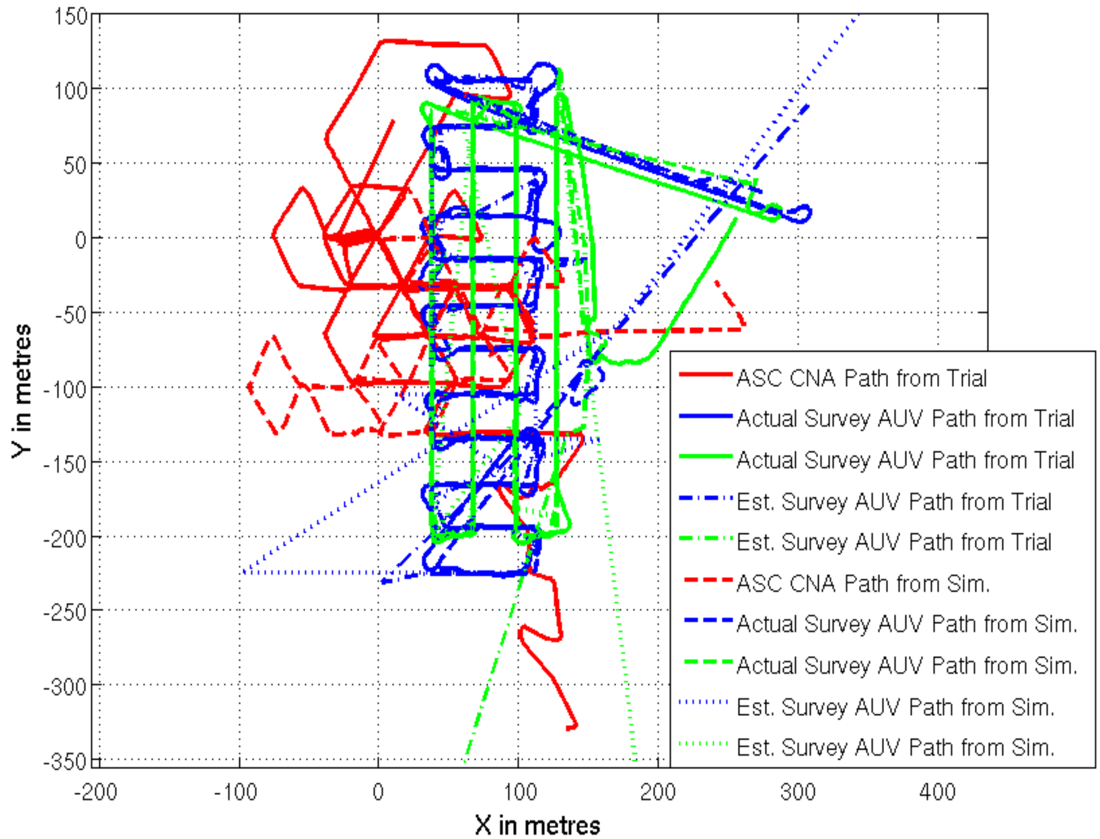

Figure 6.51: Position plots from Figure 6.47 and Figure 6.49 overlaid

Figure 6.53 shows the same harbour trial as Figure 6.47, but with reduced CNA path-planning parameters. Like some of the single survey AUV harbour trials, the log files suffer from a lag in *(x,y)* position information being passed from the frontseat to the backseat processor. In this trial, the operating region was not established correctly (it was later modified) and the green survey AUV ran outside the operating region and the end of its second leg, stopped, and began to drift to the west before being recovered. The blue survey AUV successfully completed its mission and was recovered at the park point. It was turned off in the recovery boat during transit (explaining the long line from the park point near (150, -100)). Partly due to the failure of the green survey AUV, but largely due to the reduced CNA path planning parameters, the CNA again headed in the wrong direction until restrained by the distance penalty. The error in this trial is much higher than in the trial shown in Figure 6.47. This trial was also run in the tank, the (improved) results are shown in Figure 6.54. In the tank trial, long duration (5 min or more) communication drop-outs made the CNA's estimate of survey AUV position quite poor, but the estimates corrected quickly once communication was re-established.

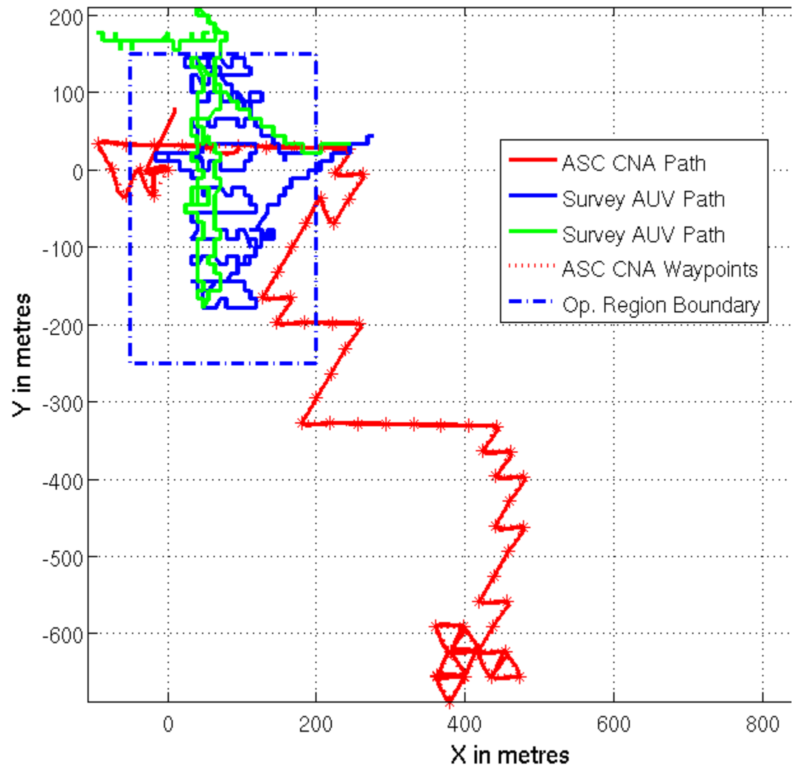

Figure 6.52: Repeat of the harbour trial in Figure 6.47 (10 m mode depth) with reduced CNA path planning parameters

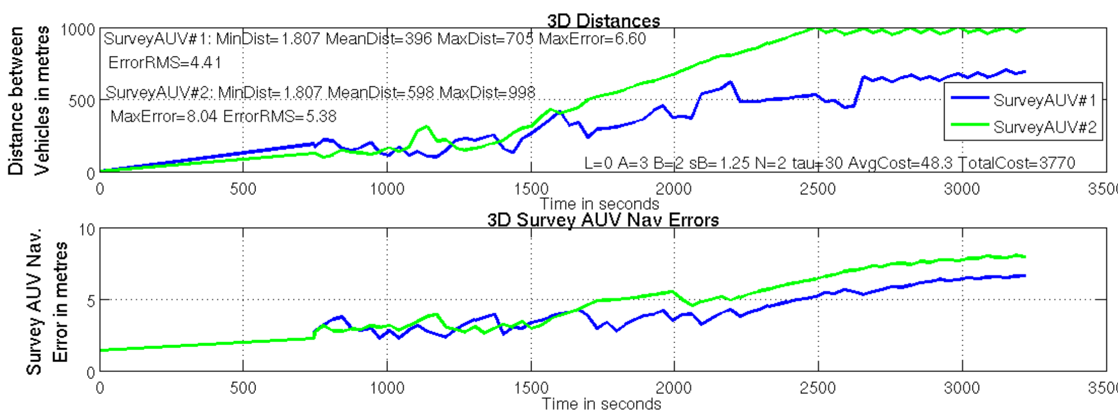

Figure 6.53: Distance and survey AUV position error vs. time from Figure 6.52

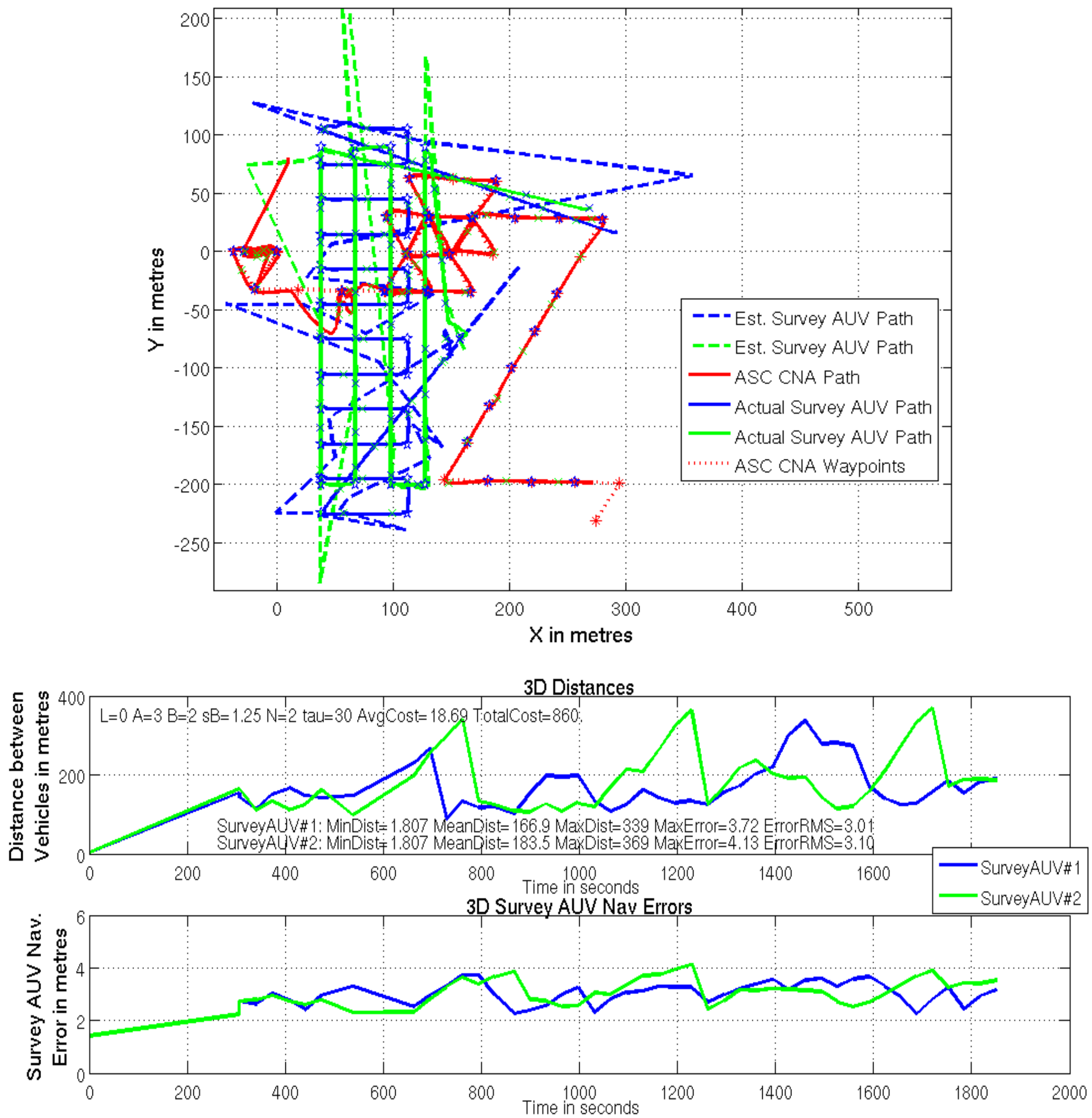

Figure 6.54: Tank trial repeating harbour trial shown in Figure 6.53 (10 m mode depth)

Figure 6.56 shows a harbour trial where the survey AUV mode depth is 5 m and the CNA path planning parameters are at the highest level (A = 5, L = 5) used in the harbour trials. The errors and distances are similar to those in Figure 6.47. The CNA typically maintains close proximity to the survey AUVs resulting in some aggressive manoeuvring near (100,50) following inputs from *BHV_AvoidCollision*. Near the beginning of the mission, the blue survey AUV had a large jump in position estimate, causing the solid blue diagonal lines heading to and from the south-east. This is a unique error in the harbour trials shown and has no apparent explanation. The solid green line going to the southwest of the plot is actually two overlapping dashed lines and are part of the CNA's erroneous estimates of the green survey AUVs position while parking. Errors like this have been common during parking and have been discussed previously. There are two additional issues in the case of multiple survey AUVs with the same park point. First, the two survey AUVs are compromising between the park behaviour and the avoid collision behavior (typically resulting in each circling the park point). This means that the AUVs are moving more at the park point than in the case of a single survey AUV. Second, with this increased movement on the surface comes poorer acoustic communication, reducing the accuracy of the CNA's estimate of the survey AUVs' current locations, in addition to its estimate of the survey AUVs' future locations (i.e. the CNA assumes the survey AUVs are moving in a straight line at their last reported speed and heading). The great advantage of having all the survey AUVs return to the same park point is that they can be recovered at the same point, reducing recovery times.

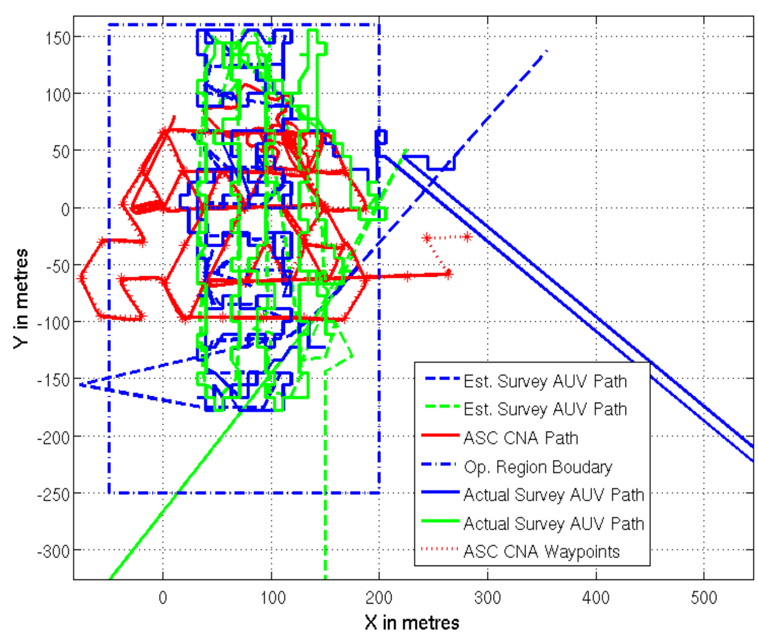

Figure 6.55: Harbour trial with Iver2 AUVs on orthogonal lawnmower paths (5-m mode depth), supported by a simulated ASC CNA

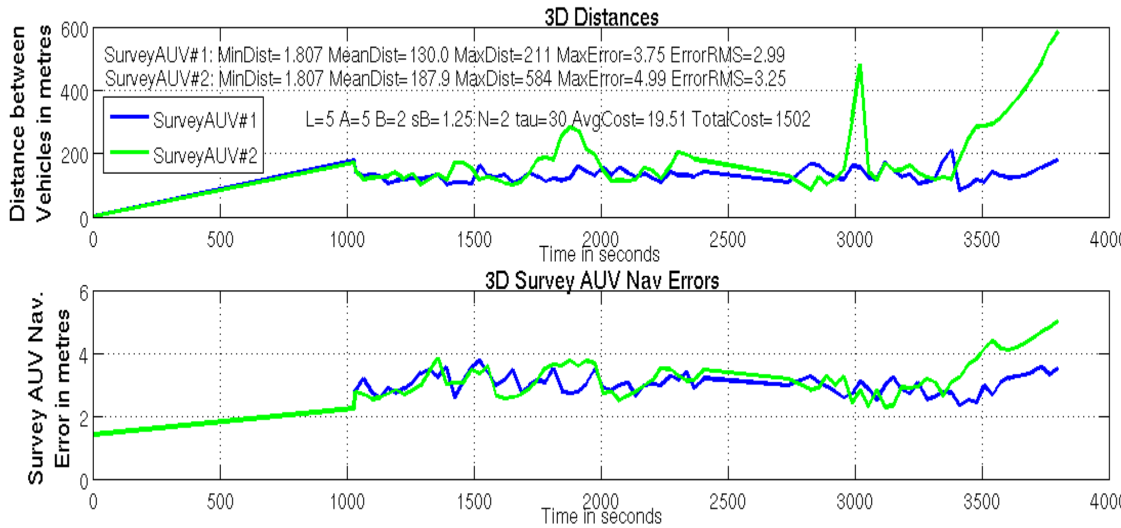

Figure 6.56: Distance and survey AUV position error vs. time

Figure 6.57 shows a tank trial repeating the harbour trial in Figure 6.56. Comparing the two figures, it can be seen that while the harbour trial was longer, the distances and errors are lower in the harbour trial. This may be due to better acoustic communications in the harbour trial.

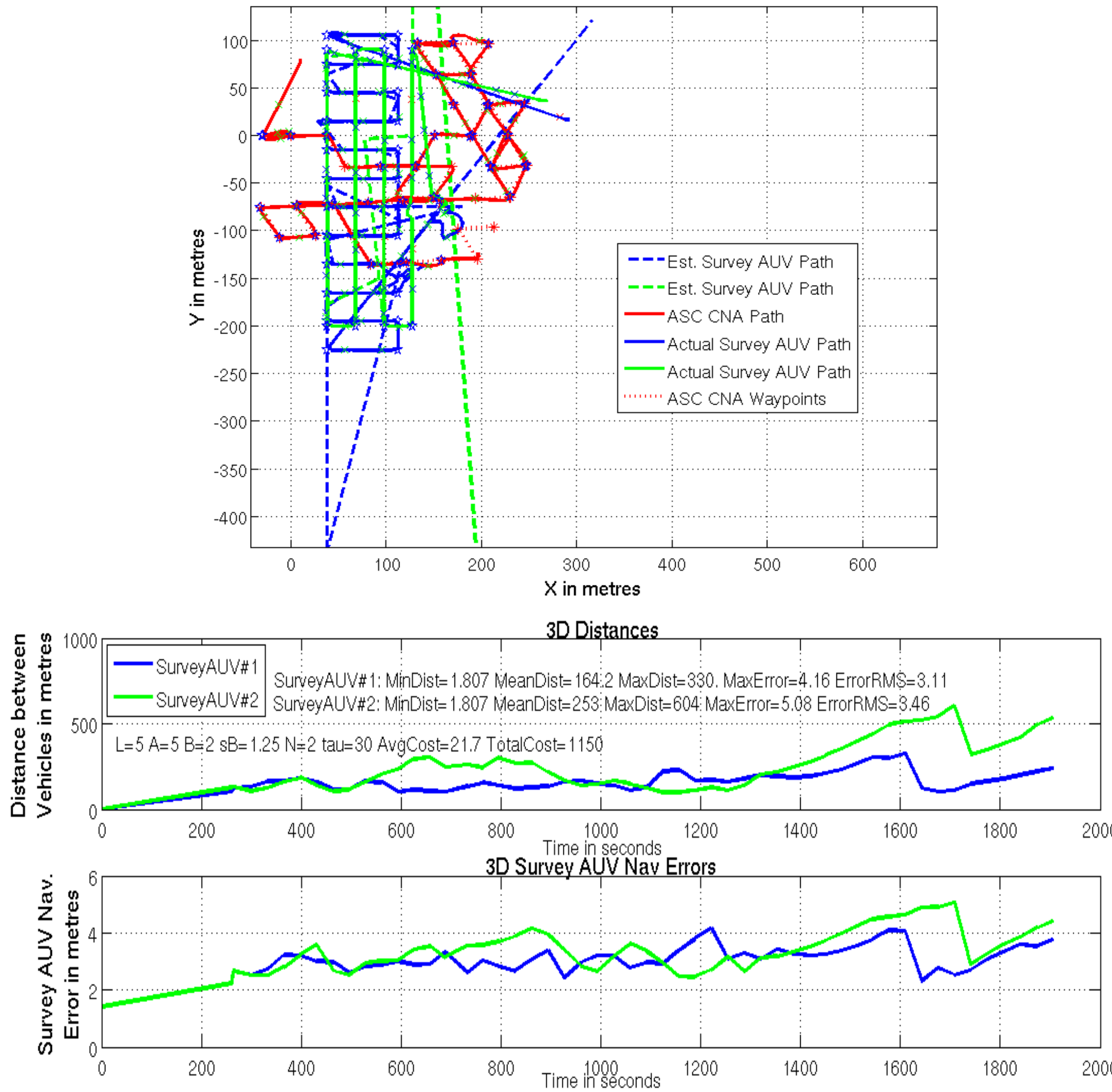

Figure 6.57: Tank trial repeating harbour trial in Figure 6.56(5-m mode depth)

Figure 6.58 shows a two survey AUV harbour trial with a mode survey AUV depth of 5 m and reduced CNA path-planning parameters. Figure 6.60 shows that, as with other trials with reduced CNA parameters, the distance penalty is required to bound the survey AUVs' error.

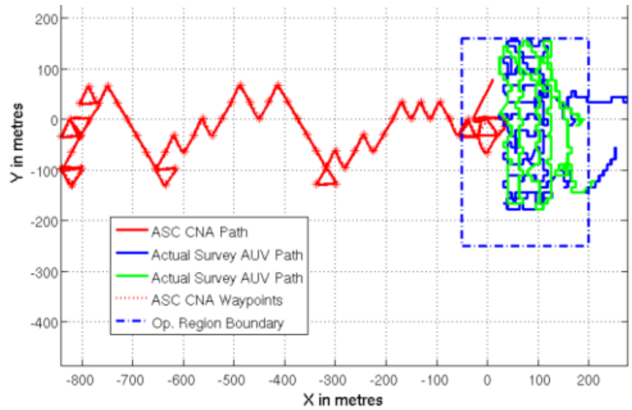

Figure 6.58: Repeat of the harbour trial in Figure 6.56 (5 m mode depth) with reduced CNA path planning parameters

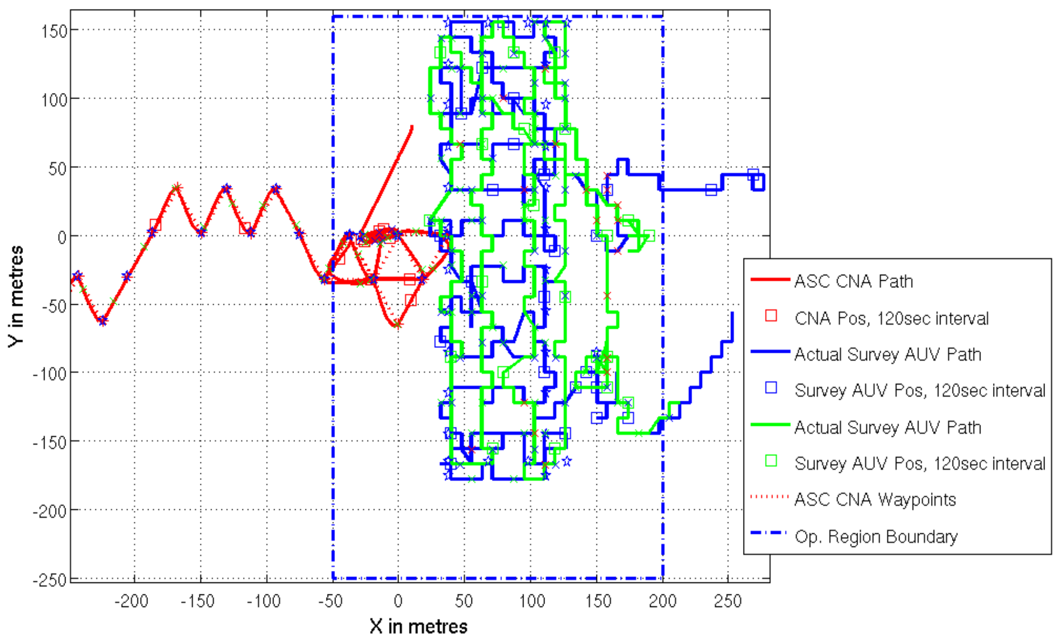

Figure 6.59: Detail view of Figure 6.58

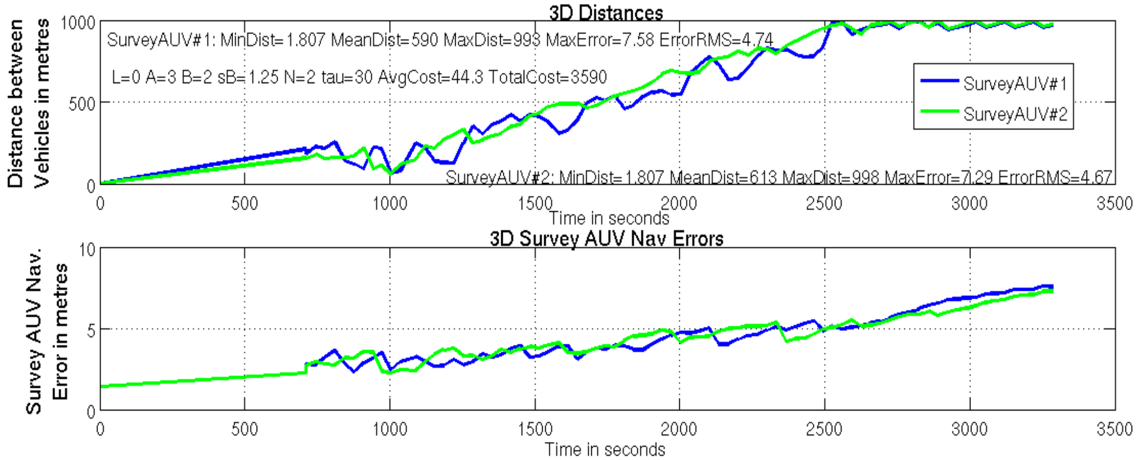

Figure 6.60: Distance and survey AUV position error vs. time for harbour trial shown in Figure 6.58

Figure 6.61 shows the better results of the Figure 6.58 harbour trial repeated as a tank trial. Notice however, that the communication update rate is much better for the green survey AUV than for the blue survey AUV, as evidenced in the differences between estimated survey AUV paths. It should also be noted that the longer legs of the green survey AUV path are more robust to communication drop-outs based on Figure 4.5.

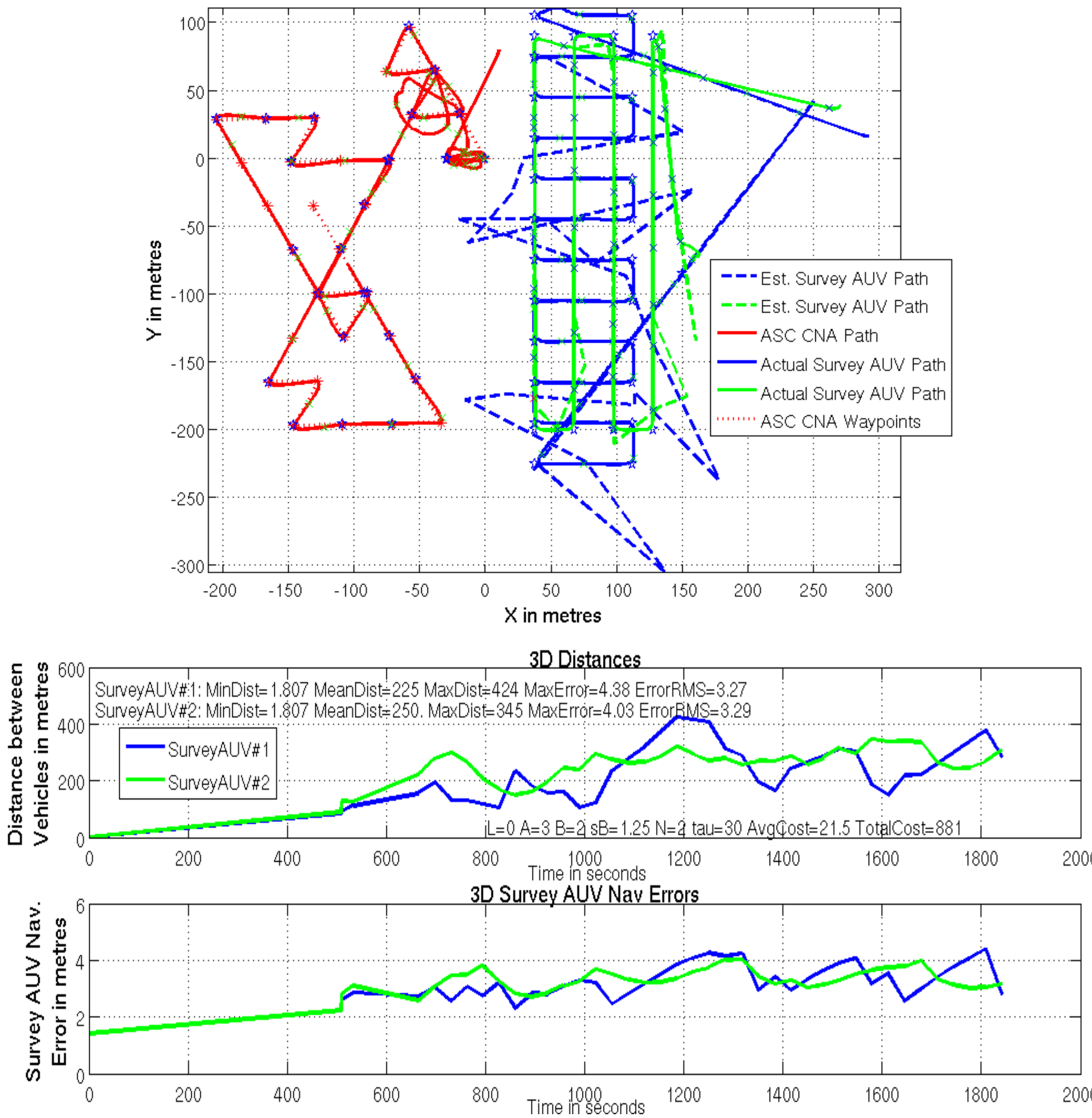

Figure 6.61: Tank trial repeating harbour trial in Figure 6.58 (5-m mode depth)

Two altitude keeping harbour trials were run using two survey AUVs. As with the other harbour trials, one trial was run with tight CNA path planning parameters and the other was run with reduced parameters. Figure 6.63 shows the tight parameters and Figure 6.66 shows the reduced parameters. As has been the case in other trials, the tighter parameters perform much better than the reduced parameters. The blue AUV surfaces once before the end of the mission. The green AUV should also surface one before the end of the mission (on its final leg), but there was a missing parameter in the altitude keeping behaviour which prevented a proper hand-off between altitude keeping and 0 m depth behaviours when the navigation error exceeded the 15 m maximum discussed in the single survey AUV trials discussion. The green survey AUV surfaced after completing the lawnmower pattern. Tank trials for both altitude keeping missions are also shown. In these trials (as with the single vehicle altitude keeping tank trials), the survey AUVs maintain constant altitude over bathymetric data collected by the US Naval Undersea Warfare Centre in Rhode Island.

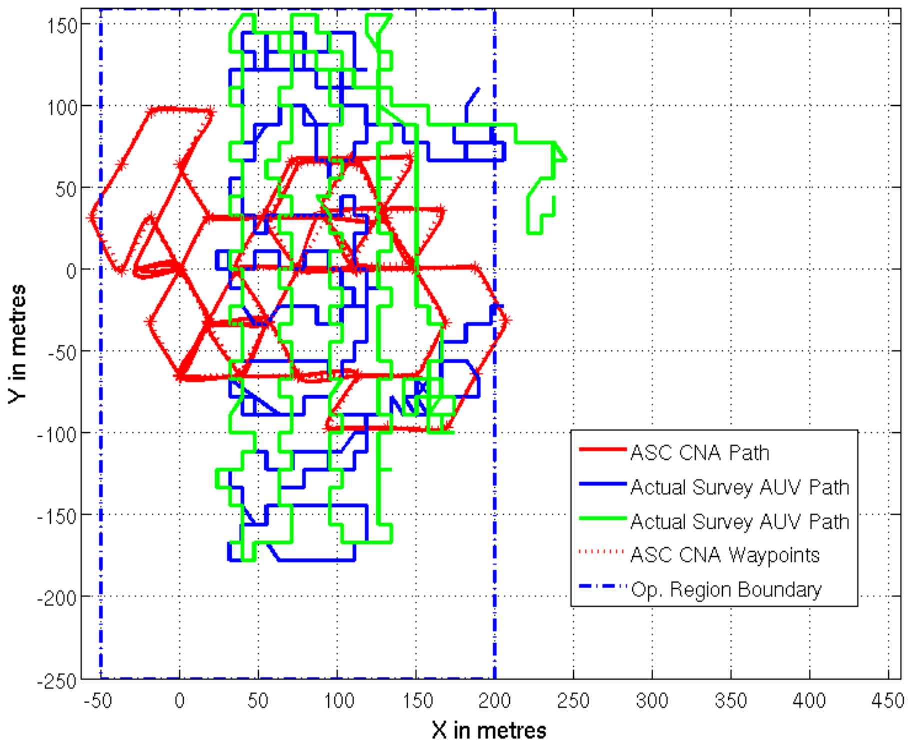

Figure 6.62: Harbour trial with Iver2 AUVs on orthogonal lawnmower paths (10 m altitude), supported by a simulated ASC CNA

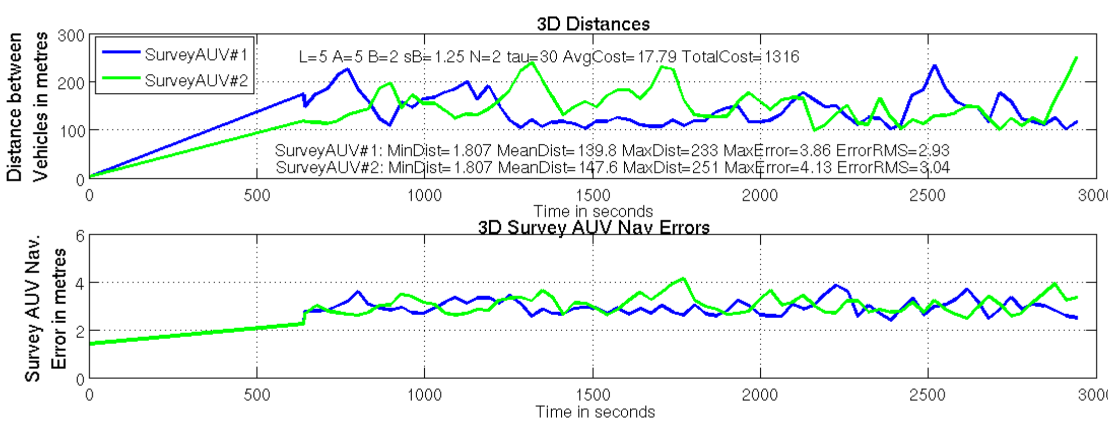

Figure 6.63: Distance and survey AUV position error vs. time

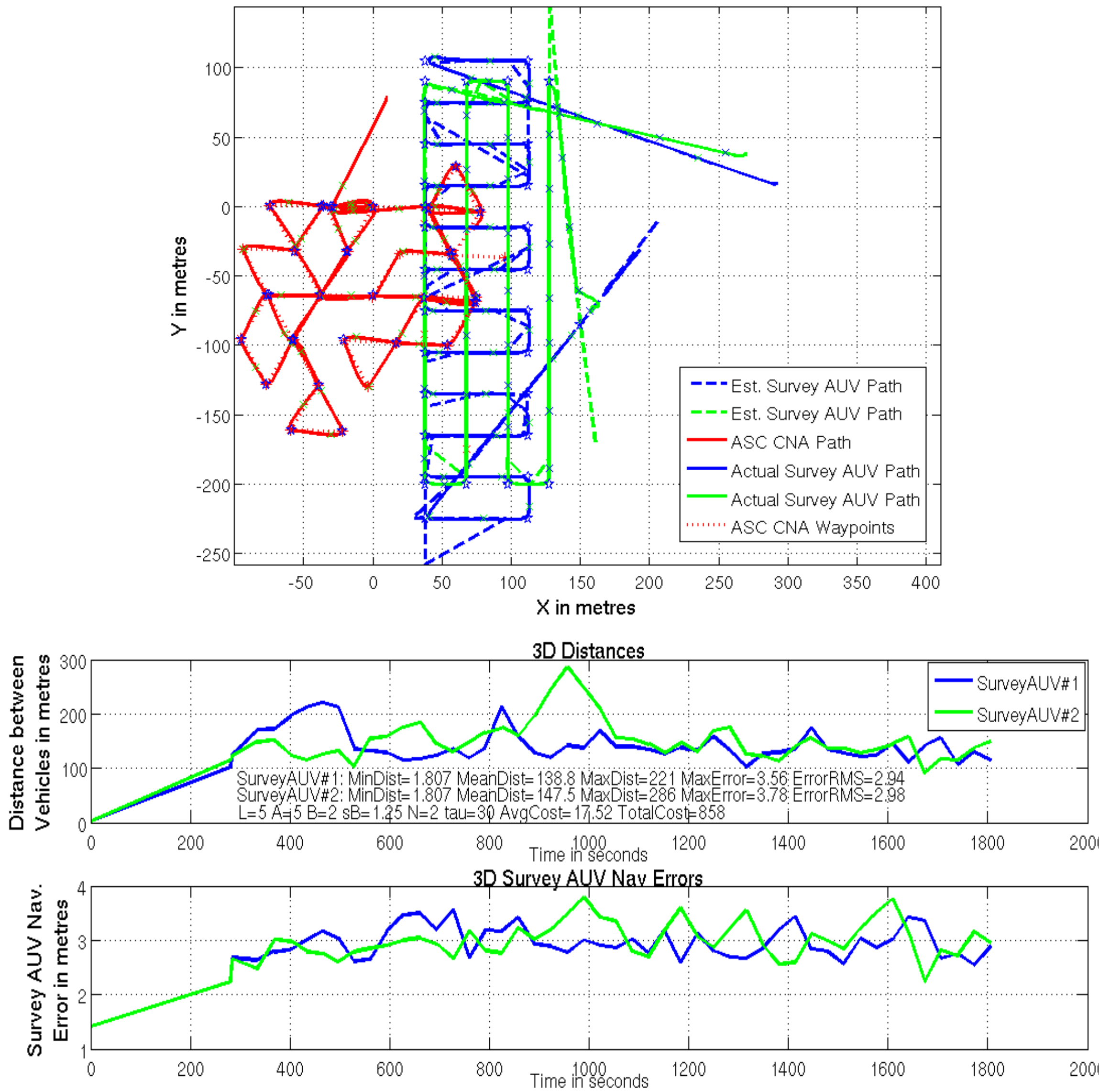

Figure 6.64: Tank trial repeating harbour trial shown in Figure 6.61 (10-m altitude keeping with tight path planning parameters)

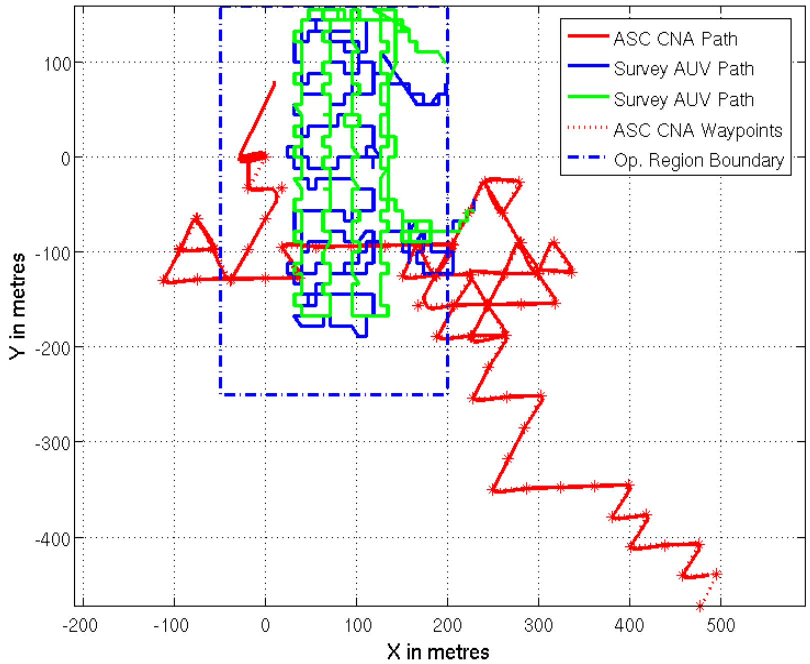

Figure 6.65: Repeat of the harbour trial in Figure 6.63 (10-m altitude keeping) with reduced CNA path planning parameters

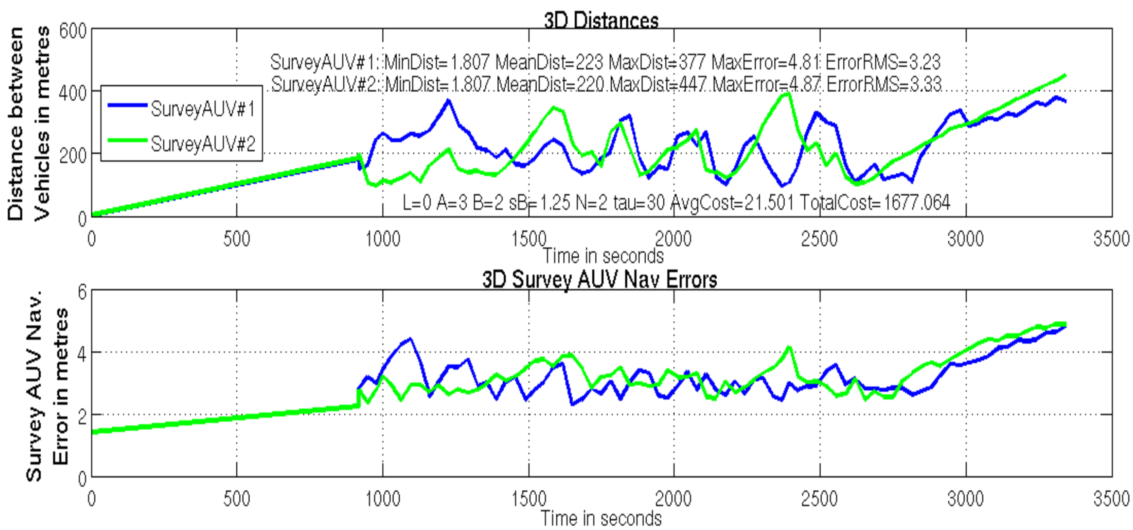

Figure 6.66: Distance and survey AUV position error vs. time from Figure 6.65

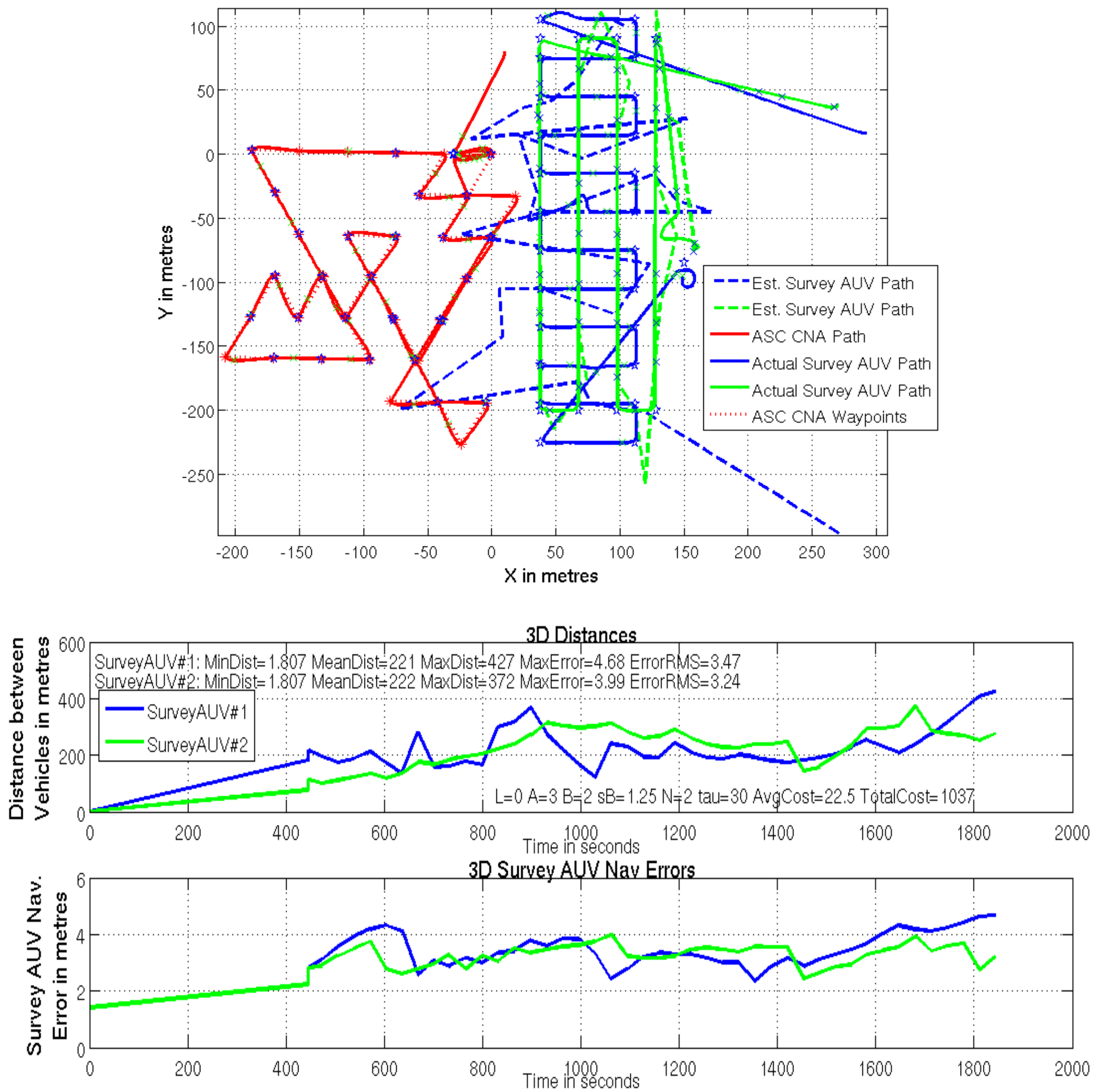

Figure 6.67: Tank trial repeating harbour trial shown in Figure 6.66 (10-m altitude keeping with reduced path planning parameters)

It was desired to run some longer harbour trials to better demonstrate the capabilities of the CNA path-planning algorithm. Due to various time constraints and vehicle problems, most of these trials could not be run. However, two runs that were largely complete were runs with two survey AUVs with parallel search areas with 10 m swath widths (see Figure 1.1). Tank trials replicating the intended missions are found in Figure B.1 and Figure B.2.

In Figure 6.69, the green survey AUV experienced a propeller shaft coupling failure (loose set screw) shortly after launch and started drifting slowly south-east. When this was noticed, it was recovered and shut down after travelling north in the recovery boat. Near the end of its mission, the blue survey AUV had a large position jump (to the southeast). Shortly afterwards, it suffered a leak and stopped. (The issues with both AUVs were resolved within a couple of days thanks to the hard work of the DRDC (Atlantic) technicians.) Despite the obvious problems, this trial is significant because (as can be seen from the plots) this is a case where the tight CNA path planning parameters failed to bound the survey AUV position error and it was the distance penalty once again that began to bound the position error.

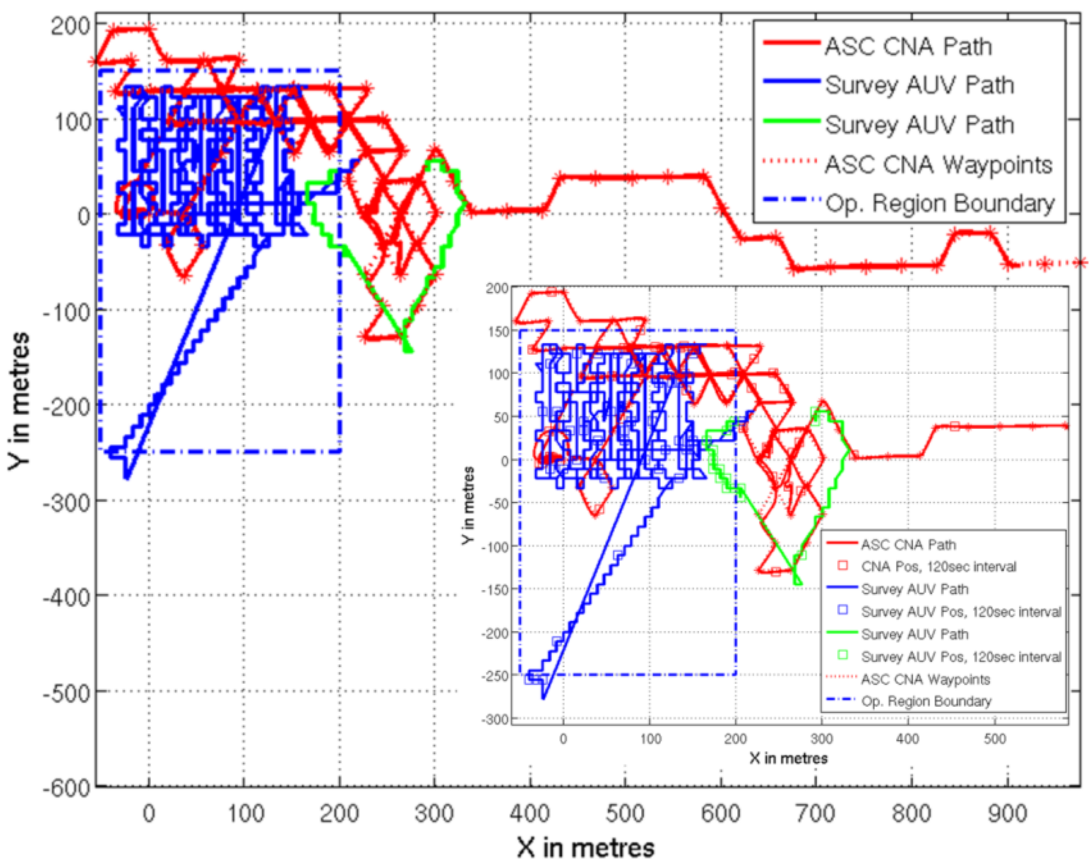

Figure 6.68: Harbour trial with Iver2 AUVs on parallel lawnmower paths (10 m mode depth), supported by a simulated ASC CNA

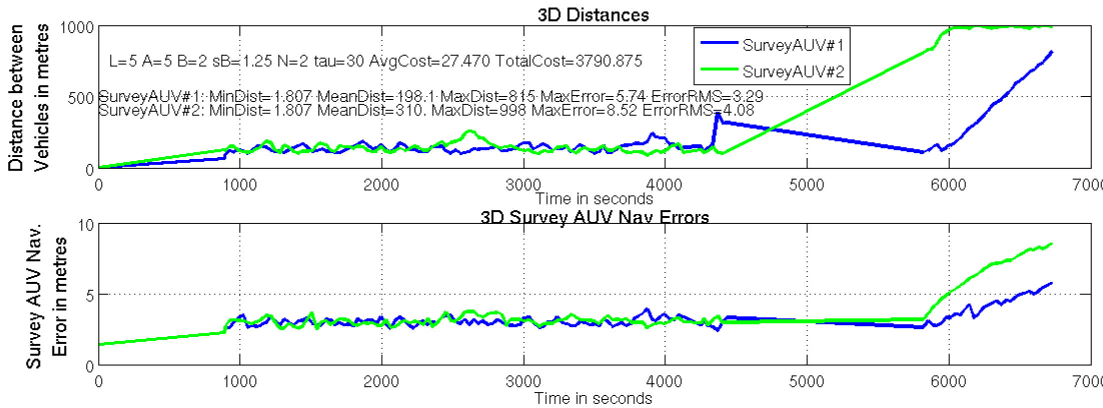

Figure 6.69: Distance and survey AUV position error vs. time from Figure 6.68

Figure 6.71 has the same survey AUV mission as Figure 6.69, but the CNA path planning parameters have been reduced. This mission obviously ran much better than the previous mission, but still there were issues. The blue survey AUV stopped (the cause is still unknown) near the north-east corner of the operating mission prior to the end of its mission and had to be recovered. After the blue survey AUV was recovered, the green survey AUV was mistakenly recovered before it completed its mission. Nevertheless, the basic features of the trial show the generally poor performance of the reduced path planning parameters being aided by the distance penalty.

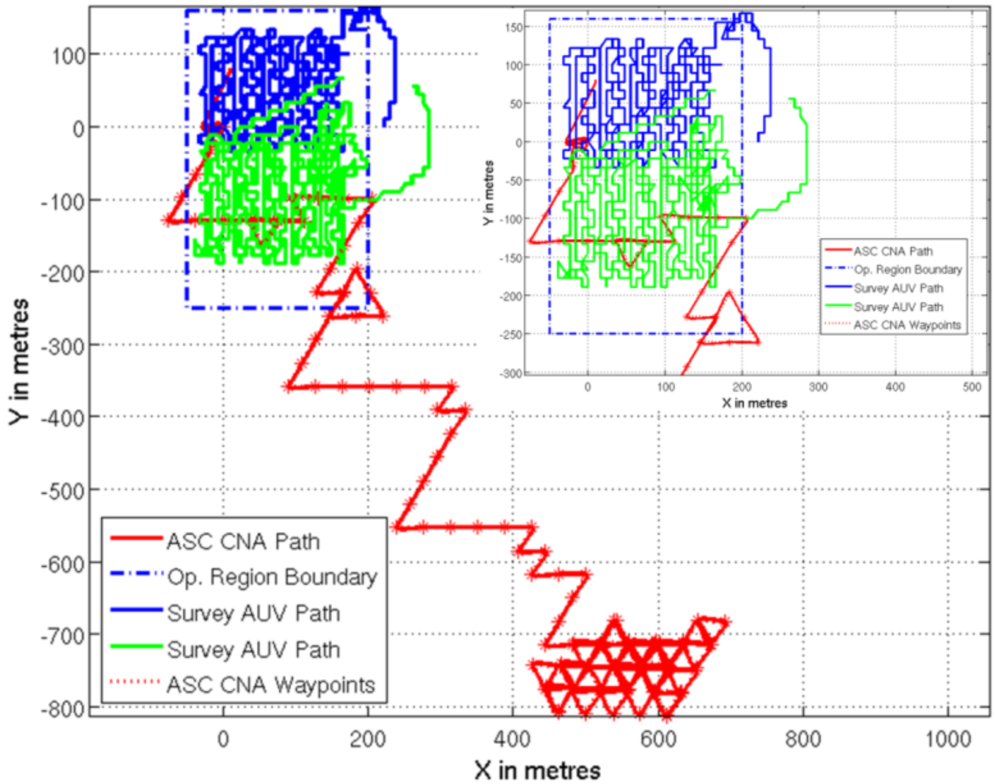

Figure 6.70: Repeat of the harbour trial in Figure 6.63 (10 m mode depth) with reduced CNA path planning parameters

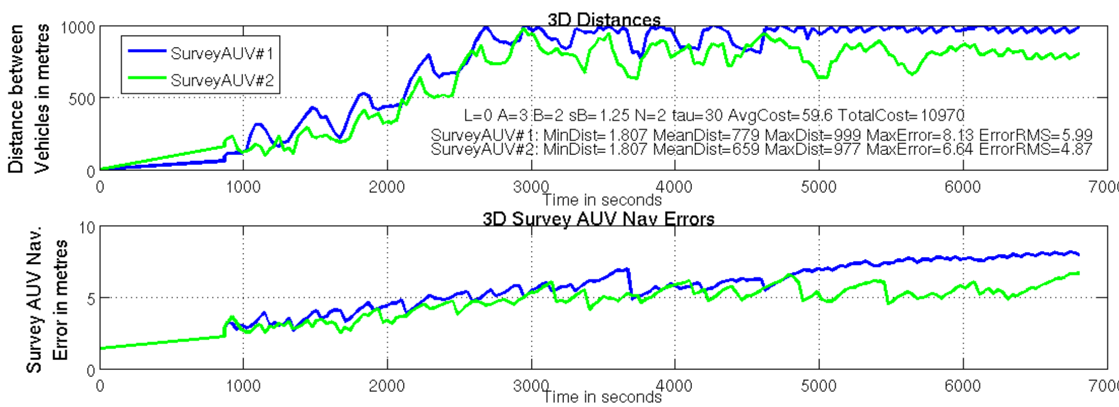

Figure 6.71: Distance and survey AUV position error vs. time from Figure 6.70

The discussion of the harbour trials has shown that the path planning algorithm shown in Chapter 3 and the implementation in Chapter 4 are robust to the realities of actual in-water conditions. These conditions include poor communications, wave action, and wind action. As we have seen, the planning algorithm does break down, especially when the survey AUVs are far apart and when the path planning parameters are low. Generally, this break down is bounded by the distance penalty, but in cases where the vehicles are too far apart (Figure 6.69) even the distance penalty may not be enough. In such as case, either two CNAs would be required or a single CNA would have to switch between survey AUVs (or groups of survey AUVs) so that some survey AUVs will be effectively aided some of the time rather than having all the survey AUVs aided ineffectively all of the time.

Chapter 7 Recommendations for Future Work

The most important item of future work is the implementation of a cooperative navigation algorithm [29] using the OWTT acoustic range measurements described in Section 1.3. This thesis has reported on adaptive path planning for a CNA vehicle. For a CNA vehicle to be useful to operational AUVs, cooperative navigation is required. Concurrent with the implementation of the cooperative navigation algorithm, the communication cycle will need to be modified so that the CNA transmits at a rate that is independent of the number of survey AUVs. In-water testing of an AUV in the role of the CNA vehicle is needed.

The first modification to the CNA path planner will be to use all waypoints transmitted by the survey AUVs when projecting survey AUV positions for all look-ahead levels instead of linking the number of waypoints used to the number of look-ahead steps. Modifying the CNA path planner to start from wherever it is (and whatever heading it has) when it receives sufficient information from each survey AUV to begin planning, rather than needing to travel to a predetermined position and heading would increase the flexibility of the path planning algorithm. This should be a fairly straightforward modification. These two modifications were not done as part of this thesis primarily to reduce the number of variables in the in-water trials. In addition, the CNA path planning algorithm should be modified to allow survey AUVs to join and leave the group aided by the CNA. This capability would add important flexibility to a CNA vehicle operating outside a research environment.

The performance of the path planning algorithm might also be improved by accepting updates to the CNA's position error estimates from the survey AUVs themselves. As an implementation of cooperative navigation will require some form of position error filtering and estimation on the survey AUVs, the survey AUV position error estimates could be sent to the CNA and be used to update the CNA's estimated ε_t^k and $\varepsilon_t^{\perp k}$. However, the CNA path planning algorithm cannot become dependent on these updates due to the lack of reliability in acoustic communication.

A more sophisticated way of inferring future survey AUV depth rather than simply assuming constant depth between acoustic updates could improve the effectiveness of the algorithm. One way of doing this could be by using the survey AUV's altitude set point and inferring water depths from an electronic chart (assuming one is available) of the operating region or a set of bathymetric data collected prior to or during the mission. However, some of these options have the potential to require many complex computations and may not be achievable underway on all autonomous marine vehicles.

Some AUV applications would benefit from a "rendezvous behaviour" to facilitate the timely arrival of an autonomous marine vehicle at a recovery point. This behaviour would have increasing priority weight over time, similar to the distance ramping used in *BHV_AvoidCollision* [98]. This time ramping would keep the behaviour out of the way during the normal mission time, but if the mission (e.g. minehunting survey) was running too long, the rendezvous behaviour would override the minehunting behaviour and cause the AUV to head for the recovery point.

Consideration should be given to implementing the CNA path planning algorithm as a MOOS-IvP behaviour rather than as a process. Implementation as a behaviour would improve coordination with other behaviours, such as collision avoidance and operating region definition, but would reduce the concreteness of the travel to best *(x,y)* decisions in the current implementation in favour of a less predictable arbitrated approach where the speed, heading, and depth decision of the path planning algorithm is compared with other behaviours such as collision avoidance and operating region definition.

Chapter 8 Conclusions

This thesis has demonstrated a path planning algorithm for an autonomous CNA vehicle (surface or subsurface) that can accommodate changes in depth by survey AUVs as they maintain a specified altitude above a significantly changing ocean floor. An important aspect of this planning algorithm not explored by others is the need to constrain the distance between the CNA and the survey AUVs in order to bound the survey AUV position error. Several different penalty equations were tested in simulation. It was found that quadratic and cubic equations were not as helpful as simpler equations. It is considered more important to limit the minimum distance between the CNA and the survey AUVs than to limit the maximum distance due to the risk of collisions.

This thesis has reported on the algorithm's success planning prior to the mission ("pre-deployment") and during the mission ("underway," based on path information acoustically transmitted by the survey AUVs). Results have been shown for both simulations and in-water testing.

In-water testing demonstrated the path planning algorithm's ability to handle the limitations of underwater communication including in the case of survey AUVs travelling at a specified altitude over a muddy (sound absorbent) seafloor. Good and poor path planning parameters (in terms of heading options and look-ahead time steps) were used in the in-water trials to illustrate that the improvements in performance seen in simulation also appear in trials. The results of the poor path planning parameters also showed the importance of the distance penalty in bounding the survey AUV position error when the path planning parameters alone were insufficient.

In addition, survey AUV paths other than lawnmower patterns have been considered, including a reactively planned path which does not allow the CNA to accurately infer the future path of the survey AUV over long periods of time. The results of these other survey AUV paths show that the algorithm is not confined to supporting the lawnmower survey pattern. However, the algorithm does perform better when the survey AUVs transmit waypoints to the CNA so that the CNA can accurately infer the future path of the survey AUV.

Pre-deployment simulations were run in MATLAB® for both an ASC and AUV CNA. Neither type of CNA vehicle seemed better than the other in reducing survey AUV position error, though future work (especially in-water trials) may come closer to a definitive result. However, eight additional evaluation factors were discussed (covertness, computational power, possible secondary tasks, navigational accuracy, in-air communications, speed, and acoustic communications reliability). Given the closeness of the position error results for an ASC or AUV CNA, it was suggested that the seven additional evaluation factors could form the actual basis for a decision on a CNA vehicle type.

References

[1] M.A. Moline, D.L. Woodruff, and N.R. Evans, "Optical Delineation of Benthic Habitat Using an Autonomous Underwater Vehicle," *Journal of Field Robotics*, vol. 24, no. 6, pp. 461-471, 2007.

[2] H.A. Kermorgant and D. Scourzic, "Interrelated Functional Topics Concerning Autonomy Related Issues in the Context of Autonomous Inspection of Underwater Structures," in *Oceans - Europe 2005*, 2005, pp. 1370-1375.

[3] Department of the Navy, USA, *The Navy Unmanned Undersea Vehicle (UUV) Master Plan*. USA: The Department of the Navy, 2004.

[4] M.R. Benjamin, H. Schmidt, P.M. Newman, and J.J. Leonard, "Nested Autonomy for Unmanned Marine Vehicles with MOOS-IvP," *Journal of Field Robotics*, vol. 27, no. 6, pp. 834-875, 2010.

[5] A.M. Percival and M.A. Stoddard, "PATHA: A Planning Aid for Tasking Heterogeneous Assests for Route Survey or Mine Countermeasures Operations," in *Oceans 2010*, Seattle, 2010, pp. 1-8.

[6] L. Paull, S. Saeedi, H. Li, and V. Myers, "An Information Gain Based Adaptive Path Planning Method for an Autonomous Underwater Vehicle using Sidescan Sonar," in *6th Annual IEEE Conference on Automation Science and Engineering*, Toronto, 2010, pp. 835-840.

[7] M. Purcell, "Deep Sea Recovery: AUVs and Air France Flight 447," in *Association for Unmanned Vehicle Systems International (AUVSI) Unmanned Systems North America 2011*, Washington, D.C., 2011.

[8] J.G. Paglia and W.F. Wyman, "DARPA's Autonomous Minehunting and Mapping Technologies (AMMT) Program: An Overview," in *Oceans '96, MTS/IEEE "Prospects for the 21st Century" Conference Proceedings*, 1996, pp. 794-799.

[9] L.E. Freitag et al., "Multi-band Acoustic Modem for the Communications and Navigation Aid AUV," in *Proceedings of MTS/IEEE Oceans 2005.*, Washington, D.C., 2005, pp. 1080-1085.

[10] J. Curcio et al., "Experiments in Moving Baseline Navigation using Autonomous Surface Craft," in *Proceedings of MTS/IEEE Oceans, 2005*, 2005, pp. 730-735.

[11] A.D. Matthews, T.C. Montgomery, D.A. Cook, J.W. Oeschger, and J.S. Stroud, "12.75-inch Synthetic Aperature Sonar (SAS), High Resolution and Automatic Target Recognition," in *Oceans 2006*, 2006, pp. 1-7.

[12] C.G. Rauch et al., "AUV Deployed Marking and Homing to Targets," , 2008, pp. 1-5.

[13] M.L. Seto, J.A. Hudson, and Y.-J. Pan, "Three-Dimensional Path-Planning for a Communications and Navigation Aid Working Cooperatively with Autonomous Underwater Vehicles," in *Autonomous and Intelligent Systems*, Burnaby, B.C., 2011, pp. 51-62.

[14] IHS Jane's. (2011, March) Jane's Fighting Ships; SANDOWN Class. Annual Book Pulication Online.

[15] IHS Jane's. (2011, May) Jane's Underwater Warfare Systems; REMUS 100. Annual Book Publication Online.

[16] R.P. Stokey, L.E. Freitag, and M.D. Grund, "A Compact Control Language for AUV Acoustic Communication," in *Oceans - Europe 2005*, Brest, Fr., 2005, pp. 1133-1137.

[17] L. Freitag, M. Grund, S. Singh, and M. Johnson, "Acoustic Communication in Very Shallow Water: Results from the 1999 AUV Fest," in *Oceans 2000 MTS/IEEE Conference and Exhibition*, Providence, R.I., 2000, pp. 2155-2160.

[18] J. Yuh, "Design and Control of Autonomous Underwater Robots: A Survey," *Autonomous Robots*, vol. 8, pp. 7-24, 2000.

[19] W.J. Marr and A.J. Healey, "Acoustic Data Transfer Limits using an Underwater Vehicle in Very Shallow Water," in *Proceedings of OMAE04, 23rd International Conference on Offshore Mechanics and Arctic Engineering*, Vancouver, 2004, pp. 711-718.

[20] J. Coleman, K. Merrill, M. O'Rourke, A.G. Rajal, and D.B. Edwards, "Identifying Error in AUV Communication," in *Oceans 2006 - Asia Pacific*, Singapore, 2006, pp. 1-8.

[21] C. Kunz et al., "Deep Sea Underwater Robotic Exploration in the Ice-covered Arctic Ocean with AUVs," in *2008 IEEE/RSJ International Conference on Intelligent Robotics and Systems*, Nice, Fr., 2008, pp. 3654-3660.

[22] S.E. Webster, L.L. Whitcomb, and R.M. Eustic, "Preliminary Results in Decentralized Estimation for Single-Beacon Acoustic Underwater Navigation," in *Robotics: Science and Systems VI*, Zaragoza, Spain, 2010, pp. 1-8.

[23] B. Butler and R. Verral, "A Precision Hybrid Interial/Acoustic Navigation System for a Long-Range Autonomous Underwater Vehicle," Defence Research and Development Canada (Atlantic), Dartmouth, N.S.,.

[24] J.J. Leonard, A.A. Bennet, C.M. Smith, and H.J.S. Feder, "Autonomous Underwater Vehicle Navigation," Massachusetts Institute of Technology, MIT Marine Robotics Laboratory Technical Memorandum 98-1, 1998.

[25] E. Desa, R. Madhan, and P. Maurya, "Potential of Autonomous Underwater Vehicles as New Generation Ocean Data Platforms," *Current Science*, vol. 90, no. 9, pp. 1202-1209, 2006.

[26] M.F. Fallon, M. Kaess, H. Johannsson, and J.J. Leonard, "Efficient AUV Navigation Fusing Acoustic Ranging and Side-scan Sonar," in *2011 IEEE International Conference on Robotics and Automation*, Shanghai, 2011, pp. 2398-2405.

[27] A Kim and R. Eustice, "Pose-graph Visual SLAM with Geometric Model Selection for Autonomous Underwater Ship Hull Inspection," in *The 2009 IEEE/RSJ International Conference on Intelligent Robots and Systems (IROS 2009)*, St. Louis, 2009, pp. 1559-1565.

[28] J. Vaganay, J. J. Leonard, J. A. Curcio, and J. S. Willcox, "Experimental Validation of the Moving Long Base-Line Navigation Concept," in *2004 IEEE/OES Autonomous Underwater Vehicles*, 2004, pp. 59-65.

[29] A. Bahr, J.J. Leonard, and M.F. Fallon, "Cooperative Localization for Autonomous Underwater Vehicles," *International Journal of Robotics Research*, vol. 28, no. 6, pp. 714-728, June 2009.

[30] R.M. Eustice, L.L. Whitcomb, H. Singh, and M. Grund, "Experimental Results in Synchronous-Clock One-Way-Travel-Time Acoustic Navigation for Autonomous Underwater Vehicles," in *2007 IEEE International Conference on Robotics and Automation*, Roma, Italy, 2007, pp. 4257-4264.

[31] A. Bahr, "Cooperative Localization for Autonomous Underwater Vehicles," WHOI/MIT, PhD Thesis 2009.

[32] G. Rui and M. Chitre, "Cooperative Positioning using Range-only Measurements between Two AUVs," in *Oceans 2010*, Sydney, Australia, 2010, pp. 1-6.

[33] T.Y. Teck and M. Chitre, "Single Beacon Cooperative Path Planning Using [sic] Cross-Entropy Method," in *IEEE/MTS Oceans'11 Conference, Hawaii, USA*, Kona, Hawaii, 2011, pp. 1-6.

[34] P. Baccou and B. Jouvencel, "Simulation Results, Post-Processing Experimentations [sic] and Comparisons Results [sic] for Navigation, Homing and Multiple Vehicles Operations [sic] with a New Positioning Method using on Transponder [sic]," in *Proceedings of the 2003 IEEE/RSJ International Conference on Robots and Systems, 2003 (IROS 2003)*, 2003, pp. 811-817.

[35] R. Panish and M. Taylor, "Achieving High Navigation Accuracy usinng Intertial Navigation Systems in Autonomous Underwater Vehicles," in *Oceans 2011 - Spain*, 2011, pp. 1-7.

[36] OceanServer Technology, Inc. (2011) Iver2 Autonomous Underwater Vehicle: Iver2 Navigation Accuracy. [Online]. http://www.iver-auv.com/navigation.html

[37] A. Cadena, "Design and Implementation of Cooperative Autonomous Underwater Vehicles for Antarctic Exploration," in *Proceedings of SPIE--The International Society for Optical Engineering, Ocean Sensing and Monitoring III*, 2011, pp. 1-12.

[38] T. Schneider and H. Schmidt, "Unified Command and Control for Heterogeneous Marine Sensing Networks," *Journal of Field Robotics*, vol. 27, no. 6, pp. 876-889, 2010.

[39] A. Bahr and J.J. Leonard, "Minimizing Trilateration Errors in the Presence of Uncertain Landmark Positions," in *Proceedings of the 3rd European Conference on Mobile Robots (ECMR)*, 2007, pp. 48-53.

[40] A. J. Shafer, M. R. Benjamin, J. J. Leonard, and J. Curcio, "Autonomous Cooperation of Heterogeneous Platforms for Sea-Based Search Tasks," in *Oceans*, Quebec City, 2008, pp. 1-10.

[41] A. Aguiar et al., "Cooperative Autonomous Marine Vehicle Motion Control in the Scope of the EU GREX Project: Theory and Practice," in *Oceans 2009 - Europe. Oceans '09.*, 2009, pp. 1-10.

[42] A. Bahr, M. R. Walter, and J. J. Leonard, "Consistent Cooperative Localization," in *2009 IEEE International Conference on Robotics and Automation*, Kobe, Japan, 2009, pp. 3415-3422.

[43] M. Perrier, L. Brignone, and M. Drogou, "Communication Constraints and Requirements for Operating Multiple Unmanned Marine Vehicles," in *The Proceedings of the Seventeenth (2007) International Offshore and Polar Engineering Conference*, 2007, pp. 1053-1058.

[44] H. Ferreira et al., "SWORDFISH: An Autonomous Surface Vehicle for Network Centric Operations," in *Oceans 2007 - Europe*, 2007, pp. 1-6.

[45] A.J. Healey, D.P. Horner, S.P. Kragelund, B. Wring, and A. Monarrez, "Collaborative Unmanned Systems for Maritime and Port Security Operations," in *7th IFAC Conference on Control Applications in Marine Systems, CAMS 2007*, Elaphusa, Croatia, 2007, pp. 1-6.

[46] M. Lindemuth et al., "Sea Robot-Assisted Inspection," *IEEE Robotics and Automation Magazine*, vol. 18, no. 2, pp. 96-107, June 2011.

[47] P. B. Sujit, Joao Sousa, and F. L. Pereira, "UAV and AUVs Coordination [sic] for Ocean Exploration," in *Oceans 2009 - Europe*, 2009, pp. 1-7.

[48] N. Michael, J. Fink, and V. Kumar, "Controlling a Team of Ground Robots via an Aerial Robot," in *IEEE/RSJ International Conference on Intelligent Robots and Systems, 2007*, San Diego, 2007, pp. 965-970.

[49] J.M. Eadie and R.D. Mace, "Autonomous Littoral Warfare Systems Evaluator - Engineering Simulation (ALWSE-ES)," Costal Systems Station, Panama City, Fla.,.

[50] J. Lok, "Autonomous Underwater Vehicle Technology Pluges Toward Maturity," *Jane's International Defence Review*, vol. 38, pp. 44-47, July 2005.

[51] C. von Alt et al., "Hunting for Mines with REMUS: A High Performance, Affordable, Free Swimming Underwater Robot," in *MTS/IEEE Conference and Exhibition Oceans 2001*, Honolulu, 2001, pp. 117-122.

[52] D. Green and C. Bernstein, "Command, Control, and Data Transport for Underwater Robots Using Acoustic Communications," in *Underwater Technology 2002 Proceedings*, 2002, pp. 343-348.

[53] A.G. Rajala, D.B. Edwards, and M. O'Rourke, "Collaborative Behavior for Vehicle Replacement in AUV Formations," in *Proceedings of the IMECE2005, 2005 ASME International Mechanical Engineering Congress and Exhibition*, Orlando, 2005.

[54] Society of Manufacturing Engineers, *Fundamentals of Manufacturing*, 2nd ed., Philip D. Rufe, Ed. Dearborn, USA: Society of Manufacturing Engineers, 2002.

[55] J.S. McCue, R.D. Blidberg, and M.J. Carter, "An Investigation into Protocols for Underwater Communication," in *Proceedings of the 7th International Symposium on Unmanned Untethered Submersible Technology (AUV 91)*, Lee, N.H., 1991.

[56] A. Rajala, M. O'Rourke, and D.B. Edwards, "AUVish: An Application-based Language for Cooperating AUVs," Center for Intelligent Systems, University of Idaho, Moscow, ID,.

[57] A. Rajala and D. Edwards, "Allocating AUVs for Mine Map Development in MCM," in *Oceans 2006 - Asia Pacific*, 2007, pp. 1-8.

[58] B. Johnson, N. Hallin, H. Leidenfrost, M. O'Rourke, and D. Edwards, "Collaborative Mapping with Autonomous Underwater Vehicles in Low-bandwidth Conditions," in *Oceans 2009*, 2009, pp. 1-7.

[59] P.B. Chapple, "Unsupervised Detection of Mine-Like Objects in Seabed Imagery from Autonomous Underwater Vehicles," in *MTS/IEEE Biloxi Oceans 2009 - Marine Technology for Our Future: Global and Local Challenges*, 2009, pp. 1-6.

[60] P. Hollesen, W.A. Connors, and T. Trappenberg, "Comparison of Learned versus Engineered Features for Classification of Mine Like Objects from Raw Sonar Images," in *Lecture Notes in Computer Science, Advances in Artificial Intelligence - 24th Canadian Conference on Artificial Intelligence, Canadian AI 2011*, 2011, pp. 174-185.

[61] M.F. Fallon, G. Papadopoulos, and J.J. Leonard, "A Measurement Distribution Framework for Cooperative Navigation using Multiple AUVs," in *2010 IEEE International Conference on Robotics and Automation*, Anchorage, 2010, pp. 4256-4263.

[62] F.R. Driscoll, P.-P. Beaujean, W. Venezia, and L. Freitag, "Development and Testing of an A-Sized Rapidly Deployable Navigation and Communication GATEWAY Buoy," in *Proceedings of MTS/IEEE Oceans 2005*, 2005, pp. 1234-1241.

[63] F.R. Driscoll, P.-P. Beaujean, and W.A. Venezia, "Development and Testing of an A-Sized Rapidly Deployable Navigation and Communication GATEWAY Buoy," *Marine Technology Society Journal*, vol. 40, no. 1, pp. 36-46, Spring 2006.

[64] T. Schneider and H. Schmidt, "pAcommsHandler: Acoustic Networking in MOOS with the WHOI Micro-Modem," in *MOOS Development and Applications Working Group (MOOS-DAWG) 2010*, Cambridge, Mass., 2010.

[65] T. Schneider and H. Schmidt, "Goby-Acomms (v2) (Including pAcommsHandler): Slow Link Networking for Robotic Marine Platforms," in *MOOS Development and Applications Working Group (MOOS-DAWG) 2011*, Cambridge, Mass., 2011.

[66] T. Schneider and H. Schmidt, "The Dynamic Compact Control Language: A Compact Marshalling Scheme for Acoustic Communications," in *Oceans 2010 IEEE - Sydney*, vol. 27, Sydney, Aus., 2010, pp. 1-8.

[67] A.J. Plueddeman, A.L. Kukulya, R. Stokey, and L. Freitag, "Autonomous Underwater Vehicle Operations Beneath Coastal Sea Ice," *IEEE/ASME Transactions on Mechatronics*, vol. 17, no. 1, pp. 54-64, February 2012.

[68] J.M. Thorleifson, T.C. Davies, M.R. Black, D.A. Hopkin, and R.I. Verrall, "The Theseus Autonomous Underwater Vehicle: A Canadian Success Story," in *MTS/IEEE Conference Proceedings Oceans '97*, 1997, pp. 1001-1006.

[69] J.S. Ferguson, "The Theseus Autonomous Underwater Vehicle: Two Successful Missions," in *Proceedings of the 1998 International Symposium on Underwater Technology, 1998*, 1998, pp. 109-114.

[70] M.R. Black and B. Butler, "Arctic Ocean Trials of Trackpoint Ultrashort Baseline Acoustic Positioning Systems," in *Proceedings of the 1994 Symposium on Autonomous Underwater Vehicle Technology, 1994 (AUV '94)*, 1994, pp. 297-302.

[71] C. Kaminski et al., "12 Days Under Ice -- An Historic AUV Deployment in the Canadian High Arctic," in *2010 IEEE/OES Autonomous Underwater Vehicles (AUV)*, 2010, pp. 1-11.

[72] H. Boggild. (2011, September) UNCLOS Survey Blog. [Online]. http://blogs.science.gc.ca/arctic-arctique/

[73] R.P. Stokey and T.C. Austin, "Sequential, Long Baseline Navigation for REMUS, an Autonomous Underwater Vechicle," in *Proceedings of SPIE, International Society of Optical Engineers*, 1999, pp. 212-219.

[74] R.P. Stokey et al., "Development of the REMUS 600 Autonomous Underwater Vehicle," in *Proceedings of MTS/IEEE Oceans, 2005*, Washington, D.C., 2005, pp. 1301-1304.

[75] Z. Deng, Y. Ge, W. Guan, and K. Han, "Underwater Map-Matching Aided Inertial Navigation System Based on Multi-Geophysical Information," *Frontiers of Electrical and Electronic Engineering in China*, vol. 5, no. 4, pp. 496-500, 2010.

[76] T.F. Fulton and C.J. Cassidy, "Navigation Sensor Data Fusion for the AUV Remus," *Marine Technology*, vol. 38, no. 1, pp. 65-69, January 2001.

[77] N. Le Bouffant, P. Pidsley, J.-P. Malkasse, and F. Florin, "Automatic MCM Mission Control for AUV Systems," in *Oceans - Europe 2005*, 2005, pp. 930-936.

[78] S. Reed, I. Tena Ruiz, C. Capus, and Y. Petillot, "The Automatic Fusion of Classified Sidescan Sonar Mosaics using CML-RTS and Markov Random Fields," in *Oceans - Europe 2005*, 2005.

[79] J.M. Saez, A. Hogue, F. Escolano, and M. Jenkin, "Underwater 3D SLAM through Entropy Minimization," in *Proceedings of the 2006 IEEE International Conference on Robotics and Automation*, Orlando, Fla., 2006, pp. 1-6.

[80] U. Holscher-Hobing and M.B. Larsen, "Aided Inertial Navigation System Solutions," in *Proceedings of OMAE2006, 25th International Conference on Offshore Mechanics and Arctic Engineering*, Hamburg, Germany, 2006, pp. 749-758.

[81] M.B. Larsen, "The Autonomous Redundant Navigation Systems of an AUV for Mine Counter Measures [sic]," in *UDT2006*, 2006, pp. 1-9.

[82] Atlas Elektronik GmbH. (2012, February) SeaOtter Mk II Autonomous Underwater Vehicle. [Online]. http://www.maridan.atlas-elektronik.com/uploads/media/SeaOtter_civil.pdf

[83] Y. Liu and X.R. Li, "Aided Strapdown Inertial Navigation for Autonomous Underwater Vehicles," *Proceedings of SPIE - The International Society for Optical Engineering*, vol. 7698, pp. 1-12, 2010.

[84] M. Benjamin, M. Grund, and P. Newman, "Multi-objective Optimization of Sensor Quality with Efficient Marine Vehicle Task Execution," in *Proceedings of IEEE International Conference on Robotics and Automation, ICRA 2006*, 2006, pp. 3226-3232.

[85] J.C. Kinsey, R.M. Eustice, and L.L. Whitcomb. (2006) www.whoi.edu. [Online]. http://www.whoi.edu/cms/files/jkinsey-2006a_20090.pdf

[86] M. Jakuba et al., "Multiscale, Multimodal AUV Surveys for Hydrothermal Vent Localization," in *Proceedings of the 14th Unmanned Untethered Submersible Technology Conference*, Durham, N.H., 2005.

[87] L. Medagoda, S.B. Williams, O. Pizarro, and M.V. Jakuba, "Water Column Current Profile Aided Localization combined with View-Based SLAM for Autonomous Underwater Vehicle Navigation," in *2011 IEEE International Conference on Robotics and Automation*, Shanghai, 2011, pp. 3048-3055.

[88] D.B. Marco and A.J. Healey, "Current Developments in Underwater Vehicle Control and Navigation: The NPS ARIES AUV," in *Oceans 2000 MTS/IEEE Conference and Exhibition*, 2000, pp. 1011-1016.

[89] J.C. Alleyne, "Position Estimation from Range Only Measurements," Naval Postgraduate School, Monterey, Cal., Mater's Thesis 2000.

[90] J.C. Hartsfield, "Single Transponder Range Only Navigation Geometry (STRONG) Applied to REMUS Autonomous Under Water [sic] Vehicles," Massachusetts Institute of Technology and Woods Hole Oceanographic Institution, Woods Hole, Mass., Thesis 2005.

[91] A. Martins, J. M. Almeida, and E. Silva, "Coordinated Maneuver for Gradient Search using Multiple AUVs," in *Proceedings of Oceans 2003*, 2003, pp. 347-352.

[92] A. Pascoal et al., "Robotic Ocean Vehicles for Marine Science Applications: The European ASIMOV Project," in *Oceans 2000 MTS/IEEE Conference and Exhibition*, Providence, R.I., 2000, pp. 409-415.

[93] M. Chitre, "Path Planning for Cooperation Underwater Range-Only Navigation using a Single Beacon," in *International Conference on Autonomous and Intelligent Systems, 2010*, Povoa de Varzim, Portugal, 2010, pp. 1-6.

[94] M.F. Fallon, G. Papadopoulos, and J.J. Leonard, "Cooperative AUV Navigation using a Single Surface Craft," *Journal of Field and Service Robotics*, vol. 26, pp. 331-340, 2010.

[95] S. Yoon and C. Qiao, "Cooperative Search and Survey using Autonomous Underwater Vehicles (AUVs)," *To appear in IEEE Transactions on Parallel and Distributed Systems*, pp. 1-14, 2010.

[96] J.A. Hudson, M.L. Seto, and Y.-J. Pan, "Three-Dimensional Mobile Navigation And Communication Aid Path Planning For Multiple Autonomous Underwater Vehicles," in *Association for Unmanned Vehicle Systems International (AUVSI) Unmanned Systems North America 2011*, Washington, D.C., 2011, pp. 1-11.

[97] M.F. Fallon, G. Papadopoulos, J.J. Leonard, and N.M. Patrikalakis, "Cooperative AUV Navigation using a Single Maneuvering Surface Craft," *The International Journal of Robotics Research*, 2010.

[98] M.R. Benjamin, H. Schmidt, P. Newman, and J.J. Leonard, "An Overview of MOOS-IvP and a Users Guide to the IvP Helm - Release 4.2.1," Massachusetts Institute of Technology, Cambridge, Mass., Technical Report MIT-CSAIL-TR-2011-037, 2011.

[99] T.B. Koay et al., "STARFISH - A Small Team of Autonomous Robotic Fish," in *3rd International Conference on Underwater System Technology: Theory and Applications 2010*, Cyberjaya, Malaysia, 2010, pp. 1-7.

[100] D.P. Eickstedt and S.R. Sideleau, "The Backseat Control Architecture for Autonomous Robotic Vehicles: A Case Study with the Iver2 AUV," *Marine Technology Society Journal*, vol. 44, no. 4, pp. 42-54, July/August 2010.

[101] S. Kemna, "BHV_OpRegionBounce: An OpRegion that can Bounce You Back," in *MOOS Development and Applications Working Group (MOOS-DAWG) 2011*, Cambridge, Mass., 2011.

[102] MASc Committee Meeting, Present: Hudson, J., Seto, M., Pan, Y.-J., Militzer, J., Gregson, P., Oct. 18, 2011.

[103] M.L. Seto and D. Hopkin, "Modelling Variable Length Tows and Altitude-keeping with Canadian Remote Minehunting and Disposal System," in *Oceans 2008*, Quebec City, 2008, pp. 1-8.

[104] International Submarine Engineering. (2008) ISE DORADO. [Online]. http://www.ise.bc.ca/dorado.html

[105] J. Pentzer et al., "Measurement of Magnetic Field Using Collaborative AUVs," in *IEEE Oceans 2010 - Sydney*, Syndey, Aus., 2010, pp. 1-7.

[106] A. Martins et al., "Autonomous Surface Vehicle Docking Manoeuvre with Visual Information," in *2007 IEEE International Conference on Robotics and Automation*, 2007, pp. 4994-4999.

[107] C. Chant, *Submarine Warfare Today: The World's Deadliest Underwater Weapons Systems*. New York: Barnes and Noble, 2006.

[108] B. Campbell and C.A. Baker, *The Canadair Argus (CL-28, CP-107): The Untold Story of Canada's Cold War Martime Hunter*. Chester, N.S., Can.: Bryler Publications, 2011.

[109] Woods Hole Oceanographic Institution (WHOI). (2012, March) Acoustic Communications, Micro Modem Related Documentation, Transducers. [Online]. http://acomms.whoi.edu/umodem/documentation.html#transducers

[110] H. Schmidt, M.R. Benjamin, A. Balasuriya, K. Cockrell, and R. Lum. (2008, December) MOOS-IvP Undersea Autonomous Network Simulator User's Guide. [Online]. http://acoustics.mit.edu/faculty/henrik/LAMSS/simguide.pdf

[111] M. Bibuli, G. Bruzzone, M. Caccia, and L. Lapierre, "Path-Following Algorithms and Experiments for an Unmanned Surface Vehicle," *Journal of Field Robotics*, vol. 26, no. 8, pp. 669-688, 2009.

[112] M.R. Benjamin, J.A. Curcio, J.J. Leonard, and P.M. Newman, "Navigation of Unmanned Marine Vehicles in Accordance with the Rules of Road," in *Proceedings of IEEE International Conference on Robotics and Automation, 2006, ICRA 2006*, 2006, pp. 3581-3587.

[113] P.M. Ludwig, "Formation Control for Multi-vehicle Robotic Minesweeping," Naval Postgraduate School, Monterey, California, Thesis 2000.

[114] Y. Watanabe, H. Ochi, T. Shimura, and T. Hattori, "Long Range Acoustic Navigation of Cruising AUV Based on Bearing Estimation," in *Oceans 2010 IEEE - Sydney*, Sydney, Aus., 2010, pp. 1-5.

[115] M. Fallon and J. Leonard, "Cooperative AUV Navigation using MOOS: MLBL," in *MOOS Development and Applications Working Group (MOOS-DAWG) 2010*, Cambridge, Mass., 2010.

[116] M. Deffenbaugh, "A Matched Field Processing Approach to Long Range Acoustic Navigation," Massachusetts Institute of Technology, Master's Thesis 1994.

[117] M. Deffenbaugh, H. Schmidt, and J. Bellingham, "Acoustic Positioning in a Fading Multipath Environment," in *IEEE Oceans '96*, 1996, pp. 596-599.

[118] S.C. Chapra and R.P. Canale, *Numerical Mehtods for Engineers*, 5th ed. New York: McGraw-Hill Higher Education, 2006.

[119] J. DeArruda, "OceanServer Iver2 Autonomous Underwater Vehicle Remote Helm Functionality," in *Oceans 2010*, 2010, pp. 1-5.

Appendix A Complete Results for Pre-Deployment Simulations

A	L	s^{CNA} (m/s)	Max Error (m)	RMS Error (m)
7	5	3.50	2.29	2.22
7	5	3.75	2.33	2.22
9	2	4.00	2.30	2.22
8	4	3.75	2.31	2.22
8	3	3.75	2.29	2.22
9	4	4.00	2.29	2.22
8	2	4.00	2.30	2.22
8	4	3.50	2.30	2.22
7	4	3.75	2.29	2.22
9	4	3.75	2.31	2.22
9	3	4.00	2.30	2.22
8	1	3.25	2.33	2.22
7	5	3.75	2.33	2.22
9	2	3.50	2.35	2.23
7	4	4.00	2.34	2.23
7	5	3.50	2.29	2.23
9	2	3.75	2.31	2.23
7	2	4.00	2.30	2.23
7	2	4.00	2.30	2.23
7	4	3.50	2.31	2.23
7	5	4.00	2.37	2.23
7	5	4.00	2.37	2.23
9	3	3.50	2.37	2.23
8	3	4.00	2.33	2.23
8	4	4.00	2.33	2.23
8	3	3.50	2.32	2.23
7	3	4.00	2.34	2.23
8	1	4.00	2.42	2.23
9	3	3.75	2.33	2.23
9	4	3.25	2.37	2.23
7	5	3.25	2.34	2.23
9	2	3.25	2.35	2.23
8	2	3.50	2.40	2.23
6	5	4.00	2.35	2.23
6	3	4.00	2.37	2.23
9	4	3.00	2.37	2.23
9	1	2.75	2.40	2.23
9	4	2.75	2.40	2.23

A	L	s^{CNA} (m/s)	Max Error (m)	RMS Error (m)
9	1	4.00	2.37	2.23
9	4	3.50	2.33	2.23
8	2	3.25	2.39	2.23
8	4	3.25	2.39	2.23
5	5	3.75	2.42	2.23
7	2	3.75	2.33	2.23
7	2	3.75	2.33	2.23
9	1	3.75	2.46	2.24
5	4	3.75	2.33	2.24
9	3	2.75	2.35	2.24
5	4	4.00	2.34	2.24
5	5	4.00	2.43	2.24
8	3	3.25	2.37	2.24
7	5	3.00	2.37	2.24
9	3	3.25	2.33	2.24
6	5	3.75	2.36	2.24
5	4	3.50	2.33	2.24
5	5	3.50	2.33	2.24
5	5	3.50	2.33	2.24
5	1	4.00	2.41	2.24
5	1	3.75	2.42	2.24
9	2	3.00	2.39	2.24
5	2	3.75	2.37	2.24
5	2	3.50	2.32	2.24
7	1	4.00	2.41	2.24
6	3	3.25	2.39	2.24
6	4	3.75	2.38	2.24
6	4	3.75	2.38	2.24
5	5	3.25	2.34	2.24
8	1	3.75	2.38	2.24
9	3	3.00	2.36	2.24
7	5	3.00	2.37	2.24
6	2	4.00	2.41	2.24
7	1	3.50	2.36	2.24
8	1	3.50	2.40	2.24
5	4	3.25	2.34	2.24
6	3	3.50	2.38	2.24
6	4	3.50	2.38	2.24
6	4	3.50	2.38	2.24

A	L	s^{CNA} (m/s)	Max Error (m)	RMS Error (m)
6	5	3.50	2.38	2.24
5	2	4.00	2.52	2.24
6	5	3.00	2.37	2.24
6	5	3.00	2.37	2.24
6	4	4.00	2.35	2.24
6	4	4.00	2.35	2.24
9	1	3.25	2.42	2.25
7	5	3.25	2.41	2.25
6	1	3.75	2.45	2.25
9	1	3.50	2.47	2.25
6	2	3.75	2.43	2.25
6	3	3.00	2.42	2.25
7	2	3.50	2.37	2.25
7	2	3.50	2.37	2.25
4	2	4.00	2.37	2.25
6	1	4.00	2.38	2.25
7	4	3.25	2.46	2.25
6	4	3.25	2.38	2.25
6	4	3.25	2.38	2.25
7	2	3.00	2.35	2.25
7	2	3.00	2.35	2.25
4	4	3.75	2.49	2.25
4	5	3.75	2.49	2.25
4	6	3.75	2.49	2.25
6	4	2.75	2.40	2.25
6	4	2.75	2.40	2.25
5	4	3.00	2.38	2.25
5	5	3.00	2.38	2.25
6	5	3.25	2.45	2.25
7	2	3.25	2.38	2.25
7	2	3.25	2.38	2.25
7	1	3.25	2.38	2.25
5	1	3.50	2.44	2.25
6	2	3.00	2.37	2.25
7	4	3.00	2.42	2.25
8	2	3.00	2.41	2.25
9	2	2.75	2.50	2.25
8	3	3.00	2.44	2.25
4	6	4.00	2.47	2.25
8	4	3.00	2.43	2.26
4	3	3.75	2.50	2.26
7	1	3.75	2.52	2.26
8	4	2.75	2.52	2.26
7	3	2.75	2.56	2.26
7	3	2.75	2.56	2.26
7	3	2.75	2.56	2.26
7	3	2.75	2.56	2.26
6	2	3.25	2.45	2.26
6	2	2.75	2.46	2.26
7	1	3.00	2.49	2.26
6	5	2.75	2.50	2.26
4	4	3.25	2.50	2.26
4	6	3.25	2.50	2.26
9	1	3.00	2.46	2.26
6	1	2.75	2.53	2.26
6	3	2.75	2.43	2.26
6	1	3.00	2.47	2.26
5	2	3.00	2.46	2.26
6	2	3.50	2.49	2.26
6	1	3.25	2.48	2.26
7	4	2.75	2.56	2.26
4	3	4.00	2.47	2.26
4	4	4.00	2.47	2.26
4	5	4.00	2.47	2.26
7	5	2.75	2.56	2.27
6	4	3.00	2.52	2.27
6	4	3.00	2.52	2.27
8	1	3.00	2.46	2.27
4	1	4.00	2.67	2.27
4	6	3.50	2.56	2.27
5	1	3.25	2.47	2.27
9	3	2.50	2.56	2.27
9	2	2.50	2.56	2.27
9	4	2.50	2.56	2.27
7	2	2.75	2.54	2.27
4	2	3.25	2.50	2.27
4	5	3.00	2.54	2.27
7	1	2.75	2.49	2.27
4	6	3.00	2.54	2.27
9	4	2.25	2.61	2.28
4	4	3.00	2.54	2.28
4	5	3.25	2.54	2.28

A	L	s^{CNA} (m/s)	Max Error (m)	RMS Error (m)
4	4	3.50	2.55	2.28
8	2	2.50	2.55	2.28
8	2	2.75	2.52	2.28
4	5	3.50	2.54	2.28
9	3	2.25	2.61	2.28
9	2	2.25	2.61	2.28
7	5	2.50	2.55	2.28
7	2	2.50	2.55	2.28
7	4	2.50	2.55	2.28
8	3	2.75	2.52	2.29
4	3	3.25	2.55	2.29
8	4	2.50	2.63	2.29
7	5	2.25	2.57	2.29
3	3	4.00	2.52	2.29
3	4	4.00	2.52	2.29
3	5	4.00	2.52	2.29
3	6	4.00	2.52	2.29
3	7	4.00	2.52	2.29
3	2	4.00	2.52	2.29
4	6	2.75	2.54	2.29
5	4	2.75	2.54	2.29
5	5	2.75	2.54	2.29
6	3	2.50	2.59	2.29
6	2	2.50	2.59	2.29
6	2	2.50	2.59	2.29
4	3	2.75	2.54	2.29
4	4	2.75	2.54	2.29
4	5	2.75	2.54	2.29
8	3	2.50	2.63	2.29
4	3	3.00	2.62	2.30
6	4	2.50	2.59	2.30
6	4	2.50	2.59	2.30
3	3	3.75	2.58	2.30
3	7	3.75	2.58	2.30
8	4	2.25	2.59	2.30
3	2	3.75	2.58	2.30
7	4	2.25	2.68	2.30
5	4	2.50	2.56	2.30
5	5	2.50	2.56	2.30
5	5	2.50	2.56	2.30
5	2	2.50	2.56	2.30

A	L	s^{CNA} (m/s)	Max Error (m)	RMS Error (m)
5	1	2.50	2.56	2.30
3	4	3.75	2.76	2.30
3	4	3.75	2.76	2.30
3	5	3.75	2.76	2.30
3	6	3.75	2.76	2.30
8	3	2.25	2.59	2.30
8	2	2.25	2.61	2.30
5	1	3.00	2.55	2.30
8	1	2.75	2.63	2.31
4	2	2.75	2.65	2.31
4	2	3.50	2.82	2.31
4	1	3.50	2.82	2.31
6	5	2.50	2.60	2.31
7	1	2.50	2.54	2.31
3	7	3.50	2.76	2.31
3	5	3.50	2.76	2.31
3	6	3.50	2.76	2.31
3	3	3.50	2.65	2.31
5	4	2.25	2.61	2.31
5	4	2.25	2.61	2.31
5	5	2.25	2.61	2.31
5	5	2.25	2.61	2.31
6	5	2.25	2.65	2.31
9	1	2.25	2.67	2.32
7	2	2.25	2.62	2.32
6	3	2.25	2.65	2.32
4	1	2.75	2.79	2.32
4	2	3.00	2.80	2.32
4	1	3.00	2.80	2.32
4	3	3.50	2.84	2.32
6	2	2.25	2.75	2.32
6	2	2.25	2.75	2.32
7	5	2.00	2.75	2.32
6	4	2.25	2.65	2.32
6	4	2.25	2.65	2.32
5	1	2.75	2.61	2.32
3	5	3.25	2.73	2.32
3	6	3.25	2.73	2.32
3	7	3.25	2.73	2.32
4	1	3.25	2.81	2.32
8	1	2.25	2.58	2.32

A	L	s^{CNA} (m/s)	Max Error (m)	RMS Error (m)
3	4	3.50	2.76	2.32
4	6	2.25	2.80	2.32
7	4	2.00	2.75	2.32
6	1	2.25	2.65	2.33
4	5	2.25	2.57	2.33
9	4	2.00	2.69	2.33
8	4	2.00	2.64	2.33
3	4	3.25	2.71	2.33
9	2	2.00	2.69	2.33
7	2	2.00	2.75	2.33
5	1	2.25	2.61	2.33
6	1	2.50	2.62	2.33
5	2	2.75	2.61	2.33
2	3	4.00	2.64	2.33
2	4	4.00	2.64	2.33
2	5	4.00	2.64	2.33
2	6	4.00	2.64	2.33
2	7	4.00	2.64	2.33
2	8	4.00	2.64	2.33
2	9	4.00	2.64	2.33
3	2	3.50	2.68	2.33
4	4	2.50	2.79	2.33
3	3	3.25	2.71	2.33
3	2	3.25	2.71	2.33
5	2	2.25	2.61	2.33
4	5	2.50	2.78	2.34
4	6	2.50	2.78	2.34
6	3	2.00	2.73	2.34
6	4	2.00	2.73	2.34
6	4	2.00	2.73	2.34
3	1	4.00	2.85	2.34
4	2	2.50	2.75	2.34
8	2	2.00	2.66	2.34
9	3	2.00	2.69	2.34
8	3	2.00	2.73	2.34
8	1	2.50	2.63	2.34
8	4	1.75	2.67	2.34
6	5	2.00	2.77	2.34
9	1	2.50	2.68	2.35
8	1	2.00	2.71	2.35
8	3	1.75	2.61	2.35
7	1	2.25	2.63	2.35
7	4	1.75	2.71	2.35
3	4	3.00	2.73	2.35
3	5	3.00	2.73	2.35
3	6	3.00	2.73	2.35
3	7	3.00	2.73	2.35
2	3	3.75	2.68	2.35
2	2	3.75	2.68	2.35
2	8	3.75	2.68	2.35
2	9	3.75	2.68	2.35
3	1	3.75	2.88	2.35
6	2	2.00	2.73	2.35
6	2	2.00	2.73	2.35
9	3	1.75	2.66	2.35
2	2	4.00	2.64	2.35
3	2	3.00	2.75	2.35
5	2	2.00	2.69	2.35
5	1	2.00	2.69	2.35
9	2	1.75	2.78	2.35
7	2	1.75	2.59	2.35
3	3	3.00	2.76	2.36
9	4	1.75	2.65	2.36
6	1	2.00	2.71	2.36
9	4	1.50	2.63	2.36
5	4	2.00	2.82	2.36
5	4	2.00	2.82	2.36
5	5	2.00	2.82	2.36
5	5	2.00	2.82	2.36
8	2	1.75	2.63	2.36
4	3	2.50	2.94	2.36
2	3	3.50	2.71	2.36
2	4	3.50	2.71	2.36
2	5	3.50	2.71	2.36
2	6	3.50	2.71	2.36
2	7	3.50	2.71	2.36
2	8	3.50	2.71	2.36
2	9	3.50	2.71	2.36
9	1	2.00	2.64	2.36
9	2	1.50	2.68	2.36
5	2	1.50	2.78	2.36
2	4	3.75	2.68	2.37

A	L	s^{CNA} (m/s)	Max Error (m)	RMS Error (m)
2	5	3.75	2.68	2.37
2	6	3.75	2.68	2.37
2	7	3.75	2.68	2.37
7	5	1.75	2.87	2.37
3	1	3.50	2.93	2.37
4	1	2.50	2.78	2.37
8	1	1.75	2.81	2.37
7	1	2.00	2.75	2.37
3	1	3.25	2.97	2.37
9	3	1.50	2.69	2.37
6	3	1.50	2.69	2.37
7	1	1.75	2.58	2.37
7	4	1.50	2.67	2.37
2	5	3.25	2.78	2.37
2	6	3.25	2.78	2.37
2	7	3.25	2.78	2.37
2	8	3.25	2.78	2.37
2	9	3.25	2.78	2.37
4	4	2.25	2.81	2.38
7	5	1.50	2.79	2.38
2	1	4.00	2.85	2.38
9	1	1.50	2.65	2.38
6	3	1.75	2.80	2.38
6	2	1.75	2.80	2.38
6	2	1.75	2.80	2.38
5	1	1.50	2.73	2.38
6	4	1.50	2.55	2.38
6	4	1.50	2.55	2.38
5	2	1.75	2.78	2.38
2	4	3.25	2.74	2.38
4	3	2.25	2.98	2.38
2	3	3.25	2.74	2.38
6	5	1.75	2.85	2.38
5	1	1.75	2.70	2.38
9	1	1.75	2.70	2.38
5	4	1.50	2.88	2.38
5	4	1.50	2.88	2.38
3	1	3.00	2.99	2.39
2	2	3.50	2.71	2.39
3	4	2.75	2.74	2.39
3	5	2.75	2.74	2.39

A	L	s^{CNA} (m/s)	Max Error (m)	RMS Error (m)
3	6	2.75	2.74	2.39
3	7	2.75	2.74	2.39
5	5	1.75	2.78	2.39
5	5	1.75	2.78	2.39
4	1	2.25	2.73	2.39
6	4	1.75	2.89	2.39
6	4	1.75	2.89	2.39
8	2	1.50	2.75	2.40
4	1	3.75	2.81	2.40
8	4	1.50	2.91	2.40
8	3	1.50	2.90	2.40
3	2	2.75	2.76	2.40
6	1	1.75	2.75	2.40
5	5	1.50	2.88	2.40
5	5	1.50	2.88	2.40
5	4	1.75	3.00	2.40
8	1	1.50	2.70	2.40
6	5	1.50	2.95	2.41
6	2	1.50	2.74	2.41
6	2	1.50	2.74	2.41
6	1	1.50	2.74	2.41
2	1	3.75	2.88	2.41
9	2	1.25	2.70	2.41
3	6	2.50	2.83	2.41
3	7	2.50	2.83	2.41
4	3	1.75	2.82	2.41
4	3	2.00	2.82	2.41
2	1	3.50	2.92	2.41
8	4	1.25	2.74	2.41
4	4	1.75	2.82	2.41
4	5	1.75	2.82	2.41
3	4	2.50	2.83	2.41
3	5	2.50	2.83	2.41
7	1	1.50	2.64	2.41
2	9	3.00	2.87	2.41
3	3	2.75	2.86	2.41
2	1	3.25	2.96	2.42
4	2	2.00	2.80	2.42
9	3	1.25	2.79	2.42
6	3	1.25	2.75	2.42
4	6	2.00	2.87	2.42

A	L	s^{CNA} (m/s)	Max Error (m)	RMS Error (m)
2	2	3.25	2.75	2.42
7	4	1.25	2.83	2.42
7	4	1.25	2.83	2.42
6	2	1.25	2.86	2.42
8	3	1.25	2.86	2.42
9	4	1.25	2.70	2.43
7	1	1.25	2.86	2.43
2	4	3.00	2.86	2.43
2	5	3.00	2.86	2.43
2	7	3.00	2.86	2.43
2	8	3.00	2.86	2.43
6	5	1.25	2.90	2.43
4	4	2.00	3.00	2.43
3	5	2.25	3.01	2.43
9	1	1.25	2.83	2.43
7	2	1.25	2.86	2.43
6	4	1.25	2.86	2.43
2	6	3.00	2.85	2.43
4	5	2.00	2.82	2.43
2	3	3.00	2.77	2.43
8	1	1.25	2.80	2.43
2	2	3.00	2.81	2.44
3	4	2.25	3.01	2.44
5	4	1.25	2.82	2.44
7	5	1.25	2.91	2.44
4	1	1.75	3.00	2.44
3	2	2.25	3.01	2.44
6	1	1.25	2.92	2.44
5	2	1.25	2.82	2.45
3	2	2.00	2.91	2.45
6	3	1.00	2.76	2.45
4	1	2.00	2.94	2.45
3	1	1.75	2.97	2.45
3	1	2.00	2.91	2.45
4	2	1.75	2.90	2.45
3	3	2.25	2.98	2.45
2	4	2.75	2.97	2.46
2	7	2.75	2.97	2.46
6	2	1.00	2.97	2.46
3	6	2.25	3.01	2.46
3	7	2.25	3.01	2.46

A	L	s^{CNA} (m/s)	Max Error (m)	RMS Error (m)
3	2	1.75	2.97	2.46
3	2	2.50	3.00	2.46
7	5	1.00	2.82	2.46
9	2	1.00	2.84	2.46
3	1	2.75	2.79	2.46
2	2	2.75	2.93	2.47
2	6	2.75	2.97	2.47
6	5	1.00	2.83	2.47
3	3	2.50	2.91	2.47
4	6	1.75	2.91	2.47
7	4	1.00	2.85	2.47
7	4	1.00	2.85	2.47
7	2	1.00	2.97	2.47
6	1	1.00	2.85	2.47
7	1	1.00	2.97	2.47
9	3	1.00	2.79	2.47
2	5	2.75	2.89	2.47
8	3	1.00	2.89	2.47
3	3	1.50	3.04	2.47
8	4	1.00	2.85	2.47
8	1	1.00	2.93	2.47
3	3	2.00	2.91	2.47
3	4	2.00	2.91	2.47
3	5	2.00	2.91	2.47
3	6	2.00	2.91	2.47
3	7	2.00	2.91	2.47
2	1	3.00	3.01	2.47
2	3	2.75	2.84	2.47
4	3	1.50	2.83	2.47
5	5	1.25	2.92	2.48
2	8	2.75	2.83	2.48
4	2	1.50	2.88	2.48
3	2	1.50	3.04	2.48
3	1	2.50	2.80	2.48
9	4	1.00	2.94	2.48
3	3	1.75	2.97	2.48
3	4	1.75	2.97	2.48
3	5	1.75	2.97	2.48
3	6	1.75	2.97	2.48
3	1	2.25	2.84	2.48
8	2	1.00	2.96	2.48

A	L	s^{CNA} (m/s)	Max Error (m)	RMS Error (m)
4	6	1.50	3.12	2.49
6	4	1.00	2.94	2.49
9	1	1.00	2.94	2.49
4	4	1.50	2.84	2.49
5	2	1.00	2.87	2.49
4	2	1.25	2.88	2.49
4	5	1.50	3.05	2.49
4	1	1.50	3.06	2.50
4	4	1.25	2.88	2.50
3	5	1.50	3.04	2.50
3	7	1.75	3.32	2.50
3	4	1.50	3.04	2.50
3	1	1.50	3.15	2.51
4	3	1.00	2.99	2.51
7	2	0.75	2.98	2.51
8	1	0.75	3.09	2.51
2	9	2.75	3.41	2.51
9	3	0.75	3.07	2.51
8	2	0.75	2.99	2.51
4	5	1.25	3.09	2.52
3	6	1.50	3.04	2.52
7	1	0.75	3.08	2.52
4	3	1.25	2.96	2.52
4	6	1.25	3.14	2.52
8	3	0.75	3.04	2.52
5	1	1.25	3.07	2.53
9	2	0.75	3.00	2.53
2	4	2.50	2.91	2.53
2	4	2.25	3.10	2.53
2	7	2.25	3.10	2.53
2	2	2.50	2.97	2.53
9	4	0.75	2.97	2.53
6	3	0.75	3.06	2.54
8	4	0.75	2.98	2.54
5	4	1.00	2.90	2.54
5	4	1.00	2.90	2.54
3	2	1.25	3.14	2.54
2	1	2.75	3.16	2.54
4	4	1.00	2.99	2.54
4	6	1.00	2.99	2.54
3	7	1.50	3.08	2.54

A	L	s^{CNA} (m/s)	Max Error (m)	RMS Error (m)
5	5	1.00	2.99	2.54
2	5	2.50	2.96	2.54
2	6	2.50	2.96	2.54
9	1	0.75	3.05	2.54
6	2	0.75	3.06	2.54
2	3	2.50	2.95	2.55
7	4	0.75	3.01	2.55
7	4	0.75	3.01	2.55
7	5	0.75	3.02	2.55
2	1	2.50	2.90	2.55
6	4	0.75	3.19	2.55
6	5	0.75	3.19	2.55
3	4	1.25	3.14	2.55
3	5	1.25	3.14	2.55
4	1	1.25	3.13	2.55
3	3	1.25	3.14	2.55
2	7	2.50	3.07	2.56
4	5	1.00	3.03	2.56
2	9	2.50	3.09	2.56
2	8	2.50	3.30	2.56
2	2	2.25	3.01	2.56
2	6	2.25	2.98	2.56
2	3	2.25	2.97	2.56
2	4	2.00	3.03	2.56
2	5	2.00	3.03	2.56
2	5	2.25	2.98	2.56
5	4	0.75	3.06	2.57
5	5	0.75	3.06	2.57
3	7	1.25	3.14	2.57
2	8	2.25	3.14	2.57
2	9	2.25	3.14	2.57
2	6	2.00	3.17	2.58
3	6	1.25	3.37	2.58
2	3	2.00	3.05	2.58
4	2	0.75	3.11	2.58
7	2	0.50	3.21	2.59
2	1	2.25	2.98	2.59
4	1	1.00	3.17	2.59
8	3	0.50	3.26	2.59
3	2	0.75	3.47	2.60
4	4	0.75	3.11	2.60

A	L	s^{CNA} (m/s)	Max Error (m)	RMS Error (m)
4	3	0.75	3.11	2.60
8	2	0.50	3.15	2.60
4	5	0.75	3.11	2.60
9	4	0.50	3.21	2.60
9	3	0.50	3.19	2.60
7	4	0.50	3.22	2.60
7	4	0.50	3.22	2.60
8	4	0.50	3.26	2.60
2	7	2.00	3.12	2.60
2	8	2.00	3.12	2.60
2	9	2.00	3.12	2.60
9	2	0.50	3.17	2.61
3	2	1.00	3.29	2.61
4	6	0.75	3.28	2.61
7	5	0.50	3.24	2.61
2	5	1.75	3.20	2.61
3	3	1.00	3.47	2.62
5	1	1.00	3.16	2.62
6	4	0.50	3.28	2.62
2	6	1.75	3.20	2.62
8	1	0.50	3.20	2.62
2	2	2.00	3.09	2.62
2	2	2.00	3.09	2.62
6	1	0.75	3.19	2.62
6	3	0.50	3.25	2.62
6	2	0.50	3.26	2.62
2	4	1.75	3.13	2.63
3	5	1.00	3.29	2.63
3	6	1.00	3.29	2.63
3	7	1.00	3.29	2.63
3	6	0.75	3.29	2.63
3	7	0.75	3.29	2.63
4	3	0.50	3.25	2.63
4	3	0.50	3.25	2.63
4	4	0.50	3.25	2.63
3	4	0.75	3.29	2.63
3	5	0.75	3.29	2.63
5	2	0.50	3.23	2.63
5	4	0.50	3.29	2.64
3	4	1.00	3.29	2.64
7	1	0.50	3.19	2.64
9	1	0.50	3.20	2.64
6	5	0.50	3.28	2.64
4	2	0.50	3.22	2.64
2	1	1.75	3.13	2.65
5	5	0.50	3.29	2.65
4	5	0.50	3.25	2.65
2	2	1.75	3.13	2.65
2	3	1.75	3.13	2.65
2	7	1.75	3.20	2.65
2	8	1.75	3.20	2.65
2	9	1.75	3.20	2.65
2	1	2.00	3.15	2.65
3	1	1.25	3.43	2.65
4	6	0.50	3.25	2.66
2	2	1.50	3.21	2.66
2	8	1.50	3.37	2.66
3	3	0.75	3.53	2.66
4	1	0.75	3.26	2.68
2	4	1.00	3.25	2.68
2	3	1.50	3.21	2.68
2	3	1.00	3.41	2.69
2	4	1.50	3.30	2.69
2	5	1.50	3.30	2.69
2	6	1.50	3.30	2.69
2	7	1.50	3.30	2.70
2	9	1.50	3.30	2.70
3	5	0.50	3.57	2.70
3	6	0.50	3.57	2.70
3	7	0.50	3.57	2.70
2	2	1.25	3.29	2.70
3	1	1.00	3.47	2.70
2	4	0.75	3.37	2.70
2	5	1.00	3.29	2.71
2	5	1.25	3.29	2.71
2	6	1.25	3.29	2.71
2	7	1.25	3.29	2.71
3	3	0.50	3.57	2.71
2	3	1.25	3.29	2.71
5	1	0.75	3.27	2.71
2	4	1.25	3.26	2.71
2	6	1.00	3.34	2.71

A	L	s^{CNA} (m/s)	Max Error (m)	RMS Error (m)
2	8	1.25	3.29	2.72
2	9	1.00	3.25	2.72
3	1	0.75	3.52	2.72
2	7	1.00	3.34	2.72
2	8	1.00	3.34	2.72
2	1	1.50	3.12	2.72
2	6	0.75	3.37	2.73
3	4	0.50	3.29	2.73
2	0	2.00	3.30	2.73
2	7	0.75	3.37	2.73
3	2	0.50	3.53	2.74
2	8	0.75	3.37	2.74
2	9	0.75	3.37	2.74
6	1	0.50	3.37	2.74
2	2	1.00	3.37	2.75
2	9	1.25	3.34	2.75
4	1	0.50	3.37	2.76
5	1	0.50	3.37	2.77
2	5	0.75	3.45	2.78
2	3	0.75	3.44	2.80
2	2	0.75	3.41	2.80
2	7	0.50	3.48	2.80
2	8	0.50	3.48	2.80
2	9	0.50	3.48	2.80

A	L	s^{CNA} (m/s)	Max Error (m)	RMS Error (m)
3	1	0.50	3.59	2.82
2	6	0.50	3.48	2.85
2	5	0.50	3.48	2.86
2	2	0.50	3.39	2.87
2	3	0.50	3.48	2.87
2	4	0.50	3.48	2.87
2	0	1.75	3.55	3.02
2	1	1.25	3.63	3.03
2	1	0.75	3.49	3.06
2	0	0.75	3.49	3.06
2	0	1.50	3.62	3.06
2	0	1.25	3.60	3.06
2	0	1.00	3.57	3.07
2	1	0.50	3.54	3.07
2	0	0.50	3.54	3.07
2	1	1.00	3.55	3.07
2	0	2.25	3.98	3.26
2	0	3.00	4.16	3.45
2	0	2.75	4.24	3.48
2	0	2.50	4.27	3.49
2	0	4.00	4.67	3.61
2	0	3.75	4.79	3.66
2	0	3.50	4.80	3.67
2	0	3.25	5.08	3.72

Appendix B Additional Tank Trials

Additional tank trials were run in anticipation of matching upcoming harbour trials. These harbour trials could not be completed due to factors including weather, AUV serviceability, and staff and facility availability. However, two of the tank trials shown were also attempted as harbour trials (Figure 6.69 and Figure 6.71). The Table B.1 summarizes both planned and attempted tank and harbour underway path planning trials. Some trials were run twice in an attempt to maximize the work accomplished in the time available on a particular day of trials.

Table B.1: Planned, attempted, and completed tank and harbour trials

N	Pattern	Depth	CNA Params	1st Harbour Trial	2nd Harbour Trial	Tank Trial
1	Lawnmower	10 m	A=5,L=5	Figure 6.18		Figure 6.20
1	Lawnmower	10 m	A=3,L=0	Figure 6.23		Figure 6.26
1	Lawnmower	5 m	A=5,L=5	Figure 6.28	Figure 6.36	Figure 6.32
1	Lawnmower	5 m	A=3,L=0	Figure 6.38	Figure 6.39	Figure 6.40
1	Lawnmower	Alt.	A=5,L=5	Figure 6.42	Figure 6.44	
1	Lawnmower	Alt.	A=3,L=0	Figure 6.46		
2	Ortho.Short	10 m	A=5,L=5	Figure 6.47		Figure 6.49
2	Ortho.Short	10 m	A=3,L=0	Figure 6.53		Figure 6.54
2	Ortho.Short	5 m	A=5,L=5	Figure 6.56		Figure 6.57
2	Ortho.Short	5 m	A=3,L=0	Figure 6.58		Figure 6.61
2	Ortho.Short	Alt.	A=5,L=5	Figure 6.63		Figure 6.64
2	Ortho.Short	Alt.	A=3,L=0	Figure 6.66		Figure 6.67
2	Parallel.Med	10 m	A=5,L=5	14FEB12: failure	Figure 6.69	
2	Parallel.Med	10 m	A=3,L=3			Figure B.13
2	Parallel.Med	10 m	A=3,L=0	Figure 6.71		Figure B.14
2	Parallel.Med	5 m	A=5,L=5			Figure B.15
2	Parallel.Med	5 m	A=3,L=0			Figure B.16
2	Parallel.Med	Alt.	A=5,L=5			
2	Parallel.Med	Alt.	A=3,L=0			
2	Orthog.Med	10 m	A=5,L=5			Figure B.1
2	Orthog.Med	10 m	A=3,L=0			Figure B.2
2	Orthog.Med	5 m	A=5,L=5			Figure B.5
2	Orthog.Med	5 m	A=3,L=0			Figure B.6
2	Orthog.Med	Alt.	A=5,L=5			Figure B.9
2	Orthog.Med	Alt.	A=3,L=0			Figure B.10
2	Parallel.Long	10 m	A=5,L=5	17NOV11: failure		Figure B.17
2	Parallel.Long	10 m	A=3,L=0			
2	Parallel.Long	5 m	A=5,L=5			Figure B.18
2	Parallel.Long	5 m	A=3,L=0			
2	Parallel.Long	Alt.	A=5,L=5			
2	Parallel.Long	Alt.	A=3,L=0			

N	Pattern	Depth	CNA Params	1st Harbour Trial	2nd Harbour Trial	Tank Trial
2	Orthog.Long	10 m	A=5,L=5	Figure 6.9(tnk)[33]	23SEP11: failure	Figure 6.7
2	Orthog.Long	10 m	A=3,L=0			
2	Orthog.Long	5 m	A=5,L=5			
2	Othog.Long	5 m	A=3,L=0			
2	Orthog.Long	Alt.	A=5,L=5			
2	Orthog.Long	Alt.	A=3,L=0			
3	Parallel.Long	10 m	A=5,L=5			
3	Parallel.Long	10 m	A=5,L=3	Figure 6.13(tnk)		Figure 6.12
3	Parallel.Long	10 m	A=3,L=0			
3	Parallel.Long	5 m	A=5,L=5			
3	Parallel.Long	5 m	A=5,L=3			Figure 6.14
3	Parallel.Long	5 m	A=3,L=0			
3	Parallel.Long	Alt.	A=5,L=5			
3	Parallel.Long	Alt.	A=3,L=0			
1	[6]: 200 ×300 m	10 m	A=7,L=1			
1	[6]: 200 ×300 m	10 m	A=7,L=3			
1	[6]: 200 ×300 m	5 m	A=7,L=1			
1	[6]: 200 ×300 m	5 m	A=7,L=3			
1	[6]: 200 ×300 m	Alt.	A=7,L=1			
1	[6]: 200 ×300 m	Alt.	A=7,L=3			
1	[6]: 100 ×600 m	10 m	A=7,L=1			
1	[6]: 100 ×600 m	10 m	A=7,L=3			
1	[6]: 100 ×600 m	5 m	A=7,L=1			
1	[6]: 100 ×600 m	5 m	A=7,L=3			
1	[6]: 100 ×600 m	Alt.	A=7,L=1			
1	[6]: 100 ×600 m	Alt.	A=7,L=3			
1	[5]:200 ×400 m	Alt.	A=5,L=5			
1	[5]:200 ×400 m	Alt.	A=3,L=0			
1	[5]:200 ×400 m	10 m	A=5,L=5			
1	[5]:200 ×400 m	10 m	A=3,L=0			
1	[5]:200 ×400 m	5 m	A=5,L=5			
1	[5]:200 ×400 m	5 m	A=3,L=0			

[33] "tnk" indicates trial is actually a tank trial

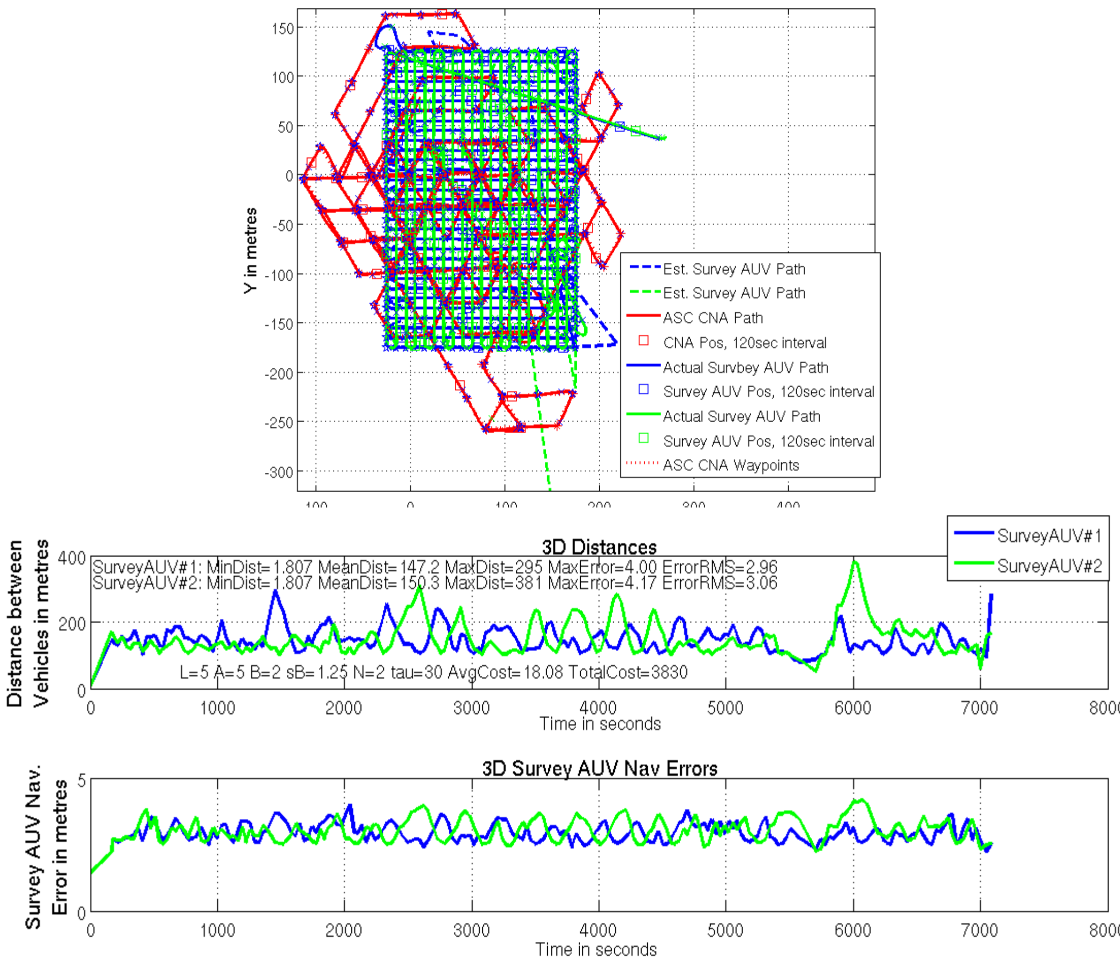

Figure B.1: Tank trial, orthogonal lawnmower legs, 10 m mode depth, tight parameters

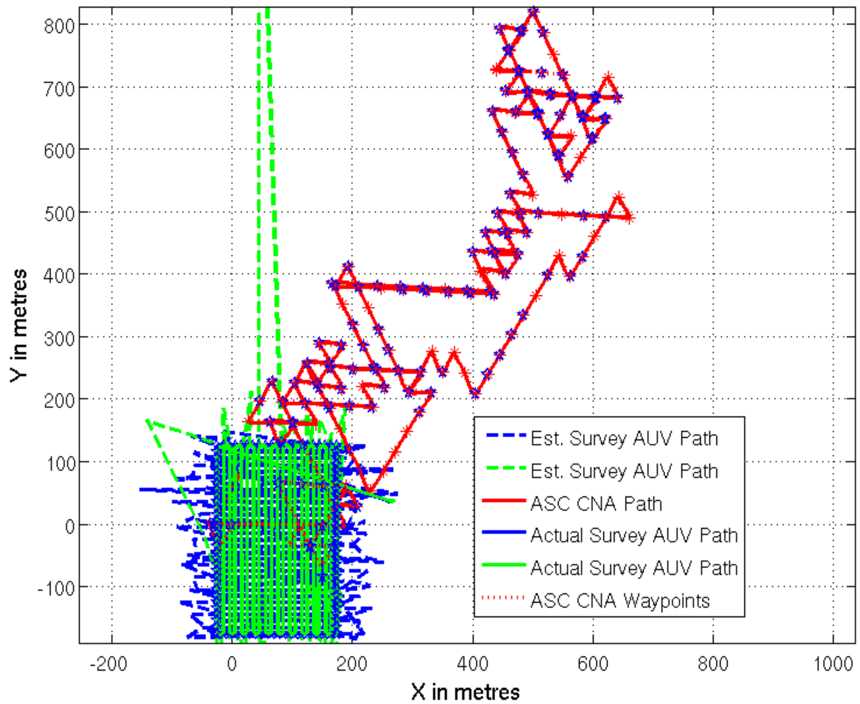

Figure B.2: Tank trial, orthogonal lawnmower legs, 10 m mode depth, reduced parameters

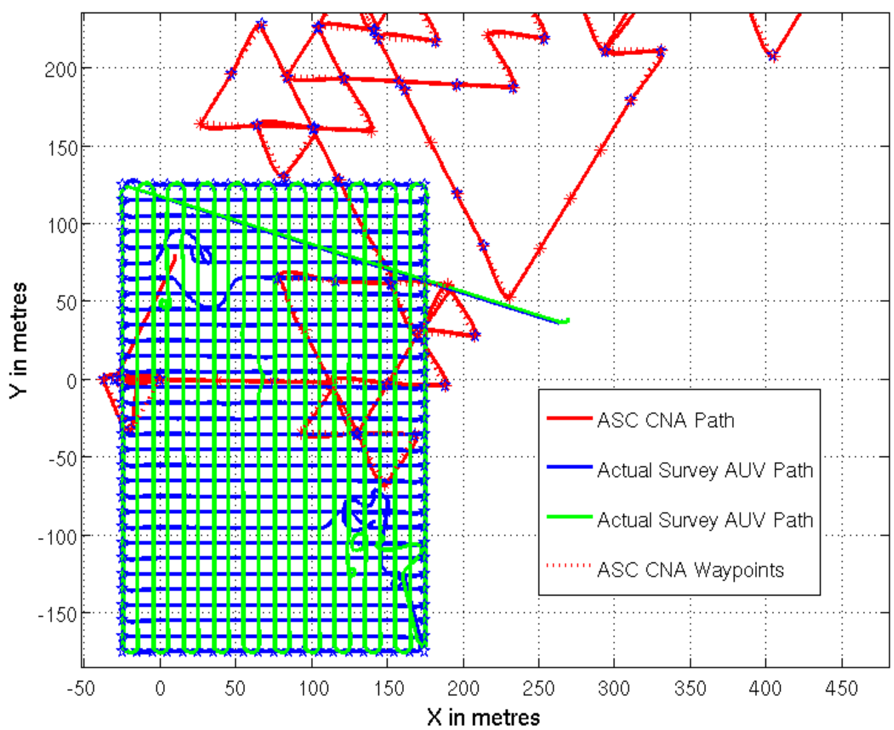

Figure B.3: Detail view of Figure B.2

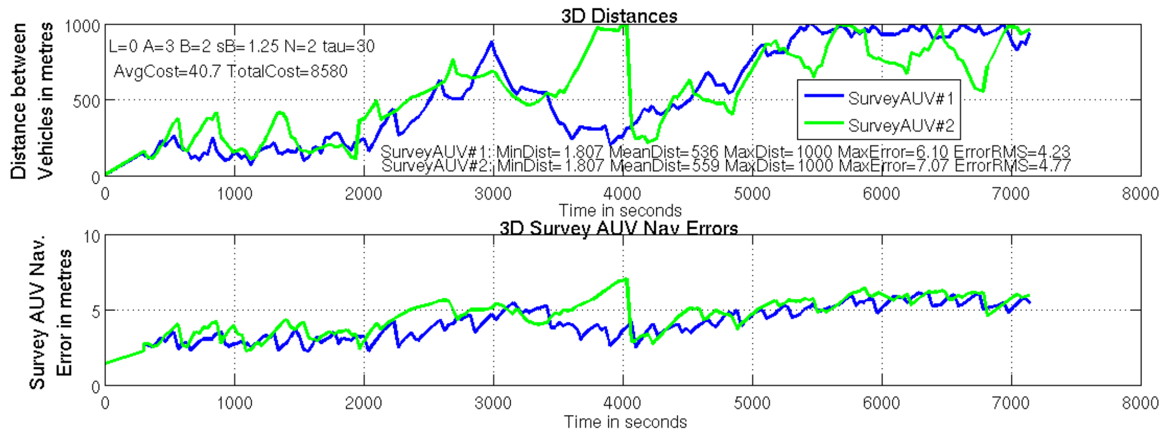

Figure B.4: Distance and survey AUV position errors vs. time for Figure B.2

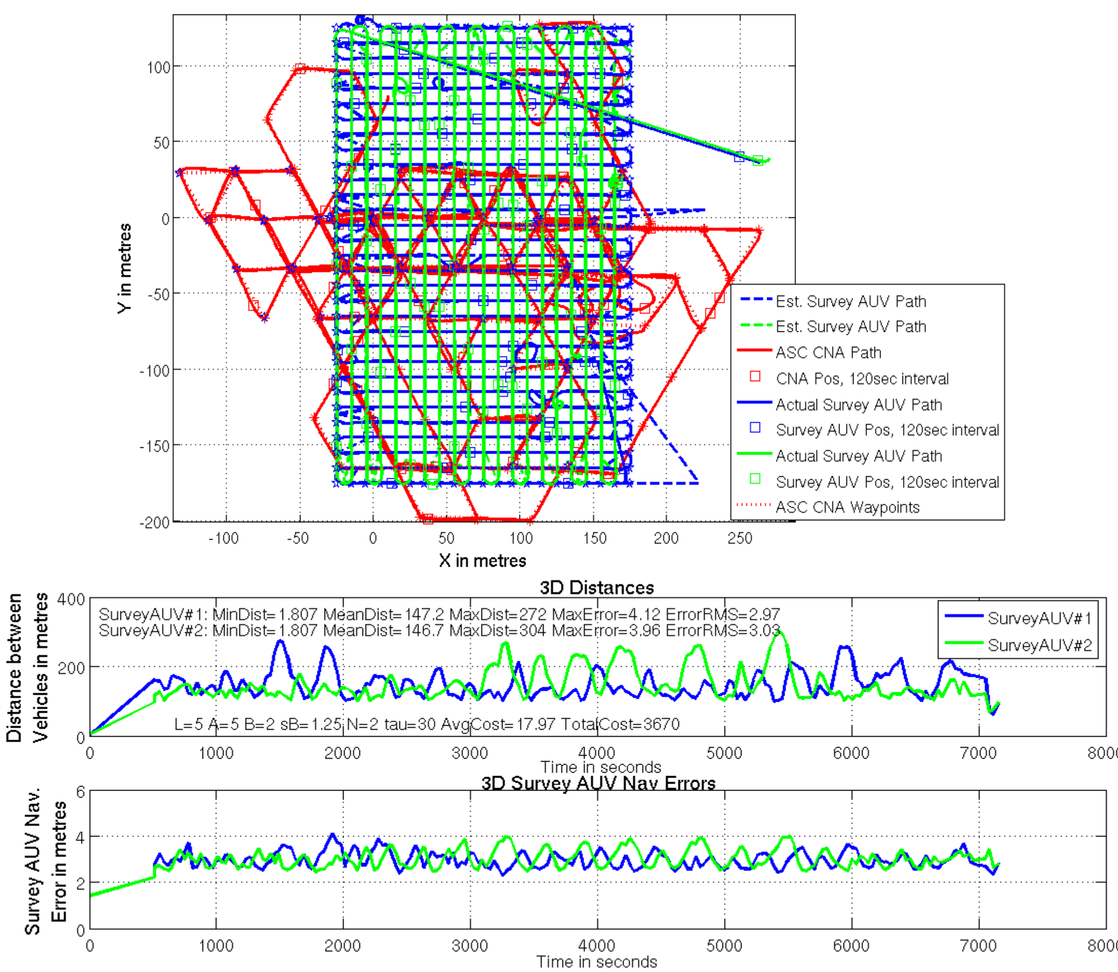

Figure B.5: Tank trial, orthogonal lawnmower legs, 5 m mode depth, tight parameters

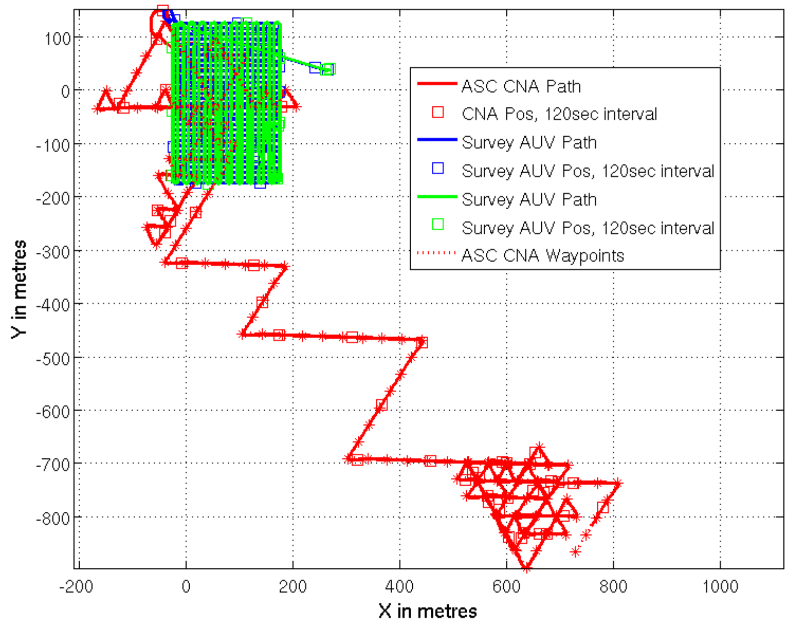

Figure B.6: Tank trial, orthogonal lawnmower legs, 5 m mode depth, reduced parameters

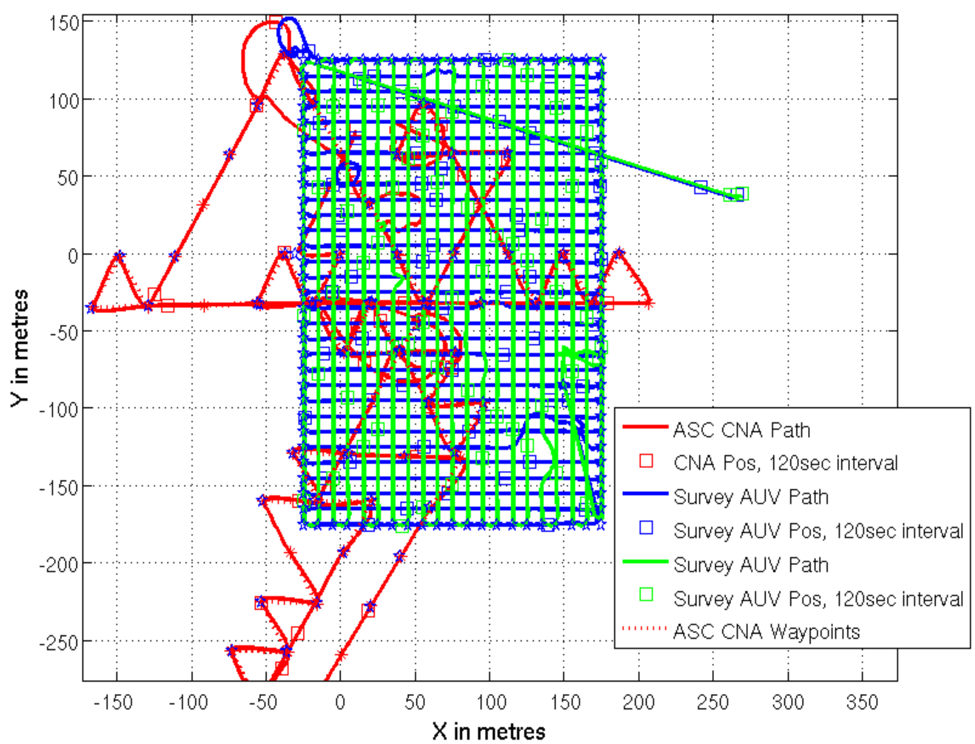

Figure B.7: Detail view of Figure B.6

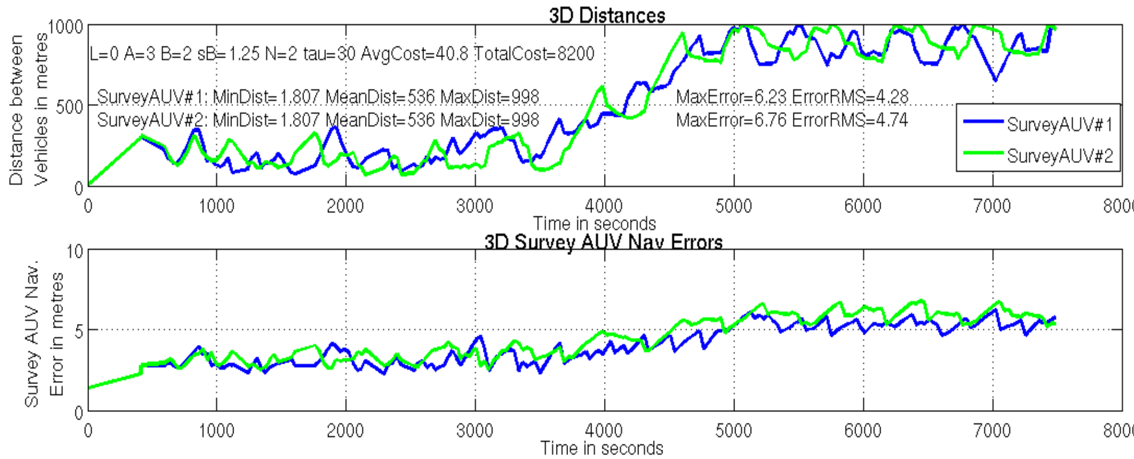

Figure B.8: Distance and survey AUV position error vs. time for tank trial in Figure B.6

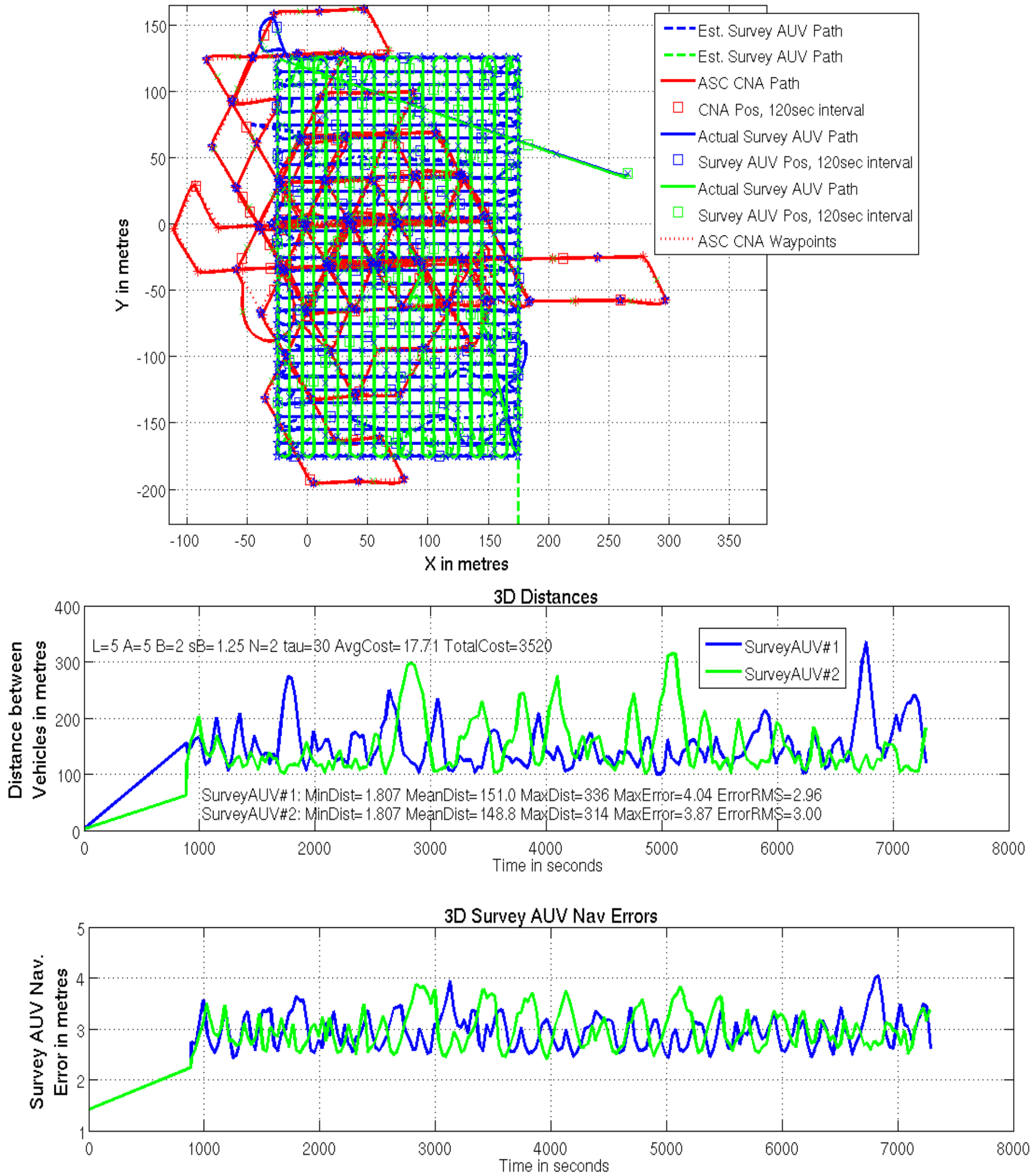

Figure B.9: Tank trial, orthogonal lawnmower legs, 10 m altitude keeping, tight parameters

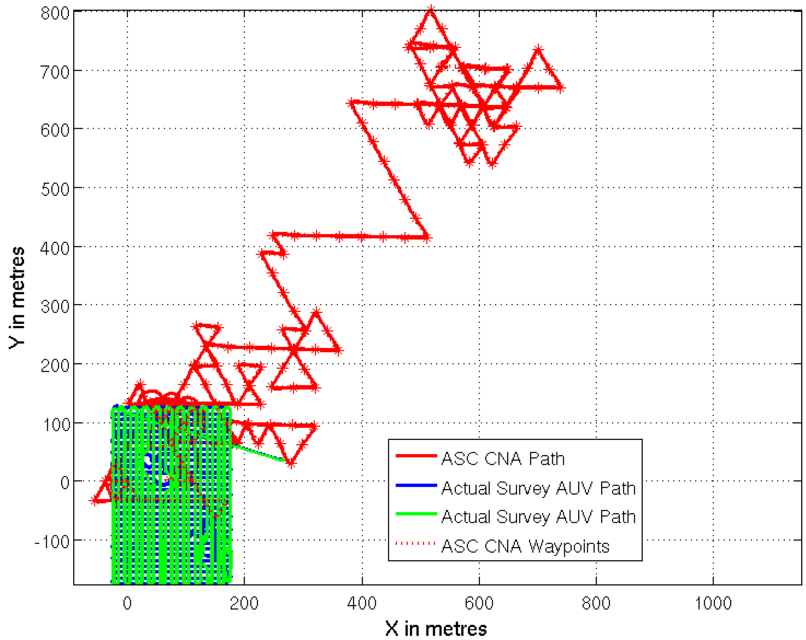

Figure B.10: Tank trial, orthogonal lawnmower legs, 10 m constant altitude, reduced parameters

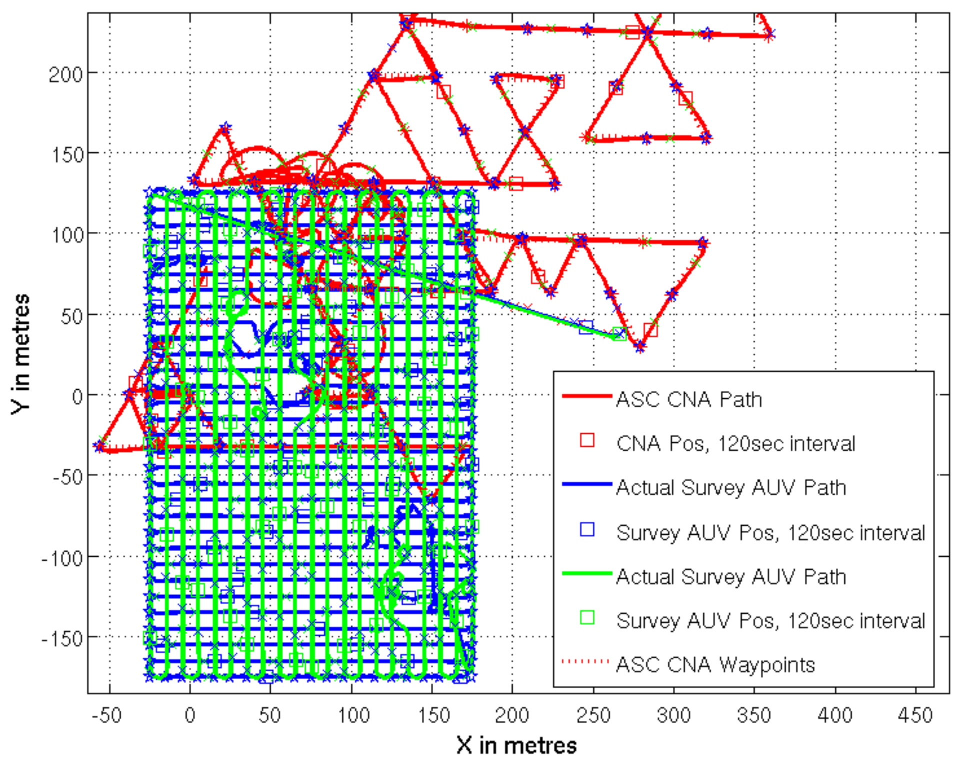

Figure B.11: Detail view of Figure B.10

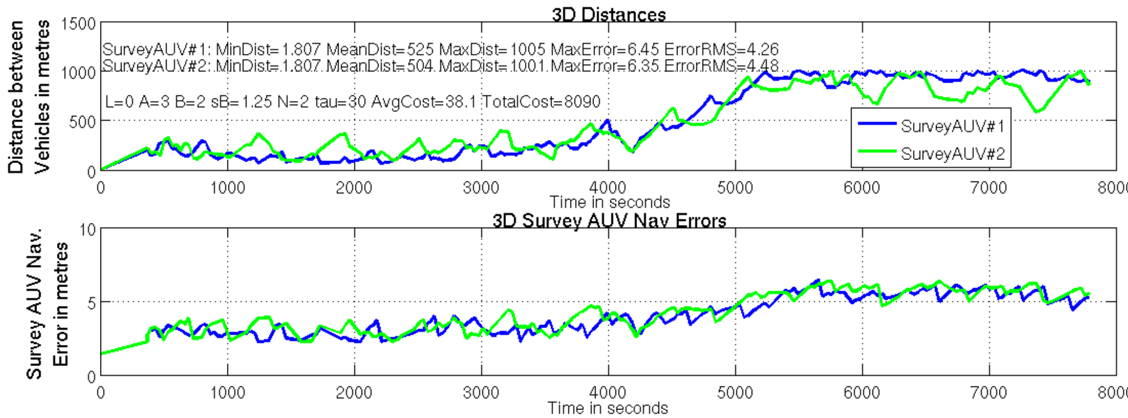

Figure B.12: Distance and survey AUV position error vs. time for tank trial in Figure B.10

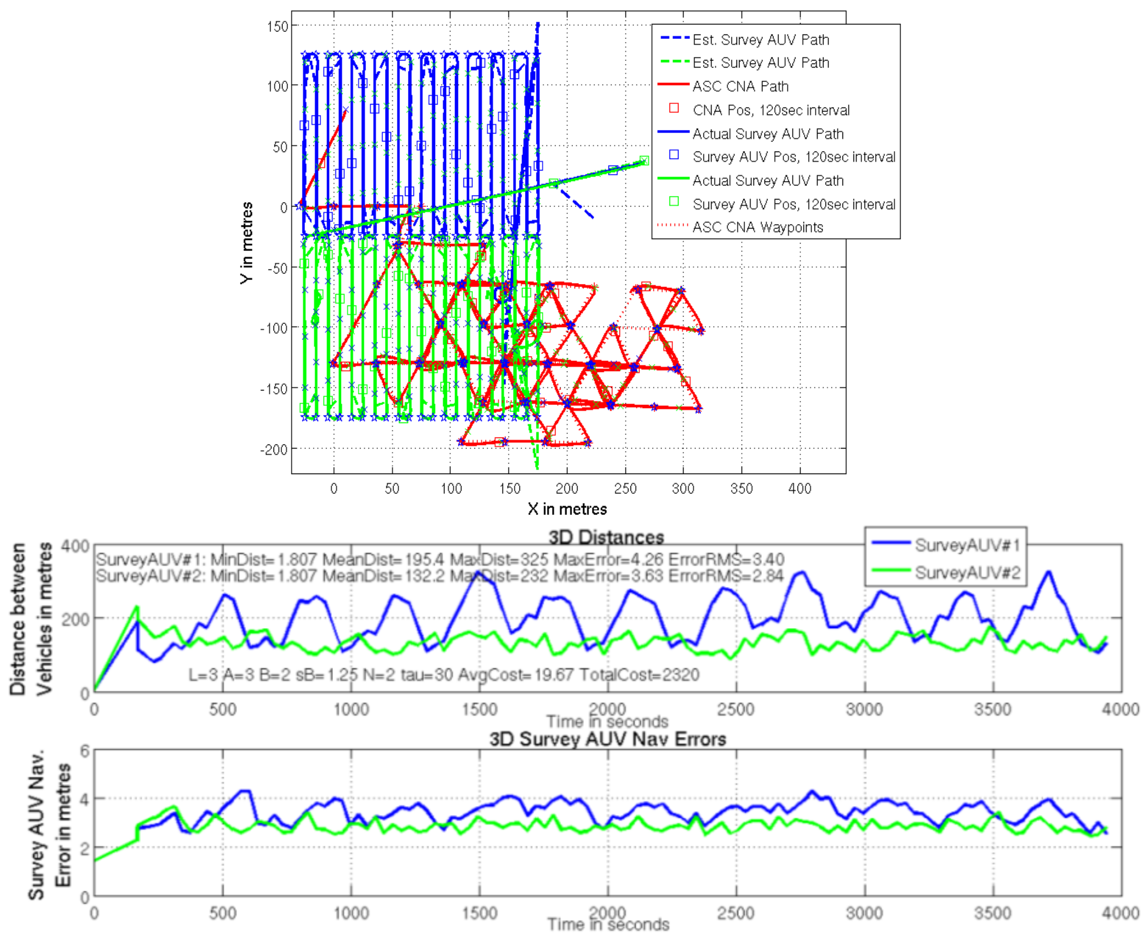

Figure B.13: Tank trial, parallel lawnmower legs, 10 m mode depth, moderately tight parameters

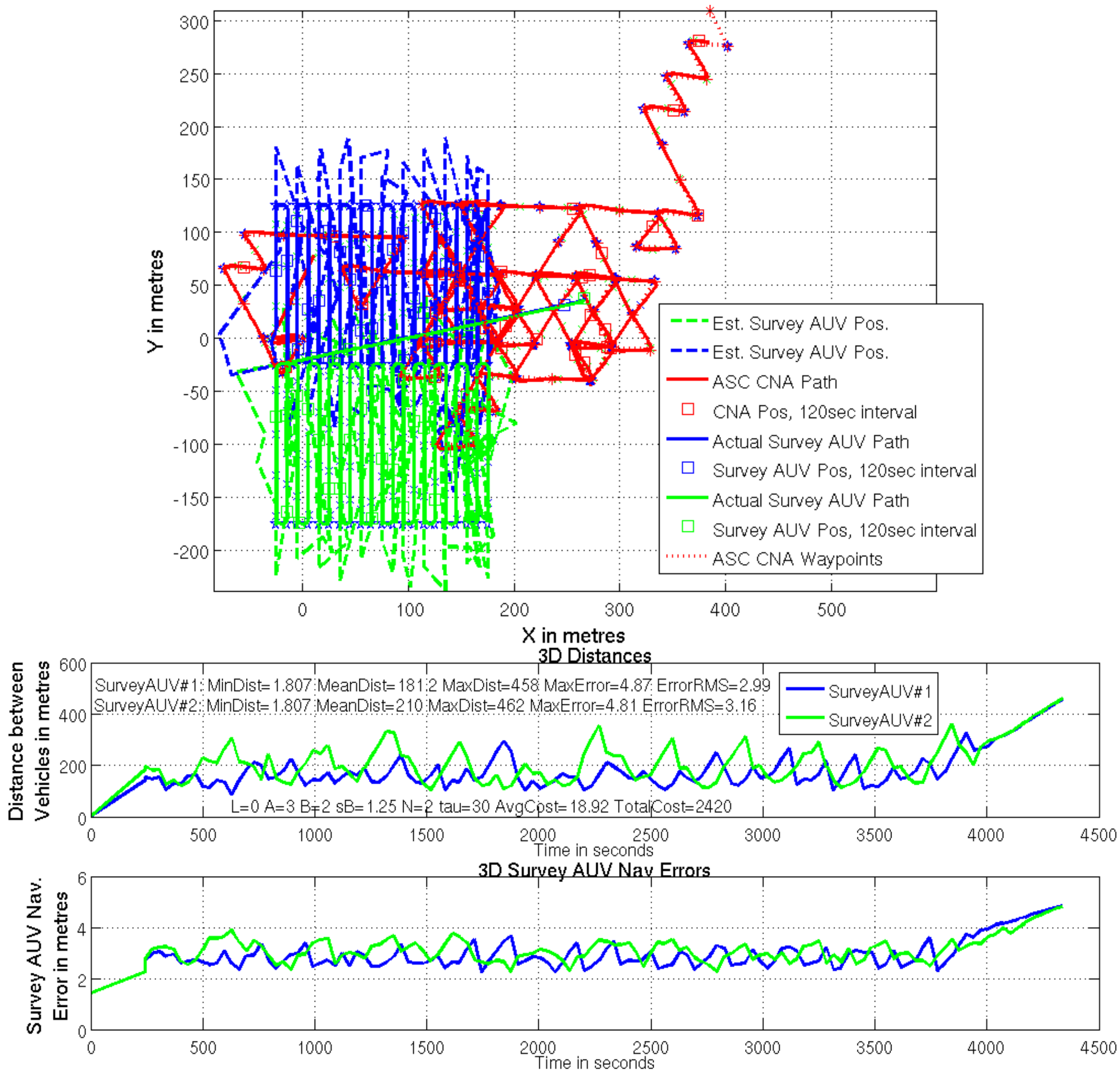

Figure B.14: Tank trial, parallel lawnmower legs, 10 m mode depth, reduced parameters

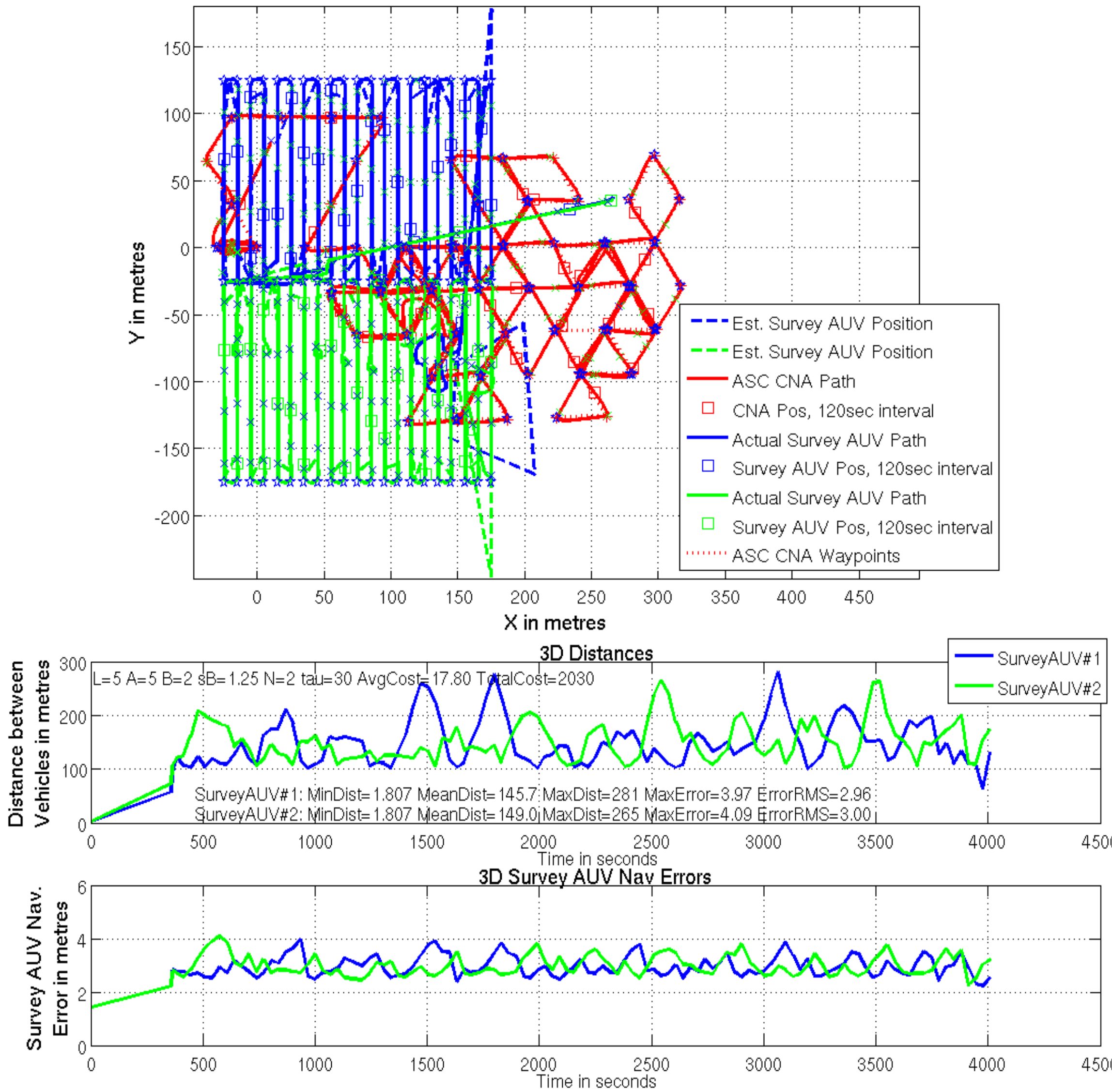

Figure B.15: Tank trial, parallel lawnmower legs, 5 m mode depth, tight parameters

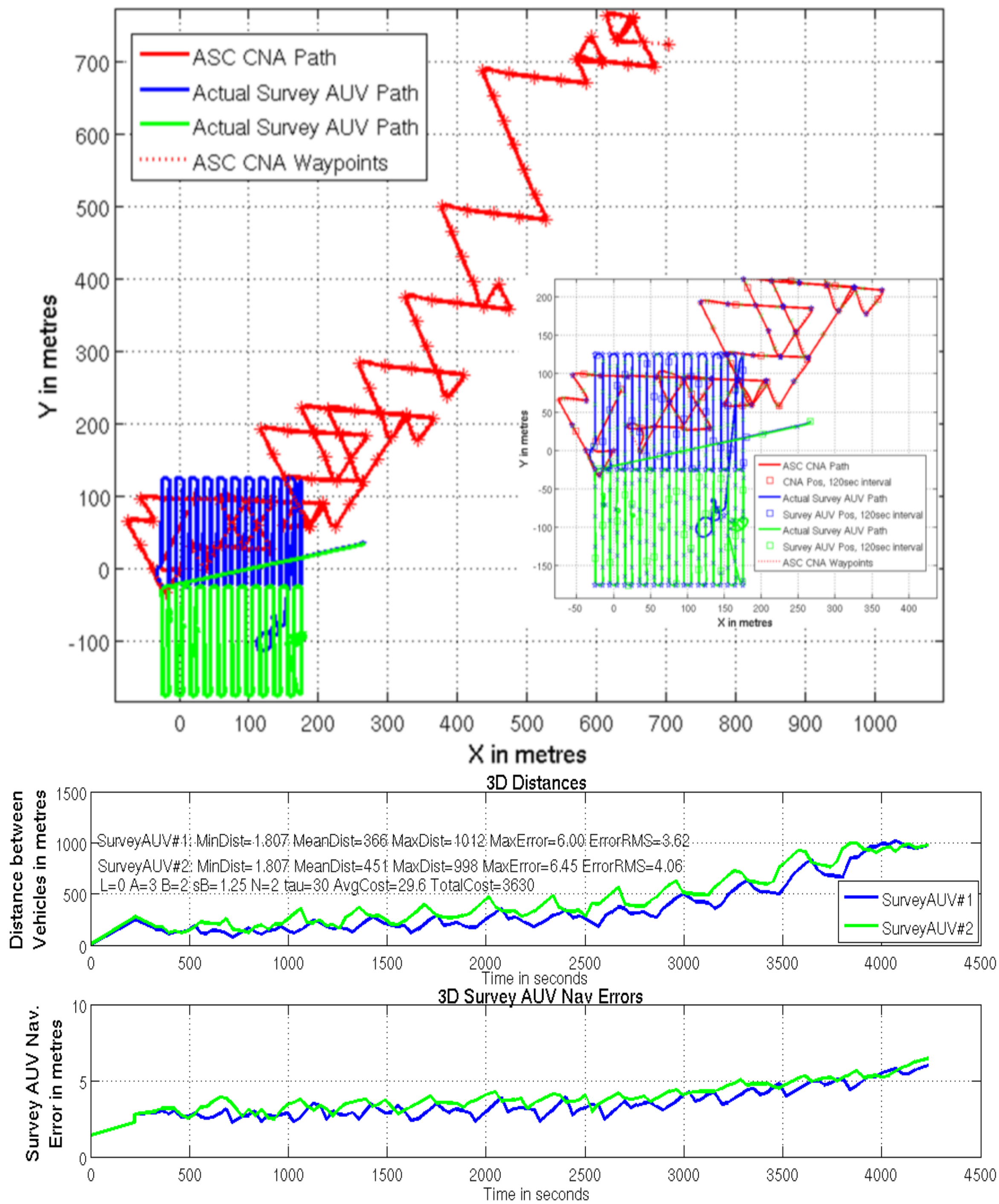

Figure B.16: Tank trial, parallel lawnmower legs, 5 m mode depth, reduced parameters

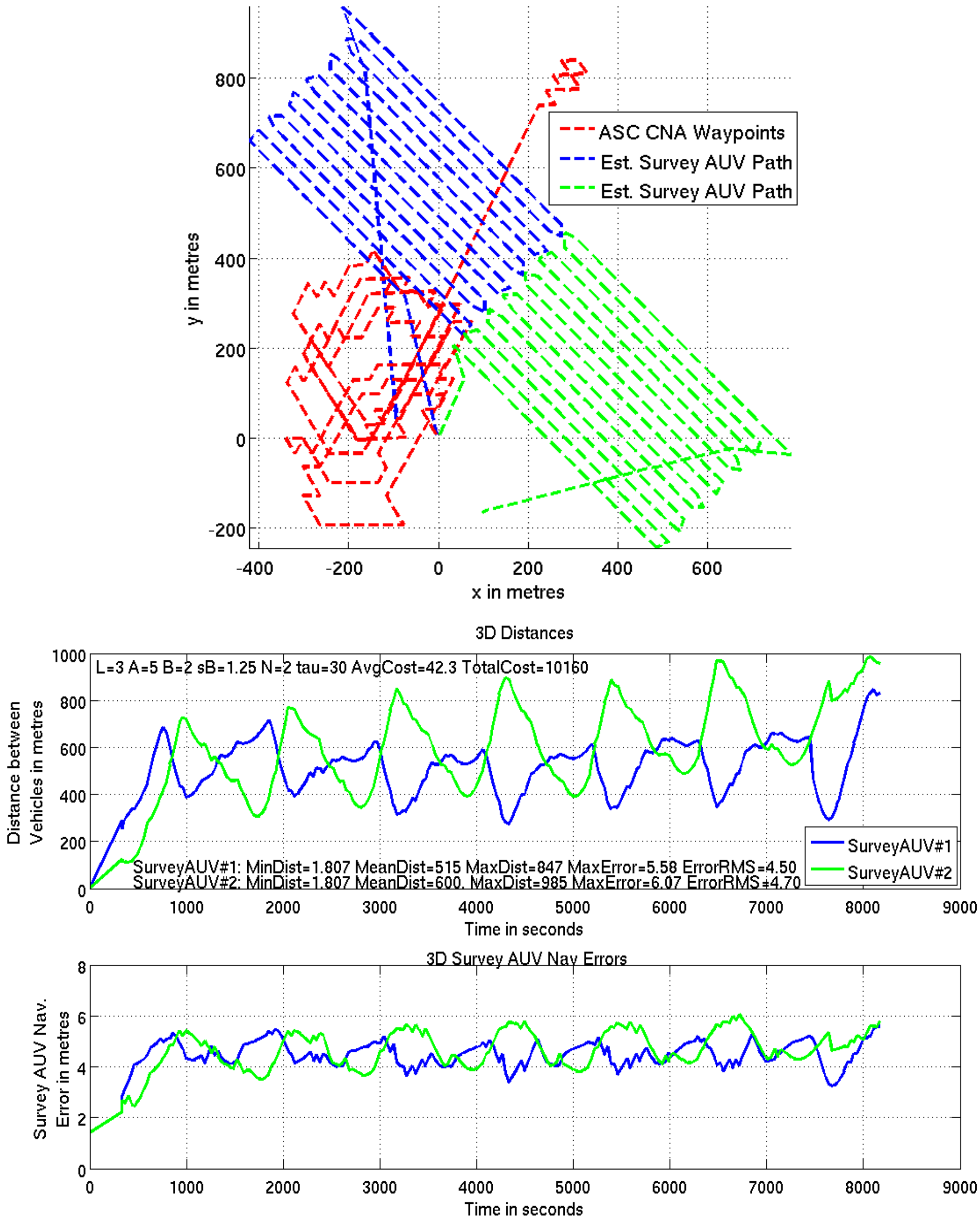

Figure B.17: Tank trial, parallel lawnmower legs, 10 m mode depth, tight parameters

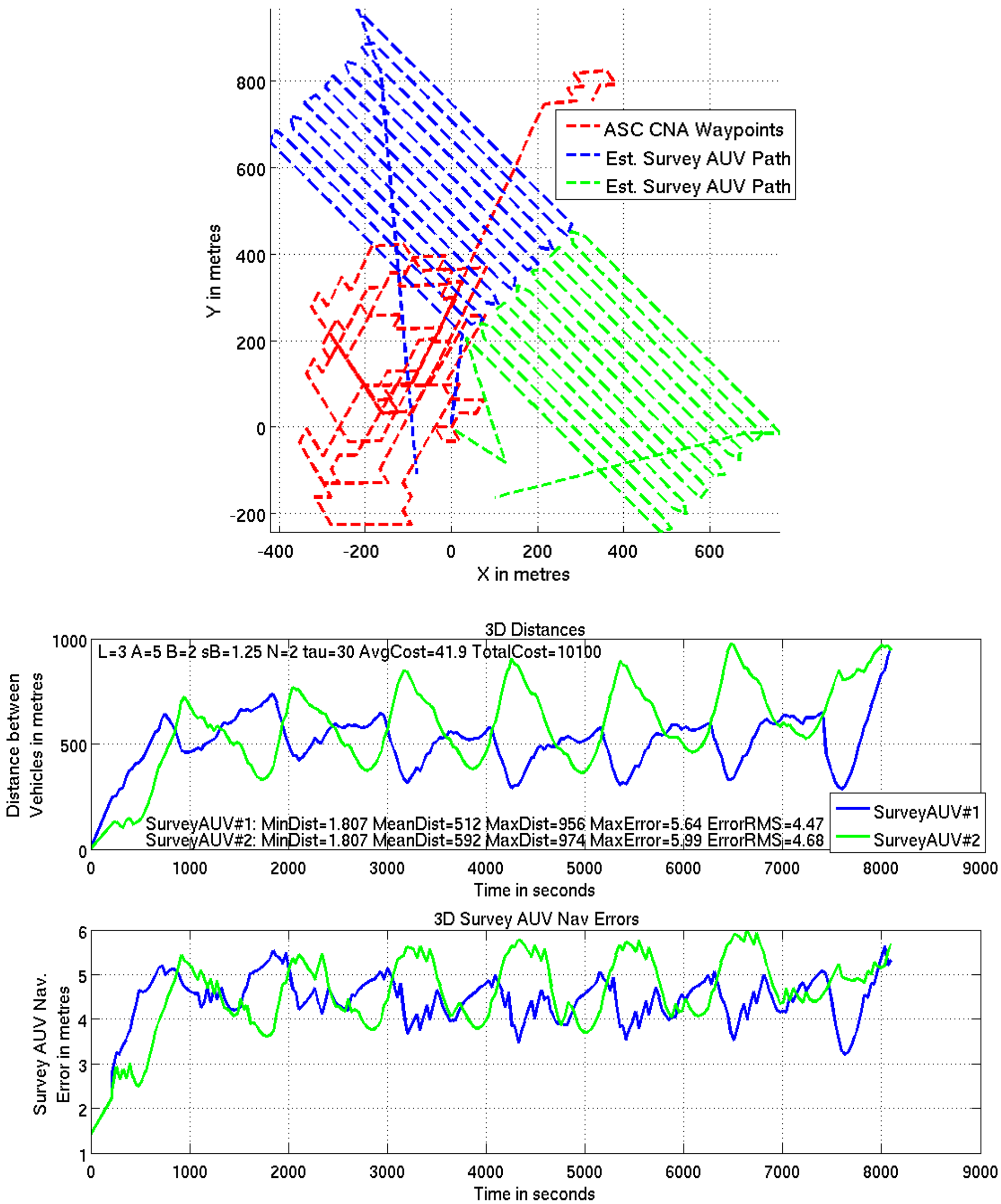

Figure B.18: Tank trial, parallel lawnmower legs, 5 m mode depth, tight parameters

Appendix C Acoustic Message used in Experiments

Below is the XML file used by *pAcommsHandler* to transmit the acoustic messages used in thesis to communicate the information used for the CNA's underway path planning.

Listing B.1: Primary status message exchanged by marine vehicles


```
<?xml version="1.0" encoding="UTF-8" ?>
- <!-- Status and Command message for testing online CNA -->
- <message_set>
- <message>
  <name>SURVEY_AUV_STATUS</name>
  <trigger>time</trigger>
  <trigger_time>3</trigger_time> <!-- 10 times proposed comm cycle time -->
  <size>32</size>
- <header>
  <id>61</id>
- <time>
  <name>Timestamp</name>
  </time>
- <src_id algorithm="to_lower,name2modem_id">
  <name>Node</name>
  <moos_var>VEHICLE_NAME</moos_var>
  </src_id>
  </header>
- <layout>
- <static>
  <name>MessageType</name>
  <value>SURVEY_STATUS</value>
  </static>
- <enum algorithm="to_lower">
  <name>Type</name>
  <moos_var>VEHICLE_TYPE</moos_var>
  <value>asc</value>
  <value>auv</value>
  <value>ship</value>
  <value>buoy</value>
  <value>glider</value>
  <value>unknown</value>
  </enum>
- <float>
  <name>nav_x</name>
  <moos_var>NAV_X</moos_var>
  <max>16000</max>
  <min>-16000</min>
  <precision>0</precision>
  </float>
- <float>
```

```
  <name>nav_y</name>
  <moos_var>NAV_Y</moos_var>
  <max>16000</max>
  <min>-16000</min>
  <precision>0</precision>
  </float>
- <float>
  <name>Speed</name>
  <moos_var>NAV_SPEED</moos_var>
  <max>9</max>
  <min>-2</min>
  <precision>1</precision>
  </float>
- <float algorithm="angle_0_360">
  <name>Heading</name>
  <moos_var>NAV_HEADING</moos_var>
  <max>360</max>
  <min>0</min>
  <precision>0</precision>
  </float>
- <float>
  <name>x1</name>
  <moos_var>X1_SELF</moos_var>
  <max>16000</max>
  <min>-16000</min>
  <precision>0</precision>
  </float>
- <float>
  <name>y1</name>
  <moos_var>Y1_SELF</moos_var>
  <max>16000</max>
  <min>-16000</min>
  <precision>0</precision>
  </float>
- <float>
  <name>x2</name>
  <moos_var>X2_SELF</moos_var>
  <max>16000</max>
  <min>-16000</min>
  <precision>0</precision>
  </float>
- <float>
  <name>y2</name>
  <moos_var>Y2_SELF</moos_var>
  <max>16000</max>
  <min>-16000</min>
  <precision>0</precision>
  </float>
- <float>
```

```
  <name>x3</name>
  <moos_var>X3_SELF</moos_var>
  <max>16000</max>
  <min>-16000</min>
  <precision>0</precision>
  </float>
- <float>
  <name>y3</name>
  <moos_var>Y3_SELF</moos_var>
  <max>16000</max>
  <min>-16000</min>
  <precision>0</precision>
  </float>
- <enum algorithm="to_lower">
  <name>frontSeatError</name>
  <moos_var>FRONTSEAT_ERROR</moos_var>
  <value>n</value>
  <value>e</value>
  <value>m</value>
  <value>sop</value>
  <value>stl</value>
  <value>sle</value>
  <value>sfp</value>
  <value>sed</value>
  <value>sup</value>
  <value>stf</value>
  <value>srp</value>
  <value>snd</value>
  <value>snc</value>
  <value>spw</value>
  <value>sti</value>
  </enum>
- <enum algorithm="to_lower">
  <name>frontMode</name>
  <moos_var>FRONTSEAT_MODE</moos_var>
  <value>normal</value>
  <value>manual_override</value>
  <value>servo</value>
  <value>stopped</value>
  <value>manual_park</value>
  </enum>
- <enum algorithm="to_lower">
  <name>powerLeakDetect</name>
  <moos_var>BATTERY_LEAK</moos_var>
  <value>false</value>
  <value>true</value>
  </enum>
- <float>
  <name>Depth</name>
```

```
  <moos_var>NAV_DEPTH</moos_var>
  <max>203</max>
  <min>-1</min>
  <precision>1</precision>
  </float>
- <float>
  <name>Altitude</name>
  <moos_var>NAV_ALTITUDE</moos_var>
  <max>203</max>
  <min>-1</min>
  <precision>1</precision>
  </float>
- <float>
  <name>Battery</name>
  <moos_var>BATTERY_PERCENT</moos_var>
  <max>100</max>
  <min>0</min>
  <precision>0</precision>
  </float>
  </layout>
- <!-- decoding -->
- <on_receipt>
- <publish>
  <moos_var>INCOMING_REPORT</moos_var>
  <all />
  </publish>
- <publish>
  <moos_var>NODE_REPORT</moos_var>
 <format>NAME=%1%,TYPE=%2%,UTC_TIME=%3$.0lf,X=%4%,Y=%5%,LA
  T=%6$lf,LON=%7$lf,SPD=%8%,HDG=%9%,DEPTH=%10%,ALTITUDE=%
  11%</format>
  <message_var algorithm="modem_id2name">Node</message_var>
  <message_var>Type</message_var>
  <message_var>Timestamp</message_var>
  <message_var>nav_x</message_var>
  <message_var>nav_y</message_var>
  <message_var algorithm="utm_y2lat:nav_x">nav_y</message_var>
  <message_var algorithm="utm_x2lon:nav_y">nav_x</message_var>
  <message_var>Speed</message_var>
  <message_var>Heading</message_var>
  <message_var>Depth</message_var>
  <message_var>Altitude</message_var>
  </publish>
- <publish>
  <moos_var type="double">%1%_NAV_UTC</moos_var>
  <format>%2$lf</format>
  <message_var algorithm="modem_id2name,to_upper">Node</message_var>
  <message_var>Timestamp</message_var>
  </publish>
```

```
- <publish>
  <moos_var type="double">%1%_NAV_X</moos_var>
  <format>%2%</format>
  <message_var algorithm="modem_id2name,to_upper">Node</message_var>
  <message_var>nav_x</message_var>
  </publish>
- <publish>
  <moos_var type="double">%1%_NAV_Y</moos_var>
  <format>%2%</format>
  <message_var algorithm="modem_id2name,to_upper">Node</message_var>
  <message_var>nav_y</message_var>
  </publish>
- <publish>
  <moos_var type="double">%1%_NAV_LAT</moos_var>
  <format>%2%</format>
  <message_var algorithm="modem_id2name,to_upper">Node</message_var>
  <message_var algorithm="utm_y2lat:nav_x">nav_y</message_var>
  </publish>
- <publish>
  <moos_var type="double">%1%_NAV_LONG</moos_var>
  <format>%2$lf</format>
  <message_var algorithm="modem_id2name,to_upper">Node</message_var>
  <message_var algorithm="utm_x2lon:nav_y">nav_x</message_var>
  </publish>
- <publish>
  <moos_var type="double">%1%_NAV_SPEED</moos_var>
  <format>%2$lf</format>
  <message_var algorithm="modem_id2name,to_upper">Node</message_var>
  <message_var>Speed</message_var>
  </publish>
- <publish>
  <moos_var type="double">%1%_NAV_HEADING</moos_var>
  <format>%2%</format>
  <message_var algorithm="modem_id2name,to_upper">Node</message_var>
  <message_var>Heading</message_var>
  </publish>
- <publish>
  <moos_var>ACOMMS_SRC_VEHICLE</moos_var>
  <message_var algorithm="modem_id2name">Node</message_var>
  </publish>
- <publish>
  <moos_var type="double">X1_%1%</moos_var>
  <format>%2%</format>
  <message_var algorithm="modem_id2name,to_upper">Node</message_var>
  <message_var>x1</message_var>
  </publish>
- <publish>
  <moos_var type="double">Y1_%1%</moos_var>
  <format>%2%</format>
```

```
  <message_var algorithm="modem_id2name,to_upper">Node</message_var>
  <message_var>y1</message_var>
  </publish>
- <publish>
  <moos_var type="double">X2_%1%</moos_var>
  <format>%2%</format>
  <message_var algorithm="modem_id2name,to_upper">Node</message_var>
  <message_var>x2</message_var>
  </publish>
- <publish>
  <moos_var type="double">Y2_%1%</moos_var>
  <format>%2%</format>
  <message_var algorithm="modem_id2name,to_upper">Node</message_var>
  <message_var>y2</message_var>
  </publish>
- <publish>
  <moos_var type="double">X3_%1%</moos_var>
  <format>%2%</format>
  <message_var algorithm="modem_id2name,to_upper">Node</message_var>
  <message_var>x3</message_var>
  </publish>
- <publish>
  <moos_var type="double">Y3_%1%</moos_var>
  <format>%2%</format>
  <message_var algorithm="modem_id2name,to_upper">Node</message_var>
  <message_var>y3</message_var>
  </publish>
- <publish>
  <moos_var>FRONTSEAT_ERROR_%1%</moos_var>
  <format>%2%</format>
  <message_var algorithm="modem_id2name,to_upper">Node</message_var>
  <message_var>frontSeatError</message_var>
  </publish>
- <publish>
  <moos_var>FRONTSEAT_MODE_%1%</moos_var>
  <format>%2%</format>
  <message_var algorithm="modem_id2name,to_upper">Node</message_var>
  <message_var>frontMode</message_var>
  </publish>
- <publish>
  <moos_var>BATTERY_LEAK_%1%</moos_var>
  <format>%2%</format>
  <message_var algorithm="modem_id2name,to_upper">Node</message_var>
  <message_var>powerLeakDetect</message_var>
  </publish>
- <publish>
  <moos_var>BATTERY_PERCENT_%1%</moos_var>
  <format>%2%</format>
  <message_var algorithm="modem_id2name,to_upper">Node</message_var>
```

```
  <message_var>Battery</message_var>
  </publish>
- <publish>
  <moos_var type="double">%1%_NAV_DEPTH</moos_var>
  <format>%2%</format>
  <message_var algorithm="modem_id2name,to_upper">Node</message_var>
  <message_var>Depth</message_var>
  </publish>
- <publish>
  <moos_var type="double">%1%_NAV_ALTITUDE</moos_var>
  <format>%2%</format>
  <message_var algorithm="modem_id2name,to_upper">Node</message_var>
  <message_var>Altitude</message_var>
  </publish>
  </on_receipt>
- <queuing>
  <ack>false</ack>
  <blackout_time>10</blackout_time>
  <ttl>300</ttl>
  <value_base>3</value_base>
  </queuing>
  </message>
  </message_set>
```